Circulating biomarkers of *Onchocerca volvulus* for diagnosis of infection and antifilarial treatment efficacy

Thesis submitted in accordance with the requirements of
the University of Liverpool
for the degree of Doctor in Philosophy
by

Cara L Macfarlane
September 2017

Abstract

Onchocerciasis, or “river blindness”, is a parasitic disease caused by the filarial worm *Onchocerca volvulus*. Significant progress in onchocerciasis control in Latin America and Africa, where 99% of cases occur, has made elimination of the disease feasible in some circumstances. However, progression to an elimination programme poses new challenges for diagnosis, as no test can detect current infection with the *O. volvulus* adult worm, and the detection of microfilariae (mf) in the skin lacks sufficient sensitivity after long-term exposure to treatment with ivermectin. To achieve the new global health goals for onchocerciasis, *O. volvulus* biomarkers with high sensitivity are needed to map areas with low levels of ongoing transmission and monitor infection recrudescence, while high specificity is required to enable discrimination between closely related filarial worms in areas with overlapping geographic distributions. Although the adult worms live in subcutaneous nodules, these nodules are highly vascularised, allowing potential biomarkers of *O. volvulus* to present in the host circulation. In this study, a longitudinal plasma sample set collected in Cameroon from individuals with onchocerciasis pre-treatment, and at four, 12 and 21 months after following one of three antifilarial treatment regimens, was used to screen for circulating protein, DNA and miRNA markers of infection and macrofilaricidal treatment efficacy in the host. Following the development of a discovery proteomic method for plasma, five individuals infected at baseline and amicrofilaridermic or with low mf burden (four patients and one patient, respectively) at 21 months were analysed. Sixteen circulating *O. volvulus* proteins were identified, of which 15 were detected 21 months post-doxycycline treatment. Eight proteins were detected in almost every individual at each time point over 21 months, while three parasite proteins changed in detection frequency among individuals by the final follow-up. An uncharacterised *O. volvulus* membrane protein enriched in female worms, A0A044VCM8, was detected in all individuals and may be a circulating marker for female worm infection. However, the protein was detected consistently over the 21 month follow-up, suggesting it is unlikely to be useful as a marker for treatment efficacy. An analysis of 18 participants before and after treatment with either doxycycline, doxycycline + ivermectin, or ivermectin, detected both parasite-derived miRNAs and *O. volvulus*-specific DNA in the circulation of the host using RT-qPCR and qPCR, respectively. However, the two parasite-derived miRNAs associated with *O. volvulus*, miR-71 and lin-4, were negative in almost all plasma samples, and did not have the specificity or sensitivity to be circulating markers for onchocerciasis. The *O.*

volvulus-specific O-150 DNA marker was detected in plasma in almost half of the same 18 individuals pre-treatment, with a decline in the proportion of positive patients detected in all treatment groups over the follow-up timeframe. Of the 58 plasma samples negative for O-150 by qPCR, 36 (62.1%) had microfilaridermia detected by parasitological evaluation. Detection of *O. volvulus* DNA in the host plasma was therefore was not sufficiently sensitive. No suitable circulating protein, DNA or miRNA markers of infection clearance and treatment efficacy were identified by 21 months post-treatment among the individuals tested. Several factors may have confounded our longitudinal biomarker analyses, such as large gaps in time between sampling in an area of ongoing transmission, where reinfections can occur and influence the prevalence or abundance of circulating biomarkers. Individuals may also have occult *L. loa* and/or *M. perstans* infection, and therefore potential biomarkers identified may not be specific for onchocerciasis. Participants in the study may have had incomplete responses to macrofilaricidal treatment, and the variable persistence of adult worms among individuals influenced the circulating biomarker profile. Ideally, biomarkers of active *O. volvulus* infection and infection clearance following macrofilaricidal treatment would be validated in clinical sample sets from areas of low endemicity or in a confirmed elimination setting, in order to reduce the possibility of reinfections over follow-up. These areas should also be free of coinfective parasites, such as *L. loa, M. perstans* or *W. bancrofti*, to ensure that biomarker(s) are detected due to infection with *O. volvulus* only. Additionally, patients would consistently respond to treatment and show a total macrofilaricidal response. In the absence of a perfect human sample set, animal models, such as new immunodeficient mouse models for onchocerciasis, would also be useful for conducting preclinical studies, where samples can be readily obtained and conditions optimally controlled. Future work should determine in an optimised sample set whether the *O. volvulus* proteins consistently detected here in plasma are indeed novel circulating markers of infection, in order to progress specific and sensitive targets for future diagnostic development.

Contents

Abstract 1
List of Figures 5
List of Tables 7
Supplementary Material 8
Acknowledgements 9
Contributors Statements 10
List of Abbreviations and Acronyms 11
Chapter 1. Introduction 13
Onchocerciasis 13
Parasite and life cycle 13
Clinical manifestations of disease 15
Epidemiological patterns and prevalence 19
Control and elimination 20
Treatment for onchocerciasis 25
Diagnosis of *Onchocerca volvulus* 30
Biomarkers for onchocerciasis 37
Recent advances in technology platforms for biomarker discovery 39
Circulating biomarkers for adult *Onchocerca volvulus*: A rationale 43
Project aims 45
Chapter 2. Methods 46
Methodology 46
Reagents and equipment 46
Human plasma 48
Ethics statement 50
Proteomic techniques 50
Protein identification: Proteome Discoverer and Mascot 55
Protein identification: MaxQuant and Andromeda 57
Bioinformatic analysis of the onchocerciasis plasma proteome: Perseus 59
Functional analysis of *Onchocerca volvulus* proteins 60
Molecular techniques 61
Statistical analysis 68

Chapter 3. Developing a discovery proteomic workflow for plasma.....70
Abstract 70
Introduction 71
Methods 73
Results 78
Discussion 93
Chapter 4. The onchocerciasis plasma proteome – a longitudinal survey.....99
Abstract 99
Introduction 100
Methods 102
Results 109
Discussion 126
Chapter 5. Nucleic acid markers of *Onchocerca volvulus* in plasma.....132
Abstract 132
Introduction 133
Methods 135
Results 141
Discussion 157
Chapter 6. Discussion.....164
Bibliography 172

List of Figures

Fig. 1. 1. Life cycle of *Onchocerca volvulus*. 15
Fig. 1. 2. Distribution and status of preventive chemotherapy for onchocerciasis worldwide, in 2015. 23
Fig. 3. 1. Percentage of protein mass in plasma 71
Fig. 3. 2. Proteomic workflow. 74
Fig. 3. 3. Plasma protein profile with 1D SDS-PAGE 79
Fig. 3. 4. Protein identifications in plasma depleted of abundant proteins. 82
Fig. 3. 5. Relative abundance of the top 12 abundant proteins (-Ig accessions) in plasma and depleted plasma. 87
Fig. 3. 6. Number of proteins in the depleted plasma and whole plasma. 88
Fig. 3. 7. Reproducibility of LC-MS/MS analyses. 89
Fig. 3. 8. Number of proteins in the depleted plasma and eluted fraction. 90
Fig. 3. 9. Protein identifications in depleted and eluted fractions combined *in silico*. 92
Fig. 4. 1. Proteomic workflow. 105
Fig. 4. 2. Number of protein groups identified in each individual at each time point. 111
Fig. 4. 3. Statistical evaluation of protein expression level changes over time. 115
Fig. 4. 4. Profile plots of *O. volvulus* proteins in plasma. 119
Fig. 4. 5. Overview of GO annotations for the *O. volvulus* proteins. 120
Fig. 4. 6. Unsupervised hierarchical clustering and principal component analysis. 125
Fig. 5. 1. Standard curves of two parasite miRNA qPCR assays. 142
Fig. 5. 2. Assessment of plasma reference miRNAs 143
Fig. 5. 3. Plasma reference and spike-in miRNA controls 144
Fig. 5. 4. Monitoring PCR inhibition using a plasma endogenous control miRNA. 146
Fig. 5. 5. Detection of a parasite miRNA in plasma after optimising the RT-qPCR. 147
Fig. 5. 6. Longitudinal evaluation of cel-miR-71-5p in two individuals with onchocerciasis before and after doxycycline-treatment. 148

Fig. 5. 7. Longitudinal detection of plasma endogenous control and spike-in miRNAs in trial individuals before and after following one of three antifilarial treatment regimens. 150
Fig. 5. 8. Standard curve of the *O. volvulus* O-150 qPCR assay and endogenous plasma control GAPDH qPCR assay. 151
Fig. 5. 9. *O. volvulus* DNA positive and endogenous control DNA positive individuals. 152
Fig. 5. 10. O-150 positive plasma samples by treatment group and time point. 154
Fig. 5. 11. Plasma reference and spike-in DNA controls.....156

List of Tables

Table 2. 1. List of powder and liquid laboratory supplies used and their sources. ...46
Table 2. 2. Buffers and solutions made in the laboratory.....48
Table 2. 3. Reference proteomes concatenated for database searching in MaxQuant. 59
Table 2. 4. Primer and probe sequences for DNA-based experiments.....67
Table 3. 1. Plasma proteins identified by 1D SDS-PAGE and LC-MS/MS. 80
Table 3. 2. Plasma proteins identified by 1D SDS-PAGE and LC-MS/MS after abundant protein depletion.....83
Table 3. 3. Top 20 high scoring proteins identified in plasma by in-solution proteolysis and LC-MS/MS. 84
Table 3. 4. Top 20 high scoring proteins identified in depleted plasma by in-solution proteolysis and LC-MS/MS. 85
Table 3. 5. Protein accessions unique to the bound abundant protein fraction. 91
Table 4. 1. Parasitology of participants selected for the current study.....104
Table 4. 2. Protein identifications in the onchocerciasis plasma proteome.....110
Table 4. 3. The 20 most abundant proteins in the onchocerciasis plasma proteome. 112
Table 4. 4. Proteins present at only one of four time points in the trial. 113
Table 4. 5. Specificity of the 16 *O. volvulus* proteins detected in plasma.....123
Table 5. 1. Parasitology of participants selected for the current study.....137
Table 5. 2. Clinical plasma samples positive for worm miRNAs. 149
Table 5. 3. Individuals positive and negative for O-150 in plasma by qPCR. 153
Table 5. 4. Test results obtained by qPCR of plasma and by mf detection in skin snips. 155

Supplementary Material

Table S1. Protein identifications from whole plasma and depleted plasma.

Table S2. Protein identifications from depleted plasma and eluted abundant protein fraction.

Table S3. Protein identifications from depleted plasma and eluted abundant protein fraction recombined *in silico.*

Table S4. Protein identifications in the onchocerciasis plasma proteome.

Table S5. GO terms for circulating *O. volvulus* proteins.

Table S6. Details of *O. volvulus* peptide identifications.

Fig. S1. Pairwise comparisons of $\log_2$ transformed LFQ protein intensities.

Fig. S2. Distribution of sample LFQ intensities.

Fig. S3. Low abundance LFQ intensity imputation.

Acknowledgements

I would firstly like to thank my supervisors, Professor Mark Taylor and Dr Simon Wagstaff, for their input and guidance throughout my PhD. I would also like to thank the Liverpool School of Tropical Medicine for funding this PhD studentship. I would like to thank past and current members of the A-WOL laboratory for general support over the years, with a special thank you to Dr Gemma Molyneux for helping me immensely during the initial stages of my proteomics project, and for giving me an understanding of protein experiments, proteomics and the bioinformatic analyses. I sincerely appreciate her assistance, expertise, time and advice on proteomics during our time working together. I would also like to thank Mr Andrew Stevens, who has been great support over the years, Dr Joe Turner for helpful discussions regarding trial and parasite samples and filariasis, and Miss Mary Creegan for giving administrative support and for her help throughout my PhD. I would also like to thank Dr Tom Edwards and Dr Emily Adams for their useful discussions and guidance on the molecular work. Professor Alister Craig and Professor Martin Donnelly have also provided informative and constructive feedback and advice during the later stages of my PhD, and I would to thank them for always making time for me. I would also like to thank Dr Artemis Koukounari within LSTM, and Dr Simon Perkins and Miss Hayley Price at the University of Liverpool, for giving up their time to discuss statistical and bioinformatic techniques with me. Dr Eva Caamano has been an amazing friend within LSTM throughout my PhD, and I am grateful for her support and helpful discussions over the years. Finally, I would like to thank my family and friends, in particular my mum, Tom Edwards and Rebecca Chilvers, for their patience and support, and for getting many drinks in.

Contributors Statements

The contributions to all chapters:

Chapter 1. Cara L Macfarlane wrote this and Professor Mark Taylor and Dr Simon Wagstaff supervised the writing.

Chapter 2. Cara L Macfarlane wrote this and Professor Mark Taylor and Dr Simon Wagstaff supervised the writing. Advice on the statistical and bioinformatic analysis methodology was provided by Dr Artemis Koukounari, Dr Simon Perkins and Miss Hayley Price.

Chapter 3. Cara L Macfarlane performed the scientific experiments, with assistance from Dr Gemma Molyneux and Dr Gavin Laing for the LC-MS/MS analyses. Professor Mark Taylor and Dr Simon Wagstaff supervised the experimental design, work and the writing.

Chapter 4. Cara L Macfarlane performed the scientific experiments with assistance from Dr Gemma Molyneux for the LC-MS/MS analyses. Professor Mark Taylor and Dr Simon Wagstaff supervised the experimental design, work and the writing.

Chapter 5. Cara L Macfarlane performed the scientific experiments. Professor Mark Taylor and Simon Wagstaff supervised the experimental design, work and the writing.

Chapter 6. Cara L Macfarlane wrote this chapter and Professor Mark Taylor and Dr Simon Wagstaff supervised the writing.

List of Abbreviations and Acronyms

Aa	- Amino acid
ACN	- Acetonitrile
AmBic	- Ammonium Bicarbonate
ANOVA	- Analysis of Variance
APOC	- African Programme for Onchocerciasis Control
APS	- Ammonium Persulfate
BLAST	- Basic Local Alignment Search Tool
Bp	- Base Pair
BSA	- Bovine Serum Albumin
CDD	- Community Drug Distributor
cDNA	- Complementary DNA
CFA	- Circulating Filarial Antigen
CI	- Confidence Interval
Cq	- Quantification Cycle Value
CTDi	- Community Directed Treatment with ivermectin
CV	- Coefficient of Variation
d.H_2O	- Distilled water
DALY	- Disability-Adjusted Life Years
DEC	- Diethylcarbamazine
DNA	- Deoxyribonucleic acid
DOXY	- Doxycycline
DTT	- Dithiothreitol
E/S	- Excretory-secretory
EDTA	- Ethylenediaminetetracetic acid
ELISA	- Enzyme-Linked Immunosorbent Assay
FA	- Formic acid
FDR	- False Discovery Rate
GAPDH	- Glyceraldehyde 3-phosphate dehydrogenase
GEO	- Generalised onchocerciasis
H_2O	- Water
HCl	- Hydrogen Chloride
HPLC	- High-Performance Liquid Chromatography
HUPO	- Human Proteome Organization
IAA	- Iodoacetamide
ICT	- Immunochromatographic Test
Ig	- Immunoglobulin
IVM	- Ivermectin
kDa	- Kilodalton
L1	- First stage larvae
L3	- Third stage larvae
LAMP	- Loop Mediated Isothermal Amplification
LC	- Liquid Chromatography
LC-MS/MS	- Liquid Chromatography Tandem-Mass Spectrometry
LF	- Lymphatic filariasis
LOD	- Limit of Detection
LSTM	- Liverpool School of Tropical Medicine
MDA	- Mass Drug Administration
Mf	- Microfilariae
mf/mg	- Microfilariae per mg skin
miRNA	- MicroRNA
MS	- Mass Spectrometry
MS/MS	- Tandem-Mass Spectrometry
MW	- Molecular Weight
NaOH	- Sodium Hydroxide
NATOG	- N-Acetyltyramine-O,β-Glucuronide
NHS	- National Health Service

NMWL	- Nominal Molecular Weight Limit
nt	- Nucleotide
NTC	- No Template Control
NTD	- Neglected Tropical Disease
OCP	- Onchocerciasis Control Programme
OEPA	- Onchocerciasis Elimination Program for the Americas
PC	- Preventive Chemotherapy
PCA	- Principal Component Analysis
PCR	- Polymerase Chain Reaction
PhHV-1	- Phocine herpes virus 1
PSM	- Peptide Spectrum Match
PZP	- Pregnancy Zone Protein
QC	- Quality Control
Qpcr	- Quantitative PCR
RAPLOA	- Rapid Assessment Procedures for Loiasis
RDT	- Rapid Diagnostic Test
REMO	- Rapid Epidemiological Mapping of Onchocerciasis
RNA	- Ribonucleic acid
RP-LC	- Reverse Phase Liquid Chromatography
RPMI	- Roswell Park Memorial Institute
RT	- Reverse Transcription
-RT	- Minus Reverse Transcriptase control
RT-qPCR	- Quantitative Reverse Transcription PCR
SAE	- Severe Adverse Event
SD	- Standard Deviation
SDS	- Sodium Dodecyl Sulfate
SDS-PAGE	- Sodium Dodecyl Sulfate Polyacrylamide Gel Electrophoresis
SEM	- Standard Error of the Mean
STH	- Soil-Transmitted Helminths
TEMED	- Tetramethylethylenedi-Amine
TFA	- Trifluoroacetic acid
T_m	- Melting temperature
Tris	- Tris base / Trizma
WHO	- World Health Organization

Chapter 1. Introduction

Onchocerciasis

Onchocerciasis, also known as “river blindness”, is a neglected tropical disease (NTD) affecting an estimated 37 million people, with over 100 million more people at risk (1). Of the 34 countries where the disease is prevalent, over 99% of cases occur in 31 endemic African countries (2). Sub-Saharan Africa is by far the most affected region with regards to distribution and impact of disease, with minor foci in Latin America and in Yemen. Onchocerciasis is caused by the filarial nematode *Onchocerca volvulus*, which is transmitted to the human host by infected blackflies of the genus *Simulium* during a bloodmeal. The name “river blindness” derives from the insect vector breeding requirement for fast-flowing streams and rivers which confines infection to areas adjacent to river systems, and an advanced clinical manifestation of the disease which results in blindness (3). Onchocerciasis is responsible for a range of clinical presentations that affect the skin and eyes. Symptoms experienced by those infected include severe itching and various skin changes, and some people may develop eye symptoms that can progress to visual impairment and blindness. There is currently no vaccine to protect people from continued re-infection with *O. volvulus*. In endemic areas, the enormous socio-economic impact (4-7) and the substantial morbidity experienced by those infected resulted in over 1 million disability-adjusted life years (DALYs) annually (8, 9). Significant progress in interrupting disease transmission has been made in Latin America and in Africa over the last few decades by using large-scale mass treatment of all populations in endemic areas. Following the success of ongoing efforts and near elimination of onchocerciasis in Latin America, and interruption of disease transmission in some areas in Africa, elimination of the disease in the African Region is now a global health initiative (10).

Parasite and life cycle

There are eight species of filarial nematodes that infect humans, and three are responsible for causing the majority of medically important filariasis disease (11). *Wuchereria bancrofti* and *Brugia malayi* cause lymphatic filariasis, and *O. volvulus* is the sole causative agent of onchocerciasis. *O. volvulus* is a parasitic thread-like

roundworm transmitted to the human host during a bloodmeal by the intermediate black fly host of the genus *Simulium* (Fig. 1.1) (12). Once the infective third-stage larvae (L3) of the parasite are introduced into the human host, the larvae develop into sexually dimorphic mature adults after one year. The adult worms reside in vascularised subcutaneous or deeper nodules called onchocercomas, and they are typically situated over bony prominences (13). The adult female can live for up to 14 years, with a reproductive life span ranging from nine to 11 years (14). The males are around ten times smaller in size and migrate between nodules to inseminate the viviparous females, which when fertilised give birth to 1,000 to 3,000 microfilariae (mf) per day (3). Fertilised females have an enormous reproductive capacity and can produce millions of mf over the course of their life time. The mf migrate from nodules into the skin, utilising extracellular proteases to aid their migration through tissues (15), where they can live for 12 – 18 months waiting to be taken up by the blackfly vector (11). Once the mf are within their intermediate host, they migrate from the blackfly's midgut through the hemocoel to the thoracic muscles. The mf develop over two weeks by undergoing successive moults into second-stage larvae (L2) and finally into infective L3 larvae (12). The L3 larvae then migrate to the blackfly proboscis ready to infect another human during a blood meal, thus completing the parasite life cycle and transmission of the infection. Humans are the primary host for *O. volvulus* and there is no animal reservoir for the parasite.

O. volvulus, like many other filarial worms, harbour the intracellular bacteria *Wolbachia* as an obligate endosymbiont. The presence of *Wolbachia* in *O. volvulus* was first reported by Kozek and Marroquin in 1977 (16), and the endosymbiont is present in both the male and female worms, and in all the larval developmental stages (3). *Wolbachia* is fundamental for the growth, development, embryogenesis, and survival of the parasite (17).

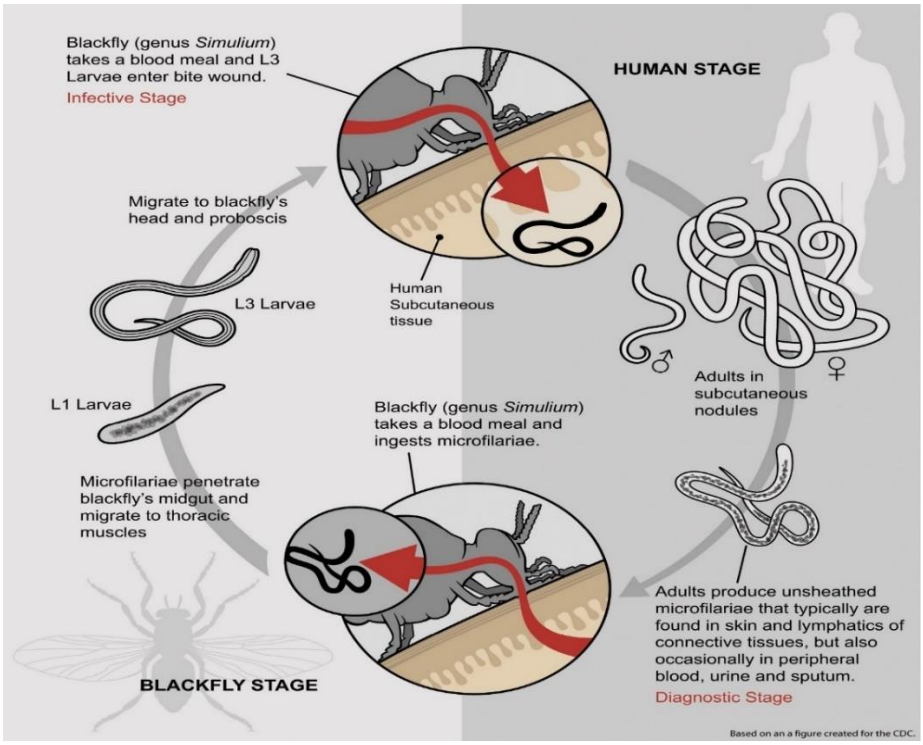

Fig. 1. 1. Life cycle of *Onchocerca volvulus* (18).

Clinical manifestations of disease

Onchocerciasis presents as cutaneous and ocular disease as a result of inflammatory reactions to the death of mf in the skin and eyes (19). Symptoms of onchocerciasis typically appear one to three years after infection, and the severity of the pathology can vary considerably amongst those affected (20). A spectrum of disease manifestations is evident and this reflects the intensity and type of host immune responses, which may be influenced by host genetic factors (21). The majority of infected individuals typically develop the generalised onchocerciasis (GEO) disease type, which is characterised by low levels of inflammation, hyporesponsive immune responses and high parasite load (22). Most individuals are asymptomatic/paucisymptomatic, presenting with a hyporesponsive immunological state that supresses anti-parasitic immunity and is unable to effectively reduce parasite loads (23). A rare but severe hyperreactive form, known as lichenified onchodermatitis or sowda, more common in particular geographical regions such as Yemen and Sudan has reduced mf and adult worm burdens associated with pronounced cellular and humoral immune responses with severe pathology (24).

Cutaneous pathology

The skin is the primary site of *O. volvulus* mf infection and the cutaneous pathology is responsible for 50% of the 1 million DALYs for onchocerciasis (25). Manifestations of the skin disease are highly variable, and the cumulative effects of chronic infection means that two or more clinical patterns may present at the same time and progress towards a variety of chronic skin manifestations (26). One of the most common and significant features of onchocerciasis is pruritus (troublesome itching), which causes extreme irritation as well as social stigma and reduced income generating capacity amongst those affected (4, 6, 27). Several different patterns of onchocercal-induced skin disease were classified by Murdoch *et al*, including; acute papular and chronic papular onchodermatitis, lichenified onchodermatitis, atrophy and depigmentation (28). Acute and chronic papular onchodermatitis affects those with the generalised onchocerciasis type. Symptoms of acute papular onchodermatitis include skin defects such as pruritic papules, vesicles and pustules, and localised erythema and oedema of the skin may also occur. The chronic form presents as a papular rash, where scattered skin lesions are flat-topped papules of variable size and height on the skin, and some lesions may be itchy. Post-inflammatory hyper-pigmentation of skin is characteristic of chronic papular onchodermatitis. The rarer severe hyperreactive form, lichenified onchodermatisis or sowda, presents as pruritic, hyperpigmented, hyperkeratotic plaques, with lichenification and lymphadenopathy. Atrophy consists of loss of skin elasticity and is also known as ‘lizard skin’. ‘Hanging groin’ presents as uni- or bilateral inelastic folds of skin that may contain enlarged lymph nodes. Onchocercal depigmentation can also cause areas of pigment-loss, and is described as ‘leopard skin’ (28).

Ocular pathology

If onchocerciasis is left to progress untreated, increasingly severe pathological outcomes such as visual impairment and blindness can result, making onchocerciasis one of the most important infectious causes of blindness worldwide (after trachoma) in number of persons affected (29, 30). Over 500,000 people are estimated to suffer from visual impairment, and blindness affects a further 270,000 people (8, 31). In untreated populations infection was once responsible for blinding the older residents of entire villages; however, the implementation of control programs in Sub-Saharan

Africa has drastically reduced the incidence of new ocular pathology and blindness. The incidence of ocular disease has been linked to a number of factors; including localisation of nodules in the upper part of the body (32), vector species (33), mf load (34), parasite strain (35), and a higher *Wolbachia* load in the blinding savannah strain of *O. volvulus* (36). Onchocercal ocular disease encompasses a wide spectrum of clinical manifestations, and mf may be found in all the tissues of the eye. Thylefors (37) and Bird *et al* (38) have produced a detailed review of the onchocercal ocular manifestations. The most common ocular pathology is typically initiated by inflammatory reaction to dead mf in the cornea provoking reversible onchocercal punctuate keratitis, which manifests as greyish 'fluffy' or 'snow-flake' opacities (37). The irreversible corneal lesion, sclerosing keratitis, may develop over several years with high ocular infection densities, as the cornea progressively loses transparency and becomes white and hard (37). Mf in the conjunctiva provoke itching, and can cause an inflammation of the iris known as chronic anterior uveitis (39). Chronic inflammation can also result in blindness due to secondary glaucoma or secondary cataract (40). In the posterior section of the eye, the optic nerve, the retina and the choroid can be affected by onchocercal lesions (38). Acute optic neuritis can lead to permanent optic atrophy and restricted visual fields (41). Retinal lesions are initially characterised by a mottled area with slight oedema, which can advance to atrophy of the retinal pigment epithelium (38). Chronic chorioretinitis may develop as an inflammation causing gradual loss of visual field, leading on to choroido-retinal or optic atrophy and eventually blindness (42).

The intracellular *Wolbachia* endosymbiont of the parasite also has a role in driving onchocercal eye disease, where bacteria released from dying and degenerating mf in the corneal stroma evokes a sequence of inflammatory responses that induce keratitis (3). By using a mouse model of onchocercal keratitis and *O. volvulus* extracts containing *Wolbachia*, the presence of *Wolbachia* has been found to be crucial for neutrophil-mediated inflammation, opacity, and corneal haze (43-45). The role of *Wolbachia* in pathogenesis of onchocercal keratitis was established, as: i) corneal inflammation does not occur in individuals with *O. volvulus* depleted of *Wolbachia* by antibiotic treatment, (ii) other *Wolbachia*-containing filarial species induce keratitis, while filarial species without *Wolbachia* do not, and iii) neutrophil recruitment to the corneal stroma was induced by isolated *Wolbachia* bacteria (3).

The role of *Wolbachia* in onchocerciasis ocular pathology has been reviewed by Tamarozzi *et al* (3). Additionally, parasite antigens similar to human autoantigens have also been implicated in inducing cross-reactive antibodies linked to the pathogenesis of posterior eye disease (46) and anterior segment lesions (47).

Other conditions associated with onchocerciasis

Systemic effects of onchocerciasis reportedly may also include low body weight, general debility, and diffuse musculoskeletal pain (39). Onchocerciasis has also been linked to epilepsy (48-50), with some epileptic individuals presenting with retarded growth, mental impairment, and delayed sexual development (50). Two other conditions that have been linked to onchocerciasis (and each other) include nakalanga syndrome and nodding syndrome (51, 52). The cause of nakalanga syndrome remains uncertain, but the condition has been described in Africa for several decades, and clinical manifestations include growth retardation, physical deformities, endocrine dysfunction, mental impairment, and epilepsy (51). Nodding syndrome has been documented in Uganda, South Sudan, and Tanzania, and is a neurological disorder affecting children (53). Nodding syndrome presents with similar features to nakalanga syndrome, and can involve head nodding episodes, stunted growth, delayed puberty, and mental impairment (51). In recent years, the blackfly vectors in onchocerciasis endemic regions have been implicated in the transmission of an etiological agent that, directly or indirectly, causes nodding syndrome and other types of epilepsy (54-56). There is also evidence suggesting nodding syndrome is an autoimmune epileptic disorder induced by molecular mimicry with *O. volvulus* antigens (particularly tropomyosin) (57, 58). Johnson *et al* reported the use of an untargeted approach for autoantibody profiling in pooled sera from individuals with nodding syndrome and pooled sera from unaffected control villagers (57). The authors identified leiomodin-1 autoantibodies were increased 33,000-fold in individuals with nodding syndrome, and autoantibodies to leiomodin-1 were detected in both sera and cerebrospinal fluid. The protein was shown to be expressed in brain structures that are thought to be affected in those with nodding syndrome, and the antibodies were found to be neurotoxic *in vitro*. The authors linked parasitic infection to autoimmune epilepsy, as leiomodin-1 antibodies purified from individuals with nodding syndrome also cross-reacted with *O. volvulus* antigens (57). Antibodies against the neuron surface protein, VGKC complex

protein, have also been studied in serum from individuals with nodding syndrome and compared to serum from unaffected siblings (59). However, 15 of the 31 individuals with nodding syndrome (48.3%) and one of the 11 controls (9.1%) tested positive (unpublished data from Idro *et al*, reported in (59)).

Epidemiological patterns and prevalence

Onchocerciasis is endemic in 31 countries in Sub-Saharan Africa, extending from Senegal in the west across to Ethiopia on the eastern boundary, and in two dispersed foci in two countries in Latin American, and in Yemen (60). In Africa, it is estimated that 86 million people live in high risk areas in 18 countries, with most of the high risk population found in Nigeria (26 million) and the Democratic Republic of Congo (28 million) (61). High risk areas for onchocerciasis range from small remote foci to an extensive adjoining area of more than 2 million km^2 spread across seven countries. In Cameroon, the Central African Republic, the Democratic Republic of Congo, Liberia and South Sudan, the population of high risk areas represents some 31 - 48% of the total population of the country (61). Onchocerciasis endemicity is principally determined by the ecology and behaviour of the insect vectors of family *Simuliidae*, therefore the greatest incidence of infection occurs in villages situated nearby rivers with *Simulium* breeding sites (11). All populations near vector breeding sites will be at risk, and the amount of exposure and the length of time a population is exposed will influence the progression and manifestations of the disease.

Two broad epidemiological patterns of onchocerciasis exist in Africa, blinding (savannah) and the non-blinding (forest), and the two patterns arise from *Onchocerca-Simulium* complexes where particular vector members are better adapted to transmit either the savannah or forest strains of *O. volvulus* (62, 63). The *Simulium damnosum* complex is the largest sibling species complex, consisting of morphologically similar sibling species and cytoforms (64, 65). Variations within the complex are minor but they exhibit adaptations to local conditions; the migratory *S. damnosum* subcomplex includes the species primarily responsible for transmission in savannah areas, while *S. yahense* and *S. squamosum* subspecies are more endemic to forest areas, and *S. sanctipauli* in the forest-savannah mosaic (39, 66). Some *Simulium* sp. such as *S. neavei* in East Africa do not fly far from breeding sites, while

S. damnosum in West Africa can fly long distances (400–500km) (39). The forest cytoforms of *S. damnosum* tend to have higher *O. volvulus* infection intensities compared to the savannah forms (63), and the non-blinding form of onchocerciasis prevalent in the forest belts typically manifests as severe skin disease, where skin disease and severe pruritus can affect 50% of the population in some communities (67). Blindness is relatively uncommon in the forest areas (8), whereas in savannah communities up to 10% of the population may be blind in villages hyperendemic for the savannah *O. volvulus* strain (20). Different vector species therefore differ in their ease of control and efficiency for onchocerciasis transmission.

In the Americas, active *O. volvulus* transmission is currently limited to two foci among Yanomami indigenes in crossborder areas of Venezuela and Brazil (68). Onchocerciasis was originally introduced into the region by the slave trade, and molecular studies indicate that it was the savannah strain that became established in the Americas (69). Twelve vector morphospecies, of which several are complexes of sibling species, were originally reported in Latin America (70). The most common complexes today are *S. ochraceum*, *S. metallicum*, *S. exiguum* and *S. guianenses*, although *Simulium* sp. in the Americas are less efficient at transmitting the parasite than those in Africa (71, 72). In Yemen, the disease likely has African origins and is endemic in the river valleys (Wadis) that channel into the Red Sea (39). Onchocerciasis in the region can cause a rare hyperreactive immune response in those affected, manifesting as a severe skin condition known as sowda.

Control and elimination

The Onchocerciasis Control Programme (OCP)

The first large-scale control programme for onchocerciasis spanned from 1974 to 2002 in West Africa, and was coordinated by the Onchocerciasis Control Programme (OCP) through the World Health Organization (WHO). The risk of onchocercal blindness was originally very high along the rivers in the West African savannah, and up to 50% of adults could be affected by blindness in highly endemic communities (73). River valleys were depopulated for fear of blindness, and the socio-economic importance of onchocerciasis was the primary reason for the implementation of the OCP in West Africa (74). At this time, vector control was the only intervention available. The OCP initiated large-scale targeting of the blackfly

vector breeding sites using weekly aerial insecticide spraying over fast-flowing rivers and streams (75). In 1989, the OCP was supplemented by large-scale distribution of Mectizan (ivermectin). Merck & Co., Inc generously promised to donate ‘as much Mectizan as necessary, for as long as necessary’ for the treatment of onchocerciasis (76). The OCP, in partnership with the World Bank, United Nations (UN), and later the Mectizan Donation Programme and nongovernmental organizations (NGOs), successfully controlled onchocerciasis in the savannah belt of nine of the 11 West African countries (75, 77). The programme prevented 40 million people from becoming infected, a further 600,000 people from onchocercal blindness, and protected 18 million children from the threat of the disease (77). Twenty-five million hectares of uninhabited arable land was also recovered for settlement and agricultural production, with the capacity to feed 17 million people annually (77).

African Programme for Onchocerciasis Control (APOC)

In 1995, the African Programme for Onchocerciasis Control (APOC) was launched to control onchocerciasis in endemic countries that were not included in the OCP (78). The African area outside the OCP comprised 85% of all infected people in the world at the time (8). Aerial larviciding was thought not to be technically feasible or cost-effective in this area, and therefore no control was undertaken until the introduction of ivermectin. The objective of the APOC was to support the establishment of effective and sustainable community-directed treatment with ivermectin (CDTi) in the remaining high risk endemic countries in Africa, and use vector control to eliminate onchocerciasis in certain foci (78). In the OCP costly mobile teams of health workers had been used to distribute ivermectin; however, a multi-country study in 1996 showed that CDTi was feasible, effective and sustainable (79). This novel approach to mass drug administration (MDA) was based on the concept that community drug distributors (CDDs) would be selected by the community, and then trained to distribute treatment, keep records and monitor adverse events (80).

Highly endemic countries to be targeted for treatment were mapped using Rapid Epidemiological Mapping of Onchocerciasis (REMO) (81). REMO was based on excluding areas unsuitable for the vector, and sampling 30-50 men in villages to

identify areas with a high prevalence of onchocercal nodules (81). Three classes of onchocerciasis endemicity were delineated based on the community prevalence of microfilaridermia: hyperendemic (mf prevalence > 60%), mesoendemic (mf prevalence 35% - 60%) and hypoendemic (mf prevalence <35%) (82). Higher mf burdens were associated with the more severe clinical manifestations. Mf prevalence is correlated with the prevalence of palpable nodules, therefore the onchocerciasis endemicity levels based on community prevalence of nodules in adults was extrapolated: hyperendemic (nodule prevalence > 45%), mesoendemic (nodule prevalence 20% - 45%), and hypoendemic (nodule prevalence < 20%) (83). CDTi was to be established in high risk areas where the prevalence of palpable nodules was higher than 20% in adults (84, 85). The APOC mapped infection in 20 countries (85), and managed annual treatment by CDTi in 16 countries where onchocerciasis was thought to be a public health problem (9).

From control to elimination: Guidelines

The original guidelines for certification of elimination of human onchocerciasis were published by the WHO in 2001 (86), and were used to verify the elimination of the disease as a public health problem in Colombia, Ecuador and Mexico. New guidelines were published by the WHO in 2016 (87), outlining the criteria for stopping MDA and verifying elimination of onchocerciasis following interruption of transmission of *O. volvulus*. The distribution and status of preventive chemotherapy for onchocerciasis worldwide in 2015 is shown in Fig. 1.2 (87). The WHO recommendations provide guidance on when to cease MDA initiatives and conduct post-treatment surveillance (PTS) activities. PTS is required for at least three to five years before elimination of onchocerciasis can be confirmed. Before the official acknowledgement of elimination by WHO Director General, the International Verification Team (IVT) must verify the elimination of *O. volvulus* transmission in the whole endemic country. Ongoing transmission is assessed using several methods aimed at identifying the infection and transmission potential in both the intermediate vector and the human host.

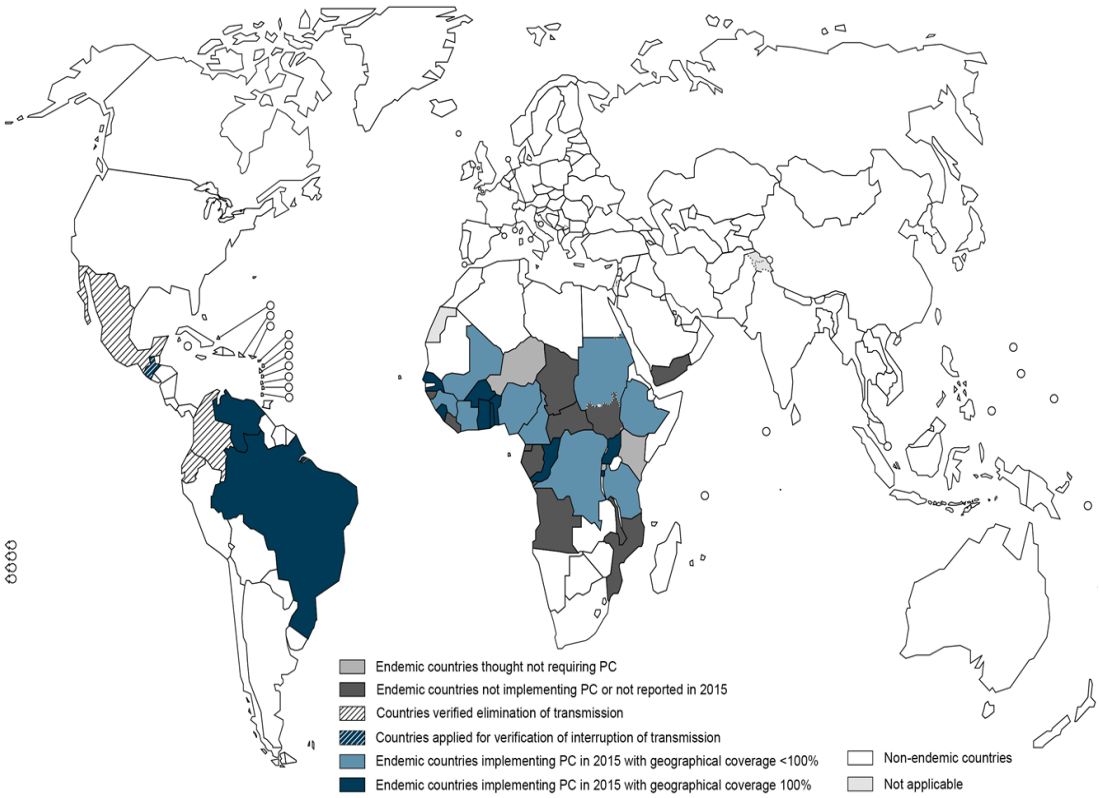

Fig. 1. 2. Distribution and status of preventive chemotherapy for onchocerciasis worldwide, in 2015 (88).

Elimination in the African Region

The APOC closed in 2015 after providing treatment through CDTi to 114 million people, covering around 60% of people who require treatment globally (60). The APOC continued to scale up the CDTi MDA campaign over its 20 years of operation, increasing coverage from 1.5 million people in 1997 to 68.4 million by 2009 (89). As evidence gathered on the interruption of transmission in some APOC areas (90-92), the feasibility of the onchocerciasis elimination in Africa came into question (93). In 2012, new goals were outlined in the WHO 2020 Roadmap for NTDs to eliminate onchocerciasis in select African countries by 2020 (10, 94), and onchocerciasis where possible by 2025 (95). With continued progress, it is estimated that onchocerciasis will be eliminated by 2020 in 12 African countries (Benin, Burundi, Chad, Kenya, Mali, Guinea-Bissau, Guinea, Malawi, Niger, Senegal, Sierra Leone and Togo) (96). With the closure of the APOC, the Expanded Special Project for the Elimination of Neglected Tropical Diseases in Africa (ESPEN) was launched in 2016 in the African Region. This programme will operate from 2016-2020 and

oversee the APOC activities. However, ESPEN has expanded to support country owned NTD programmes targeting additional infectious diseases that are responsive to preventive chemotherapy (PC): lymphatic filariasis (LF), trachoma, soil transmitted helminths (STHs) and schistosomiasis (97). The term PC encompasses the approach of treating at risk populations for human helminth diseases in order to prevent transmission of or morbidity from the infections (98). The Regional focus has now been shifted to integrated rather than vertical control of NTDs and scaling-up MDA for PC diseases (99).

Achieving the ambitious elimination goals for onchocerciasis will involve addressing a number of challenges pertinent to the 'endgame' (100, 101). Treatment with ivermectin will need to be expanded to onchocerciasis hypoendemic communities not previously targeted by the APOC, and this will require remapping areas of infection using more sensitive techniques, as nodule palpation is only reliable in highly endemic areas (99, 102). Effective geographic and therapeutic coverage and compliance is also paramount in order to sustainably break transmission (101). Despite long-term intervention efforts some areas in Africa have encountered challenges in reducing the onchocerciasis prevalence. For example, in Cameroon some communities have remained mesoendemic for onchocerciasis despite 15 years of CDTi (103), while in Ghana persistent transmission occurs despite long-term control (104). An additional barrier to treatment occurs in areas where onchocerciasis is coendemic with another filarial infection, *Loa loa,* known as loiasis or tropical eye worm, where ivermectin can cause severe adverse events (SAEs) in individuals with high levels of microfilaraemia (105). Therefore, to work towards onchocerciasis elimination in Africa will require adopting different approaches in transmission zones where transmission persists in areas under control, or are hypoendemic and where co-endemic loiasis is a risk factor (106).

Onchocerciasis Elimination Program of the Americas (OEPA) and Yemen

In 1992, the Onchocerciasis Elimination Program of the Americas (OEPA) launched with the objective of eliminating new onchocercal ocular morbidity and interrupting transmission in the Americas by 2007 (107). This public–private partnership coordinated the establishment of biannual large-scale ivermectin treatment to all the endemic areas in the region using mobile teams, with over 85%

therapeutic coverage achieved in all endemic countries (108). Onchocerciasis originally occurred in 13 discrete foci in six countries: Colombia, Guatemala, Brazil, Ecuador, Venezuela and Mexico. By 2015, transmission was interrupted in 11 of the 13 foci (109). The first country in the world to be verified and acknowledged as free of onchocerciasis by WHO was Colombia in 2013, followed by Ecuador in 2014, Mexico in 2015, and Guatemala in 2016 (60). The remaining two endemic foci are in a transmission zone, the "Yanomami area", that connects at the border of Brazil and the Bolivarian Republic of Venezuela, and includes the indigenous Yanomami people with a population of 26,715 (109). Elimination efforts are now centred on the Yanomami people with high coverage quarterly treatments to advance onchocerciasis elimination. Mf prevalence has decreased from 27.6% in 2008 to 7.8% in 2013 in the Venezuelan South focus, and from 14.7% in 2007 to 4% in 2012 in the Brazilian Amazonas focus (109).

In Yemen, there was no national control programme for onchocerciasis due to upheaval and social unrest (110). In 2016, areas of known transmission were mapped and the WHO, in partnership with the Ministry of Health and Population and other international partners, launched the first MDA with ivermectin, with the objective of eliminating onchocerciasis in Yemen (60).

Treatment for onchocerciasis

Historical treatment of onchocerciasis

One of the earliest methods used to manage onchocerciasis was the removal of superficial subcutaneous nodules, known as nodulectomy. This method was more widely practiced in the Americas where head nodules were more prevalent, and was used to reduce the risk of mf migration to ocular tissues (111). Nodulectomies are not considered efficacious for controlling transmission, as removal of nodules does not significantly alter microfilaridermia levels (112, 113) due to nodules present in deeper tissues, or remove early adult worm infections (114, 115).

Before the introduction of ivermectin in the late 1980's, the chemotherapy used for treatment of onchocerciasis was suramin and diethylcarbamazine-citrate (DEC). Suramin killed the adult and mf stages, and was administered as a single weekly injection for six weeks (116). Suramin was very toxic due to its high protein-binding affinity and alteration of enzyme function (117), and treatment could result in optic

neuropathy, nephrotoxicity, and sometimes death (118, 119). DEC was identified as a antifilarial drug in the late 1940's, and was effective for rapidly killing the mf (120). DEC was provided as a daily tablet over several weeks, and regular retreatment was required as mf would repopulate the skin over 6-12 months (121). DEC administration was associated with SAEs, known as Mazzotti reactions, which included systemic reactions occurring in multiple systems (120, 122) and ocular reactions (123-125). A more detailed overview of DEC-induced SAEs have been described by Awadzi and Gilles (122). The severity of adverse events experienced after DEC treatment is related to mf infection intensity, as the severity increases with higher numbers of mf killed (126). Attempts to reduce the toxicity of suramin and DEC, such as using lower doses and using other drugs as SAE suppressants, induced less side-effects but there was also reduced efficacy (127-129). In the 1970's, it became evident that both drugs could aggravate onchocercal eye lesions and progress ocular pathology, and their use for onchocerciasis ceased (119, 130). DEC in combination with albendazole is currently used for treatment of lymphatic filariasis, but only in areas where onchocerciasis is not coendemic (131).

Current treatment by mass drug administration

Ivermectin is the only drug used in MDA programmes for the treatment of onchocerciasis (132). It is also an effective treatment for other helminth infections, such as ascariasis, strongyloidiasis, and trichuriasis, and ectoparasites such as scabies and lice (133). In the African Region, ivermectin is given annually in CDTi programmes and semi-annually in some priority areas in West Africa (87). Treatment is a standard dose of 150 μg/kg to all adults and children over 15 kg (excluding pregnant and breastfeeding women, and the sick) (11), which has to be sustained for more than 15 years due to the long life span of the adult female parasite. Ivermectin is known as a 'microfilaricide', as it immobilises the mf by hyperpolarisation of glutamate-sensitive channels (134). The microfilaricidal effect clears the mf over days, and also exerts an 'embryostatic' effect on the adult worm, where the release of more mf is temporarily blocked (132). Early studies with ivermectin showed that 14 days after treatment, the mf densities had decreased to around 99% of pretreatment levels and this effect was sustained over one year post-treatment (135, 136). The mf are the causative agent of disease and the parasite stage taken up and transmitted by the vector; therefore, regular treatment can prevent

development of onchocercal clinical manifestations and interrupt transmission by clearing the dermal reservoir until the adult worms naturally die. Although ivermectin has been shown to have a moderate effect on the adult worms when given four times a year for consecutive years (137), most are not killed and can continue producing mf several months after treatment.

Ivermectin is a well-tolerated and safe microfilaricide; however, adverse events can occur as a result of the host response to dying mf. Adverse events are typically of the Mazzotti type, and include exacerbation of pruritus, oedema, headache, fever and sustained postural hypotension, typically within a week of treatment (138). The incidence and severity of adverse events is related to higher mf infection intensities (138), and also to the activation of innate inflammatory responses to *Wolbachia* lipoproteins released from dying mf (139).

Treatment in areas co-endemic for *Loa loa*

Complications from MDA with ivermectin can occur in areas that are endemic for onchocerciasis and another filarial worm, *L. loa*. *L. loa*, also known as tropical eye worm, is the causative agent of loiasis, an African disease that is endemic to equatorial rainforest areas of Central and West Africa (140). *L. loa* mf reside in the blood, and the adult worms reside and migrate through subcutaneous tissues (141). Although infection prevalence of *L. loa* can be very high in some communities, it is not considered a public health problem and treatment is usually not required (142). SAEs following ivermectin treatment, first reported in 1991 and during early CDTi initiatives in Cameroon, are attributable to high *L. loa* parasitaemias (> 30 000 mf/ml of blood) (143-145). SAEs include encephalopathic reactions, coma and even death (146). Ivermectin remains the treatment for onchocerciasis hyper- and mesoendemic areas that are coendemic for *O. volvulus* and *L. loa*, as the risk is considered justifiable given the health burden of onchocerciasis within communities. However, adjusted treatment strategies were outlined by the Mectizan Expert Committee (MEC)/APOC for early identification and management of SAE cases in these areas (147).

Areas at higher risk of experiencing SAEs were identified following the development of a field-applicable Rapid Assessment Procedure for Loiasis (RAPLOA) (140, 148). This method used a questionnaire centred on identifying

individuals with subcutaneous migration of adult *L. loa* under the eye conjunctiva. A strong correlation was observed between prevalence of a history of eye worm and the *L. loa* mf prevalence at the community level, and a threshold of 40% prevalence of *L. loa* eye history was set as a predictor for high risk communities. RAPLOA was adopted for large-scale mapping in 11 APOC countries that were potentially endemic for loiasis (149), and 10 countries were found to have high risk areas for loiasis, where an estimated 14.4 people live (140). However, this method is not a universal predicator for areas at high risk of SAEs, as recent studies in Bas Congo, DRC demonstrated the events were 16 times higher in medium risk areas (RAPLOA prevalence between 20 - 40%) compared to the low loiasis prevalence areas (150). In addition, for onchocerciasis hypoendemic areas not previously covered by the APOC, the extent of overlap with high risk loiasis areas, termed "hypoendemic hotspots", is not clear (151). In these areas, alternative treatment strategies will be required to meet the onchocerciasis elimination targets (105).

Alternative treatment strategies

The chemotherapy strategy currently used for treatment of onchocerciasis does not affect the adult worm reservoir within the host, and therefore regular MDA is necessary for many years. Extensive research has been undertaken to identify alternative strategies that safely target the adult worm and effectively treat onchocerciasis. Several trials have demonstrated that antibiotics, namely doxycycline, when given daily over several weeks kill the adult worms, and are 'macrofilaricidal'. The macrofilaricidal properties are due to the anti-*Wolbachia* activity of the drug, where >90% depletion of the obligate endosymbiont results in long-term sterilisation of the female worm (>24 months), and a slow and sustained killing of the adult worm population (over 20 - 27 months) (152-155). A 5-week 100 mg daily regimen (156) and a 4-week 200 mg daily regimen have comparable clinical outcomes (152), killing ~50% adult female worms. A 6-week 200 mg daily regimen has been shown to kill >60% adult female worms (152, 157) although this increases to >70% when newly acquired infections were taken into account (152, 158). Modelling approaches demonstrated that doxycycline treatment has an estimated average efficacy of 91%–94%, irrespective of the treatment regimen, and considerably reduces adult worm longevity from approximately 10 years to 2–3 years (159). The effects of doxycycline also extend to the migratory mf, where

Wolbachia depletion has been shown to impede development to the infective L3 stage in the blackfly vector (160). The slow and sustained killing of the adult worms and block in mf production delivers a markedly improved safety profile compared to other antifilarial drugs, as the parasite-mediated or *Wolbachia*-mediated inflammatory adverse events are avoided (11). A major advantage of anti-*Wolbachia* treatment, however, is that it is safe for onchocerciasis treatment in loiasis co-endemic areas (157, 161), as *L. loa* do not harbour the *Wolbachia* endosymbiont and are therefore not affected by antibiotic chemotherapy (162, 163).

While doxycycline is clearly very valuable for onchocerciasis treatment and for interrupting transmission, it is considered to be more suitable for 'test and treat' strategies, rather than community-wide MDA strategies. Limitations of doxycycline for community-based drug administration include the contraindication of treating children under 9 years of age and pregnant women, and the logistics of delivering multiple-week treatment regimens (158, 164). However, large community studies in Cameroon have demonstrated a significant proportion of communities were eligible to receive doxycycline, and of those treated there was a very high level of compliance (97.5%) to the 42 day treatment programme (161). Furthermore, the long-term effectiveness of the community-directed doxycycline treatment was demonstrated four years later, where the mf prevalence was found to be lower in those who had received doxycycline and subsequent rounds of MDA with ivermectin (17%) relative to those who had only received ivermectin (27%) (165). Alternative strategies for community treatment would be particularly useful where responses to ivermectin have been sub-optimal, such as areas in Ghana where microfilaridermia persists in 'hotspots' despite multiple rounds of treatment with ivermectin (166-168). A recent trial showed that in an area with ivermectin suboptimal response, a 6-week 100 mg daily doxycycline regimen followed by standard ivermectin treatment at 3 and 12 months resulted in 97% of patients without microfilaridermia after 20 months, while the placebo group remained at pretreatment levels (169).

A macrofilaricide that is sufficiently efficacious and can be delivered with shorter treatment regimens is highly desirable. Different chemotherapy regimens of other antibiotics, such as azithromycin and rifampicin, have also been evaluated for onchocerciasis. Azithromycin was shown not to be macrofilaricidal for onchocerciasis when studied at different doses (250 mg/day or 1,200 mg/week) and

treatment durations (five days or six weeks) (170, 171). Rifampicin was also not effective following a 5-day 20 mg/kg daily regimen (171), but macrofilaricidal activity was observed after a 2- or 4-week 10 mg/kg daily course (172). However, the 2- and 4-week rifampicin regimen was inferior to a 6-week doxycycline treatment course for onchocerciasis (172). Since 2007, the Anti-*Wolbachia* Consortium, or A-WOL (http://awol.lstmed.ac.uk/), has sought to identify new anti-*Wolbachia* drugs with shorter treatment times of a week or less, and to also optimise regimens of existing drugs and re-purposed registered drugs for use in more constricted populations (173). A recent trial showed that one of the identified drugs, minocycline, had a trend for stronger potency with a 3-week 200 mg daily minocycline treatment regimen compared to a 3-week 200 mg doxycycline regimen (absence of *Wolbachia* in female worms was 72.7% and 64.1%, respectively) (174). However, a 4-week 200 mg daily doxycycline treatment course had superior macrofilaricidal efficacy over the shorter courses of minocycline and doxycycline (absence of *Wolbachia* in female worms was 98.8%) (174). High-dose rifampicin has also shown promise in preclinical *in vivo* mouse models of *Onchocerca ochengi* adult worm infection (the closest phylogenetic relative of *O. volvulus*)(175), achieving >90% *Wolbachia* depletion with a 14-day 35 mg/kg daily rifampicin regimen (176). Rifampicin at this high dose given regularly over 2 weeks had no serious side effects associated with the treatment, and the high 35 mg/kg dose has also been shown to be safe in human trials when administered to individuals with tuberculosis (177). A-WOL has screened over 2 million compounds for *in vitro* anti-*Wolbachial* activity, the hits of which have been progressed through standard pipelines to deliver the next generation of macrofilaricide. The outputs of this approach include three new repurposing opportunities, two new drug candidates in formal development and dozens of novel lead series ready for development as macrofilaricides.

Diagnosis of *Onchocerca volvulus*

Clinical diagnosis

Diagnosing onchocerciasis can be challenging due to the accessibility of different developmental stages that occupy several tissues in the host, as well as co-infections with other filarial species with skin dwelling mf, such as *Mansonella streptocerca,* or blood dwelling mf, such as *Mansonella perstans*, found in skin snips

contaminated by blood (32). Diagnosis of onchocerciasis may be by clinical examination, which can include examining the skin for onchodermatitis (178, 179), slit-lamp examination to detect mf in the cornea and anterior chamber of the eye, and nodule palpation (102, 180). Subcutaneous nodule palpation can be used to estimate adult worm prevalence, and this was the basis of the REMO strategy adopted by the APOC to map areas that were hyper- and mesoendemic for onchocerciasis (81). However, this method lacks sensitivity in hypoendemic areas where nodule prevalence will be lower, and deeper nodules or early developing infections will be missed (102, 114), and where lymphomas and other subcutaneous structures can lead to a false positive diagnosis.

Parasitological diagnosis

The 'gold standard' in onchocerciasis diagnostics has been the skin snip to identify mf infection in the skin. The skin snip involves taking a bloodless skin biopsy and culturing the sample in saline, resulting in the migration of mf out of the tissue and into the saline. Using microscopy, infection intensity can be assessed by counting the mf, and the infection burden may be expressed as number of mf per mg of skin (mf/mg), or more precisely as mf/biopsy or mf/snip due to the variability in skin biopsy weight. The skin snip is relatively simple to perform with basic equipment, and is highly specific when used by skilled parasitologists or health workers. However, taking a skin biopsy is an unpopular, painful and invasive procedure, and not always acceptable to communities (181). People may also refuse to give multiple skin snips, and this is important for collecting longitudinal follow-up data in clinical trials and for surveillance and monitoring (90, 91). Skin snips lack sensitivity in areas undergoing MDA with ivermectin, as mf are often absent from the skin for several months following treatment (182). Skin snips are also insensitive when levels of microfilaridermia are low, such as in hypoendemic areas and during the prepatent period (the time it takes from infection initiation to mf appearing in the skin) which is estimated to be between 9 to 15 months (183). The new WHO guidelines for stopping MDA and verifying elimination of onchocerciasis recommend the use of skin snip in phase 1 (treatment phase) of elimination programmes, but not to verify elimination (87). Mf in the eyes can be detected using slit-lamp examinations (184), however after years of interventions there is now much less ocular involvement with onchocerciasis.

The DEC patch test is another means for indirectly detecting mf, and involves applying topical DEC to an area of skin to provoke a localised Mazzotti reaction. The individual is observed over 24 - 48 hours, and infection can be determined by the appearance of dermal papules (185, 186). A ready-to-use DEC containing patch (LTS-2 patch) has also recently been trialled in order to circumvent the time-consuming DEC patch preparation (187). The DEC patch has been found to be more sensitive than skin snip at low levels of microfilaridermia (188), although others have found prevalence estimates using DEC patch test were comparable to those obtained by skin snip (189). However, the DEC patch test is not specific for *O. volvulus*, and false positives can occur in individuals infected with loiasis (190). The use of the DEC patch test is also only recommended during the treatment phase of elimination programmes (87, 191).

USG as an *Onchocerca* diagnostic tool and measure of treatment response

Ultrasonography (USG) can be used to detect adult worm motility in the host through non-invasive ultrasound examination of palpable onchocercomas, and this method has been shown to be consistent and more reliable than nodule palpation for detecting onchocercomas (192). As the technique is non-invasive, this may also improve patient compliance. USG of nodules can therefore be useful for longitudinal monitoring of changes in the number and size of nodules and in adult worm motility within the host. This technique has also been used in longitudinal clinical trials to verify the impact of drug treatment on the adult worms *in vivo* (157, 192, 193). In one study analysing a subset of individuals with palpable nodules 21 months after receiving doxycycline, doxycycline + ivermectin, or ivermectin, USG examination recorded reduced parasite motility in individuals treated with doxycycline + ivermectin and doxycycline relative to the ivermectin group (157). However, USG has some limitations for measuring the macrofilaricidal treatment response. Firstly, ultrasound examination is unable to determine the number and sex of adult worms, and therefore information is qualitative only. This method is also unable to assess embryogenesis and spermatogenesis of the adult worms. USG examinations will also only identify a small proportion of worms shown to be "vital" in histology, due to either dense host tissue or because of the echo dense connective tissue around the nodule (192).

Molecular diagnosis

The sensitivity of the skin snip can be significantly improved by using polymerase chain reaction (PCR) to detect the *Onchocerca* genus-specific 150 bp tandem repeat sequence (188, 194-197). To achieve species-specificity, hybridisation with an *O. volvulus*-specific probe can also be used (198). A recent estimate of the true genome-wide copy number of the O-150 repeats in *O. volvulus* is 5,920 (199), and detection by skin snip PCR offers improved sensitivity and specificity over parasitological and immunological diagnosis methods for onchocerciasis. In addition to conventional PCR analysis, real time qPCR assays and loop mediated isothermal amplification (LAMP) methods have recently been developed for highly sensitive and specific amplification of *O. volvulus* DNA targets in skin biopsies (200-204). Limitations of the skin snip PCR include the expensive equipment and reagents, the trained personnel required to conduct the tests, and the inability to distinguish between dead or moribund mf and living motile mf. The skin snip PCR technique will also be less sensitive if microfilaridermia is very low or absent, and will therefore not be appropriate for use for a number of months following ivermectin treatment. To the best of our knowledge, O-150 has not been validated to determine treatment response to ivermectin. However, in a study assessing the O-150 qPCR assay in individuals who had recently (< 20 months), not recently (>20 months) or not been treated with ivermectin, nine individuals were positive by skin snip microscopy and 17 were positive by qPCR (202). Skin snip PCR is currently not suitable as a point-of-care diagnostic tool, and new WHO guidelines recommend that this test may be used in limited situations where a number of children are found to be positive by the *O. volvulus Ov*-16 antibody-based test (where *Ov*-16 seropositivity is >0.1%) (87). This may enable differentiation of actual infection from antibody exposure to the parasite in sentinel populations.

PCR for detection of *O. volvulus* DNA can also be used for xenomonitoring of the black fly vector population (205). Entomological evaluation by O-150 PCR aims to determine the prevalence of the infective-L3 stage by pool-screening hundreds of blackfly heads using an *O. volvulus*-specific O-150 DNA probe (206, 207). Molecular xenomonitoring has been used to assess infection transmission dynamics after years of ivermectin control in Latin America (208-210) and some areas in Africa (90, 91). More recently, an isothermal LAMP assay (211) and a non-

instrumented nucleic acid amplification (NINA)-LAMP assay have been developed for detection of parasite DNA in the vector (212). A speciation assay has also been developed based on differentiation between *O. volvulus* and *O. ochengi* mitochondrial DNA sequences, which can be used in high-throughput high-resolution melt (HRM)- as well as lower throughput conventional restriction fragment length polymorphism (RFLP) analyses (213). Entomological assessment of the infective *Simulium* population by PCR is a recommended diagnostic tool for use in onchocerciasis elimination programmes, and flies should be collected when they will be most abundant (during daylight hours and during the peak transmission season) (87). Following evaluation by PCR, an upper limit of the 95% confidence interval for the prevalence of flies with infective L3 larvae should be less than one infected black fly in 1000 parous flies (<1/1000), equating to less than a 0.1% prevalence, or one infected black fly in 2000 flies tested, equating to less than a 0.05% prevalence (87). Limitations of xenomonitoring by PCR include the challenge of collecting a large number of black flies sufficient to represent the potential infective vector reservoir, the cost of molecular supplies and equipment for PCR, and trained personnel to conduct the tests. The presence of other species of *Onchocerca* in the blackfly vectors may also confound molecular testing for xenomonitoring if an *O. volvulus*-specific probe is not used to detect the O-150 DNA sequence.

Antibody detection tests

Much of the initial effort to develop immunodiagnostics for onchocerciasis focussed on antibody detection assays, as attempts to produce antigen detection tests were largely unsuccessful (214). The early serological tests involved developing antibody detection assays using *O. volvulus* parasite extracts, however this was encumbered by the need to obtain adult worms from nodules since there was no suitable laboratory host (214). Most of the assays using native material from *O. volvulus* (215-217), or closely related *Onchocerca* species (218), as well as alternative filarial worms that could be laboratory cultured (219, 220), were highly sensitive but lacked specificity for onchocerciasis. The development of recombinant *O. volvulus* antigens, such as *Ov*33 (221) and *Ov*16 (222), enhanced the specificity of onchocerciasis diagnosis relative to native antigens. However, sensitivity for detecting infection using individual recombinant antigens varied, and so to improve

the sensitivity a cocktail of recombinant *O. volvulus* antigens was employed (223-226). A multicentre trial was initiated by the WHO's Special Programme for Research and Training in Tropical Diseases (WHO/TDR) to test a panel of antigens for sensitivity and specificity (227), and three were selected (*Ov*16 (222, 228), *Ov*7 (229) and *Ov*11 (230)) as the preferred antigen cocktail. Although the antigen 'tri-cocktail' had an epidemiological sensitivity of 70–80% (depending on the area), and a specificity of 96–100%, enzyme-linked immunosorbent assay (ELISA) was the basis for onchocerciasis antibody detection, and the test was not adopted for routine operational use (20, 231).

*Ov*16 antibody detection tests

The specificity of onchocerciasis immunodiagnosis was further improved by assessing the IgG_4 antibody subclass rather than total IgG (232, 233). In particular, the detection of IgG_4 antibodies to the recombinant *O. volvulus* antigen *Ov*16, to which antibodies develop during the pre-patent period of infection (228), has been the most widely used and employed in a number of immunoassay formats. Using a cocktail of antigens that were also available alongside the anti-*Ov*16 assay did not improve the performance of the test (234). A lateral flow rapid-format card test for detection of anti-*Ov*16 IgG_4 was developed in 2000 and later assessed for field use (235, 236), but the test was never commercialised. An anti-*Ov*16 ELISA has been operationalised as a serological surveillance tool for routine evaluations in Latin America (237-239), and in some countries in Africa (240-242). Guidelines for using serological evaluation for elimination involves assessing infection exposure in children under 10 years in sentinel populations to identify areas with ongoing transmission (87). The sample cohort should be representative of the entire transmission zone, and a sample size of 2000 children is recommended to assess whether the prevalence is $\leq$0.1 % at the upper bound of the 95% confidence interval (87, 240). The 0.1% threshold was extrapolated from experience in OEPA areas, however, it is not technically feasible to measure the 0.1% threshold prevalence specified by the elimination guidelines as the *Ov*16 serology tests are not 100% specific (234). Several different versions of the *Ov*16 ELISA are currently in use, and in hyper and mesoendemic areas the *Ov*16 ELISA has a high sensitivity (80-90%) and up to 99% specificity. However, the lower sensitivity of the ELISA increases the sample size that is required, for example a test that is 80% sensitive

would mean a 25% increase in the sample size, and without 100% test specificity representative areas would rarely ever make the 0.1% cut-off (234). Representative areas for transmission assessment may also not meet the current specified sample size of 2000 children.

More recently, a rapid diagnostic test (RDT) using recombinant *Ov*16 to detect IgG_4 antibodies was developed (243), and is now commercially available as a point-of-care RDT for field use (Alere SD BIOLINE Onchocerciasis IgG_4 Rapid Test, Suwon, Republic of Korea). However, it will be important to compare the performance of the RDT to the ELISA format before operationalising the RDT for use in programmatic decision-making regarding onchocerciasis elimination. Although the RDT has been compared to the ELISA using samples where the infection status is known and in a programmatic setting in Togo (234, 244, 245), the *Ov*16 antibody tests have primarily been assessed in populations with high onchocerciasis prevalence. In hyperendemic and mesoendemic areas, the RDT had a sensitivity of ~80% for detecting people with mf positive skin snips; however, in untreated hypoendemic areas and in hyperendemic areas that had been treated for some time, the RDT had a sensitivity of 40-60% for detecting people with mf positive skin snips (234). Similarly, the RDT's sensitivity compared to the ELISA was over 90% in samples from people where infection status was known, but was 40-65% in samples from low or suppressed transmission areas (234). A recent study that compared onchocerciasis diagnostic tests in a setting in Tanzania that has suppressed transmission reported that based on a randomised, age-stratified analysis, the *Ov*16 antibody RDT was positive in 38 (5.5%) participants, with 1 (0.5%), 1 (0.4%), and 2 (0.8%) children aged 0-5, 6-10, and 11-15 years, respectively (246). The authors concluded that although MDA in this area had had a significant impact on transmission, the specificity of the test could result in a number of false positives identified, such that the area would have failed to meet WHO criteria for stopping MDA in this instance (246). The guidelines issued by the WHO recognise that evidence for the usefulness of the *Ov*16 immunoassays to assess interruption of transmission is still limited, and an operational research priority is the validation of *Ov*16 RDT (87). Additional uncertainties highlighted in the new WHO guidelines regarding the use of *Ov*16 serology in elimination settings include the need to better understand the dynamics and sero-reversion rate of the *Ov*16 antibody response.

Onchocerciasis diagnosis via antibody profiling has proven useful as a surveillance tool for assessing infection prevalence in untreated communities, as well as for monitoring elimination programs in Latin America working to interrupt transmission. The major shortcoming of antibody-profiling assays is that due to the long half-life of antibodies, antibody detection tests are unable to distinguish between past and current infections (247). In addition, diagnosis of ongoing transmission using *Ov*16 serology will miss those individuals who do not mount a detectable antibody response against the *Ov*16 antigen (248).Therefore, alternative diagnostic tests that are able to detect *active* infection with *O. volvulus* adult worms are required to distinguish new patent and ongoing infections from historical infection exposure.

Biomarkers for living adult *Onchocerca volvulus*

A circulating biomarker for *O. volvulus* that could be used to detect active infection or determine infection intensity would be highly advantageous over the currently available diagnostic tools for onchocerciasis. The onchocercomas where adult worms reside are highly vascularised (249, 250), and therefore parasite antigens, metabolites, RNA and DNA may all be present in the host circulation as markers of infection. The progression from an onchocerciasis control to an elimination programme in Africa poses additional challenges for disease diagnosis, as well as for community wide surveillance and evaluation of ongoing infection transmission or recrudescence. As declining levels of disease endemicity no longer prove to be cost-effective for current MDA-based strategies, 'end-game' scenarios will be dependent upon continued surveillance and case management by 'test and treat' strategies. For those areas that will no longer require MDA, over-prescribing drugs wastes resources. Therefore, diagnostic tools with high sensitivity and specificity for active *O. volvulus* infection are required to accurately map hypoendemic areas with low levels of ongoing transmission, and make informed decisions regarding treatment provision and intervention cessation. In addition, an *O. volvulus*-specific marker of the adult worms would be valuable for quantifying treatment efficacy for both established and new candidate drugs, and for monitoring patient drug response (251).

Circulating antigen detection tests for onchocerciasis were first described in the early 1980s (252, 253), and development of diagnostic tools to identify adult *O. volvulus* infection has continued to be an active area of research ever since. The earlier antigen detection assays lacked the necessary sensitivity and specificity for a diagnostic test, and were directed towards unknown antigens (252, 253). Later tests showed more promise, with one study reporting the use of indirect ELISA to detect *O. volvulus* antigen in serum and urine with sensitivities of 92.3% and 85.9%, respectively (254). The positivity of this ELISA with both serum and urine also correlated well with mf densities in skin. However, the specificify was not determined, and the antiserum used in the ELISA was raised against a crude soluble antigen extract, and so there may be cross-reactivity due to multiple binding sites for similar epitopes found in other parasitic worms (214). Other *O. volvulus* antigen detection assays for serum have also been susceptible to high false positive rates (255) and cross-reactivity with other geographically relevant filarial parasites (such as *L. loa* and *M. perstans*)(256). Therefore, while several immunoassays have been developed and tested (252-257), none were progressed for specific and sensitive diagnosis of onchocerciasis.

For lymphatic filariasis, a sensitive immunochromatographic test (ICT), the Alere Filariasis Test Strip, is used in the Global Programme to Eliminate Lymphatic Filariasis (GPELF) to qualitatively or semi-quantitatively detect the circulating filarial antigen (CFA) of *W. bancrofti* (258-260). Levels of CFA can be quantified using the Trop-Ag ELISA kit (TropBio, Townsville, Australia). A sensitive ICT for detection of circulating filarial antigens from the dog heartworm, *Dirofilaria immitis*, is also available (261). Several longitudinal macrofilaricidal drug trials have demonstrated a significant decline in CFA levels over the months and years following macrofilaricidal treatment (262-265). Furthermore, studies have shown that the levels of filarial antigens may correlate to the adult worm infection intensity (266-268) and to mf densities in the blood or skin (254, 260). Circulating filarial markers can therefore be used to determine infection prevalence, infection intensity and treatment efficacy. A similar rapid format diagnostic test for active *O. volvulus* infection that demonstrated a significant, reproducible, dynamic alteration following elimination of adult worms is highly desirable.

Recent advances in technology platforms for biomarker discovery

Proteomics

Increasingly sophisticated omics-based methods are currently being used to identify biomarkers of *O. volvulus* infection. The availability of filarial worm genomes and advances in transcriptomics and proteomics will help elucidate the unique biology of the parasite and interaction with the human host, and aid in identifying novel targets for onchocerciasis diagnosis. High-quality genome assemblies with reconstruction of whole chromosomes were obtained for *O. volvulus* in 2016 (199). In the same year, transcriptomic and proteomic profiles of both *O. volvulus* and its *Wolbachia* endosymbiont in the intermediate vector and human host stages were also published (269). This included L1, L2, L3, moulting L3, L4, and adult male and female stages, which enabled identification of stage-specific pathways important for the parasite adaption in the human host. Additionally, new biomarkers of *O. volvulus* patent infection were identified by using immunomics (270) to profile host antibody responses from well-characterised human samples to a protein array generated from 397 parasite stage-specific proteins (269). This study reported seven novel antigenic *O. volvulus* biomarkers from IgG_4 responses in infected individuals, one of which, OVOC10469, has been tested and validated in a luciferase immunoprecipitation system (LIPS) immunoassay (269). An integrated multiomic-based approach using data from the *O. volvulus* genome, proteome, and transcriptome has also led to the identification of novel antigens as candidates for serodiagnosis of onchocerciasis (271). Of the 241 immunoreactive proteins detected, many of the major diagnostic antigens over the past 25 years were included, in addition to 33 new proteins.

Metabolomics

Metabolomics is another technology that has shown promise for identifying small molecules, or metabolites, of *O. volvulus* infection. Metabolomics using mass spectrometry (MS)-based approaches enables nonbiased analysis of all the molecules that are present in the host body fluids by aligning against libraries of known biochemicals (272). Metabolite profiling, in which a smaller subset of metabolites are measured, may then be used to measure potential biomarkers of infection (273). For onchocerciasis, metabolite profiling of infection-associated markers in human

plasma and serum has identified metabolites that are able to discriminate between infected and non-infected individuals (273, 274). In one study, the use of a discovery liquid chromatography-MS (LC-MS) based approach identified a set of molecules that, in combination, deliver a statistically relevant characteristic of onchocerciasis infection (273). The African sample set, consisting of 73 serum and plasma samples, enabled the discovery of a set of 14 biomarkers that could discriminate between *O. volvulus*–positive and negative individuals by multivariate statistical analysis. A more recent metabolomic analysis analysed the serum metabolic profiles of 10 *O. volvulus*-infected and 10 uninfected individuals, which identified 286 known metabolites, as well as putative metabolites based on KEGG, HMDB and HMT databases (274). Their non-targeted metabolomic approach produced a global view of the metabolic variations that occur in individuals infected with *O. volvulus*, and enabled the discovery of important metabolites and associated pathways that could be useful as biomarkers of onchocerciasis (274).

Metabolomic analysis of urine from onchocerciasis infected individuals has additionally identified the biomarker N-acetyltyramine-O,β-glucuronide (NATOG), a neurotransmitter-derived secretion metabolite from *O. volvulus* (275). NATOG has been detected at a significantly reduced concentration in urine from individuals tested 20 months post-doxycycline treatment compared with untreated *O. volvulus*-positive patients and placebo-treated patients (275), and found to be detectable before the appearance of mf in jirds infected with the onchocerciasis model nematode *Litomosoides sigmodontis* (276). The diagnostic utility of NATOG has also recently been evaluated in two separate studies (277, 278). In one report, an assessment of NATOG specificity revealed that NATOG values were found to be elevated in mono- and co-infection (*L. loa* and *Mansonella perstans*) samples only in the presence of *O. volvulus* (277). The authors proposed NATOG as a biomarker for tracking active onchocerciasis infections, and provided a threshold concentration value of NATOG for future diagnostic tool development (277). However, in a separate evaluation, Lagatie and colleagues reported on the limited diagnostic applicability of NATOG due to the lack of discrimination between nodule-positive amicrofilaridermic individuals and the control groups (278).

Metabolomics could be a useful alternative to protein-based diagnostics due to the very limited half-lives of metabolites and because they are the result of

combinatorial effects of the genome, the transcriptome, the proteome and the environment (274). Biomarker identification from metabolomic analyses is challenging however, due to the constant dynamic changes of the metabolites, small intermediates, or end products of enzyme-catalysed biochemical reactions (274). Plasma and serum of uninfected and infected hosts have also been analysed for nematode-specific phospholipids, however analysis of the host phospholipid profiles showed that parasite phospholipids were below the limit of detection (279).

Parasite-derived microRNAs

More recently, small RNA markers for onchocerciasis have become an area of diagnostic interest. The most extensively studied small RNAs include microRNAs (miRNAs), small interfering RNAs (siRNAs), and piwi-interacting RNAs (piRNAs) (280); however, in parasitic worms particular attention has been given to miRNAs. MiRNAs are small (~22 nt in length) non-coding RNAs that function as post-transcriptional gene regulators, typically by inducing gene silencing of their target (281). The miRNA–target interaction is initiated by the 'seed' sequence, which consists of nucleotides 2–7 at the 5′ end of a miRNA (282). MiRNA populations have been identified in at least 35 species of parasitic helminths (283), and have been implicated in several important physiological processes such as development, differentiation and homeostasis, and possibly drug resistance (284). Parasite miRNAs may also have potential roles in host-pathogen interactions and immune regulation (285-288). Many miRNA families are highly conserved with homologues in nematodes (289), however some have been found to be filarial specific (289) and unique to a species (290, 291). Furthermore, both gender- and stage-specific miRNA expression in parasitic worms has been observed (289, 290, 292, 293). MiRNAs in parasitic helminthiases have recently been reviewed by Cai *et al* (283).

Parasite-derived miRNAs have been identified in the host biofluids for a number of parasitic nematodes, including filarial worms such as *O. volvulus, O. ochengi, L. loa, D. immitis, Brugia pahangi* and *L. sigmodontis*, and trematodes, *Schistoma japonicum* and *Schistoma mansoni* (251, 287, 291, 294-297). MiRNAs are also present in mammalian extracellular body fluids such as plasma, where they are believed to be particularly stable due to their association with specific proteins or by encapsulation in small lipoprotein vesicles (298, 299). Host miRNAs have been

proposed as potential markers of parasite infection due to the correlation between the status or progression of various diseases and miRNA dysregulation (300, 301). The potential of circulating host miRNAs as biomarkers has been investigated with infections of *S. japonicum* (302, 303), *S. mansoni* (295), and *Opisthorchis viverrini* (304, 305), although with mixed results. For example, while one group found that levels of the host miRNA miR-192 in serum could potentially be a biomarker and prognostic indicator for *O. viverrini*-induced cholangiocarcinoma (ICC) (304), another study that identified a panel of eight miRNAs associated with *O. viverrini*-ICC in plasma did not include miR-192 in their panel (305). The host miRNA miR-223 has also been put forth as a potential circulating biomarker for infection with *S. japonicum* (302); however, higher levels of miR-223 in the circulation may also be indicative of other conditions, such as gastric cancer (306).

With respect to onchocerciasis, six putative *O. volvulus* miRNAs have been identified in host plasma using Illumina high-throughput sequencing (291), two of which, miR-71 and lin-4, were present in plasma from infected individuals living in Cameroon. In another study, 21 miRNA candidates predicted to be released by *O. volvulus* were discovered through sequencing and bioinformatic analysis of onchocerciasis-infected sera (251). However, there was no overlap in the parasite miRNAs identified in the two studies, and the 21 putative *O. volvulus* miRNA identifications by Tritten *et al* (251) were questioned by Quintana *et al* (291). In the study of Quintana and collegues, the reads of nucleotide (nt) sequences detected and aligned to the *O. volvulus* genome were present in ≥ 2 copies to avoid analysis of sequencing artefacts, and only reads >16 nt were analysed in line with the default criteria of miRdeep2 alignments. Following further bioinformatic analysis of miRNA content, sequence reads had to map perfectly to the genome and be 18 to 30 nt in length to be included for analysis. Quintana *et al* (291) criticised the findings of Tritten *et al* (251), as 13 of the 21 reported miRNAs were < 17 nt long or detected in only one read, and therefore did not meet their more stringent analysis criteria. Additionally, a further three sequences were found to perfectly align to human ribosomal RNA, and two were identified as part of longer sequences in European control serum. Therefore, miRNAs specific to *O. volvulus* have yet to be confidently identified in the host. Although several studies have demonstrated the conserved nature of RNA secretion/excretion by nematodes (251, 287, 291, 296, 307), the

identification of novel miRNAs from *O. ochengi* in nodule fluid holds promise that *O. volvulus*-specific miRNAs may also be present in the blood (291).

Circulating biomarkers for adult *Onchocerca volvulus*: A rationale

While several interesting protein, metabolite and nucleic acid candidates have been identified using various technologies, no potential biomarkers identified in recent years have yet been progressed to diagnostic development for field use. Additionally, all studies have identified the potential *O. volvulus* biomarkers in the host by testing infected vs uninfected cohorts. Therefore, aside from the metabolite NATOG, whether any of the markers could be used to monitor treatment efficacy or patient drug response is unknown. The ideal circulating diagnostic marker for *O. volvulus* would be specific and sensitive for active adult worm infection, in addition to tracking the progressive impact of treatment and control strategies on the adult worm population within the host.

We possess a unique plasma sample set collected sequentially from patients enrolled in a randomised double-blind phase II trial conducted in Cameroon over a two year period (157). Treatment arms consisted of macrofilaricidal (doxycycline), microfilaricidal (ivermectin), or a combination of the two treatments, and this sample set includes supporting parasitological and clinical data on treatment outcome. In addition, the trial undertook parasitological screening for coinfective filarial parasites *L. loa* and *M. perstans*. This sample set could be used to discover circulating markers of onchocerciasis infection and treatment efficacy, by identifying markers present at baseline in plasma that dynamically change in abundance or prevalence over time following antifilarial therapy. Proteomics provides a promising platform for the discovery of circulating biomarkers in human plasma, and several novel circulating *O. volvulus* antigens have recently been identified using proteomic analyses of infected vs uninfected cohorts (269, 271). The plasma proteome also mirrors the physiology of an individual, representing a dynamic reflection of both genes and the environment (308). The proteome is probably the most ubiquitously affected in disease, response and recovery (309), and an affluence of proteins are introduced into the circulation from tissue leakage and foreign proteins introduced by microorganisms (310). Although based on a high technology platform, high-depth coverage discovery proteomics, followed by high-throughput selected reaction

monitoring (SRM) for verification of potential candidates, could enable the progression of potential biomarkers to immunoassay-based validation (311). Proteins are therefore also a practical target, as they more tractably translate into a point of care diagnostic format e.g. antigen detection test.

As a comparative study of other potential biomarkers in our unique sample set, parasite nucleic acids could also be investigated as circulating markers of infection and treatment efficacy. Detection of parasite-derived miRNAs would verify active infection in the host, and preliminary studies have also shown that miRNAs originating from *S. mansoni* enabled the differentiation between uninfected and infected serum in humans (295). Although the *O. volvulus* miRNAs sequenced from host biofluids have been inconsistent between studies (251, 291), miR-71 and lin-4 have been identified in a number of host-parasite models, and therefore appear to be more reliable as secreted/excreted parasite miRNA candidates. Detection of conserved circulating *O. volvulus*-associated miRNAs would provide information on the diagnostic potential of parasite-derived miRNAs for onchocerciasis. Detection of the *O. volvulus*-specific O-150 DNA repeat sequence in the host circulation would also be advantageous over current diagnostics tests such as the skin snip-PCR, which is insensitive for months following microfilaricidal treatment and involves obtaining painful invasive skin snips. In *O. volvulus*, the genome-wide copy number of the O-150 repeats has recently been estimated to be 5,920 (199), increasing the likelihood of detecting the sequence in the host circulation. The detection of circulating O-150 may enable diagnosis of active infection by adult worms irrespective of mf status, and the levels of circulating parasite DNA may provide an indication of adult infection intensity.

Following identification of protein markers of *O. volvulus* infection and infection clearance in a unique longitudinal plasma sample set, protein candidates with the necessary sensitivity and specificity could be progressed for diagnostic development for use in onchocerciasis 'end game' strategies, where diagnostic tests of adult worm infection are a high priority for programmatic support for disease elimination. The assessment of circulating parasite nucleic acids will also provide additional information on the potential of alternative diagnostic tools for onchocerciasis.

Project aims

This thesis aims to investigate whether proteomic analysis of plasma from onchocerciasis-infected individuals can identify circulating protein markers of active adult worm infection. Potential diagnostic biomarkers were analysed to determine any dynamic change in abundance or prevalence following treatment with doxycycline over a two-year follow-up period in a subset of five patients. Further studies compared potential *O. volvulus* miRNA and DNA biomarker dynamics in an expanded plasma sample set from 18 trial participants treated with doxycycline, ivermectin or a combination of both.

The aims of this project can therefore be summarised as:

1. To develop a proteomic workflow that will reduce the redundancy in plasma proteome analysis by discovery liquid chromatography tandem mass spectrometry (LC-MS/MS), in order to improve the depth of plasma proteome coverage and improve detection of less abundant circulating parasite and host proteins.

2. To use the proteomic workflow and shotgun LC-MS/MS to analyse a unique longitudinal plasma sample set and identify circulating protein markers of active onchocerciasis infection, and then track the dynamic changes in protein abundance and prevalence over time to identify markers of adult worm death and treatment efficacy.

3. To determine the suitability of selected parasite-derived miRNAs and DNA as potential biomarkers of active onchocerciasis, and determine any dynamic change in their abundance and prevalence following treatment.

Chapter 2. Methods

Methodology

This chapter details the complete methodology for all the experiments conducted and presented in this thesis. In subsequent individual experimental chapters (Chapters 3 - 5), the methods that are relevant to each chapter are briefly outlined, which refer back to the methodology provided in this chapter.

Reagents and equipment

The powder and liquid laboratory supplies that were used in experimental work and their sources are listed in Table 2.1. All reagents and equipment were maintained in the conditions recommended by the manufacturer's storage instructions.

Type	Product	Company
Powder	Glycine	Sigma-Aldrich
	Tris Base (Tris, or Trizma)	Sigma-Aldrich
	Sodium dodecyl sulfate (SDS)	Sigma-Aldrich
	Ammonium persulfate (APS)	Thermo Scientific
	Ammonium bicarbonate (AmBic)	Sigma-Aldrich
	Dithiothreitol (DTT)	Bio-Rad
	Iodoacetamide (IAA)	Sigma-Aldrich
	Tryptic digest bovine serum albumin (BSA)	Bruker
	MassPrep *Escherichia coli* digestion standard	Waters
Liquid	Ethanol	Sigma-Aldrich
	2-Propanol (isopropanol)	Sigma-Aldrich
	30% Acrylamide-Bis solution	Bio-Rad
	N,N,N′,N′-Tetramethylethylenediamine (TEMED)	Sigma-Aldrich
	Acetonitrile (ACN)	Sigma-Aldrich
	0.1% (v/v) formic acid (FA)	Pierce
	HPLC-grade trifluoroacetic acid (TFA)	Sigma-Aldrich
	HPLC-grade H_2O	Sigma-Aldrich
	RNaseZap	Thermo Scientific
	Distel laboratory disinfectant	Starlab
	Nuclease-free H_2O	Ambion
	TE Buffer pH 8.0	Integrated DNA technologies

Table 2. 1. List of powder and liquid laboratory supplies used and their sources.

The solutions and buffers prepared in the laboratory are provided in Table 2.2. Double distilled water (d.H_2O) was made in-house and dispensed from specialised laboratory taps. An UltraBasic UB-10 benchtop pH meter (Denver Instruments) was used to measure and adjust pH, and the pH of solution was altered using either HCl or NaOH. Other 'specific-use' laboratory reagents, kits, equipment and software and the suppliers are detailed in the relevant methods subsections described below. All protein-containing samples were stored in Protein Lo-Bind microcentrifuge tubes (Eppendorf), and all nucleic acid-containing samples were stored in DNA Lo-Bind microcentrifuge tubes (Eppendorf).

Solution name	Components	Concentration	Amount	Adjustment
Resolving gel	30% Acrylamide/Bis solution Tris SDS d.H_2O APS TEMED	37.5:1 1.5 M 20% (w/v) 10% (w/v) 	4 ml 2.5 ml 50 µl 3.4 ml 75 µl 7.5 µl	Tris was first adjusted to pH 8.8
Stacking gel	30% Acrylamide/Bis solution Tris SDS d.H_2O APS TEMED	37.5:1 0.5M 20% (w/v) 10% (w/v) 	0.65 ml 1.25 ml 50 µl 3.025 ml 25 µl 2.5 µl	Tris was first adjusted to pH 6.8
10 x running buffer	Tris Glycine SDS d.H_2O	250 mM 1.92 M 1% w/v 	30 g 144 g 10 g ~1 L	
Running buffer	10 x running buffer d.H_2O	1 x 	100 ml 900 ml	
70% Ethanol	Ethanol d.H_2O	70% (v/v) 	700 ml 300 ml	
High pH elution buffer	Glycine d.H_2O	100 mM 	375 mg ~50 ml	Glycine solution was adjusted to pH 2.5

Low pH elution buffer	Glycine d.H_2O	100 mM	375 mg ~50 ml	Glycine solution was adjusted to pH 10
Destaining solution	CAN AmBic	100% 25 mM	500 ml 500 ml	
*Reduction solution	DTT AmBic	60 mM 25 mM	1.5 mg 1 ml	
*Alkylation solution	IAA AmBic	170 mM 25 mM	10 mg 1 ml	
Trypsin stock solution	Trypsin AmBic	 25 mM	20 µg 100 µl	
+RapiGest	RapiGest AmBic	 25 mM	1 mg 100 µl	
+Reduction solution	DTT AmBic	60 mM 25 mM	9.2 mg 1 ml	
+Alkylation solution	IAA AmBic	170 mM 25 mM	33 mg 1 ml	

Table 2. 2. Buffers and solutions made in the laboratory.

*For use with in-gel tryptic digestion method.

+For use with in-solution tryptic digestion method.

Human plasma

European control plasma

For protein-based experiments in Chapter 3, the uninfected control plasma was lyophilised plasma (Sigma-Aldrich), prepared by the manufacturer from pooled human blood with 4% trisodium citrate as the anticoagulant. Plasma was reconstituted in d.H_2O to the specified volume and aliquoted out for storage at -20 ^oC. For molecular experiments in Chapter 5, plasma from an individual was obtained through the national health service (NHS, UK) and aliquoted out for storage at -20 ^oC until use. An alternative plasma source was obtained as the lyophilised plasma was found to have lower levels of extracellular nucleic acids relative to plasma of trial participants. Frozen plasma was thawed gently on ice before use. For all experiments, plasma samples were initially centrifuged at 16 000 x g for 5 min to pellet insoluble material.

Onchocerciasis-infected plasma

Plasma from individuals infected with onchocerciasis were obtained from a double-blind, randomised, phase II field trial conducted over two years in Cameroon (157). The trial was community based and was conducted in six satellite villages (Bifang, Ebendi, Eka, Ngalla, Dinku and Olurunti) in Widikum, in the North West Province of Cameroon (situated between latitude 5^{o} N 43–5^{o} N 54 and between longitude 9^{o} E 41^{o} E 44). The trial commenced on the 1st July 2003 and concluded on the 31st March 2005. At the time of the trial, the area was hyperendemic for onchocerciasis with a community prevalence of *L. loa* ranging from 3.36%–14.29% (312). Eligibility criteria for inclusion comprised: *O. volvulus* microfilaridermia >10 mf/mg, adults aged 15 – 60, a minimum body weight of 40 kg, and in good health. Exclusion criteria included: *L. loa* microfilarial load >8000 mf/ml, irregular range for hepatic and renal enzymes (AST and creatinine [3–126 µmol/l]), pregnancy, lactation, ivermectin intolerance, alcohol or drug abuse, or anti-filarial therapy in the last 12 months. Enrolled individuals were assigned to one of three drug regimens:

(i) DOXY: Doxycycline (2 × 100 mg capsules daily) for six weeks plus non-matching ivermectin-dummy pill at month four (lactose tablet).

(ii) DOXY+IVM: Doxycycline (2 × 100 mg capsules daily) for six weeks plus ivermectin (150 µg/kg oral dose) at month four.

(iii) IVM: Matching doxycycline-placebo for six weeks plus ivermectin (150 µg/kg oral dose) at month four.

Blood plasma was collected in BD Vacutainer® EDTA blood collection tubes from the trial participants at baseline and then at four, 12 and 21 months after the start of DOXY or DOXY-placebo treatment. At each time point, *O. volvulus* microfilaridermia was assessed by obtaining two skin snips of approximately 1 mg and immersing them in saline overnight. The next day, saline samples were moved to glass slides for microscopy, and the total number of liberated mf were counted to obtain the average number of mf/snip. At the final follow-up post-treatment, a subset of participants from each treatment group had palpable nodules removed. Further details on the methodology can be found in the study report (157). In brief, worm death was verified by evidence of calcification without cuticle or near complete adsorption, body wall had loss of integrity, absence of nuclei and absence of *O. volvulus* lysosomal aspartic protease (APR) staining.

Some of the enrolled participants had or developed co-infections with *L. loa* and *M. perstans* over the duration of the trial. Coinfections with other filarial worms were assessed by collecting 50 µl finger prick blood at each sampling time point and preparing thick blood smears to count the numbers of *L. loa* and *M. perstans* mf using microscopy.

Plasma samples selected for use in this thesis were from participants infected only with *O. volvulus* by parasitological examination*;* however, we cannot rule out that the individuals selected did not have occult loiasis and/or mansonelliasis. Parasitological information for the individuals is provided in the relevant chapters. Plasma from the trial participants was stored at the Liverpool School of Tropical Medicine (LSTM) at -80 ^{o}C, and gently thawed on ice before use. For all experiments, plasma was centrifuged at 16 000 x g for 5 min to remove insoluble material prior to any experimental work.

Ethics statement

The experimental protocol for the trial from which the human plasma was obtained was designed in accordance with the general ethical principles outlined in the Declaration of Helsinki. The trial was approved by ethics committees of the Tropical Medicine Research Station, Kumba and the Research Ethics Committee of The Liverpool School of Tropical Medicine. The trial is registered with the current controlled trials registry, no: ISRCTN48118452.

Proteomic techniques

Determining protein concentration

The protein concentration of plasma samples was determined using the BCA Assay (Pierce), following the manufacturer's instructions. Briefly, neat or diluted samples were added to a 96 well plate (Nunclon) in duplicate at a 10 or 25 µl volume, before addition of 200 µl of BCA working reagent (WR) to give a ratio of 1: 20 or 1:8 sample:WR, respectfully. To determine protein concentration, a standard curve of protein (BSA) diluted in the same diluent as the sample was included on each plate. After an incubation at 37 °C for 30 min, a plate-reader was used to measure absorbance at 562 nm. A standard curve was generated using the

absorbance values from the diluted standards, and from this the protein concentration in the sample wells could be calculated. Additionally, a NanoDrop™ spectrophotometer (Thermo Scientific) was used to cross-validate the protein concentrations obtained with the BCA assay for samples with low protein concentrations, or when a sample was stored in a buffer (glycine elution buffers) that interfered with the BCA Assay absorbance measurements. Protein concentrations were measured at A280 nm absorbance by initial blanking of instrument using the same buffer as the sample, followed by addition of 2 µl of sample in triplicate to obtain the average concentration from the three absorbance readings.

Preparation of SDS-polyacrylamide gels

One-dimensional sodium dodecyl sulfate polyacrylamide gels (1D SDS-polyacrylamide gels) at 12% (w/v) were hand-cast, according to Laemmli (247). Gel casting stands and casting frames from the Mini-PROTEAN Tetra Cell Casting Module (Bio-Rad) were used to prepare the gels. The resolving gel was prepared fresh (see Table 2.2. for solutions used) and poured to fill 2/3's of the glass plate, followed by addition of d.H_2O for the remaining 1/3 of the plate. The gels were left to polymerise for one hour wrapped in cling film. Stacking gel was prepared fresh, and the solution was mixed thoroughly before pouring over the set resolving gel fraction. A 1.0 mm comb was inserted in the stacking gel, and the gel was left to polymerise for one hour. Gels could be stored in d.H_2O for several days prior to use.

1D SDS-PAGE

To separate plasma by one-dimensional sodium dodecyl sulfate polyacrylamide gel electrophoresis (1D SDS-PAGE), samples were diluted to the desired concentration and mixed with 2x Laemmli Reducing Sample Buffer (Bio-Rad). The protein/buffer mixture was heated at 95 °C for 10 min, and then stored on ice until use. The (SDS-PAGE) Mini Cell Apparatus (Bio-Rad) was assembled to include hand cast 12% polyacrylamide gels submerged in Tris-Glycine Running buffer (see Table 2.2). The protein mixture was then loaded into individual gel lanes. To estimate the molecular weight (MW) of separated proteins and to ensure the gels had run correctly, 5 µg pre-stained Kaleidoscope Precision Plus Protein Standard (Bio-Rad) or ProtoMarker Protein Standard (National Diagnostics) was also loaded into one gel lane. The gels were run at 200 V for 45 min, and then washed three times in

d.H_2O for 15 min with constant agitation. Gels were immersed in GelCode Blue (Thermo Scientific) to stain and agitated for 1 hour, and then the GelCode Blue stain was poured off and the gels were de-stained overnight in d.H_2O with continual agitation.

Plasma protein depletion

Pierce Top 12 Abundant Protein Depletion Spin Columns were used to remove ~95% of the abundant protein portion of the plasma proteome. The columns target 12 abundant plasma proteins, including: α1-acid glycoprotein, α1-antitrypsin, α2-macroglobulin, albumin, apolipoprotein A-I, apolipoprotein A-II, fibrinogen, haptoglobin, IgA, IgG, IgM and transferrin. Plasma was diluted to 600 µg in a 10 µl final volume and added to a single-use spin column. The spin columns were gently agitated to facilitate mixing, before undergoing end-over-end mixing for 75 min. The spin column was then centrifuged at 1000 x g for 2 min, and the flow-through was collected and stored at -20 ^{o}C.

Elution of abundant proteins

Recovery of abundant plasma proteins captured by the Pierce Top 12 Abundant Protein Depletion Spin Columns was achieved by using a combination of low pH and high pH incubations on-column to elute the bound proteins.

Immediately following plasma depletion, spin columns were resealed using Parafilm M. The elution method consisted of two incubations with 400 µl 100mM glycine.HCl pH 2.5 buffer, followed by one incubation with 400 µl 1M Tris-HCl pH 7.4 buffer, and then two incubations with 100mM glycine.HCl pH 10 buffer (see Table 2.2). Each incubation step consisted of: addition of 400 µl buffer (a volume sufficient to cover the spin column antibody resin) to the column and gentle agitation to facilitate mixing. Columns were end-over-end mixed for 10 min, and then centrifuged at 1000 x g for 2 min. The flow-through was collected and the eluate fractions were immediately neutralised with an equal volume of 1M Tris-HCl pH 7.4 buffer. All flow-through fractions were pooled to a final volume of ~3.6 ml.

Protein elution was confirmed by adding an equal volume of reducing sample buffer (Bio-Rad) to the spin-column resin and boiling at 95 ^{o}C for 10 min, followed by visualisation on a 1D polyacrylamide gel.

Concentrating protein-containing samples

Concentration of the depleted plasma samples was achieved using Amicon Ultra-0.5 Centrifugal Filter Units (Merck Millipore) with nominal molecular weight limit (NMWL) of 3 kDa, as per the manufacturer's instructions. Briefly, the filter units were first washed with d.H_2O by centrifuging for 30 min at 14000 x g. The depleted plasma (500 µl) was then added to the column and centrifuged at 14000 x g for 30 min, giving ~ 48 µl concentrated material. The concentrated flow-through from the device was stored at -20 ^oC.

Abundant plasma protein eluate underwent diafiltration and concentration simultaneously using Amicon Ultra-4 Centrifugal Filter Units (Merck Millipore) with NMWL of 3 kDa. Filter units were first washed for 40 min at 4000 x g in a swing bucket rotor. The eluted protein fraction was then added to the column and centrifuged at 4000 x g for 40 min, giving ~94 µl concentrated material. Diafiltration was necessary to remove the glycine buffers used for eluting proteins off the depletion spin column. Buffer exchange was achieved by the addition of 25 mM AmBic to the filter unit to a final volume of 4 ml, and centrifuging at 4000 x g for 40 min. The process of "washing out" was repeated for three successive steps until the concentration of the glycine buffer was sufficiently reduced.

In-gel tryptic digestion

Individual 1D-SDS polyacrylamide gel bands were excised using a scalpel and placed in separate Eppendorf tubes. Destaining solution (see Table 2.2 for solutions) was added in 20 µl volumes to each gel slice and then heated at 37 °C for 10 min. The destaining solution was removed and this process repeated until the band was completely translucent. The reduction solution was then added at 20 µl to each gel band and incubated at 37 °C for 60 min. After removal of the reduction solution, 20 µl alkylation solution was added to the gel slices and incubated at 37 °C for 45 min in the dark. The alkylation solution was then removed and the bands washed with d.H_2O, before dehydrating the gel slices in 20 µl of 100% ACN. The gel slices were left to stand for one hour, and then any excess ACN was removed. Proteolysis was achieved by adding 10 µl Trypsin at final concentration of 0.2 µg to the individual gel bands, and incubating at 37 °C overnight. The next day, formic acid at 1% (v/v)

was added and samples mixed by vortexing. The peptide solution was collected and transferred to a new Eppendorf before centrifuging at 13 000 x g for 15 min to remove all insolubles. The peptide supernatant fraction was collected and 0.1% (v/v) formic acid was added for downstream LC-MS/MS analysis. The recovered peptide fractions were stored at -20 ^{o}C until use.

In-solution tryptic digestion

Depleted plasma samples were prepared by first diluting 20 µg protein in 80 µl 25 mM AmBic and 5 µl of 1% (w/v) RapiGest SF Surfactant (Waters), and heating at 80 °C for 10 min. The reduction solution (see Table 2.2 for solutions) was then added at 5 µl and vortexed to mix, before incubating samples at 60 °C for 10 min. Following this, 5 µl alkylation solution was added and the sample vortexed before incubating for 30 min at room temperature in the dark. Trypsin solution was added to depleted plasma at a 30:1 protein:trypsin ratio and incubated overnight at 37 °C. The following day, protein digestion was confirmed by visualising 10 µl sample on a 1D SDS-polyacrylamide gel. The enzyme and RapiGest detergent were inactivated by the addition of 1 µl trifluoroacetic acid (TFA) to a final concentration of 0.5% (v/v), and samples were incubated at 37 °C for 45 min. To remove any insoluble material, samples were centrifuged at 13000 x g for 15 min and the peptide supernatant was then collected and stored at -20 ^{o}C until use.

Plasma and eluted abundant plasma protein samples were prepared by diluting 100 µg protein in 160 µl 25 mM AmBic following the same protocol, with volumes of the RapiGest, reduction and alkylation solutions doubled from 5 µl to 10 µl. Trypsin was added at a 50:1 protein:trypsin ratio, and the volume of TFA was maintained at 1 µl.

RP-LC-MS/MS

In-gel and in-solution tryptically digested peptide samples were diluted to 60 ng/µl in 0.1% formic acid for analysis using LC-MS/MS. Peptide samples were initially separated by reversed-phase liquid chromatography (RP-LC) using a DIONEX UltiMate™ 3000LC chromatography system. Peptides (10 µl = ~600 ng) were injected onto the analytical column (Dionex Acclaim® PepMap RSLC C18, 2 µm, 100 Å, 75 µm i.d. x 15 cm, nanoViper), which was maintained at 35 °C and at a nanoflow rate of 0.3 µl/min^{-1}. Peptides were separated over linear chromatographic

gradients composed of buffer A (2.5 % acetonitrile: 0.1% formic acid) and buffer B (90% acetonitrile: 0.1 % formic acid). Samples were separated over a one hour chromatographic gradient for analyses in Chapter 3, and a two hour gradient for analyses in Chapter 4. MS pre- and post-run quality controls (QC's) included a tryptic digest of bovine serum albumin (BSA) (Bruker), MassPREP *Escherichia coli* digest standard (Waters) and HPLC-grade H_2O, with a H_2O run interspersed regularly between sample LC-MS/MS analyses.

To minimise albumin contamination of depleted plasma peptide samples, LC-MS/MS analyses of depleted plasma were conducted prior to whole plasma or the eluted abundant plasma protein fraction LC-MS/MS analyses. QC's used for depleted samples were *E. coli* digest standard and HPLC-grade H_2O pre- and post-study run. The eluting peptides were analysed online in a LTQ-Orbitrap Velos mass spectrometer (Thermo Fisher Scientific, Schwerte, Germany) coupled to the HPLC system with an electro spray ion source. The mass spectrometer was operated in the data-dependent mode, where a full scan MS spectra survey (from *m/z* 200 to 4000) was acquired in the Orbitrap with high-resolution (40,000-60,000). The ion-trap operated with CID MS/MS (with wide band activation) on the 20 most intense ions. Dynamic exclusion was enabled to avoid repeatedly selecting intense ions for fragmentation and this was set at 500 with an exclusion duration of 20 seconds. Charge states of 1 were rejected. The minimum MS signal threshold was set at 500 counts and the MS/MS default charge state was 2 with a 1.2 *m/z* isolation width, normalised CID at 35V and an activation time of 10 ms.

Protein identification: Proteome Discoverer and Mascot

Proteome Discoverer and Mascot

Raw data from the human plasma (Sigma-Aldrich) LC-MS/MS analyses in Chapter 3 were informatically processed using Proteome Discoverer (Version. 1.4, Thermo Scientific™). The Proteome Discoverer workflow consisted of four workflow nodes: Spectrum Files, Spectrum Selector, Mascot database and Target Decoy PSM Validator. Individual thermo raw files, containing MS and tandem mass spectrometry (MS/MS) data from individual LC-MS/MS analyses, were uploaded to the Proteome Discoverer software. Files were then converted to Mascot generic format files (MGF) for analysis with Mascot protein identification software (Matrix

Science) (313). An in-house Mascot server (Version 2.4, Matrix Sciences) was employed to identify proteins in plasma samples by searching the non-redundant human reference proteome database, downloaded from UniProt (www.uniprot.org/) (314). The human proteome database was accessed on December 7th 2015; containing 70, 075 protein sequences, and last modified September 29th 2015 at the time of use (available from: http://www.uniprot.org/proteomes/UP000005640).

Mascot search engine for proteome database searching

Mascot search parameters were set-up within the 'Mascot database' workflow node within Proteome Discoverer to include: 10 ppm peptide mass tolerance and with a fragment mass tolerance of 0.8 Da, maximum two missed cleavages allowed, carbamidomethylation was set as fixed modification, and methionine oxidation and deamidation as variable modifications. Target decoy database search was applied with a relaxed False Discovery Rate (FDR) <0.05 and strict FDR <0.01, and no ion score cut-off. Protein identifications were filtered in Proteome Discoverer based on Mascot significance threshold <0.05, medium and high peptide confidence, and >1 unique peptide.

Target decoy database searches are required for large scale proteomic experiments, such as LC-MS/MS analysis of plasma, to determine the FDR. A more detailed overview of these methods has been described by Nesvizhskii (315). Briefly, it is recommended to repeat the proteome database search, with the same search parameters, against a database containing the sequences reversed or randomised. As no true matches are expected from the 'decoy' database, the number of matches identified provides an estimate of the number of false positives in the results obtained from the real or 'target' database search (316). The quantity reported for the FDR is calculated by the equation: FDR = FP / (FP + TP), where FP is false positive matches and TP is true positive matches (317).

Protein inference in Mascot

Protein inference within Mascot is based on the "Principle of Parsimony". The human proteome is characterised by high sequence redundancy, and in discovery proteomics a peptide often cannot be uniquely ascribed to just one protein of origin. If the identified peptide sequences match to multiple proteins, the minimum set of proteins that cannot be distinguished based on the peptide information are reported

as a protein group, with a lead protein identifier for which there is the most peptide evidence (318). Protein grouping was enabled to reduce redundancy among protein identifications. 'Unique peptides' are peptide sequences that are unique to a protein group in a data set, and one or several unique peptides may be identified per group. Unique peptides are common to the proteins that comprise the group, and are not present in the proteins from any other protein group identified.

Mascot employs probability based scoring with a 5% confidence threshold, and this has been described in more detail by Perkins and colleagues (313). Briefly, each protein reported in Mascot is assigned a Protein Score, which has been calculated from the summed score of the individual peptides (or Ions Scores) matching the protein. Higher scores represent a more confident overall match. The Ion Score is a measure of how well the experimentally observed MS/MS spectrum matches the theoretical peptide in the database. An individual Ion Score signficance threshold value is calculated for the proteome database searched, and peptides equal to or greater than this number can be considered significant matches ($P = < 0.05$). Therefore, proteins identifed by one or more peptides with a significant Ion Score are more confident matches. Protein identifications were filtered to include proteins with a Mascot significance threshold <0.05.

Protein identification: MaxQuant and Andromeda

MaxQuant and Andromeda

Raw data from LC-MS/MS analyses of plasma from five selected trial participants, discussed in Chapter 4, were informatically processed using MaxQuant (Version 1.5.3.30) software and integrated search engine, Andromeda (319, 320). MaxQuant was selected for this analysis as it is a quantitative proteomics software package that has been designed for analysing large MS data sets. An overview of the MaxQuant and Andromeda computational workflows, and the parameters and configuration options, have recently been reviewed by Tyanova and colleagues (321). Briefly, Thermo raw files obtained from individual LC-MS/MS analyses were uploaded to MaxQuant, where the depleted and eluted protein fraction files for an individual were recombined as one file for proteomic analysis.

Search parameters and settings were: default settings for orbitrap instrument, two missed cleavages allowed, carbamidomethylation was set as fixed modification, and

methionine oxidation and deamidation as variable modifications. Target decoy reverse database search was applied with a peptide and protein FDR <0.05. The 'match between runs' feature was also activated. Label-free quantitation (LFQ) was performed with a minimum ratio count of 1 (322).

'Match between runs' is unique to the MaxQuant computational platform, and it enables the transfer of peptide identifications from an LC-MS run, where a peptide was identified by MS/MS, to a different LC-MS run file, where MS/MS data was not acquired for this peptide, or no peptide was assigned (321). Transfer of peptide identifications is based on retention time, accurate mass calculation and the peptide features individual mass tolerances (323). Use of the 'match between runs' function increases the number of peptides available for quantification, thereby producing a more complete quantitative profile across samples (321). This function is also particularly useful for identification of low abundant peptides, which are variably detected between different untargeted LC-MS/MS analyses.

'MaxLFQ' is the label-free quantification (LFQ) technology incorporated in the MaxQuant workflow for comparative proteomic analyses. The MaxLFQ algorithms for calculating protein intensity profiles have been described in detail by Cox *et al* (322). Briefly, LFQ intensity is the relative protein quantification across all samples, and is represented by a normalised protein intensity profile (321).

Custom proteome database

A custom proteomic database was prepared in-house by concatenating reference proteomes downloaded from UniProt (314) (Table 2.3). The concatenated database was composed of three reference proteomes: human (accessed December 7th 2015; containing 70, 075 protein sequences, and last modified September 29th 2015 at the time of use), *O. volvulus* (accessed November 11th 2015; containing 12, 994 protein sequences, and last modified July 27th 2015 at the time of use) and *Wolbachia* endosymbiont of *O. ochengi* (accessed November 24th 2015; containing 647 protein sequences, and last modified September 18th 2015 at the time of use). The proteome of the *Wolbachia* endosymbiont from *O. volvulus* was not publicly available at the time, therefore the proteome of the *Wolbachia* endosymbiont of *O. ochengi* was incorporated as this species of filarial worm is very closely related to *O. volvulus*.

A common contaminants database provided by MaxQuant software was also used during the proteome database searching in order to enable downstream filtering of non-biologically relevant protein identifications.

Organism	No. of protein sequences	Access date	Available from
Human	70, 075	7.12.15	http://www.uniprot.org/proteomes/UP000005640
O. volvulus	12, 994	11.11.15	http://www.uniprot.org/proteomes/UP000024404
Wolbachia endosymbiont of *O. ochengi*	647	24.11.15	http://www.uniprot.org/proteomes/UP000007516

Table 2. 3. Reference proteomes concatenated for database searching in MaxQuant. The reference proteomes for humans, *O. volvulus* and the *Wolbachia* endosymbiont of *O. ochengi* were downloaded from UniProt. An amalgamated database was prepared in-house to identify proteins in the plasma of trial participants infected with onchocerciasis.

Bioinformatic analysis of the onchocerciasis plasma proteome: Perseus

The protein identifications from MaxQuant, provided as a proteinGroups.txt output file, were uploaded to Perseus software (Version 1.5.2.6), which is provided as part of the MaxQuant computational platform for data analysis (324). LFQ intensity values formed a data matrix with the individuals and protein groups as dimensions. Protein grouping is automatically applied in MaxQuant, such that proteins with similar peptides were combined into a protein group, and a lead protein accession represented the group. However, all proteins were manually assessed at the peptide level in order to assign Swiss-Prot protein accessions as the lead for a protein group where a TrEMBL accession containing the exact same peptides had been listed as the group lead. Swiss-Prot proteins are proteins which have been manually annotated and reviewed by curators at UniProt, while TrEMBL proteins are automatically annotated and have not yet been reviewed. Proteins marked as ‘only identified by site’ and ‘reverse’ (REV) were filtered out of the data matrix. Proteins that were ‘only identified by site’ are those identified only by a modification site

with an FDR >0.05. Proteins marked as ‘reverse’ were identified by the target decoy search, with an FDR above the prespecified cut-off (> 0.05). ‘Contaminants’ (CON) are proteins, such as keratins, that have been identified as a common contaminant in proteomic data sets. Proteins marked as ‘contaminants’ were screened, and the majority were filtered out of the data matrix.

Proteins with >1 unique peptide (peptide sequences that are unique to a protein group in the data set) were retained, and the LFQ intensities of the final data set were then $\log_2$ transformed. Although the ‘match between runs’ feature was used, a proportion of the data set still had missing values where the protein was not detected. Data imputation was performed within Perseus ahead of conducting some statistical analyses. The data matrix was first reduced to include only proteins that were detected in three or more of the five individuals (>60%) at all four sampling time points (pretreatment, months four, 12 and 21). This criterion was selected as these proteins were relatively consistently detected across individuals and time, and missing values could be due to the under-sampling of low abundance proteins during LC-MS/MS analyses. Imputation was achieved by drawing random values from a distribution meant to simulate expression below the detection limit, using a down-shift of 1.8 and distribution width of 0.5 to simulate the assumption of low abundant proteins giving rise to missing values (324). For each sample, the distribution of LFQ intensities was examined by plotting frequency histograms following data filtering and data imputation, to make sure an approximately normal distribution was maintained.

Functional analysis of *Onchocerca volvulus* proteins

Sequence conservation between the *O. volvulus* proteins identified in our data set and proteins of geographically relevant parasite species, such as *L. loa*, *W. bancrofti* and soil transmitted helminths (STHs), was assessed using the Basic Local Alignment Search Tool (BLAST) within UniProt, with default search settings (http://www.uniprot.org/blast/) (325). Other *Onchocerca* species that do not infect humans, and filarial nematodes such as *B. malayi* that are not endemic to Africa, were excluded as peptide or protein conservation among these species would not affect a diagnosis of onchocerciasis. The percentage sequence similarity over the total protein length of the top BLAST protein hit for each *O. volvulus* protein was

determined using the Clustal Omega global alignment tool within UniProt (http://www.uniprot.org/align/) (326). The UniProt Peptide Search was used to determine whether the peptides experimentally detected by LC-MS/MS and used for *O. volvulus* protein inference were also present in other relevant parasite species (http://www.uniprot.org/peptidesearch/). Gene ontology searching was performed using the EBI QuickGO web-browser (https://www.ebi.ac.uk/QuickGO/) (327) by uploading experimentally-obtained UniProt accession identifiers. Data from the recent stage-specific proteome analyses *O. volvulus* by Bennuru and colleagues (269) was also used in our bioinformatic analyses to identify proteins enriched in specific life cycle stages of the worm and proteins that may be secreted (SignalP-HMM prediction) (269, 328). The entire *O. volvulus* stage-specific data set is available as a hyperlinked Excel workbook at: http://exon.niaid.nih.gov/transcriptome/O_volvulus/v245/Ov-v245-web.xlsx.

Molecular techniques

miRNA extraction from plasma

Small RNA (< 1000 nt) was extracted from human plasma samples using the miRCURY™ RNA Isolation Kit – Biofluid (Exiqon), following the manufacturer's instructions. Briefly, 300 µl of plasma was centrifuged at 16 000 x g for 5 min to pellet insoluble material, and 200 µl supernatant was collected for use as the starting volume for RNA extraction. All solutions provided in the kit were prepared following the instructions outlined in the 'Instruction manual v.1.7 (Nov 2015)'. Prior to starting the extraction, Proteinase K (Qiagen) at a final concentration of 2 µg/µl was added to each sample and incubated for 10 min at 37 °C. To minimise technical variation between samples, MS2 carrier RNA (Qiagen) at 1 µg/60 µl lysis buffer and a synthetic RNA spike-in mixture (Exiqon) at 1 µl/60 µl lysis buffer were homogenised in the lysis buffer prior to the addition to samples. Exiqon RNA spike-in mix is used to monitor RNA isolation, and consists of three pre-mixed synthetic miRNAs UniSp2, UniSp4 and UniSp5, corresponding to high, medium and low abundance miRNAs, respectively. To remove any contaminating DNA, on-column DNase treatment was applied. The extracted small RNA was eluted into 50 µl RNase free H_2O and stored at -80 ^oC pending use.

miRNA extraction from filarial worms

Adult male *O. ochengi* and L4 *L. loa* were sourced from a biobank at the LSTM, UK. The details of the methodology used to obtain *O. ochengi* have previously been described (175). Briefly, *O. ochengi* worms were extracted from excised cow nodules in Cameroon, and stored in complete sterile RPMI medium at -80 ^{o}C. *L. loa* L3 stage worms were injected into the scroft and groin of NSG mice and later extracted after culling the mouse at 88 days, before storing under the same conditions. Due to scarcity of *O. volvulus* material and as the miRNAs of interest have also been reported in the closely related *O. ochengi* (291), total RNA was extracted from *O. ochengi* to validate parasite miRNA qPCR assays and for use as a positive control.

Total RNA was extracted from two adult male *O. ochengi* worms using the miRCURY™ RNA Isolation Kit – Cell and Plant (Exiqon), following the manufacturer's instructions. All solutions provided in the kit were prepared following the instructions outlined in the 'Instruction manual v.2.4 (Nov 2015)'. Briefly, the *O. ochengi* worms were gently thawed and then promptly transferred to lysis buffer, where they were homogenised using the MagNA Lyser (Roche Diagnostics Ltd) at speed 4000 for 30 sec. The on-column DNA removal (Qiagen) was performed to remove any residual DNA. RNA was eluted into 50 µl of Elution Buffer and stored at -80 ^{o}C pending use. The same extraction procedure was also used to extract total RNA from two L4 *L. loa* worms.

Determining RNA concentration

For plasma RNA samples, as only small RNA was extracted and plasma has very low levels of RNA, quantification by optical spectrophotometry or Nanodrop is considered to give inaccurate readings. RNA used in downstream applications was therefore based on initial sample input (200 µl plasma).

For parasite RNA samples, total RNA and absence of contaminating DNA was quantified using Qubit RNA BR Assay Kit and Qubit dsDNA HS Assay Kit, respectively, for Qubit 3.0 Fluorometer (ThermoFisher), following the manufacturer's instructions. Briefly, the Qubit working solution was prepared by diluting the Qubit Assay Reagent 1:200 in Qubit Buffer, to a volume sufficient to accommodate all standards and samples. Thin-wall, clear, 0.5 ml Qubit assay tubes

were used when preparing samples and standards. Two standards are required to calibrate the Qubit 3.0 Fluorometer, and the standards were prepared by adding 190 µl Qubit working solution and 10 µl of each standard to the appropriate tube, and mixing by vortexing. For the samples to be measured, 2 µl of RNA-containing sample was added to 198 µl of Qubit working solution, and samples mixed by vortexing. All tubes were then incubated at room temperature for 2 min. The Qubit 3.0 Fluorometer was calibrated by selecting the correct Qubit Assay type and reading the standards in the correct order. The concentration of RNA or DNA was measured in triplicate for each sample, and the three measurements for each sample averaged to give a final concentration.

miRNA primers

All miRNAs in each RNA-containing sample were reverse transcribed into cDNA using a universal RT reaction provided in the Universal cDNA Synthesis Kit II (Exiqon). LNA-enriched miRNA-specific qPCR primers were used to enhance specificity for target templates. All miRNA qPCR primers were purchased from Exiqon, and prepared by adding 220 µl nuclease-free H_2O to the tube and vortexing to mix. Primers were stored in aliquots at -20 ^oC.

Six human miRNA qPCR assays, recommended as potential candidate reference genes for plasma, were initially tested in European control plasma: hsa-miR-16-5p; hsa-miR-103a-3p; hsa-miR-425-5p; hsa-miR-93-5p; hsa-miR-191-5p; and hsa-miR-484. miRNA-specific qPCR primers for the two parasite miRNAs, lin-4 and miR-71, were purchased from Exiqon for cel-miR-71-5p and bma-lin-4. The work presented in this thesis refers to the lin-4 and miR-71 as bma-lin-4 and cel-miR-71-5p, respectively, following the naming convention assigned by their homology to miRNAs listed in miRBase (release 21, http://www.mirbase.org). miRNA qPCR assays were also purchased for the synthetic miRNA spike-ins supplied by Exiqon: Sp2, Sp4, Sp5 and Sp6.

Validation of miRNA primers

The linearity of the two parasite miRNA qPCR assays, cel-miR-71 and bma-lin-4, was determined by preparing five log_{10} serial dilutions of *O. ochengi* cDNA for each assay, with each dilution performed in triplicate reactions. To measure the reproducibility of each assay, the dilution series experiments were repeated three

times over consecutive days to enable calculation of the inter- and intra-assay coefficient of variation (CV) for both cel-miR-71-5p and bma-lin-4.

To determine the limit of detection (LOD) for the parasite qPCR assays, cel-miR-71-5p and bma-lin-4 PCR products were retrieved following their amplification by qPCR, and purified using the QIAquick PCR Purification Kit (Qiagen), following the manufacturer's instructions. Briefly, all buffers were prepared as specified prior to using the kit. Five volumes of Buffer PB were added to 1 volume of the PCR sample and mixed, before adding to a QIAquick spin column. Purified DNA was eluted from the column by after adding 30 µl Buffer EB to the centre of the QIAquick membrane and incubating at room temperature for 1 min, before centrifuging. The flow-through was collected and the purified miRNA amplicon stocks were quantified using the Qubit 3.0 Fluorometer (ThermoFisher, UK). The copy number in each miRNA amplicon stock was determined using scienceprimer.com. A 1:10 dilution series spanning over 10^5 to 10^0 copies per reaction was prepared for both cel-miR-71-5p and bma-lin-4, with nine reactions conducted per dilution. The 95% LOD for each assay was determined using a probit regression analysis in SPSS (Version 23, IBM Corp). Specificity of the parasite miRNA assays was evaluated by observing a single peak in the melt curve analysis, and by the negative reactions in European control plasma and 'no template' controls (NTCs).

The linearity of a human miRNA, hsa-miR-16-5p, was determined by preparing standard curves with five $\log_{10}$ serial dilutions of European control plasma cDNA, in three replicate reactions. The experiment was repeated three times on consecutive days to measure the inter- and intra-assay CV.

miRNA RT-qPCR

Reverse transcription

The two-step miRCURY LNA™ Universal RT microRNA PCR (Exiqon) methodology was utilised for both plasma and parasite samples, following the manufacturer's instructions with minor modifications. For cDNA synthesis, a reaction tube was prepared to a final volume of 10 µl, and consisted of: 5x Reaction buffer (2 µl), Nuclease-free H_2O (4.5 µl), Enzyme mix (1 µl), synthetic RNA spike-in Sp6 or nuclease-free H_2O if omitted (0.5 µl), and RNA-containing sample (2 µl).

A no reverse transcriptase control (-RT), where nuclease-free H_2O was added in place of the Enzyme mix, was also prepared for each sample to check for DNA contamination. For plasma samples, RNA input volumes into the reverse transcription (RT) and qPCR systems, respectively, were empirically determined in European control plasma and a subset of trial participant plasma samples. RNA volumes tested were 2 µl, 4 µl and 7 µl (maximum volume for RT reaction). RT was performed with a TC-4000 Thermal Cycler (Bibby Scientific Ltd). The RT thermocycling parameters were as follows: 42 °C for 60 min, 95 °C for 5 min, followed by a cool down to 4 ^{o}C. One RT reaction was performed per sample.

qPCR

Real time-qPCR was performed with ExiLENT SYBR® Green master mix (Exiqon) in 10 µl reaction volumes, which consisted of: 2x PCR Master mix (5 µl), primer mix (1 µl) and diluted cDNA template (4 µl). It is recommended by the kit manufacturer to dilute cDNA obtained from total cellular RNA to 1:80 in nuclease-free H_2O and to dilute cDNA obtained from biofluid small RNA to 1:40 in nuclease-free H_2O. cDNA obtained from worms was diluted to the desired concentration for the experiment, and the optimal plasma cDNA input for qPCR was determined by testing cDNA in dilutions of 1:5, 1:10, 1:20 and 1:40. The CFX384 C1000 Thermal Cycler (Bio-Rad) was used for qPCR, with Microseal® Skirted 384-Well PCR Plates (Bio-Rad) and adhesive Microseal® 'B' PCR Plate Sealing Film (Bio-Rad). Thermocycling parameters for qPCR were as follows: 95 °C hold for 10 min, 40 cycles of 95 °C for 10 sec and 60 °C for 1 min with a ramp rate of 1.6 °C/sec. Fluorescence was monitored during the 60 ^{o}C step, using the FAM channel. Melt curve analysis was performed between 60 and 95 °C at a ramp rate of 0.5 °C/sec.

All experiments included a positive control, a -RT control for each sample tested, and a NTC obtained from a mock RNA extraction using d.H_2O in place of sample. Each sample was initially tested in duplicate. A qPCR assay was determined positive if the amplification signal crossed the threshold in fewer than 40 cycles and was amplified in both reaction replicates. The optimal threshold for each qPCR assay was determined using the standard curve method. A single peak at the correct melting temperature (T_m) was also required for each product, as determined by the melt curve analysis. The anticipated T_m for bma-lin-4 and cel-miR-71-5p was determined

from repeated standard curves prepared from *O. ochengi* cDNA. Samples with amplification in one qPCR reaction were retested in triplicate, and were only considered positive if amplification occurred in two or more reactions, with a Cq < 40 and the correct T_m in all positive reactions.

DNA extraction

DNA was extracted from clinical plasma samples using the QIAamp DNA Blood Mini Kit (Qiagen) following the manufacturer's instructions. Briefly, 300 µl of plasma was centrifuged at 16 000 x g for 5 min to pellet insoluble material, and 200 µl of supernatant was collected as starting volume for extraction. To control for technical variation between samples, phocine herpes virus-1 DNA (PhHV-1) (Clinical Virology Department, Erasmus MC, Netherlands) was diluted 1:1000 in nuclease-free H_2O and spiked at 1 µl/200 µl lysis buffer. The extracted DNA was eluted into 50 µl Buffer AE after a five min on-column incubation, and stored at -80 ^oC pending use. Plasma DNA input used in downstream applications was based on initial sample volume input.

The *O. volvulus* DNA was originally obtained from a human onchocercoma, and stored in a biobank at the LSTM, UK at -80 ^oC.

Primers for DNA-based experiments

All primers purchased for DNA-based experiments were resuspended in TE Buffer pH 8.0 (Integrated DNA Technologies, IDT) at a stock concentration of 100 µM before storing in aliquots at –20 ^oC. Primers and probe sequences are provided in Table 2.4.

Target	Primer and probe sequences
GAPDH	F 5′- CCACTCCTCCACCTTTGAC -3′ R 5′- ACCCTGTTGCTGTAGCCA -3′
PhHV-1	F 5′- GGGCGAATCACAGATTGAATC -3′ R 5′- GCGGTTCCAAACGTACCAA -3 Probe 5′- VIC-TTTTTATGTGTCCGCCACCATCTGGATC-BHQ1 -3′
O-150	F 5′- TCGCCGTGTAAATGTGGAA -3′ R 5′- AACTGATGACCTATGACCCTAATC -3′ Probe 5′- FAM-GGACCCAATTCGAATGTATGTACCCGT-Zen/Iowa Black FQ -3′

Table 2. 4. Primer and probe sequences for DNA-based experiments.

Glyceraldehyde 3-phosphate dehydrogenase (GAPDH) was selected as the plasma endogenous control, and a qPCR assay for GAPDH was purchased from Sigma. The qPCR assay was assessed using standard curves prepared from a series of five 1:2 dilutions of European control plasma DNA, with three replicate reactions per dilution. Standard curve experiments were repeated three times on alternate days. Primers and a TaqMan probe for viral DNA spike-in PhHV-1 (accession no. Z68147.1) were purchased from IDT.

For amplification of *O. volvulus* DNA, a pre-validated TaqMan qPCR assay specific to *O. volvulus* tandem repeat O-150 DNA sequence (accession no. J04659) (201) was purchased from IDT. The details of the primers/probe and their design have been reported elsewhere (201). O-150 qPCR assay specificity was verified using Primer-BLAST (329), and confirmed by testing negative in European control plasma reactions and NTC reactions. The linearity of the TaqMan assay was assessed from standard curves prepared from five 1:1 serial dilutions of *O. volvulus* DNA, in three replicate reactions per dilution. Three standard curves were prepared over consecutive days to determine the intra- and inter-assay CV. The LOD for the assay has been reported elsewhere (201).

qPCR for DNA-based experiments

All qPCR experiments were performed in 20 µl final volumes using the CFX384 C1000 Thermal Cycler (Bio-Rad) with Microseal® Skirted 384-Well PCR Plates (Bio-Rad) and adhesive Microseal® 'B' PCR Plate Sealing Film (Bio-Rad). Reaction

mixtures for GAPDH qPCR consisted of: 2X SsoAdvanced™ Universal SYBR® Green Supermix (Bio-Rad), 400 nM primers, nuclease-free H_2O, and 4 µl DNA from clinical plasma samples. Cycling parameters consisted of: a hold at 98.0 ºC for 3 min, 40 cycles of 98.0 ºC for 10 sec and 60 ºC for 20 sec. Fluorescence was monitored during the 60 ºC step, using the FAM channel. Melt curve analysis was performed between 60 and 95 °C at a ramp rate of 0.5 °C/s.

Reaction mixes for PhHV-1 qPCR contained 2X TaqMan Fast Advanced Master Mix (Life Technologies, Thermo Scientific), 100 nM primers and probe, nuclease-free H_2O and 4 µl DNA from plasma. *O. volvulus* O-150 qPCR reaction mixtures included 2X TaqMan Fast Advanced Master Mix (Thermo Scientific), 300 nM primers, 250 nM probe, nuclease-free H_2O and 4 µl DNA from clinical samples. Cycling parameters for PhHV-1 and O-150 qPCR assays consisted of: a pre-PCR read at 60 °C for 30 sec, a hold at 95 °C for 20 sec, 40 cycles of 95 °C for 3 sec and 57 °C for 20 sec, and a final extension at 60 °C for 30 sec. Fluorescence was monitored during the 57 ºC step, using the FAM channel for O-150 and the VIC channel for PhHV-1.

Experiments included a positive control and a NTC obtained from a mock DNA extraction using d.H_2O in place of sample. Each sample was initially tested in duplicate. A qPCR assay was counted as positive if the amplification signal had a Cq < 40 and was amplified in both replicate reactions. The standard curve method was used to set the optimal threshold for each qPCR assay. Samples with amplification in one reaction were retested in triplicate, and were only considered positive if amplification occurred in > two reactions.

Statistical analysis

Data obtained from proteomic and molecular experiments were maintained in Excel spreadsheets, and analysed using Perseus (MaxQuant), GraphPad Prism 5, SPSS (Version 23, IBM Corp) and CFX Manager™ (Bio-Rad) software packages. Figures were prepared using GraphPad Prism 5, Perseus and BioVenn (http://www.biovenn.nl/) (330) software. Prior to conducting statistical analyses, data sets were tested for normality. When data was found to be normal, or could be normalised by transformation, parametric tests were used. To assess whether a statistically significant difference was present between the outcomes of independent

groups when data was not normally distributed, the non-parametric Kruskall-Wallis test was used. The non-parametric Friedman's test was used to test for differences in repeated-measures data of dependent samples. When statistically significant differences between groups were identified, Dunn's post hoc test (with 95% confidence intervals) was used to ascertain which groups were significant from the others.

The reproducibility of protein LFQ intensities between different samples was assessed using scatter plots of protein LFQ intensities to calculate R^2 values (322). To compare means between two groups, in which the groups consisted of measurements taken at different time points from the same individuals, a paired t-test was used. Multiple pairwise comparisons were made between imputed proteomic data collected from four trial time points. Volcano plots were then used to plot $-\log_{10}$ transformed p-values against $\log_2$ fold change in average protein intensity between two time points. We acknowledged that this approach risked increasing the chance of making a Type I error (rejecting the null hypothesis when it is true, e.g. falsely identifying proteins as differentially expressed when they are not), particularly when performing multiple t-tests on the same data. After consulting a statistician and bioinformaticians, several types of repeated-measures designs for dependent variables were discussed, including: repeated-measures ANOVA, logistic regression, and linear mixed models. Repeated-measures ANOVA was not suitable for this experimental design given the small sample size and high-dimensional data set (the dimension of repeated measurements per subject is greater than the number of subjects). A dependent t-test was therefore selected for preliminary analyses of potentially interesting proteins between time points ahead of conducting more computationally sophisticated analyses. Confounding or interacting variables (covariates) possibly predictive of the outcomes under study, such as: patient age, gender, weight, village, number of nodules, number of mf or nodulectomy outcomes, were not investigated due to the small and heterogeneous sample set.

Additionally, principal component analysis (PCA) and unsupervised hierarchical clustering were conducted on imputed proteomic data. Unsupervised hierarchical clustering was performed using Euclidean distance with average linkage for both row (proteins) and column (patients).

Chapter 3. Developing a discovery proteomic workflow for plasma

Abstract

Plasma represents the largest and deepest version of the human proteome, and the most clinically relevant and informative of human biological samples. However, the complexity and huge range in protein concentrations in plasma poses significant challenges for proteomic discovery studies. Attempts to reduce the large dynamic concentration range of the plasma proteome incorporated the use of Pierce Top 12 Abundant Protein Depletion Spin Columns, which the manufacturer's claim depletes 95% of the 12 most abundant plasma proteins. On-column high and low pH washes were used to recover the bound abundant plasma proteins, and the depleted and eluted protein fractions were analysed by untargeted liquid chromatography tandem-mass spectrometry (LC-MS/MS). The relative abundance of albumin decreased by 93.4% following depletion, and six of nine abundant proteins assessed (albumin, α2-macroglobulin, apolipoprotein A-1, apolipoprotein A-11, haptoglobin and transferrin) were significantly reduced ($P < 0.05$) in the depleted plasma relative to plasma. Fibrinogen and α1-acid glycoprotein were significantly more abundant in depleted plasma relative to plasma, while there was no significant difference in α1-antitrypsin. However, 63.7% fewer novel protein accessions were identified by LC-MS/MS without depletion. The eluted plasma fraction contained 133 proteins, showing that a high number of non-targeted proteins were bound to the immunoaffinity column, some of which were not found in the depleted fraction. Recombining the two fractions *in silico* improved the proteome coverage from 145 proteins in the depleted fraction to 208 (43.4% increase) proteins in the combined sample. Recovering the bound abundant plasma proteins, and concatenating the depleted and eluted protein identifications further improved the plasma proteome coverage. Merging the two fractions will also provide a better indication of the relative protein abundances in plasma for quantitative analyses. This proteomic workflow reduced the redundancy of plasma analyses by discovery LC-MS/MS, which improved plasma proteome coverage and increased the number of novel low abundance circulating proteins identified.

Introduction

Blood and its derivatives, plasma and serum, are the primary sample types used in clinical diagnostic testing. These biofluids are easy to obtain by minimally invasive methods, and their analysis can provide a snap-shot of an individual's physiology at a given point in time. The plasma proteome comprises a subset of 'classical' plasma proteins that carry out their functions in the blood, as well as an affluence of proteins introduced into the circulation by secretion from blood and tissue cells, tissue leakage, and foreign proteins introduced by microorganisms (310). It is estimated that more than 1,000,000 proteins could be circulating in blood at any given time when the number of protein variants and isoforms are taken into account (331). Plasma therefore represents the most extensive example of the human proteome, and the most clinically relevant and informative of human biological samples (331, 332). Despite the complexity of the human plasma proteome, 99% of the protein mass in plasma is made up of only 22 proteins (Fig. 3.1)(310).

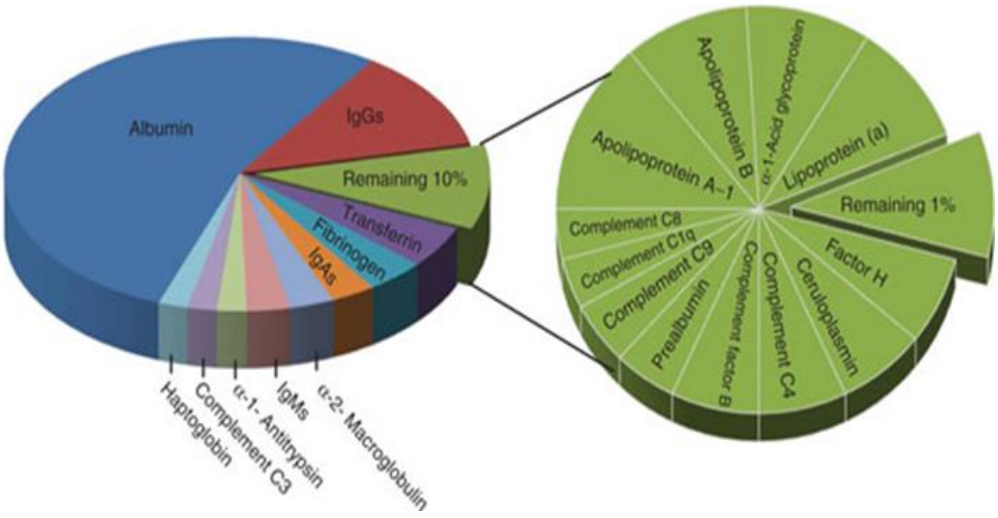

Fig. 3. 1. Percentage of protein mass in plasma (333).

Approximate weighting of the 22 most abundant proteins in plasma. Ten proteins that make up around 90% of total protein mass in plasma are depicted on the left. On the right, the remaining 10% is further divided. Thousands of low abundance proteins, including potential biomarkers, comprise the 1% of the plasma proteome mass. IgA, immunoglobulin A; IgG, immunoglobulin G; IgM, immunoglobulin M.

Albumin alone comprises 55% of the proteome, while other high to medium abundance plasma proteins, such immunoglobulins and complement proteins, form

the remainder (333). Potential biomarkers and clinically relevant tissue-leakage proteins are generally present at sub-nanogram concentrations, and comprise the remaining 1% of the plasma protein mass.

Discovery, or shotgun, proteomics typically utilises a liquid chromatography (LC) system coupled to a tandem mass spectrometer (MS/MS) to perform a hypothesis-free, or untargeted, analysis that aims to identify large numbers of proteins in complex biological mixtures (334). As no prior knowledge is necessary, discovery-based LC-MS/MS attempts to produce an unbiased characterisation of the proteome within a sample (333). MS-based shotgun proteomics employs a bottom-up strategy, whereby proteins are digested into their constituent peptides prior to LC-MS/MS analysis, and protein inference is achieved through assigning peptide sequences to proteins in downstream bioinformatic analyses (335). However, the complexity and huge range in protein concentrations in plasma poses significant challenges for proteomic discovery studies. While the dynamic range of MS instrumentation used for shotgun experiments is 4-5 orders of magnitude (336), the dynamic range in protein concentration within the plasma proteome spans over 10 orders of magnitude (310, 332). For example, the plasma concentrations of albumin and interleukin 6, which are normally present at 35-50 mg/ml and 0-9 pg/ml, respectively, differ by a factor of 10^{10} (337). Comparatively less (around 2–5 fold less) circulating proteins are identified relative to the number of proteins that can be identified evaluating cell and tissue extracts, using similar protein inputs and LC-MS/MS instruments (338-340).

An additional challenge of analysing complex biological mixtures using LC-MS/MS is that the more abundant peptides tend to ‘drown out’ or suppress ion signals from the less abundant peptides. ‘Under-sampling’ can occur when the complexity of the digested peptides surpasses the analytical ability of the MS instrument, such as where more peptides elute from the LC-column than can be analysed per unit time, or peptides at low-abundance are below the detection limit for MS/MS (341, 342). This results in data acquisition redundancy, such that only a fraction of the peptides that are detectable by LC-MS/MS are actually identified (342, 343).

Aim of the study

The aim of this study was to develop a proteomic workflow that would significantly reduce the abundant portion of the plasma proteome, in order to improve the depth of proteome coverage and increase the number of low abundance proteins identified by shotgun LC-MS/MS analysis. The method could then be scaled-up for a prospective MS-based discovery study of circulating onchocerciasis protein markers using a unique longitudinal plasma sample set (157).

Methods

Human plasma

Lyophilised plasma (Sigma-Aldrich), prepared from pooled human blood by the manufacturer, was reconstituted in d.H_2O and stored in aliquots at -20 ^oC. All proteomic workflows used aliquots of the same pooled human plasma.

Proteomic workflow

Plasma was processed using the protein processing methodology and bioinformatic analysis described in Chapter 2. The method has been briefly described and illustrated in Fig. 3.2.

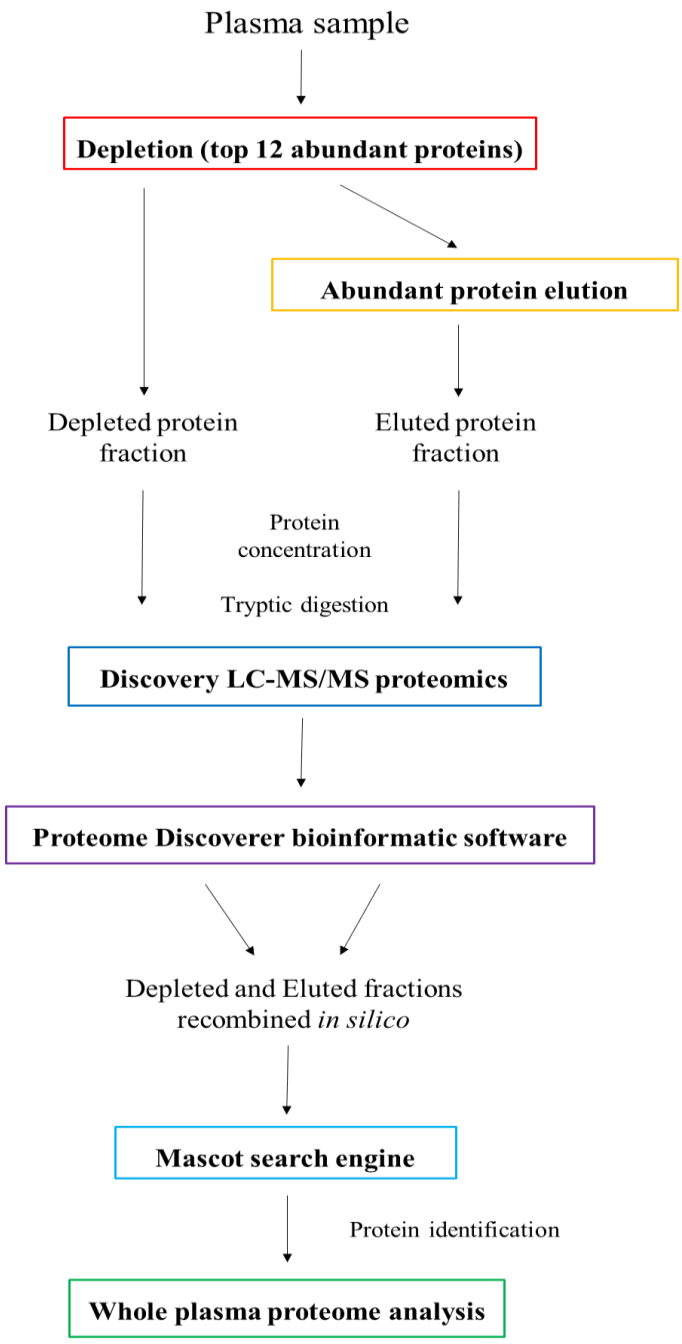

Fig. 3. 2. Proteomic workflow.

Plasma was separated into two distinct fractions: a low abundance protein fraction with the top 12 abundant plasma proteins depleted, and an eluted abundant protein fraction following removal of bound protein from the immunoaffinity column. Depleted and eluted fractions were both concentrated and then tryptically digested in-solution for bottom-up proteomics. Each fraction was analysed once by discovery LC-MS/MS. Matching depleted and eluted fractions were recombined in Proteome Discoverer, and protein accessions were identified using Mascot search engine and the human reference proteome. Lists of protein identifications were filtered in Proteome Discoverer prior to bioinformatic analysis.

Protein concentration

Plasma protein concentration was determined using the BCA Assay (Pierce), according to the manufacturer's instructions. A NanoDrop (Thermo Scientific) spectrophotometer was used to cross-validate protein concentrations.

1D SDS-PAGE

1D sodium dodecyl sulfate polyacrylamide gel electrophoresis (1D SDS-PAGE) was performed by hand-casting 12% (w/v) mini-polyacrylamide gels according to Laemmli (344). Plasma was mixed with 2x Laemmli Reducing Sample Buffer (Bio-Rad) and heated at 95 °C for 10 min before loading on to the SDS-PAGE apparatus. A pre-stained Precision Plus Protein Kaleidoscope Standard (Bio-Rad) or ProtoMarker Protein Standard (National Diagnostics) were used as a molecular weight markers. The gels were stained with GelCode Blue (Thermo Scientific).

Plasma protein depletion

The complexity of the plasma proteome was reduced using Pierce Top 12 Abundant Protein Depletion Spin Columns, according to the manufacturer's instructions. The Pierce Top 12 Protein Depletion Columns reportedly deplete greater than 95% of the 12 most abundant plasma proteins: α1-acid glycoprotein, α1-antitrypsin, α2-macroglobulin, albumin, apolipoprotein A-I, apolipoprotein A-II, fibrinogen, haptoglobin, IgA, IgG, IgM and transferrin.

Plasma samples were diluted to 600 µg in a 10 µl final volume and added to a single-use spin column. They were gently agitated to facilitate mixing before undergoing end-over-end mixing for 75 min. After centrifuging at 1000 x g for 2 min, the flow-through was collected and stored at -20 ^{o}C.

Recovery of abundant plasma proteins

Abundant proteins captured by the Pierce Top 12 Abundant Protein Depletion Spin Columns were recovered using a combination of on-column high and low pH washes. Protein elution consisted of: two 10 min incubations with a 100mM glycine.HCl pH 2.5 buffer, followed by a 10 min incubation with a 1M Tris-HCl pH 7.4 buffer, and then two 10 min 100mM glycine.NaOH pH 10 buffer incubations.

Eluate collected after each buffer incubation was immediately neutralised by an equal volume of 1M Tris-HCl pH 7.4, and all flow-through fractions were pooled.

Concentration of proteins

Depleted plasma samples were concentrated using Amicon Ultra-0.5 Centrifugal Filter Units (Merck Millipore) with nominal molecular weight limit (NMWL) of 3 kDa. The samples were centrifuged at 14000 x g for 30, and the concentrated flow-through from the device was stored at -20 ^{o}C.

The immunoaffinity column eluate was simultaneously concentrated and diafiltrated using Amicon Ultra-4 Centrifugal Filter Units (Merck Millipore) with NMWL of 3 kDa. Pooled eluate from the column was centrifuged at 4000 x g for 40 min to a final volume of ~94 µl. Buffer exchange was achieved by addition of 25 mM Ammonium Bicarbonate (AmBic) to the filter concentrate to a final volume of 4 ml, followed by centrifugation. The process of 'washing out' was repeated three times.

In-gel tryptic digestion

1D SDS-polyacrylamide gel bands were excised and individually tryptically digested following the in-gel trypsin proteolysis protocol outlined in Chapter 2. Briefly, individual bands were destained, and then reduced, alkylated and dehydrated, before an overnight incubation at 37 ^{o}C in a Trypsin (Thermo Scientific™) solution. The following day, gel slices in solution were centrifuged to remove insolubles and the peptide supernatant removed for LC-MS/MS analysis.

In-solution tryptic digestion

Depleted plasma was prepared by diluting 20 µg protein in a final volume of 80 µl 25 mM AmBic and 1% (w/v) RapiGest SF Surfactant (Waters), followed by an incubation at 80 °C for 10 min. After reduction and alkylation, samples were incubated overnight at 37 ^{o}C in a Tryspin (Thermo Scientific™) solution prepared at a 30:1 protein:trypsin ratio. To inactivate the enzyme and detergent, 1 µl trifluoroacetic acid (TFA) was added and samples incubated for 45 min at 37 °C. The samples were centrifuged at 13000 x g for 15 min to remove all insoluble material before removing the peptide supernatant and storing at -20 ^{o}C.

Plasma and the abundant plasma protein eluate from immunoaffinity columns were prepared using the same protocol, but with 100 ug protein added to 160 µl AmBic, and all volumes of solutions used in subsequent steps were doubled. Trypsin solution was added at a 50:1 protein:trypsin ratio.

RP-LC-MS/MS

A more detailed explanation of methodology is provided in Chapter 2. In brief, peptide samples were diluted to 60 ng/µl in 0.1% formic acid, and 10 µl (~600 ng protein) of sample was separated by reversed-phase liquid chromatography (RP-LC) over a 1 hour linear chromatographic gradient using a DIONEX UltiMate™ 3000LC chromatography system. The eluting peptides were analysed online in a LTQ-Orbitrap Velos mass spectrometer (Thermo Fisher Scientific, Schwerte, Germany) coupled to the HPLC system with an electro spray ion source. The mass spectrometer was operated in the data-dependent mode and dynamic exclusion was enabled to avoid repeatedly selecting intense ions for fragmentation.

Bioinformatic analysis

Proteome Discoverer

Raw data sets were informatically processed using Proteome Discoverer software (Version 1.4, Thermo Scientific™) and an in-house Mascot server (Version 2.4, Matrix Sciences) (313). Protein identification was performed using the non-redundant UniProt human reference database and Mascot search engine. The methodology is described in detail in Chapter 2.

Protein inference in Mascot

Protein inference in Mascot involves protein grouping, where the minimum set of proteins that account for the observed peptide matches are reported as a group, and a lead protein accession assigned. Protein grouping was enabled to reduce redundancy, with one or more unique peptides identified per group. Immunoglobulin (Ig) accessions were comparatively excluded for some analyses due to the difficulty in distinguishing between specific antibody sequences at the peptide level (345, 346).

Determining relative protein abundance

Proteins identified in Mascot are each assigned a Protein Score, which has been calculated from the summed score of the individual peptides (or Ions Scores) matching a protein. Higher scores represent a more confident overall match. The Ion Score is a measure of how well the experimentally observed MS/MS spectrum matches the theoretical peptide in the database.

The number of peptide spectrum matches (PSMs) identified by MS/MS for each protein was used as a relative measurement for assessing differences in protein abundances (347). The number of PSMs reported for a protein comprise the total number of identified peptide spectra for that protein. The number of PSMs can be higher than the number of peptides used for protein identification, as the same peptides can be repeatedly detected as PSMs.

Comparisons of the proteins identified between different sample types was performed using BioVenn (http://www.biovenn.nl/) (330).

Statistical analysis

Differences in top plasma protein abundance between plasma and depleted plasma were assessed using Welch's t-test, and significance threshold was set at $P < 0.05$.

Results

1D SDS-PAGE for plasma profiling

1D SDS-PAGE was used to visualise the plasma protein profile (Fig. 3.3). By incrementally increasing the protein concentration of plasma, the resolution of other proteins in the sample was not significantly enhanced. A protein around the molecular weight (MW) of albumin (~66 kDa) dominated the plasma proteome. As the protein concentration was increased, the density of this band increased and dominated the gel, as well as affecting protein migration through the gel matrix.

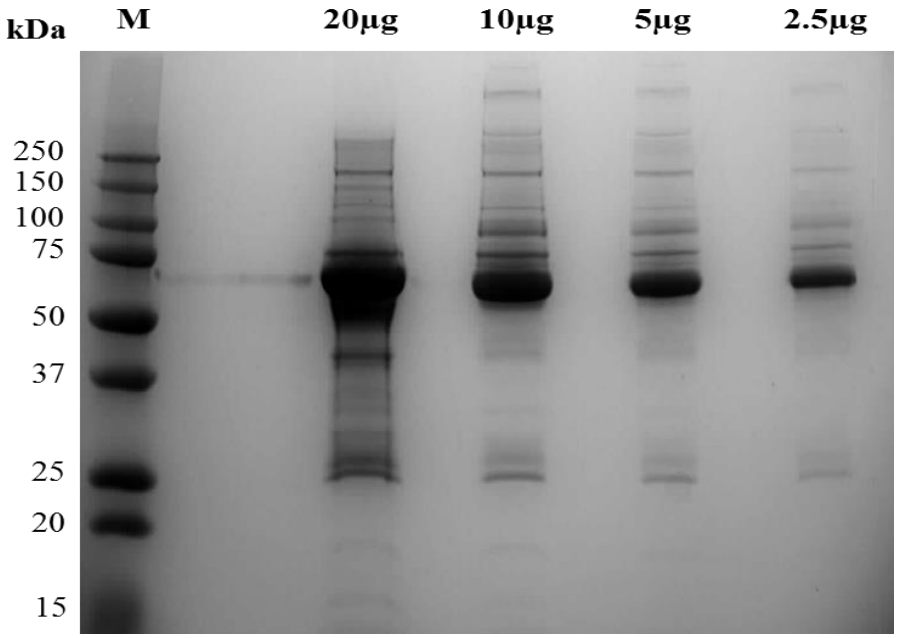

Fig. 3. 3. Plasma protein profile with 1D SDS-PAGE.

1D polyacrylamide gel showing classical plasma protein profile dominated by a subset of abundant proteins. As more protein is added, the protein profile is altered and the gel becomes increasingly overloaded with albumin, affecting successive protein migration down the gel. M: Molecular weight marker (kDa); Lane 1: plasma protein (20 µg); Lane 2: plasma protein (10 µg); Lane 3: plasma protein (5 µg); Lane 4: plasma protein (2.5 µg).

To ascertain the identity of the protein bands, the 22 gel bands were excised and analysed using LC-MS/MS. Protein identifications for individual bands were obtained through Proteome Discoverer, using Mascot search engine and the UniProt human reference proteome database. This led to the identification of seven distinct proteins across 22 bands (Table 3.1). The most abundant plasma protein, serum albumin, was the top scoring hit in 15 of the 22 (68.2%) protein bands. Albumin has high affinity and multiple binding sites for many classes of molecules (348), and can also adsorb onto many different surfaces as structural modifications are easily induced. The other six proteins identified were abundant plasma proteins or common contaminants (keratin). Separation of plasma using 1D SDS-PAGE demonstrated that only the highly abundant proteins in plasma can be detected, and the majority of proteins were masked by albumin.

Band	Accession	Description	% Protein coverage	No. peptides	MW (kDa)
1	P04114	Apolipoprotein B-100	23.67	108	515.3
2	P02768	Serum albumin	64.86	39	69.3
3	P02768	Serum albumin	65.68	41	69.3
4	P02768	Serum albumin	68.80	42	69.3
5	P02768	Serum albumin	63.38	39	69.3
6	P02768	Serum albumin	72.74	45	69.3
7	P02768	Serum albumin	65.02	41	69.3
8	P02768	Serum albumin	67.32	43	69.3
9	P02768	Serum albumin	67.16	43	69.3
10	P02768	Serum albumin	64.86	40	69.3
11	P02768	Serum albumin	63.71	39	69.3
12	P02768	Serum albumin	65.02	41	69.3
13	P02768	Serum albumin	66.83	42	69.3
14	P02768	Serum albumin	69.79	43	69.3
15	P02768	Serum albumin	65.02	44	69.3
16	P02675	Fibrinogen beta chain	68.64	31	55.9
17	P01009	Alpha-1-antitrypsin	57.89	24	46.7
18	A0A087WU08	Haptoglobin	50.18	17	31.4
19	P02768	Serum albumin	56.49	33	69.3
20	P02647	Apolipoprotein A-I	78.28	26	30.8
21	P04264	Keratin, type II cytoskeletal 1	30.12	22	66.0
22	P04264	Keratin, type II cytoskeletal 1	35.25	27	66.0

Table 3. 1. Plasma proteins identified by 1D SDS-PAGE and LC-MS/MS.

The top scoring protein from each excised gel band obtained from 1D SDS-PAGE and LC-MS/MS analyses of whole plasma. The human reference proteome database was searched using Mascot through Proteome Discoverer. For each excised gel band, the top scoring UniProt protein accession and the description is listed. The number of peptides identified for each protein and percentage of protein coverage by the identified peptides are also detailed. MW (kDa), molecular weight (kilodaltons).

Depletion of abundant plasma proteins

To overcome the vast dynamic range of the plasma proteome, the top 12 abundant proteins (constituting ~ 95% total protein mass in plasma) were removed using immunoaffinity spin columns. Flow-through from the spin column was visualised using 1D SDS-PAGE, and the individual bands were analysed using LC-MS/MS (Fig. 3.4) (Table 3.2). Gel bands from the depleted plasma fraction were fainter due to the removal of most of the plasma protein mass, and the dilution from a 10 µl starting volume to ~500 µl final volume from the spin column flow-through. Keratin, type I and II cytoskeletal proteins were the top scoring protein in most of the bands, indicating contamination was introduced during sample processing (349). Where this occurred, the next highest scoring protein listed was selected as the representative protein for each band.

LC-MS/MS analysis of the depleted plasma fraction separated by 1D-SDS-PAGE identified 13 distinct protein accessions in 17 gel bands. This was an improvement on the seven distinct protein accessions identified in 22 bands by LC-MS/MS analysis of whole plasma separated by 1D SDS-PAGE. Nine accessions were uniquely identified in the depleted plasma fraction relative to whole plasma, of which two were abundant protein variants (alpha-1-antitrypsin and fibrinogen gamma chain) and one was an uncharacterised protein. Four abundant plasma proteins (albumin, fibrinogen, alpha-1-antitrypsin and apolipoprotein A-I) targeted for removal by the immunoaffinity column were identified as a top scoring protein in six of the 17 bands (35.3%) from depleted plasma. However, the presence of albumin was markedly reduced in the depleted plasma fraction relative to whole plasma, as only two of 17 bands (11.8%) relative to 15 of 22 bands (68.2%), respectively, identified albumin as the top scoring protein. This indicated effective but incomplete removal of some abundant proteins targeted by the immunoaffinity column, and insufficient protein coverage of the plasma proteome using 1D SDS-PAGE and LC-MS/MS analyses.

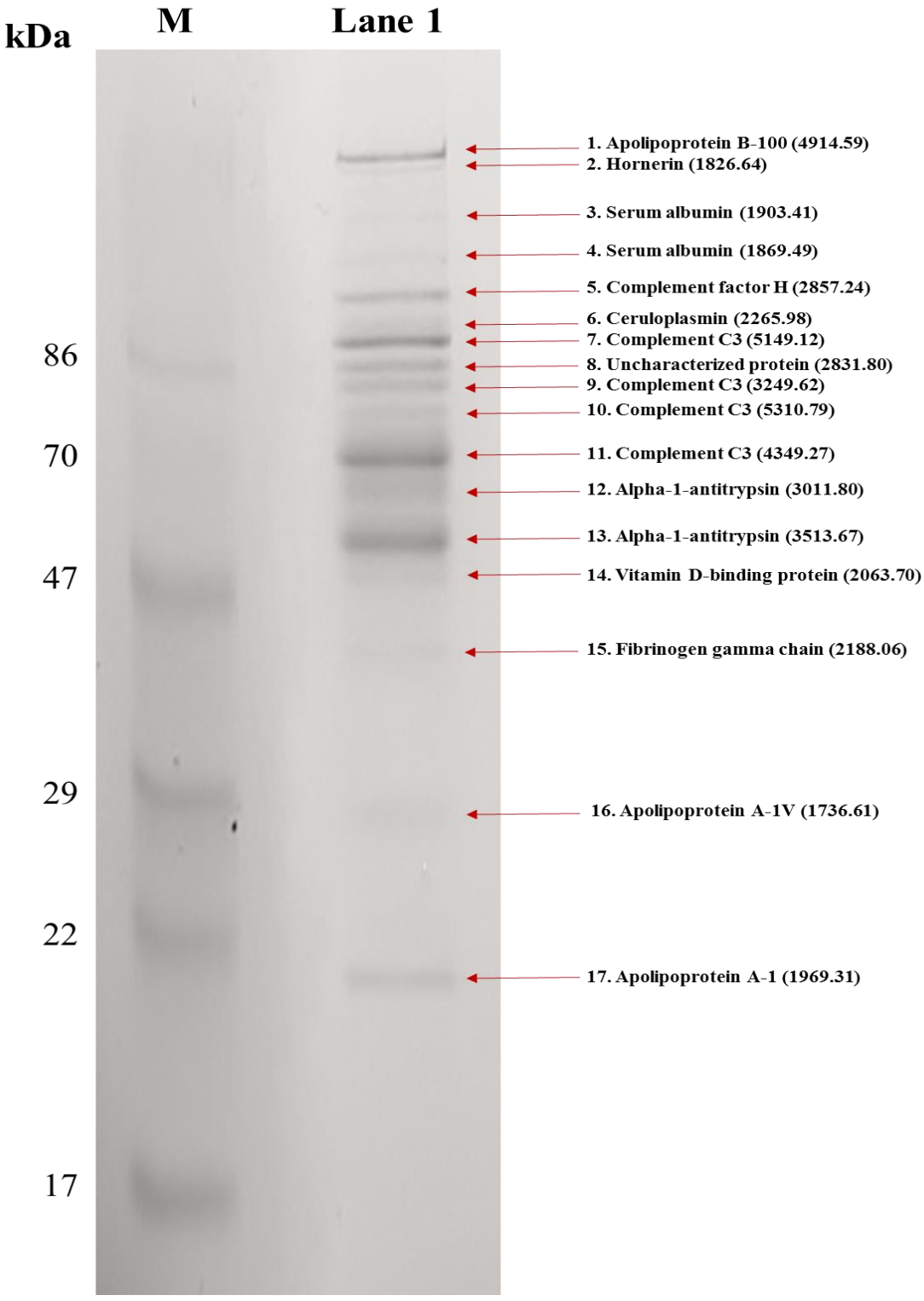

Fig. 3. 4. Protein identifications in plasma depleted of abundant proteins.

Plasma depleted of the top 12 abundant proteins (10 µl volume) was visualised on a 12% (w/v) polyacrylamide gel, and the gel bands analysed using LC-MS/MS. The human reference proteome database was searched with Mascot through Proteome Discoverer. The top scoring protein identification (excluding keratins) for each gel band are indicated along with the Mascot Protein Score. M: Molecular weight marker (kDa).

Band	Accession	Description	% Protein coverage	No. peptides	MW (kDa)
1	P04114	Apolipoprotein B-100	38.31	138	515.3
2	Q86YZ3	Hornerin	17.12	17	282.2
3	P02768	Serum albumin	69.79	37	69.3
4	P02768	Serum albumin	69.79	37	69.3
5	P08603	Complement factor H	53.94	52	139.0
6	P00450	Ceruloplasmin	47.61	37	122.1
7	P01024	Complement C3	47.62	66	187.0
8	B4E1Z4	Uncharacterised protein	46.37	53	140.9
9	P01024	Complement C3	52.56	63	187.0
10	P01024	Complement C3	52.38	69	187.0
11	P01024	Complement C3	47.81	62	187.0
12	P01009	Alpha-1-antitrypsin	60.53	25	46.7
13	A0A024R6I7	Alpha-1-antitrypsin	57.66	26	46.7
14	D6RF35	Vitamin D-binding protein	57.77	25	53.0
15	C9JEU5	Fibrinogen gamma chain	67.87	26	50.3
16	P06727	Apolipoprotein A-IV	62.12	25	45.4
17	P02647	Apolipoprotein A-I	71.91	22	30.8

Table 3. 2. Plasma proteins identified by 1D SDS-PAGE and LC-MS/MS after abundant protein depletion.

The top scoring protein from each excised gel band obtained from 1D SDS-PAGE and LC-MS/MS analyses of a depleted plasma sample. Keratin contaminated samples had keratin removed as the top scorer. For each excised gel band, the top scoring protein accession and the description is listed. The number of peptides identified for each protein accession and percentage of protein coverage by the identified peptides are also provided. MW (kDa), molecular weight (kilodaltons).

Whole proteome in-solution proteolysis

To improve the plasma proteome coverage by LC-MS/MS, a whole proteome in-solution proteolysis method was adopted. Following in-solution digestion of a single plasma and depleted plasma sample, both were analysed by LC-MS/MS. The resultant output following bioinformatic processing was a list of proteins that had been identified in a sample ranked by the Mascot Protein Score (supplementary

Table S1). The top 20 highest scoring proteins identified from a single LC-MS/MS analysis of plasma (Table 3.3) and abundant protein depleted plasma (Table 3.4) were compared.

No.	Accession	Description	% Protein coverage	No. peptides	No. PSMs
1	P02768	Serum albumin	78.98	55	1243
2	A0A087X130	Ig kappa chain C region	49.78	7	200
3	A0A087WZW8	Protein IGKV3-11	45.49	6	199
4	P01024	Complement C3	43.48	64	137
5	P01023	Alpha-2-macroglobulin	40.16	43	108
6	P04114	Apolipoprotein B-100	21.63	76	90
7	P02787	Serotransferrin	59.03	36	94
8	P00738	Haptoglobin	64.78	25	95
9	A0A087WV47	Ig gamma-1 chain C region	42.92	15	102
10	P01009	Alpha-1-antitrypsin	45.22	17	77
11	P00739	Haptoglobin-related protein	43.68	17	75
12	A0A0G2JL54	Complement C4-B	29.74	37	55
13	A0A0G2JPR0	Complement C4-A	28.96	37	55
14	P02671	Fibrinogen alpha chain	22.63	19	56
15	P02679	Fibrinogen gamma chain	59.38	21	66
16	P02647	Apolipoprotein A-I	62.92	18	45
17	P02675	Fibrinogen beta chain	52.92	19	50
18	A0A087WXL8	Ig gamma-3 chain C region	31.72	11	57
19	E9PFZ2	Ceruloplasmin	32.45	21	40
20	P01861	Ig gamma-4 chain C region	42.51	9	60

Table 3. 3. Top 20 high scoring proteins identified in plasma by in-solution proteolysis and LC-MS/MS.

The 20 highest scoring proteins in plasma, based on the Mascot Protein Score. The number of peptides and peptide spectrum matches identified for each protein accession, and percentage of protein coverage by the identified peptides are provided.

No.	Accession	Description	% Protein coverage	No. peptides	No. PSMs
1	P01024	Complement C3	72.70	126	346
2	P0C0L5	Complement C4-B	46.39	66	114
3	A0A0G2JPR0	Complement C4-A	45.93	65	113
4	P08603	Complement factor H	61.66	61	122
5	P02774	Vitamin D-binding protein	66.24	37	108
6	P02790	Hemopexin	65.58	30	100
7	P00450	Ceruloplasmin	53.80	51	100
8	P04114	Apolipoprotein B-100	22.24	85	102
9	P02671	Fibrinogen alpha chain	40.18	33	92
10	P02768	Serum albumin	73.73	40	82
11	P01009	Alpha-1-antitrypsin	68.66	31	87
12	P02675	Fibrinogen beta chain	68.02	34	85
13	P04264	Keratin, type II cytoskeletal	56.37	34	62
14	P00738	Haptoglobin	71.18	33	73
15	P04003	C4-binding protein alpha chain	52.43	26	54
16	P04217	Alpha-1B-glycoprotein	45.25	16	68
17	P13645	Keratin, type I cytoskeletal	58.73	30	52
18	P02749	Beta-2-glycoprotein 1	69.57	22	61
19	P04196	Histidine-rich glycoprotein	39.05	21	52
20	B4E1Z4	Uncharacterised protein	36.18	45	67

Table 3. 4. Top 20 high scoring proteins identified in depleted plasma by in-solution proteolysis and LC-MS/MS.

The 20 highest scoring proteins in depleted plasma, based on the Mascot Protein Score. The number of peptides and peptide spectrum matches identified for each protein accession, and percentage of protein coverage by the identified peptides are provided.

Albumin was the top scoring protein in plasma, and Ig protein accessions were the 2nd and 3rd highest scoring proteins (Table 3.3). The number of peptide spectrum matches (PSMs) identified for albumin and the 2nd highest scoring protein was 1243 and 200 PSMs, respectively. PSMs can serve as relative measure to determine differences in the abundance of proteins identified in a LC-MS/MS analysis (347). The relative abundance of albumin detected was therefore more than 6 times higher than that of the other abundant plasma proteins. Eight of the top 12 plasma proteins

were identified (IgG subclasses and fibrinogen chain accessions were counted as single parent proteins, respectively), and only one lower abundance plasma protein (haptoglobin-related protein) was identified within the 20 highest scoring proteins.

In the plasma depleted of abundant proteins, albumin was the 10th top scoring accession (Table 3.4). Although albumin had not been completely removed and remained an abundant protein, there was a significant reduction in the number PSMs identified for albumin in the depleted plasma relative to whole plasma by LC-MS/MS. Eighty-two PSMs compared to 1243 were detected in the depleted plasma and whole plasma, respectively. Therefore, the relative abundance of albumin detected by LC-MS/MS had decreased by 93.4% after using the immunoaffinity spin columns for abundant plasma protein removal. Additionally, no Ig accessions were identified in the top 20 of depleted plasma compared to five identified in whole plasma. Seven proteins not among the 22 most abundant plasma proteins were also identified as high scoring proteins in depleted plasma. Of the 12 proteins specifically targeted for removal, four were identified within the top 20 highest scoring proteins in the depleted sample: albumin, fibrinogen, α1-antitrypsin and haptoglobin.

Performance of immunoaffinity depletion

In order to evaluate the overall efficiency of the immunoaffinity column for removal of the top 12 abundant protein targets, the number of PSMs for each protein was compared in the depleted plasma and whole plasma. The immunoglobulins targeted for removal (IgG, IgA and IgM) were not included due to the difficulty in distinguishing between specific antibodies at the peptide level (345, 346). PSMs for fibrinogen subchain (α, β, γ) accessions were also grouped into the one parent protein.

As was previously discussed, the number of albumin PSMs was significantly higher in the LC-MS/MS analysis of whole plasma compared to depleted plasma (Fig. 3.5). Six proteins (albumin, α2-macroglobulin, apolipoprotein A-1, apolipoprotein A-11, haptoglobin and transferrin) were significantly reduced ($P < 0.05$) in the depleted plasma. Two proteins (fibrinogen and α1-acid glycoprotein) were significantly more abundant in depleted plasma relative to plasma, and no significant difference was observed in α1-antitrypsin between the two samples. The greater number of PSMs in depleted plasma for two of the proteins targeted for

removal is most likely due to the significant reduction of albumin, which enabled more efficient surveying of ion signals from the less abundant peptides.

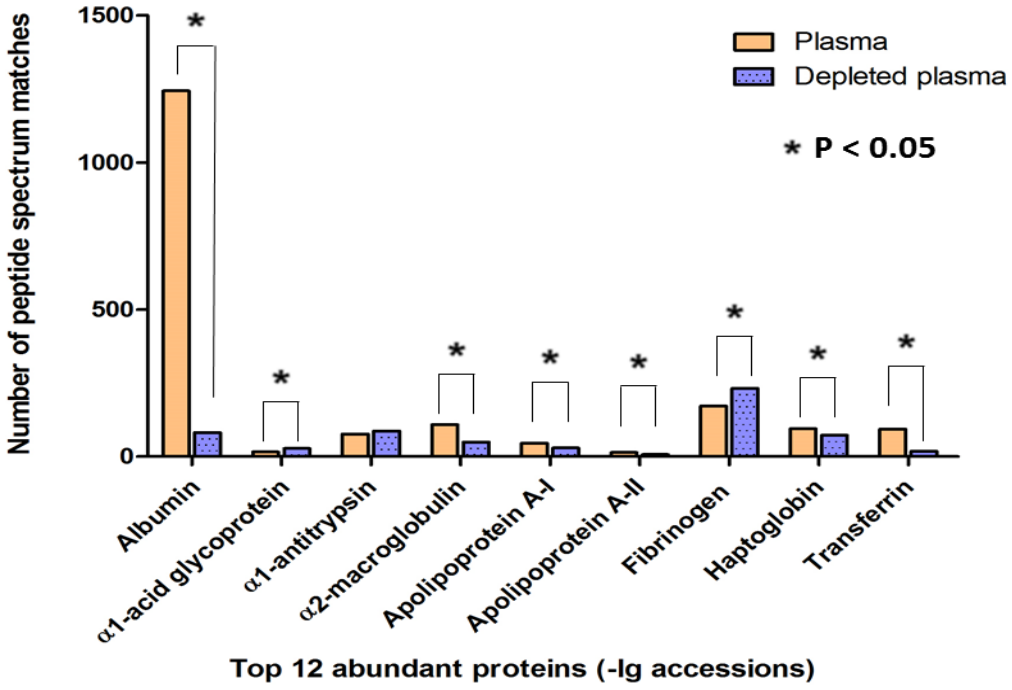

Fig. 3. 5. Relative abundance of the top 12 abundant proteins (-Ig accessions) in plasma and depleted plasma.

The number of PSMs identified for nine of the 12 abundant plasma proteins targeted for removal in both plasma and the depleted plasma. IgG, IgA and IgM were excluded due to the difficultly accurately assigning ambiguous Ig peptides. Six proteins (albumin, α2-macroglobulin, apolipoprotein A-1, apolipoprotein A-11, haptoglobin and transferrin) were significantly reduced ($P < 0.05$) in the depleted plasma relative to plasma following removal by the immunoaffinity column. Fibrinogen and α1-acid glycoprotein were significantly more abundant in depleted plasma relative to plasma, while there was no significant difference in α1-antitrypsin ($P > 0.05$).

Use of the immunoaffinity spin column did not appear to have a notable effect on the number of proteins that could be identified in plasma by LC-MS/MS, as 168 and 143 proteins were detected in the depleted plasma and whole plasma, respectively (Fig. 3.6). Eighty-two proteins were identified in both samples, and so the number of proteins uniquely identified in plasma and depleted plasma was comparable. However, after removal of all ambiguous Ig accessions, 80 and 29 proteins were novel to depleted plasma and whole plasma, respectively. Therefore, 63.7% fewer

novel protein accessions were identified when abundant plasma proteins were not removed prior to LC-MS/MS analysis. Nine Ig accessions were identified in the depleted fraction compared to 35 Ig accessions in plasma, three of which overlapped. Following the removal of Ig accessions, depletion of abundant proteins was effective for increasing the plasma proteome coverage detectable by LC-MS/MS.

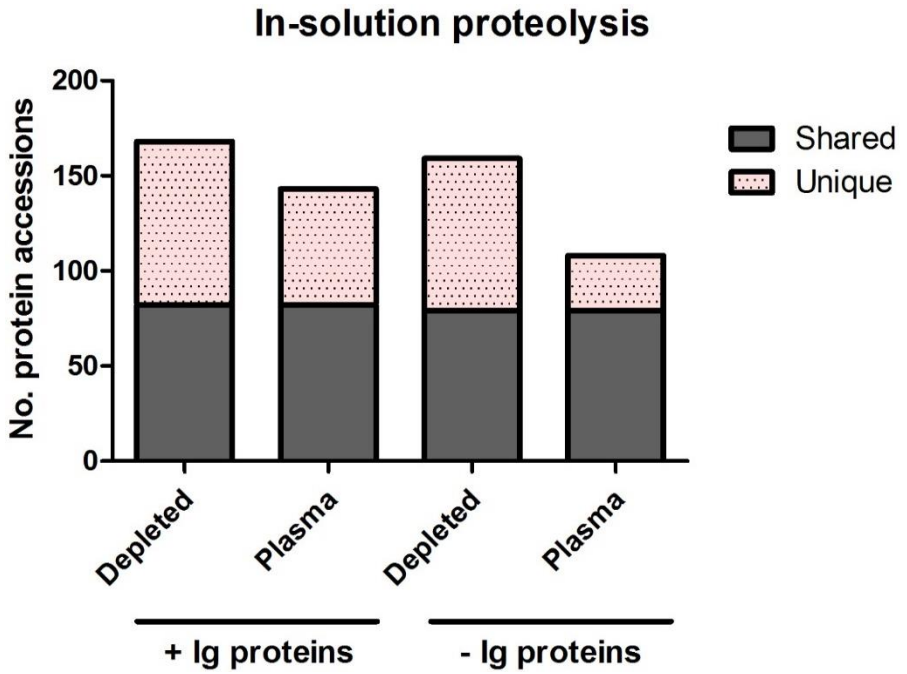

Fig. 3. 6. Number of proteins in the depleted plasma and whole plasma.
The number of protein accessions identified from depleted plasma and whole plasma after in-solution proteolysis and LC-MS/MS analysis. The number of proteins identified were initially comparable in the two samples until the Ig accessions were removed. Considerably more novel proteins were identified by LC-MS/MS after removal of the abundant plasma proteins and ambiguous Ig accessions.

Reproducibility of discovery LC-MS/MS

To assess the reproducibility of shotgun LC-MS/MS, three repeat LC-MS/MS analyses were conducted for depleted plasma and whole plasma, respectively. The three LC-MS/MS analyses of depleted plasma showed a 66.3% overlap in the protein accessions identified, with a total of 150, 153 and 168 proteins detected from the individual analyses (Fig. 3.7A). There was a 56.7% overlap in protein accessions identified in whole plasma, with a total of 135, 134 and 143 proteins per replicate LC-MS/MS analysis (Fig. 3.7B). The top scoring and higher abundance proteins of

both plasma and depleted plasma were consistently detected across their respective replicate series. However, the lower abundance proteins, which were identified by a limited number of PSMs, were differentially detected over the repeat LC-MS/MS analyses. This demonstrated that detection of the more abundant proteins is reproducible using LC-MS/MS analyses, but lower abundance proteins can be variably detected due to sampling bias in discovery LC-MS/MS analyses.

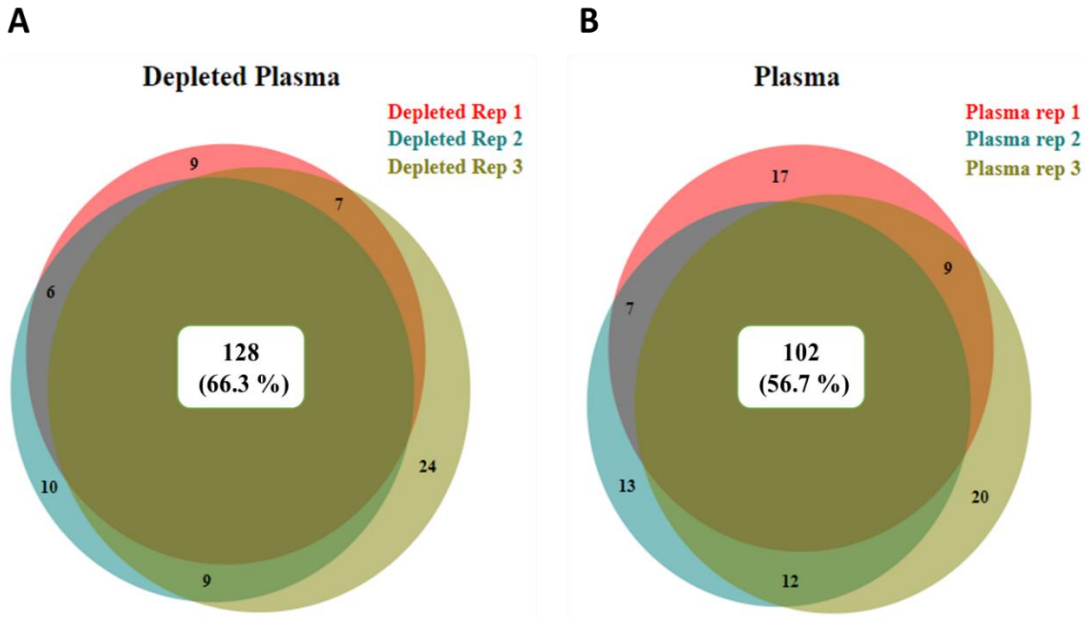

Fig. 3. 7. Reproducibility of LC-MS/MS analyses.

A. Depleted plasma was analysed in triplicate LC-MS/MS analyses, and the protein accessions identified in each replicate analysis were compared. Of the proteins identified, 66.3% were present in all three replicates, and novel proteins were also identified in every replicate.

B. Whole plasma was analysed in triplicate LC-MS/MS analyses and the protein accessions identified were compared. There was a 56.7% overlap between the three replicates, and novel proteins were detected in each analysis.

Protein profile of the eluted abundant protein fraction

To investigate the proteins that were bound to the Pierce Top 12 Abundant Protein Depletion Spin Columns, plasma was depleted and an extreme pH buffer wash protocol was used to elute the bound abundant proteins off the column. The depleted plasma and abundant protein eluate were digested in-solution and analysed using LC-MS/MS (protein lists supplied in Table S2). Although the immunoaffinity

column targeted 12 abundant plasma proteins, 133 protein accessions were identified in eluted fraction. Of these, 94 were not Ig accessions. The bound protein fraction was therefore effectively eluted by the buffer washes. Nine of the top 12 proteins targeted by the columns for removal were identified as the highest scoring proteins, although all 22 abundant plasma proteins were detected in the eluted fraction. After excluding Ig accessions 45 proteins (33.8%) were detected by 1-3 PSMs, indicating low abundant proteins which were not targeted for removal, were bound to the immunoaffinity column.

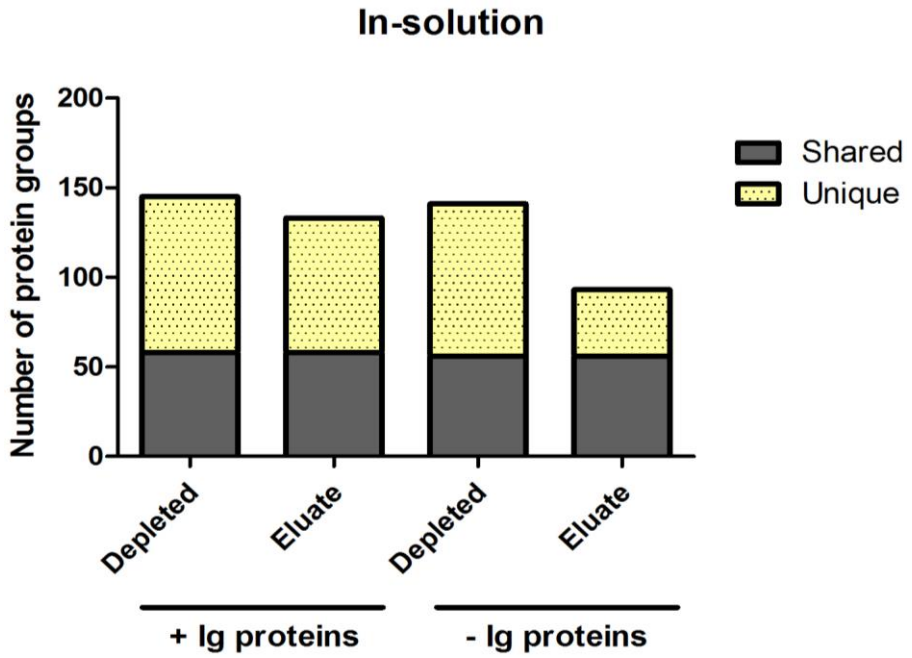

Fig. 3. 8. Number of proteins in the depleted plasma and eluted fraction.
Number of protein accessions identified from a depleted and eluted fraction subject to in-solution proteolysis and LC-MS/MS analysis. The number protein accessions identified in both fractions was initially comparable, despite the columns only targeting 12 abundant proteins. After removal of Ig accessions, considerably more novel proteins were identified in the depleted sample relative to the eluted fraction. However, a number of novel and shared proteins remained in the eluted fraction, even after removal of Ig accessions.

A comparable number of protein accessions, 145 and 133, were identified in the matching depleted and eluted abundant protein fractions, respectively (Fig. 3.8). Eighty-seven and 75 accessions were novel to the depleted and eluted fractions, and 58 protein accessions were common to both samples. Six Ig accessions were identified in the depleted plasma compared to 39 in the eluted fraction, two of which

were common to both fractions. Therefore, a total of 38 protein accessions were uniquely identified in the eluted fraction after exclusion of ambiguous Ig accessions. Of all the proteins that were unique to the bound fraction, 19 (25.3%) were not Ig, keratin or protein fragment accessions (Table 3.5). This verified that there is unspecific binding of non-targeted proteins to the immunoaffinity column and/or binding to proteins targeted by the column, and that eluting the abundant proteins will identify additional accessions unique to the eluted fraction.

Accession	Description	% Protein coverage	No. peptides	No. PSMs
P68871	Hemoglobin subunit beta	68.03	8	9
P00751	Complement factor B	12.07	9	10
Q8IZF3	Adhesion G protein-coupled receptor F4	2.01	1	4
P69905	Hemoglobin subunit alpha	28.87	4	4
P00748	Coagulation factor XII	1.46	1	1
H9KV48	Plasma protease C1 inhibitor	4.54	2	2
A0A096LPE2	Protein SAA2-SAA4	13.94	3	3
C9JEV0	Zinc-alpha-2-glycoprotein	5.29	1	1
G3V2D1	Ribosomal protein S6 kinase alpha-5	2.74	1	1
O43866	CD5 antigen-like	4.03	1	1
Q9BXE4	FKSG51	6.45	1	1
H0Y4U7	ATP-binding cassette sub-family A member 9	0.38	1	1
Q8WZ42	Titin	0.03	1	1
Q99459	Cell division cycle 5-like protein	1.12	1	1
E7EQY3	Pregnancy-specific beta-1-glycoprotein 5	2.70	1	1
Q5T0H8	Gelsolin	4.35	1	1
Q9Y2H5	Pleckstrin homology domain-containing family A member 6	0.76	1	1
F5GX11	Proteasome subunit alpha type-1	2.94	1	1
Q9ULJ8	Neurabin-1	1.37	1	1

Table 3. 5. Protein accessions unique to the bound abundant protein fraction. Nineteen accessions identified as novel to the high abundant protein eluate fraction following in-solution digestion; excluding Ig, keratin and protein fragment accessions.

Global plasma proteome analysis

To establish a global view of the plasma proteome, and reduce redundancy by pooling protein identifications that may have overlapping peptides, the depleted plasma and eluted abundant protein fractions were recombined *in silico* (Table S3). The plasma proteome coverage was increased from 145 to 208 (43.4%) protein identifications in the depleted and combined sample, respectively. The number of concatenated proteins identified was a small reduction from the 220 total proteins (shared protein accessions and those unique to both fractions) identified in the separate depleted and eluted fraction analyses (Fig. 3.9).

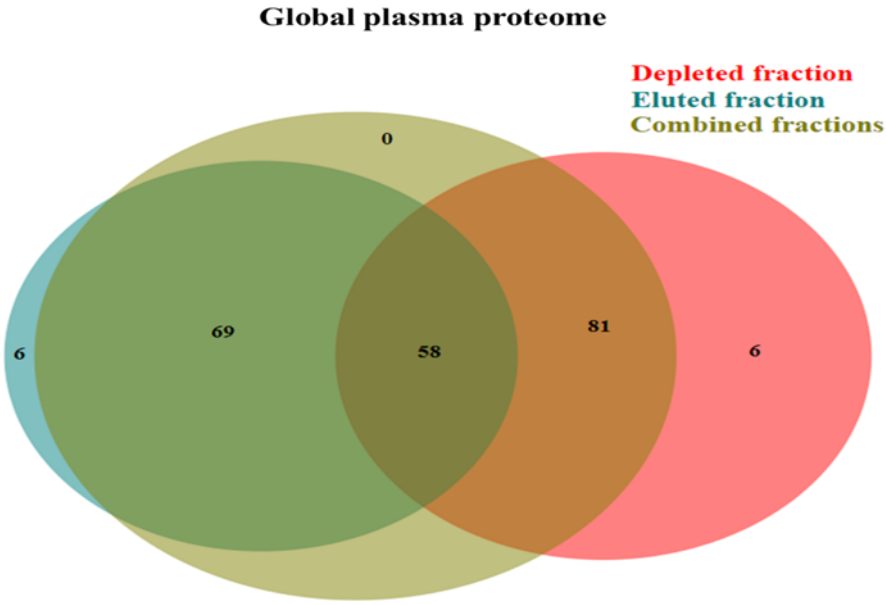

Fig. 3. 9. Protein identifications in depleted and eluted fractions combined *in silico*. The contribution of the protein accessions that were unique to and shared by the depleted, eluted and concatenated fractions are shown. Six proteins uniquely identified in both the depleted and eluted fractions were not found in the concatenated sample.

Six additional accessions were identified in the depleted and eluted sample that were not in the recombined plasma. This was due to the peptides (used for protein inference) being reassigned to other protein accessions as more peptide evidence became available from combining eluted and depleted fractions. Therefore, analysis of abundant plasma protein and depleted fractions by LC-MS/MS and concatenation of the fractions *in silico* improved coverage of the plasma proteome relative to LC-MS/MS analysis of whole or depleted plasma.

Discussion

The aim of this study was to develop a proteomic workflow to reduce the redundancy in plasma proteome analysis by LC-MS/MS, in order to improve detection of less abundant circulating proteins while maintaining throughput for larger experimental applications. The data presented verifies that plasma as a clinical sample for untargeted proteomic profiling is inherently complex, and the presence of a subset of high abundant proteins, most notably albumin, will impact the number of proteins that can be identified using LC-MS/MS. Use of immunoaffinity depletion columns to remove ~95% of the abundant plasma proteome revealed that targeted proteins remained present at high levels in depleted plasma, but considerably more novel proteins were still identified relative to whole plasma. Analysing the depleted plasma fraction and bound abundant protein fraction using LC-MS/MS and then concatenating the protein identifications *in silico* improved the proteome coverage relative to LC-MS/MS analysis of whole plasma or depleted plasma. Furthermore, as the number of PSMs for individual proteins in the eluted abundant protein and depleted fraction are also combined *in silico*, merging the two fractions provides a better indication of the relative protein abundances in plasma for quantitative analyses. This proteomic workflow reduced the redundancy of plasma analyses by discovery LC-MS/MS, which improved plasma proteome coverage and increased the number of novel low abundance circulating proteins identified.

Shotgun LC-MS/MS of plasma is confounded by the vast dynamic range in protein mass, whereby only a small fraction of the proteome can be surveyed (310, 333, 343). In our plasma analysis, albumin was detected at a relative abundance 6 times higher than that of the 2nd highest scoring Ig protein accession (1243 and 200 PSMs, respectively). Reducing the dynamic range in plasma is therefore essential to improve the proteome coverage in discovery-based LC-MS/MS. Techniques such as abundant protein depletion or low abundant protein enrichment are typically used to achieve this. We opted to use immunodepletion, as while several studies have shown the two methods to be comparable (350-354), enrichment requires greater sample volumes (>1.0 ml) (353). 1D SDS-PAGE was initially used to visualise the plasma protein profile, but it did not have sufficient resolution to separate more than 22 protein bands, and albumin was consistently identified as the lead protein in 15 of the 22 (68.2%) excised gel bands. This resulted in a massive underrepresentation of

the plasma proteome, and even many other high abundance proteins were omitted from this profile. The depletion of albumin and 11 other abundant plasma proteins using immunoaffinity depletion columns showed that more distinct proteins could be identified following separation by 1D SDS-PAGE. The presence of albumin was markedly reduced, as only two of 17 bands (11.8%) compared to 15 of 22 bands (68.2%) in the depleted plasma and whole plasma, respectively, identified albumin as the lead protein. However, four of the abundant proteins targeted for depletion (albumin, fibrinogen, α1-antitrypsin and apolipoprotein A-I) were still the high scoring proteins in some depleted plasma gel bands. This demonstrated that the top 12 abundant plasma proteins targeted by the immunoaffinity column had not been completely removed following depletion, and that 1D SDS-PAGE and LC-MS/MS analyses yielded inadequate coverage of the plasma proteome.

In-solution proteolysis of plasma and depleted plasma for bottom-up shotgun LC-MS/MS enabled protein identifications to be ranked according to the individual Mascot Protein Scores, and the relative abundance of individual proteins could be compared by using the number of PSMs. The abundant protein profile in depleted plasma included seven proteins that are not among the 22 most abundant plasma proteins, compared to one identified in the top 20 highest scoring proteins in whole plasma. This showed an improved depth of proteome coverage was achieved following depletion. However, four abundant plasma proteins were still identified in the top 20 highest scoring proteins in the depleted plasma (albumin, fibrinogen, α1-antitrypsin and haptoglobin). Furthermore, albumin was the 10^{th} top scoring protein, indicating there was still high levels of abundant plasma proteins in the depleted sample. Incomplete depletion of abundant plasma proteins using depletion methods has been frequently reported (355-357).

To evaluate the immunoaffinity columns, the relative levels of the individual top abundant proteins in whole plasma and depleted plasma were comparatively assessed by the total number of PSMs for each protein, excluding IgG, IgA and IgM (347). The relative abundance of albumin detected by LC-MS/MS had decreased by 93.4% following depletion, and six proteins (albumin, α2-macroglobulin, apolipoprotein A-1, apolipoprotein A-11, haptoglobin and transferrin) of nine analysed were significantly reduced in the depleted plasma relative to plasma. Fibrinogen and α1-acid glycoprotein were significantly more abundant in depleted

plasma relative to plasma, and there was no significant difference in abundance of α1-antitrypsin. Comparison of depleted plasma and whole plasma showed that 63.7% fewer novel protein accessions were identified when abundant plasma proteins were not removed prior to LC-MS/MS analysis. The improved proteome coverage in the depleted plasma was due to the significant reduction of albumin, as this enables more efficient peptide separation and data-dependent selection of low-abundance ions in LC-MS/MS analyses (358). Therefore, although there was not total depletion and high levels of the top 12 abundant proteins remained, the depth of plasma proteome coverage had been considerably improved following immunoaffinity depletion.

The number of proteins that were identified in both plasma and depleted plasma are similar to that of other studies using similar methodologies. One study that depleted the top 20 abundant plasma proteins identified 120 proteins in plasma and 154 in the depleted plasma across three LC-MS/MS replicates (359). In another study, 114, 118 and 113 proteins were identified in three depletion columns after depletion of the top 14 abundant proteins and bioinformatic exclusion of Ig accessions (360). Liu and colleagues also identified an average of 122 proteins from five separations of plasma using IgY-12 depletion column and five individual LC-MS/MS analyses (361). Only proteins with >2 distinct peptides from all the replicate analyses were included, and the Ig identifications were removed (361). Many proteomic experimenters exclude proteins detected by fewer than two peptides as they are considered low confidence protein identifications (362). Proteins identified by a single unique peptide were included here, as the depletion of single peptide protein identifications can result in a large portion of the proteome (20-25% of all expressed proteins) being lost (363). The likelihood of selecting and identifying a peptide, let alone several peptides, from a low abundance, and possibly more biologically significant, protein during LC-MS/MS analysis is extremely small (364). Furthermore, the ‘two-peptide’ rule can actually result in increased false discovery rates and a substantial loss in sensitivity relative to when single-peptide protein hits are not removed (363-365).

The reproducibility of technical LC-MS/MS replicates was assessed using three repeat LC-MS/MS analyses for both a depleted plasma and plasma sample. While a similar number of proteins were detected across the three LC-MS/MS replicate

analyses for both samples, there was a 66.3% and 56.7% overlap in the protein accessions identified for depleted plasma and plasma, respectively. Under-sampling is one explanation for the limited overlap in proteins identified from repeat LC-MS/MS analyses of a sample (342). Similar findings were reported in another study assessing replicate analyses of fractions obtained from a plasma depletion/elution workflow (366). He, *et al* analysed four distinct fractions (male-bound fraction, female-bound fraction, male-unbound fraction and female-unbound fraction) in duplicate and found a 40.1%, 44.7%, 52.3%, 45.8% overlap, respectively, in the proteins identified from duplicate analyses of each sample (366). Abundant protein identifications are typically reproducible in discovery-based LC-MS/MS, while the lower abundance proteins cause most of the perceived variability. The protein accessions that differed between technical replicates were primarily proteins with identified by one peptide. Variation in the peptide sequences identified for a given protein also contributed to the lower reproducibility in replicate analyses. Therefore, technical LC-MS/MS replicates are not sufficiently reproducible in protein discovery studies of complex biological mixtures, and perhaps not worth the increased MS analytical time.

Immunodepletion of abundant plasma proteins can result in biases and incomplete proteome coverage due to cross-reactions with the column antibodies, or because proteins bind to carrier proteins like albumin (367). Several studies have recovered a high number of non-targeted proteins following their elution off the column (360, 361, 366, 368, 369). Therefore, excluding this plasma fraction may mean valuable biological information is lost. Despite the immunoaffinity depletion column reportedly targeting 12 abundant plasma proteins, 133 protein accessions were identified in the eluted fraction following in-solution proteolysis and LC-MS/MS. All 22 abundant plasma proteins were detected in the bound portion, however 33.8% of the protein accessions had 1-3 PSMs and were low abundance plasma proteins. In the bound plasma proteome, 56.4% of proteins were unique and were not detected in the depleted plasma. Of all the proteins that were novel to the bound fraction, 25.3% were not ambiguous Ig, contaminating keratin or protein fragment accessions. This verified that untargeted proteins are removed by immunoaffinity depletion columns, and that recovering the bound protein fraction improved the plasma proteome coverage. In addition to albumin being a carrier

protein, some of the proteins that were identified are known to associate with or are structurally similar to target proteins of the column. For example, fibronectin binds to fibrinogen (370), and the sequence of haptoglobin-related protein is >90% identical to that of haptoglobin (371). Other studies that have investigated the eluted protein fraction also identified several plasma proteins that were identified here, including apolipoprotein B-100 (360), zinc-α2–glycoprotein, haemoglobin and complement proteins 3, 4 and H (361). Although non-targeted proteins bind to the depletion columns to different extents, individual non-target proteins have been shown to bind in a reproducible manner (361). This is important if the elution method is to be used for quantitative analyses.

The plasma proteome coverage was further improved by recombining the depleted plasma and eluted abundant protein fractions *in silico.* This enabled a more comphrehensive view of the plasma proteome to be established, and increased the proteome coverage by 43.4% relative to when only the depleted plasma was analysed using LC-MS/MS. Recombining the fractions also provided additional peptide evidence for protein inference, and therefore the likelihood of reporting the 'correct' representative protein was increased. An additional benefit of evaluating both fractions by LC-MS/MS and bioinformatically analysing as a unified sample is that the number of PSMs for individual proteins identified from the eluted and depleted fraction are also combined. Concatenating the two fractions provides a more accurate indication of the relative protein abundances in plasma for comparative quantitative LC-MS/MS analyses.

To further increase the number of proteins identified by discovery LC-MS/MS, more pre-fractionation or separation steps are required ahead of MS-based analysis. Multi-dimensional separations of complex samples can be achieved using 2-D strong cation exchange-RP-LC separation (SCX/HPLC or MudPIT), capillary electrophoresis coupled to HPLC (HPLC/CE), as well as various affinity-based separations (372). The inclusion of multi-dimensional LC-MS/MS can increase the proteome coverage up to 200-700 protein identifications (355, 373). However, even the Human Proteome Organization (HUPO) plasma proteome study, involving 18 laboratories with diverse methods and instruments, produced fewer than 900 high confidence protein identifications (341). Although advances in proteomic workflows have since enabled the identification of over 1,000 (374, 375) and 5,000 plasma

proteins (376), a major bottleneck of large-scale MS-based approaches is the labour and time required to perform the additional steps. The inclusion of several different sample preparation steps decreases throughput by increasing the overall analysis time in terms of manual handling and at the MS-level (367).

In conclusion, this proteomic workflow consisted of abundant plasma protein depletion and abundant protein recovery, followed by analysis of each fraction by LC-MS/MS and recombining the fractions *in silico*. This has been shown to reduce the redundancy in plasma proteomic analyses and improve the depth of plasma proteome coverage. This method will increase the likelihood of detecting less abundant circulating parasite and host proteins in the onchocerciasis plasma proteome. In addition, another method that could further increase the number of protein identifications and be integrated into our proteomic workflow is the use of longer RP-LC separation gradients. A study that used this method increased the number of proteins identified from 154 to 192, simply by doubling the RP-LC separation time (359). Incorporation of longer RP-LC gradients in subsequent analyses would improve the accessibility of the plasma proteome for discovery LC-MS/MS, while maintaining sufficient throughput, as no additional manual handling would be required.

Chapter 4. The onchocerciasis plasma proteome – a longitudinal survey

Abstract

A point-of-care diagnostic test for onchocerciasis that has high sensitivity and specificity for active infection with adult *Onchocerca volvulus* is a high priority for programmatic support for disease elimination. This study used an untargeted liquid chromatography tandem-mass spectrometry (LC-MS/MS)-based proteomic workflow to identify circulating protein markers that are present in the host plasma during infection and dynamically change over two years following macrofilaricidal treatment. We applied the proteomics methodology developed in Chapter 3 to a longitudinal plasma sample set from five individuals, collected pretreatment and at months four, 12 and 21 post-treatment. Sixteen *O. volvulus* proteins were identified in plasma, and no *Wolbachia* proteins were detected. Five of the *O. volvulus* proteins were identified consistently in individuals, and three consistently in most individuals, over the two year period. Three *O. volvulus* proteins changed in detection frequency among individuals by month 21. Ten of the 16 (62.5%) parasite proteins are enriched in male worms, while one protein, A0A044VCM8, consistently identified in individuals over time is enriched in female worms. None of the *O. volvulus* proteins identified here are predicted to be secretory, and so the proteins are most likely either derived from excreted products or released from moribund or dead parasites. The current study has therefore identified the *O. volvulus* protein A0A044VCM8 as a potential circulating candidate marker for adult female infection in plasma. However, no proteins met our biomarker criteria, and all but one of the *O. volvulus* proteins were still present in one or more individuals 21 months after treatment. The onchocerciasis plasma proteome was largely unchanging following macrofilaricidal treatment, as no parasite or human proteins statistically significantly changed over time, and no proteins were present in all individuals at baseline and absent at a later sampling time. It may be that 21 months is too short a follow-up time to kill all worms and clear parasite proteins from the host. Furthermore, during the long term follow-up period patients may become re-infected, in addition to the inter-individual variability in infection intensity and response to treatment, influencing changes in protein abundance.

Introduction

The progression from an onchocerciasis control to an elimination programme in Africa poses considerable challenges for disease diagnosis and the detection of ongoing infection transmission or recrudescence. A point-of-care diagnostic test with high sensitivity and specificity for active *O. volvulus* infection is urgently needed to accurately map hypoendemic areas with low levels of ongoing transmission, and make informed decisions regarding treatment provision and intervention cessation. An *O. volvulus*-specific marker of the adult worms would also be advantageous for quantifying treatment efficacy for both established and candidate antifilarial drugs and for monitoring patient drug response (251). The *Ov*16 antigen, to which antibodies develop during the pre-patent period of infection (228), can be used for serological evaluation of infection exposure in children under 10 years in sentinel populations, in order to identify areas with ongoing transmission (87). However, the major shortcoming of antibody-profiling assays is that due to the long half-life of antibodies, antibody detection tests are unable to distinguish between past and current infections (247).

Rapid format tests to detect circulating filarial antigens (CFA) are commercially available for *W. bancrofti* causing lymphatic filariasis (258, 259), and the dog heartworm *D. immitis* (261). Several longitudinal macrofilaricidal drug trials have also demonstrated that levels of CFA significantly decline in over the months and years following macrofilaricidal treatment (262-265). Additionally, studies have shown that the levels of filarial antigens may correlate to the adult worm infection intensity (266-268) and to mf densities in the blood or skin (254, 260). Circulating filarial markers may therefore be used to determine infection prevalence, infection intensity and treatment efficacy.

Multiomic-based discovery methods and metabolite profiling of infection-associated markers for onchocerciasis have identified a number of novel antigens (269, 271) and metabolites able to discriminate between infected and non-infected individuals (273, 274). Metabolomic analysis of urine from infected individuals has additionally identified a neurotransmitter-derived secretion metabolite from *O. volvulus*, N-acetyltyramine-O-glucuronide (NATOG), which is elevated only in the presence of *O. volvulus* in samples with mono-infection and co-infections with *L. loa*

and *M. perstans* (275, 277). NATOG has also been detected at a significantly reduced concentration in urine from individuals tested 20 months post-doxycycline treatment compared with untreated *O. volvulus*-positive patients and placebo-treated patients (275). However, the limited diagnostic applicability of NATOG for discriminating between amicrofilaridermic nodule-positive and control groups was reported in a separate evaluation (278). Analyses of nematode-specific phospholipids in plasma and serum of uninfected and infected hosts have also shown limited diagnostic potential, as the parasite phospholipids were below the limit of detection (279). While the overall progress in this research area has been encouraging, no potential biomarkers identified in recent years have been progressed to diagnostic development for field use. Additionally, all studies have identified the potential *O. volvulus* biomarkers in the host by testing infected vs uninfected cohorts. Therefore, aside from NATOG, whether any of the markers could be used to monitor treatment efficacy or patient drug response is unknown.

Proteomics provides a potential platform for discovery of circulating biomarkers in human plasma, and proteins are also a practical target as they more tractably translate into a point-of-care diagnostic format, such as an antigen detection test. In Chapter 3, it was shown that plasma is a challenging clinical sample to analyse using LC-MS/MS due to a subset of high abundant proteins and a dynamic range in protein concentration spanning over 10 orders of magnitude (310, 332). A proteomic pipeline for plasma was presented that would be amenable to scale-up for an onchocerciasis biomarker discovery study, using a unique longitudinal plasma sample set (157). This sample set will enable tracking of the dynamics of infection clearance over two years within the onchocerciasis plasma proteome, and allow each patient to serve as their own control rather than infected vs uninfected of a random sample cohort

Aim of the study

The aim of this study was to use a discovery proteomic workflow to identify protein biomarkers from *O. volvulus*, the *Wolbachia* endosymbiont of the parasite, or the host, that are present in the host plasma during infection and dynamically change over 21 months following macrofilaricidal treatment. We applied the proteomics

methodology developed with human plasma in Chapter 3 to a longitudinal plasma sample set of individuals infected only with *O. volvulus*. Plasma from five individuals collected pretreatment, and at four, 12 and 21 months post-doxycycline treatment, were analysed using untargeted label-free LC-MS/MS to discover protein markers of infection, infection intensity and/or treatment efficacy in the onchocerciasis plasma proteome. For a potential biomarker of onchocerciasis infection and infection clearance, we sought: i) proteins that were present at baseline and absent at one or more successive time points; ii) proteins that statistically significantly changed (P = <0.05) over time, with >1.5 fold change in protein abundance between the time points.

Methods

Onchocerciasis plasma samples

Plasma samples were obtained from a double-blind, randomised, field trial conducted over two years in Cameroon (157). The trial was community based and was undertaken in Widikum, in the North West Province of Cameroon. Details of the trial are available in the study report by Turner *et al* (157), and also outlined in more detail in Chapter 2. Briefly, adults aged 15–60, in good health and with *O. volvulus* skin microfilaridermia > 10 mf/mg were enrolled in the trial. There were three treatment arms in the study: 1) doxycycline + placebo (DOXY), 2) doxycycline + ivermectin (DOXY+IVM), 3) and placebo + ivermectin (IVM). Participants in the DOXY group only were selected for this pilot study in order to track the effects of worm killing from macrofilaricidal treatment on the onchocerciasis plasma proteome. The DOXY regime consisted of:

DOXY: Doxycycline (2 × 100 mg capsules daily) for six weeks plus non-matching ivermectin-dummy pill at month four (lactose tablet).

Plasma from the trial participants was collected at baseline, and then at four, 12 and 21 months post-treatment. At each time point, *O. volvulus* microfilaridermia was assessed by microscopy. The prevalence and density of *L. loa* and *M. perstans* microfilaraemia in participants was also recorded at every time point of the trial.

Pilot study sample set

The pilot sample set selected here for proteomic analysis consisted of five individuals from the DOXY group, with non-haemolysed plasma available at all four time points of the study. Of the 21 individuals in the DOXY group, four participants had a plasma sample absent at one or more time points and nine participants had visible haemolysis in plasma taken at one or more time points. Haemolysis was determined by visually inspecting samples for pink/orange/red colour. Haemolysed samples were preferentially excluded as lysis of erythrocytes causes the liberation of intracellular components, such as proteins and metabolites, which could modify the proteomic profile of the sample (377). In addition, iron from haemoglobin can catalyse oxidation and protein cleavage reactions, further contributing to pre-analytical variability between samples (378). A small number of participants were selected for the pilot study as MS-based proteomic biomarker discovery studies typically involve analysing a small number of samples in considerable depth, after which targeted analyses are used to identify the candidates of interest in a larger sample set (379, 380).

Parasitological details of participants for this study can be found in Table 4.1. The median age was 40 years, with a range from 25 to 49 years. The ratio of female to male participants was 2:3. Men and women of different ages were selected to identify a biomarker indicative of infection and infection clearance in a general onchocerciasis population, and reduce the effect of confounding variables. Patients were also selected considering nodulectomy data, which was collected from seven participants. One patient with low microfilaridermia (9 mf/mg) was included in this analysis as this patient had <20% live worms in nodules removed at 21 months, and therefore evidence of macrofilaricidal treatment response was available.

The trial plasma samples were stored at -80 ^{o}C, and gently thawed on ice before use. A 100 µl aliquot was spun at 16 000 x g to pellet and remove any cellular debris, and all samples were processed at the same time throughout the experiment.

Patient ID	Sex	Age	Baseline mf count (mf/mg)	T4 mf count (mf/mg)	T12 mf count (mf/mg)	T21 mf count (mf/mg)
1	M	49	31.5	2	57.5	9
2	F	45	9.5	14	37.5	0
3	M	26	120	0	5.5	0
4	M	40	15.5	0	0	0
5	F	25	40	1	2	0

Table 4. 1. Parasitology of participants selected for the current study (157).

Parasitology of the five patients selected for longitudinal analysis, detailing the number of mf/mg skin snip at baseline, and four, 12, and 21 months post-treatment. T4, month four; T12, month 12; T21, month 21. F, female; M, male.

Proteomic workflow

Twenty plasma samples, from the five individuals sampled at four time points, were processed using the protein processing methodology outlined in Chapter 2 and Chapter 3, and bioinformatic analysis described in Chapter 2. The method has been briefly described and illustrated in Fig. 4.1.

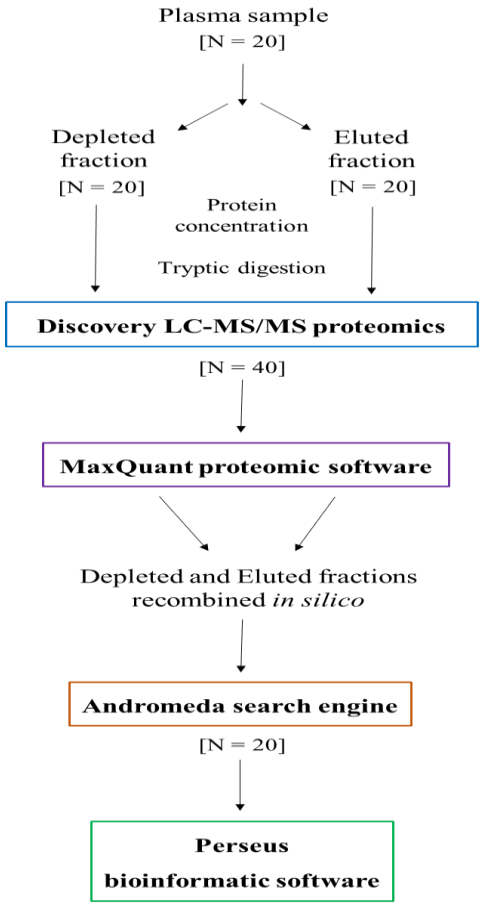

Fig. 4. 1. Proteomic workflow.

Plasma samples from five trial participants at four time points (N = 20) were each separated into two distinct fractions: a low abundance protein fraction with the top 12 abundant plasma proteins depleted (N = 20), and an eluted abundant protein fraction (N = 20). Depleted and eluted fractions were both concentrated and then tryptically digested in-solution for bottom-up proteomics. Each fraction was analysed once by discovery LC-MS/MS (N = 40). Matching depleted and eluted fractions were recombined in the MaxQuant proteomic software prior to further bioinformatic analysis. Proteins were identified using the integrated Andromeda search engine (N = 20), using a custom concatenated proteome comprising the reference proteomes of human, *O. volvulus* and the *Wolbachia* endosymbiont of *O. ochengi*. Data output from MaxQuant/Andromeda platform was bioinformatically processed using Perseus software. N = Number of samples analysed.

Plasma proteome fractionation

Pierce Top 12 Abundant Protein Depletion Spin Columns were used to deplete the top 12 abundant plasma proteins, as per the manufacturer's instructions. The 12 plasma protein targets for depletion include: α1-acid glycoprotein, α1-antitrypsin, α2-macroglobulin, albumin, apolipoprotein A-I, apolipoprotein A-II, fibrinogen, haptoglobin, IgA, IgG, IgM and transferrin. The bound abundant plasma proteins were then eluted off the column by end-over-end mixing using a combination of two 10 min 100mM glycine.HCl pH 2.5 buffer washes, followed by two 10 min 100mM glycine.NaOH pH 10 washes, with a 10 min 1M Tris-HCl pH 7.4 neutralisation wash interspersed. Eluate collected from every glycine buffer wash was immediately neutralised by an equal volume of 1M Tris-HCl pH 7.4 and all flow-through fractions were pooled to a final volume of ~3.6 ml per individual sample.

Sample preparation for LC-MS/MS

Protein concentration for the depleted plasma fractions was achieved using Amicon Ultra-0.5 Centrifugal Filter Units (Merck Millipore) with nominal molecular weight limit (NMWL) of 3 kDa, as per manufacturer's instructions. The pooled eluted abundant protein fractions were simultaneously concentrated and diafiltrated using Amicon Ultra-4 Centrifugal Filter Units (Merck Millipore) with NMWL of 3 kDa, following the manufacturer's instructions. Buffer exchange was achieved by the addition of 25 mM AmBic to the filter concentrate followed by centrifugation. All samples were then tryptically digested in-solution.

RP-LC-MS/MS

Peptide samples were initially separated by RP-LC using a DIONEX UltiMate™ 3000LC chromatography system. Peptide samples (10 µl = 600 ng) were separated over two hours using linear chromatographic gradients. All peptide samples from the depleted protein fractions were injected on column prior to the eluted fraction peptide samples. The eluting peptides were analysed online in a LTQ-Orbitrap Velos mass spectrometer (Thermo Fisher Scientific, Schwerte, Germany) coupled to the HPLC system with an electro spray ion source. The mass spectrometer was operated in the data-dependent mode and dynamic exclusion was enabled to avoid repeatedly selecting intense ions for fragmentation.

Protein identification: MaxQuant and Andromeda

Details of the protein identification parameters, and the bioinformatic and statistical analyses are provided in Chapter 2, and have been briefly outlined here. Raw data from LC-MS/MS analyses were informatically processed using MaxQuant (Version 1.5.3.30) software and integrated search engine, Andromeda (319, 320). MaxQuant was selected for this analysis as it is a quantitative proteomics software package that has been designed for analysing large MS data sets (321). Briefly, Thermo raw files obtained from individual LC-MS/MS analyses were uploaded to MaxQuant, where the depleted and eluted protein fraction files for an individual were recombined as one file for proteomic analysis.

Search parameters and settings were: default settings for orbitrap instrument, two missed cleavages allowed, carbamidomethylation was set as fixed modification, and methionine oxidation and deamidation as variable modifications. Target decoy reverse database search was applied with a peptide and protein FDR <0.05. The 'match between runs' feature was also activated. Label-free quantitation was performed with a minimum ratio count of 1 (322).

The 'match between runs' feature enables the transfer of peptide identifications from an LC-MS run, where a peptide was identified by MS/MS, to a different LC-MS run file, where MS/MS data was not acquired for this peptide, or no peptide was assigned (321, 323). This increases the number of peptides available for quantification, thereby producing a more complete quantitative profile across samples (321). 'MaxLFQ' is the label-free quantification (LFQ) technology incorporated in the MaxQuant workflow for comparative proteomic analyses (322). Briefly, LFQ intensity is the relative protein quantification across all samples, and is represented by a normalised protein intensity profile (321).

Custom proteome database

A custom proteomic database was prepared in-house by concatenating three reference proteomes: human, *O. volvulus* and *Wolbachia* endosymbiont of *O. ochengi*. A common contaminants database provided by MaxQuant was also used during database searching.

Bioinformatic analysis: Perseus

The protein identifications from MaxQuant were uploaded to Perseus software (Version 1.5.2.6), which is provided as part of the MaxQuant computational platform for data analysis (324). Protein grouping is automatically applied in MaxQuant. Proteins marked as 'only identified by site' and 'reverse' were filtered out of the data matrix. Proteins marked as 'contaminants' were screened, and the majority filtered out. Proteins with >1 unique peptide were retained and the LFQ intensities of the final data set were $\log_2$ transformed.

For a potential biomarker of onchocerciasis infection and infection clearance following treatment, we sought:

i) Proteins that were present at baseline and absent at one or more successive time points.

ii) Proteins that statistically significantly changed (P = <0.05) over time, with >1.5 fold change in protein abundance between the time points.

Data imputation was performed within Perseus ahead of conducting statistical analyses. Imputation was achieved by simulating random low abundance protein intensities meant to mimic protein expression below the detection limit (324).

Functional analyses of *Onchocerca volvulus* proteins

UniProt BLAST search was used to assess sequence conservation between the *O. volvulus* proteins experimentally identified here and proteins of geographically relevant parasite species, such as *L. loa*, *W. bancrofti* and STHs (325). Other filarial species that are not endemic to Africa or not infective to humans were excluded from this analysis. The percentage sequence similarity over the total protein length of the top BLAST protein hit for each *O. volvulus* protein was determined with the Clustal Omega global alignment tool (326). The UniProt Peptide Search tool was used to verify whether *O. volvulus* peptides experimentally detected were also present in proteins from other relevant parasite species. Gene ontology searching was performed using the EBI QuickGO web-browser (327). Data from the recent stage-specific proteome analyses of *O. volvulus* by Bennuru and colleagues (269) was also used in our bioinformatic analyses.

Statistical analysis

The reproducibility of the LFQ values between any two LC-MS/MS runs was assessed using scatter plots of protein LFQ intensities to calculate R^2 values (322). To compare changes in protein abundance between the trial sampling times for the imputed data set, multiple paired t-tests were used for pairwise comparisons of all time points. Volcano plots were used to plot $-\log_{10}$ transformed p-values against $\log_2$ fold change in average protein intensity between two time points. Principal component analysis (PCA) and unsupervised hierarchical clustering were also conducted on imputed data in Perseus.

Results

Protein identification

To identify potential protein markers of *O. volvulus* infection and infection clearance, plasma from five individuals with onchocerciasis sampled at baseline and at successive time points following macrofilaricidal treatment were analysed using LC-MS/MS. MaxQuant/Andromeda proteomic software searched 691081 spectra in 40 LC-MS/MS analyses, which identified 141658 PSMs in total, corresponding to 4062 distinct peptides. The use of different plasma/serum samples, sample preparation, depletion, fractionation, and bioinformatic analyses in proteomics experiments are known to result in significantly different proteins being identified (381). However, the data output here is line with what we could expect based on the data from the HUPO Plasma Proteome Project (362) and Plasma PeptideAtlas (381). Proteins identified as ‘reverse’, ‘only identified by site’, and most common contaminants were removed from the data set. Albumin, gelsolin, hornerin and thrombospondin-1, although marked as contaminants, were included in the data set as they can localise extracellularly and appeared consistently among the samples. Protein identifications after filtering are provided in Table S4.

The resultant filtered output yielded a total of 1165 proteins corresponding to 352 protein groups with one or more unique peptide, and an FDR <0.05% at the peptide and protein level. Eighty-one percent of proteins were identified by two or more peptides. Of the proteins identified, 336 (95.5%) were of human origin, 16

(4.5% of the data set) originated from *O. volvulus*, and none were detected from *Wolbachia* (Table 4.2). The onchocerciasis plasma proteome contained 80 Ig accessions (22.7%), six accessions (1.7%) with a variant/isoform/alternative peptide sequence from the canonical protein form, and 17 uncharacterised proteins (4.8%). A total of 89357 PSMs were detected for the included proteins, corresponding to 2771 unique peptides and a total of 4001 peptides in the entire data set. The protein groups were identified primarily by MS/MS, with 64% of the data set having associated PSMs and 23% identified using the match-between runs feature, leaving only 13% missing values in the data set.

Proteome	**Protein groups**	**Ig accession**	**Protein variant**	**Uncharacterised protein**	**Unique peptides**	**Peptides**
Human	336	80 (23.8%)	6 (1.8%)	3 (0.9%)	2749	3979
O. volvulus	16	0	0	14 (87.5%)	22	22
Wolbachia	0	0	0	0	0	0
Total	352	80 (22.7%)	6 (1.7%)	17 (4.8%)	2771	4001

Table 4. 2. Protein identifications in the onchocerciasis plasma proteome.
The contributions of the three reference proteomes to the total data set are shown. The table details the total number of protein groups identified and the number per proteome. The total number of protein groups and the number contributed by individual reference proteomes for Ig accessions, protein variants and uncharacterised proteins are also listed, along with the number of unique peptides and peptides in the data set. The proportion of a protein subset (i.e. Ig accession) within each proteome is also detailed.

Quality assessment of the proteomic analysis

Prior to analysis of the data set, experimental variability was assessed using scatterplots for pairwise comparison of $\log_2$ transformed LFQ protein intensities between the 20 samples. The coefficient of determination (R^2) for multi-scatter plot comparisons ranged between 0.898-0.989, indicating a strong positive association between intensities of individual proteins identified across different samples, and that the protein quantification in the untargeted analysis had good reproducibility (Fig. S1). The distribution of protein intensities in each sample was examined by

plotting histograms to confirm an approximately normal distribution (Fig. S2). The total number of proteins detected across different patients at a given time point ranged between 261–302, with a data set average of 289 ± 9.631 (SD) proteins identified (Fig. 4.2). This showed there was generally good concurrence in the numbers of proteins identified.

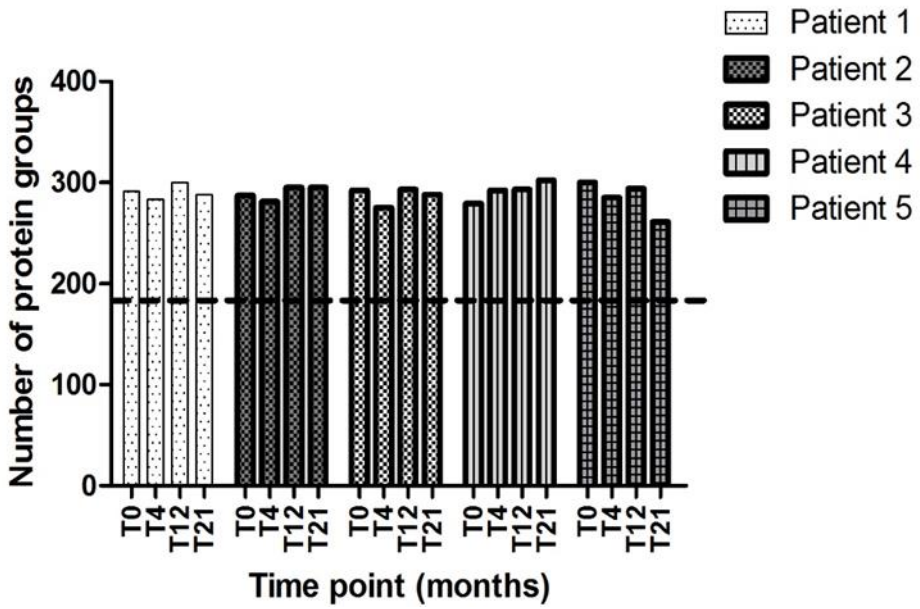

Fig. 4. 2. Number of protein groups identified in each individual at each time point. Of the 352 protein groups identified, 182 (51.7%) were identified in all patients at all time points. The core proteins in this data set are indicated below the horizontal dashed line. T0, baseline; T4, month four; T12, month 12; T21, month 21.

The onchocerciasis plasma proteome

The top 20 most abundant proteins in the onchocerciasis plasma proteome are listed in Table 4.3. The top abundant proteins were identified by descending order of total PSMs to determine which proteins were identified most frequently by MS/MS in all samples collectively. These proteins encompass 54055 (60.5%) of the total PSMs used for peptide assignment. All of the top 20 proteins identified in the onchocerciasis plasma proteome are secreted human proteins, however only six (complement C3, albumin, α2-macroglobulin, serotransferrin, fibrinogen, apolipoprotein A-I) are among the 22 most abundant proteins in plasma. Albumin was the 2nd most abundant protein here, and only five of the 12 top abundant proteins that were targeted for depletion were identified (same as the previous listed minus

complement C3). Furthermore, no Ig accessions were in the top 20 most abundant proteins. Therefore, our fractionation of plasma prior to LC-MS/MS analyses enabled more low abundance proteins to be identified. All 12 depleted abundant proteins were still consistently detected in every patient at every time point. The core proteome included 177 human proteins (97.3%) and five *O. volvulus* proteins (2.7%) that were present in every individual at every time point. The remaining proteins consisted of 159 from human (93.5%) and 11 from *O. volvulus* (6.5%).

No.	Accession	Description	Protein coverage (%)	No. peptides	Total PSMs
1	P01024	Complement C3	72.7	135	10181
2	P02768	Serum albumin	94.6	111	9834
3	P01023	Alpha-2-macroglobulin	71.6	95	4708
4	P02787	Serotransferrin	83	83	3451
5	P02790	Hemopexin	66.9	29	3041
6	P02671	Fibrinogen alpha chain	51.7	46	1893
7	P00747	Plasminogen	69.8	60	1856
8	P01042	Kininogen-1	43.2	37	1826
9	P02749	Beta-2-glycoprotein 1	60.9	22	1771
10	P04217	Alpha-1B-glycoprotein	58.2	19	1732
11	P04196	Histidine-rich glycoprotein	55.8	26	1708
12	P01008	Antithrombin-III	56.2	37	1684
13	P02647	Apolipoprotein A-I	77.2	32	1650
14	P01011	Alpha-1-antichymotrypsin	40.9	22	1554
15	P02675	Fibrinogen beta chain	79.4	45	1299
16	P01031	Complement C5	43.1	65	1227
17	P00734	Prothrombin	60.1	32	1223
18	P19823	Inter-alpha-trypsin inhibitor heavy chain H2	38.1	35	1206
19	P02765	Alpha-2-HS-glycoprotein	49	12	1124
20	P43652	Afamin	45.4	31	1087

Table 4. 3. The 20 most abundant proteins in the onchocerciasis plasma proteome. The 20 most abundant proteins collectively detected across the data set was determined by the total number of PSMs identified by MS/MS per protein across all samples.

Longitudinal analysis: the search for a biomarker

To identify potential markers of infection and infection clearance in the onchocerciasis plasma proteome, the data set was first screened in search of proteins that were present in all five individuals at baseline and absent at one or more follow-up time points. However, no *O. volvulus* or human proteins met this criterion. Proteins that were identified as distinct to a single time point were human proteins found to be only present in one individual (Table 4.4), indicating that their appearance was not a consequence of infection or treatment.

Time point	Accession	Description	% Protein coverage	No. peptides	No. patients
0	P02452	Collagen alpha-1 (I) chain	1.2	2	1
4	A0A0C4DH31	Protein IGHV1-18	12	2	1
4	P01593	Ig kappa chain V-I region AG	27.8	3	1
4	Q8NH87	Olfactory receptor 9G1	6.9	1	1
12	A6NKQ9	Choriogonadotropin subunit beta	36.4	3	1
12	A0A075B6J0	Protein IGLV1-40	31.4	2	1
21	A0A075B7D8	Protein IGHV3OR15-7	18.5	2	1
21	A0A0B4J1X8	Protein IGHV3-43	18.6	2	1
21	J3KN67	Tropomyosin alpha-3 chain	22.5	8	1
21	P31749	RAC-gamma serine/threonine-protein kinase	8.7	1	1
21	Q96CW1	AP-2 complex subunit mu	3.1	1	1
21	A0A087WVW2	Ig gamma-3 chain C region	3.1	1	1

Table 4. 4. Proteins present at only one of four time points in the trial.
Proteins specific to an individual time point and the number of individuals the proteins were detected in. T0, baseline; T4, month four; T12, month 12; T21, month 21.

A presence/absence based assessment was next used to identify changes in protein detection frequency among individuals at each time point. Proteins that were present in ≥80% individuals at a time point, that showed ≥60% increase/decrease in the detection frequency among individuals at another time point of the study were

investigated further. Thirteen proteins met this criterion, 10 from human and three from *O. volvulus*. Of the human proteins, 60% declined in detection frequency among individuals at month four relative to baseline, but were detected in more individuals again at months 12 and 21 (C-reactive protein, leukocyte immunoglobulin-like receptor subfamily A member 3, peroxiredoxin-2, prostaglandin-H2 D-isomerase, TBC1 domain family member 2A and vascular cell adhesion protein 1). Two human proteins also increased in detection frequency from baseline over the duration of the study (14-3-3 protein epsilon and fibrous sheath-interacting protein 2). Among the three *O. volvulus* proteins, two (A0A044SN57 and A0A044U885) declined in frequency of detection at month 21 relative to the earlier time points, while one protein (A0A044TBP5) was present in all five individuals at months four, 12 and 21, but only two individuals at baseline. No human proteins showed a convincing decline or increase in detection among individuals to indicate a change as a result of 'infected' vs 'treated'. Although it is a small sample set, the three *O. volvulus* proteins showed interesting detection frequency profiles among individuals, with a change by month 21.

In order to statistically infer differential protein expression over time, the data matrix was further filtered down to 269 proteins based on detection in at least three of the five patients at every time point. The 269 proteins included 261 (97%) human proteins and 8 (3%) from *O. volvulus*. Missing values, that were here considered to be below the limit of detection, were imputed by simulating random numbers meant to mimic LFQ intensities of low abundance proteins (324). Correct imputation of low abundance LFQ values and normal data distribution was confirmed by visualising a histogram of LFQ intensities for each sample (Fig. S3). Multiple paired t-tests were used to conduct pairwise comparisons of differential expression of individual proteins between each of the time points. The average fold-change versus significance for proteins was visualised in volcano plots (Fig. 4.3). Proteins were considered to be potentially interesting here if the change in expression was statistically significant ($P = <0.05$) and a fold change in average expression >1.5 was observed. Only one protein, haemoglobin subunit β, met this criterion in one pairwise comparison ($P = 0.0082$; 1.95 fold decrease in abundance from baseline to month four). Haemoglobin subunit β had statistically significantly declined from baseline to month four of sampling. Haemoglobin indicates lysis of erythrocytes in

the plasma samples, and this result is likely indicative of various degree of haemolysis detected between different samples. Haemoglobin subunit α also decreased 2 fold in abundance by month 12, although this was not statistically significant (P = 0.0514).

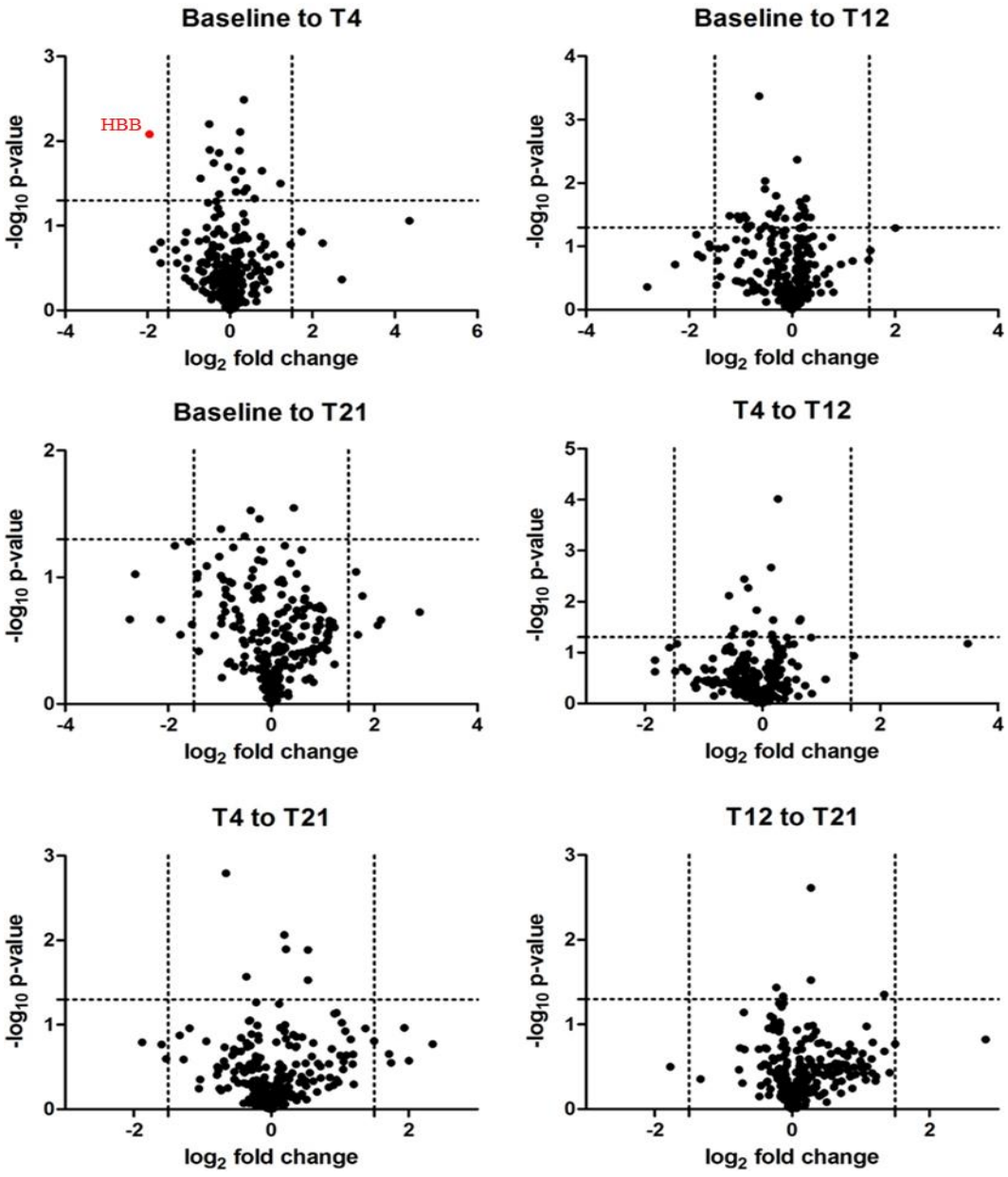

Fig. 4. 3. Statistical evaluation of protein expression level changes over time.
Volcano plots displaying the results of multiple paired t-tests for pair-wise comparison of changes in protein intensities between each time point. The p-value was transformed to the negative $\log_{10}$ scale and plotted on the y axis, and the $\log_2$ fold change in mean protein intensity between two time points was plotted on the x axis: horizontal and vertical lines indicate p values <0.05 and fold change >1.5, respectively. Red dots signify proteins with a

statistically significant change in expression and >1.5 fold change in the averaged protein abundance between a given sampling period, while black dots represent proteins that did not. Therefore, only one protein, haemoglobin subunit β (HBB), met this criterion between baseline and month four. T4, month four; T12, month 12, T21, month 21.

Onchocerca volvulus proteins in plasma

Although no clear biomarkers of infection clearance or treatment efficacy were identified in this study, 16 protein markers of *O. volvulus* infection were identified. We sought to evaluate these 16 proteins further by assessing LFQ protein intensity profile plots and further investigating what is currently known about the *O. volvulus* proteins.

Averaging patient LFQ intensities for individual *O. volvulus* proteins at each time point showed that the relative abundance of all parasite proteins was fairly stable over time (Fig. 4.4). Although missing values for the proteins that were not consistently detected means this is not a true representation of this population average, there was still no notable change in the mean protein abundance at any sampling time. One exception was protein A0A044U885, ribonucleoside-diphosphate reductase, which showed a 2-fold decline in the average abundance from baseline to four months, and then a very gradual increase at both months 12 and 21. However, a 6-fold decrease in patient 2 skewed the average fold change at month four, and by month 12 A0A044U885 was detected at near baseline values again in this patient. Earlier longitudinal analyses in this study identified A0A044U885 as a protein that declined in patient detection frequency at month 21 relative to the preceding time points. The protein was detected in three patients at baseline, four patients at months four and 12, but only one patient at 21 months.

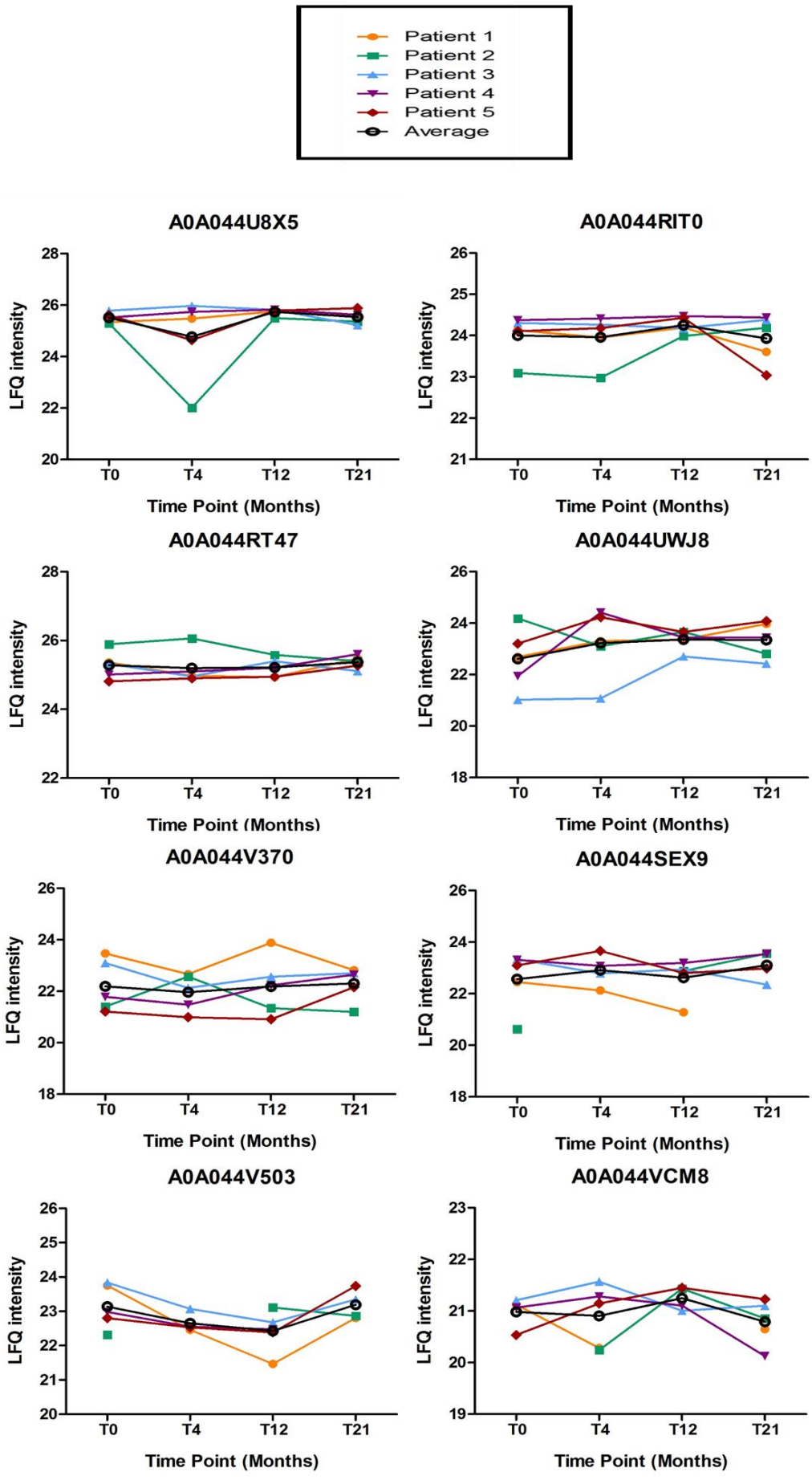
Patient 1
Patient 2
Patient 3
Patient 4
Patient 5
Average
A0A044U8X5
A0A044RIT0
A0A044RT47
A0A044UWJ8
A0A044V370
A0A044SEX9
A0A044V503
A0A044VCM8
LFQ intensity
Time Point (Months)
T0
T4
T12
T21

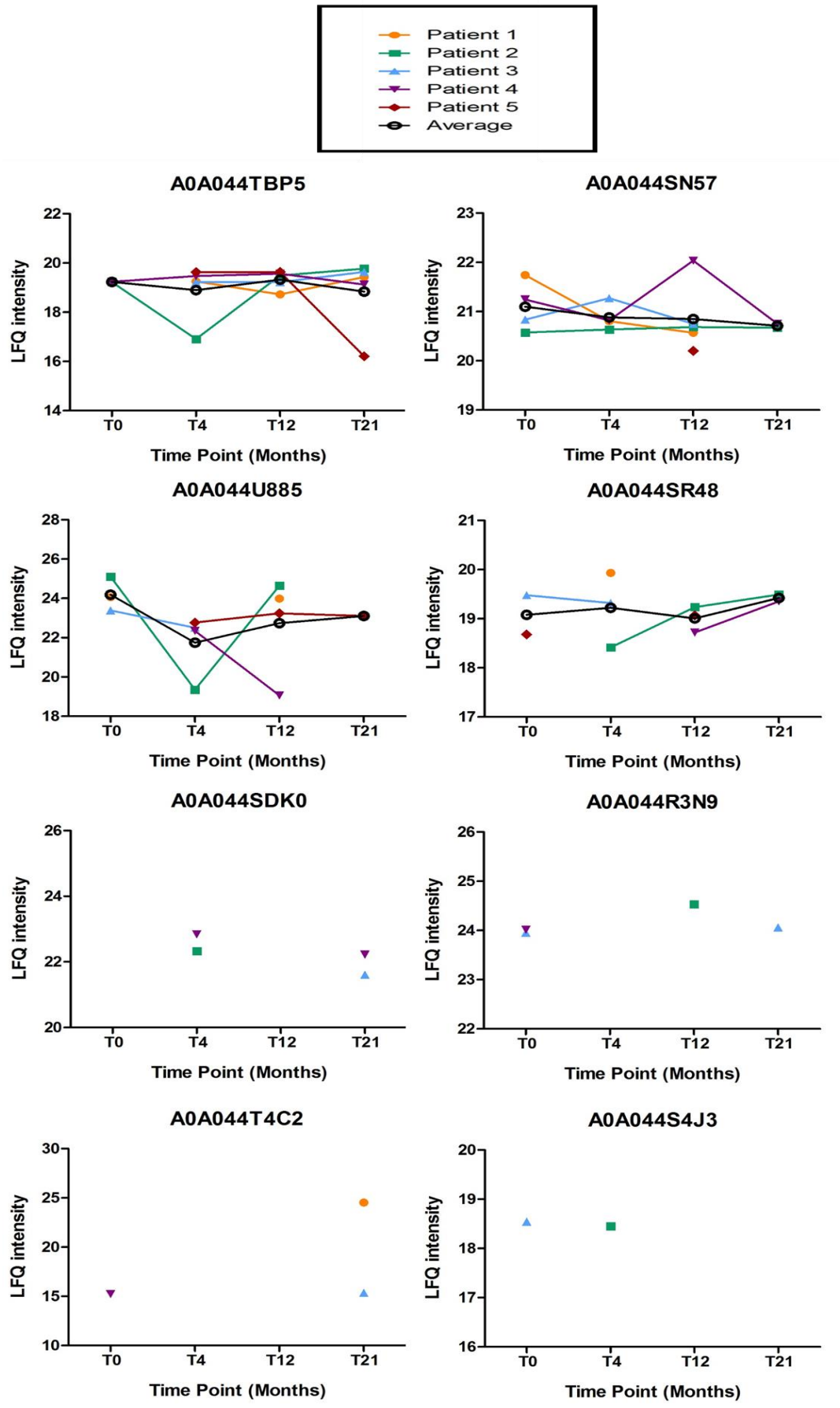
Patient 1
Patient 2
Patient 3
Patient 4
Patient 5
Average
A0A044TBP5
A0A044SN57
A0A044U885
A0A044SR48
A0A044SDK0
A0A044R3N9
A0A044T4C2
A0A044S4J3
LFQ intensity
Time Point (Months)
T0
T4
T12
T21

Fig. 4. 4. Profile plots of *O. volvulus* proteins in plasma.
The relative quantitative value (LFQ intensity) of individual *O. volvulus* proteins was plotted for the frequency of appearance and abundance profile in each patient over time. The averaged protein profile is included where there are sufficient data points.

The protein accessions from *O. volvulus* were searched using EBI Quick-GO to gain insight into the cellular origin within the parasite, and the biological processes and functions that they may be involved with. All the parasite proteins identified in this data set were TrEMBL accessions, therefore all annotations were obtained electronically from predicted or partially confirmed proteins. The search identified annotations for 10, 11 and 10 of the proteins for cellular compartment, biological process and molecular function, respectively. An overview of the main GO terms identified for all proteins are provided in Fig. 4.5, and the complete list of GO terms identified for each protein is provided in Table S5. Of the annotated proteins, the majority were membrane-associated or nuclear, and the remaining were intracellular and cilium-related. The biological processes identified were diverse, but proteins linked to multicellular organism development, protein modification and transport were the most frequently observed processes. Response to stress, reproduction, signal transduction and oxidation-reduction processes were less frequently observed among the proteins. Binding was the predominant molecular function, followed by catalytic and receptor activity. There was no obvious link between the biological processes or molecular functions of the five proteins consistently detected across the data set.

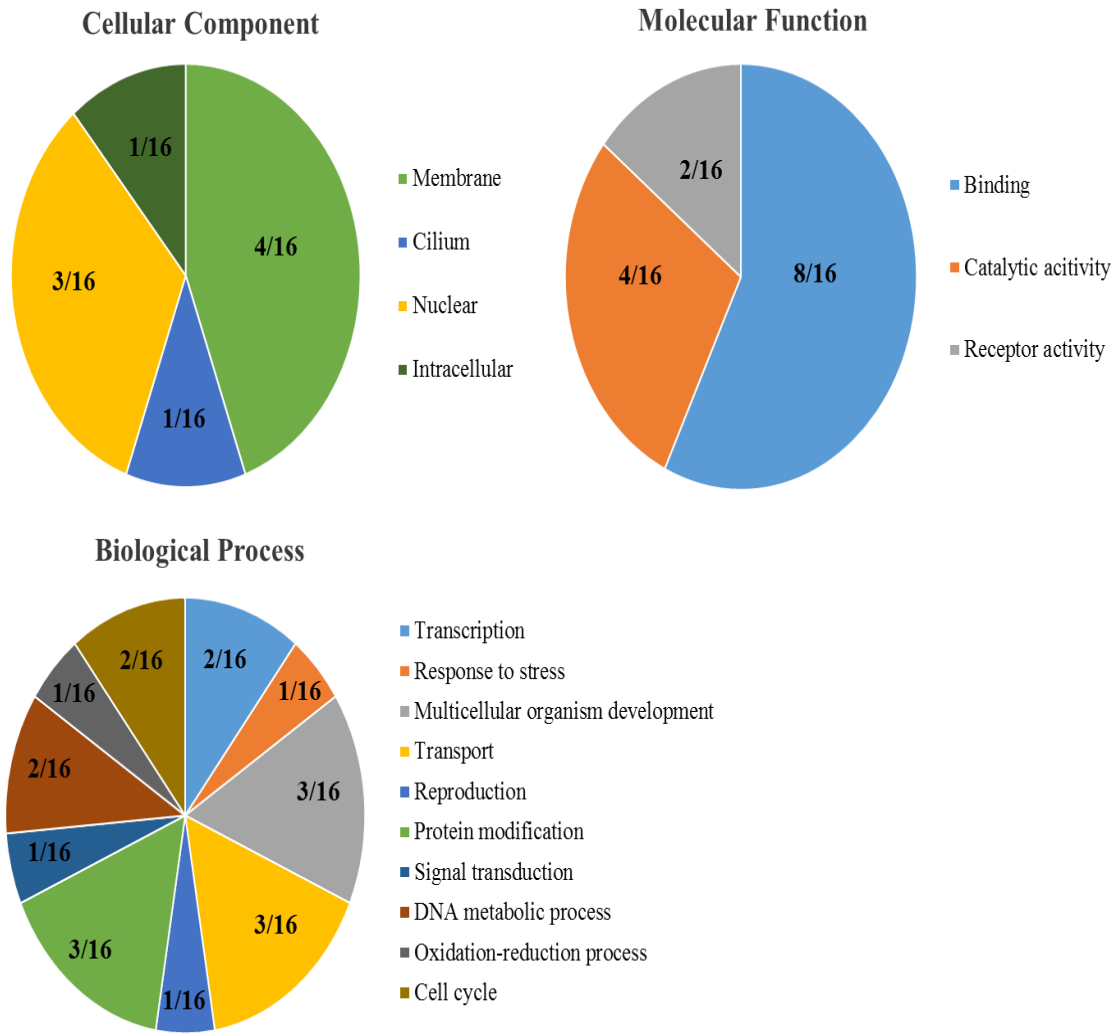

Fig. 4. 5. Overview of GO annotations for the *O. volvulus* proteins.

The cellular compartment, molecular function and biological process GO terms were investigated for the 16 *O. volvulus* proteins. Gene ontology searching of protein accessions was performed using the EBI QuickGO web-browser with no search restrictions.

The 16 *O. volvulus* proteins identified in the host plasma here were also identified in a recent stage-specific proteomic analysis of *O. volvulus* (269). We searched this large and comprehensive bioinformatic data set to try and obtain information pertinent to our proteins. Their stage-specific analysis revealed that the expression of 1 and 10 of the proteins identified here were enriched in the female and male worms, respectively, relative to the other stages. The remaining five proteins were enriched in the mf, L1 or L2 stages. An uncharacterised 11 kDa protein, A0A044VCM8, was highly associated with expression in female worms, and this protein functions in cytochrome-c oxidase activity and copper ion binding. Bennuru and colleagues also reported that cytochrome c oxidase activity was enriched in the adult females compared to all other stages (269). This may provide preliminary evidence for the identification of a female worm protein in the host plasma. Furthermore, A0A044VCM8 was identified relatively consistently (in 4-5 individuals) at every time point, and could be a potential marker for assessing the infection prevalence of adult female *O. volvulus*. Four of the five proteins that were present in every individual across the duration of the trial were enriched in the adult males relative to all other stages. Two of these proteins, A0A044RT47 and A0A044U8X5, were annotated, and reportedly function in nucleic acid binding and protein tyrosine phosphatase activity, respectively. This ties in with the findings by Bennuru *et al* that identified nucleotide binding, peptidase activity and phosphoprotein phosphatase activity as the top GO processes enriched in adult male *O. volvulus* (269). The *O. volvulus* proteins that were either detected less frequently in individuals at baseline (A0A044TBP5) or less frequently at month 21 (A0A044SN57 and A0A044U885) relative to other time points were also enriched in the adult males. A0A044TBP5 functions in DNA and zinc ion binding, transcription factor activity, steroid hormone receptor activity. A0A044SN57 functions in catalytic activity, Rab geranylgeranyltransferase activity, protein kinase activity and ATP binding. A0A044U885 functions in ribonucleoside diphosphatereductase activity, ATP binding and oxidoreductase activity.

The stage-specific *O. volvulu*s data set from Bennuru *et al* was also further evaluated to identify whether any of our proteins had been recognised as a secreted protein using SignalP-HMM prediction (269, 328). All 16 *O. volvulus* proteins detected in the onchocerciasis plasma proteome are not predicted to be secretory

proteins. Consequently, there is not an obvious presence of secreted proteins, and so the *O. volvulus* proteins are either derived from excreted products or released from moribund or dead parasites.

Specificity of *Onchocerca volvulus* proteins

The *O. volvulus* proteins and the peptides used for protein identification were evaluated using BLAST and global alignment tools to evaluate sequence conservation among other relevant parasite species. The top BLAST hit among geographically relevant parasite species (such as *W. bancrofti*, *L. loa* and STHs, as described in the Methods) and percentage sequence identity are listed (Table 4.5). All *O. volvulus* proteins experimentally identified here showed the highest levels of sequence conservation with *L. loa* or *W. bancrofti*, two filarial nematodes with overlapping geographical distributions to *O. volvulus.* Thirteen (81.3%) of the *O. volvulus* proteins had a high level of sequence identity (>70% ID) to orthologs from *W. bancrofti* or *L. loa*. However, only five (38.5%) of these proteins had a high level of sequence similarity along the total length of the *O. volvulus* protein (>70% length). Therefore, although the majority of the *O. volvulus* proteins had highly conserved sequence segments, 10 (62.5%) of the 16 proteins had peptide sequences that were not highly conserved along the total length of the protein. Additionally, a search of the peptides identified from our LC-MS/MS analyses revealed that only 4 (25%) are present in other relevant parasites, thus providing more confidence that the proteins identified were indeed from *O. volvulus*. The peptide sequences are provided in Table S6.

Encouragingly for a potential marker for female worm infection, a protein identified here that was previously found to be enriched in female worms, A0A044VCM8, had only 26.3% total sequence similarity with the top BLAST hit protein from *L. loa*. Although the peptide of A0A044VCM8 identified by LC-MS/MS was also found to be present in *L. loa* and *W. bancrofti,* individuals evaluated here were negative for co-infective mf . The *O. volvulus* protein that was detected less frequently in individuals at baseline relative to other time points, A0A044TBP5, had a high level of sequence identity and sequence similarity along the protein length with a *L. loa* protein (79.5% ID, with 87.5% similarity over the protein length). Of the two *O. volvulus* proteins detected less frequently at month 21

compared to all earlier time points, A0A044SN57 had a high level of sequence identity with a *L. loa* protein, but a low level of sequence similarity over the total length of the protein (88.2% ID, with 35.0% similarity over the protein length), while A0A044U885 had both high levels of sequence identity and similarity (90.7% ID, with 94.3% similarity over the protein length) with a *L. loa* protein. The peptides identified by MS/MS for A0A044TBP5, A0A044SN57 and A0A044U885 were only found in *O. volvulus* among the relevant parasite species.

***O. volvulus* proteins**			**Top BLAST hit**		**Global Alignment**		
Accession	**Peptide length**	**Protein length**	**Species**	**% ID**	**% Length**	**Length of similarity**	**Peptide search (100% identity)**
A0A044U8X5	15	491	*L. loa*	73.1%	86.8%	426	None
A0A044RIT0	12	902	*W. bancrofti*	84.1%	22.4%	202	None
A0A044RT47	20	403	*W. bancrofti*	46.2%	36.7%	148	None
A0A044UWJ8	14	954	*L. loa*	66.0%	84.4%	805	None
A0A044V370	10	1,622	*W. bancrofti*	88.1%	31.9%	517	None
A0A044SEX9	17	1,499	*W. bancrofti*	84.4%	71.2%	1068	*L. loa*
A0A044VCM8	11	99	*L. loa*	92.3%	26.3%	26	*W. bancrofti* *L. loa*
A0A044V503	9	1,204	*L. loa*	93.8%	98.6%	1187	*W. bancrofti* *L. loa*
A0A044TBP5	25	542	*L. loa*	79.5%	87.5%	474	None
A0A044SN57	13	932	*L. loa*	88.2%	35.0%	326	None
A0A044U885	13	1,013	*L. loa*	90.7%	94.3%	955	None
A0A044SR48	16	697	*W. bancrofti*	75.4%	22.8%	159	None
A0A044R3N9	10	199	*L. loa*	90.8%	65.8%	131	*L. loa*
A0A044SDK0	21	476	*L. loa*	82.3%	30.9%	147	None
A0A044T4C2	32	428	*W. bancrofti*	89.5%	13.8%	59	None
A0A044S4J3	11	485	*W. bancrofti*	69.7%	18.1%	88	None

Table 4. 5. Specificity of the 16 *O. volvulus* proteins detected in plasma.

The 16 *O. volvulus* proteins, with the length of peptide experimentally identified and the length of parent protein (number of amino acids) recorded. The top BLAST hit among relevant parasite species, and the percentage of sequence identity is listed. Clustal Omega global alignment of the top BLAST hit and the *O. volvulus* protein was used to determine the number of identical and similar sequences and calculate the percentage sequence similarity along the total length of the protein. The peptides experimentally identified for *O. volvulus* by LC-MS/MS were also searched for sequence conservation among relevant parasite species. All *O. volvulus* proteins identified shared high sequence identity to orthologs from *L. loa* or *W. bancrofti*, however 10 of the 16 proteins had peptide sequences that were not highly conserved along the total length of the protein. The majority of the peptides identified by LC-MS/MS, from which the *O. volvulus* proteins were inferred, were also not found in

other relevant species, and therefore they can be confirmed as circulating *O. volvulus* proteins.

Intra- and inter-individual variability of the plasma proteome

In the absence of any candidate biomarker meeting our criteria, unsupervised hierarchical clustering was performed to elucidate grouping among samples and visually identify any patterns in the data. Clustering of protein expression levels by individual patients rather than by time point was evident (Fig. 4.6A). This indicated that overall, the plasma proteomes did not cluster by time, but there was considerably higher inter- rather than intra-individual variability. Principal component analysis (PCA) was also used to investigate underlying differences between samples. The most obvious grouping was observed in all plasma samples taken from patient 3, while an individual sample from patient 2, 4 and 5 appeared to be outliers (Fig. 4.6B). These same samples also showed distinct branching in the hierarchical clustering.

Inspection of the drivers of the PCA separation revealed that complement factor H-related protein 1, haemoglobin subunits α and β, pregnancy zone protein (PZP), and a canonical and a variant sequence of α1-antitrypsin 1 were the main outliers. A natural variant of α1-antitrypsin 1 with a single amino acid difference was identified in all individuals except patient 3, while the canonical peptide sequence was not detected in patient 5. Complement factor H-related protein 1 was also 5-6 fold higher in patient 3 at months 12 and 21 compared to in the other patients. Similarly, there was up to a 6 fold difference in relative abundance of haemoglobin α and β between different individuals, likely due to varying degrees of haemolysis between plasma samples. The relative protein abundance of PZP in both female patients (2 and 5) was on average 3.6 - 4.6 fold higher than in the male patients (1, 3 and 4) over the duration of the study. PZP is one of the main pregnancy associated proteins, and is present in plasma at higher concentrations in pregnant and non-pregnant females relative to that in males (382). The six protein outliers were removed and the analyses repeated; however, intra-individual proteome similarity was still the main driver of clustering and correlation among protein expression levels. Although such heterogeneity is not ideal, our label-free workflow was robust enough to capture the natural variation of protein abundances and isoforms between individuals.

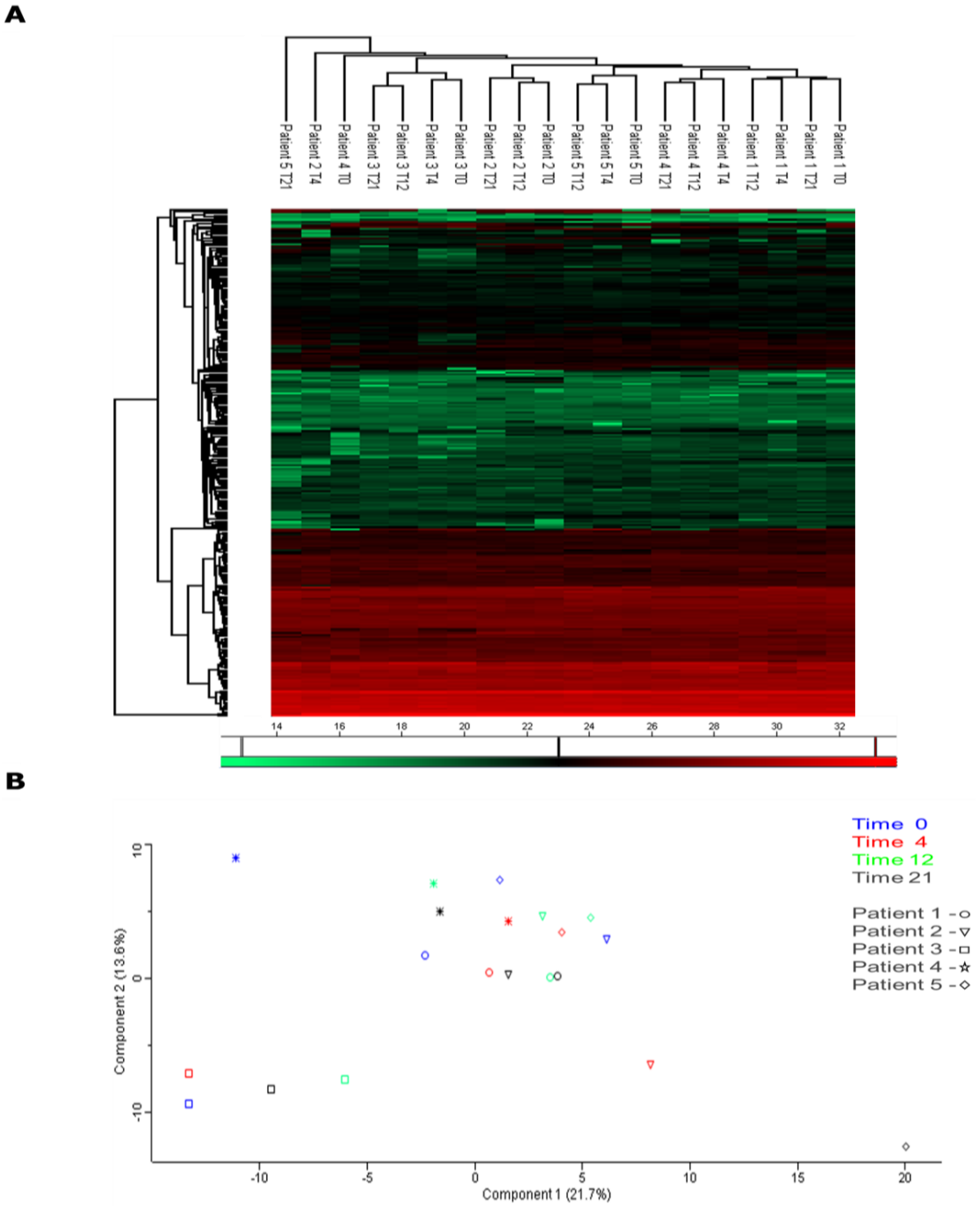

Fig. 4. 6. Unsupervised hierarchical clustering and principal component analysis.

A. Unsupervised hierarchical clustering identified clustering by individual patients rather than by time point, indicating considerable inter-individual variability of plasma proteomes. Scale represents $\log_2$ relative protein intensities from highest (red) to lowest (green).

B. PCA of the LFQ intensities at baseline (blue); month four (red); month 12 (green); and month 21 (black). Individual patients are indicated by: Patient 1 (circle); Patient 2 (triangle); Patient 3 (square); Patient 4 (star); Patient 5 (diamond). PCA did not differentiate by any time point, but samples from patient 3 were grouped, while three other plasma samples were notable outliers.

Discussion

The work presented here describes a shotgun LC-MS/MS analysis of the onchocerciasis plasma proteome, and for the first time, an assessment of the longitudinal effect of macrofilaricidal treatment on the host plasma proteome. Sixteen proteins from *O. volvulus* were detected in the plasma of individuals with onchocerciasis, while proteins from the *Wolbachia* intracellular bacteria of the worm were not detectable. Five *O. volvulus* proteins were identified consistently in all individuals at every time point over the two year period following doxycycline treatment, and a further three identified in nearly all individuals over two years. Three *O. volvulus* proteins changed in detection frequency among individuals by month 21; two proteins were detected less frequently at the final follow-up while one protein was detected in more patients at months four, 12 and 21 relative to baseline. Potential parasite protein candidates for infection prevalence and ongoing infection clearance were therefore identified in this data set. However, the onchocerciasis plasma proteome was found to be largely unchanging over 21 months following macrofilaricidal treatment, as no parasite or human proteins statistically significantly changed in abundance over time, and no proteins were present in all individuals at baseline and absent at a later time point.

The current study aimed to track the dynamic profile of onchocerciasis protein markers over time in the host following macrofilaricidal treatment, using an unbiased proteomic analytical approach. However, the statistical analyses identified only one human protein between baseline and month four that met our candidate criteria for a biomarker, showing a statistically significant difference in protein relative abundance, with >1.5 average fold change between the time points. This protein was haemoglobin subunit β, and the differential expression will be as a result of varying degrees of haemolysis between individual samples. Assessment of the protein detection frequency among individuals at each time point showed that no human proteins declined or increased in detection among individuals to indicate macrofilaricidal treatment efficacy. Three worm proteins were either more or less frequently detected among individuals by month 21 relative to baseline. Two *O. volvulus* proteins, A0A044SN57 and A0A044U885, were the closest to an indicator of treatment efficacy, as these proteins were detected less frequently among the five patients at 21 months relative to preceding time points. Conversely, the parasite

protein A0A044TBP5 was detected less frequently at baseline relative to successive time points.

In addition to the three *O. volvulus* proteins as potential indicators of treatment efficacy at month 21, five *O. volvulus* proteins (A0A044U8X5, A0A044RIT0, A0A044RT47, A0A044UWJ8 and A0A044V370) were identified in every individual at every time point, and a further three (A0A044SEX9, A0A044VCM8 and A0A044V503) were identified in almost every individual (4-5 patients) at every time point. These eight proteins could potentially serve as markers of adult worm infection prevalence. Based on the *O. volvulus* proteomic data by Bennuru and colleagues, all but two of the potential parasite markers of infection or infection clearance were shown to be enriched in the adult males relative to other worm stages, and one to be enriched in the female and one during the mf stage (269). Therefore, the higher expression in the male worms relative to females indicates that the majority of these proteins may not be circulating markers of adult female worms. However, one 11 kDa uncharacterised protein consistently detected over time, A0A044VCM8, is enriched in female worms compared to the other worm stages (269), and could potentially serve as a circulating marker of adult female worm infection. This protein is annotated as a membrane protein. As five individuals is a very small sample size, these observations would need to be verified in a larger cohort to verify the consistency of the findings.

The stage-specific *O. volvulu*s data set from Bennuru *et al* was also evaluated to identify whether any of our parasite proteins had been recognised as a secreted protein (269, 328). Approximately 20% of *O. volvulus* genes are believed to be secreted by classical secretion mechanisms, and around 42% are thought to be secreted through non-classical mechanisms (269). Excretory/secretory (E/S) products are released by all filarial worms, and they are important components of the parasite which are involved in diverse functions such as host immune response modulation, host tissue remodelling, alteration of host tissue nutritional status, and larval tissue migration enhancement (383, 384). However, all 16 *O. volvulus* proteins detected here in the onchocerciasis plasma proteome are not predicted to be secretory proteins. Therefore, the *O. volvulus* proteins are either excreted products or released from moribund or dead parasites. Although we did not identify any secreted proteins, the relative concentration of proteins from skin-dwelling parasites will be very low

relative to plasma proteins, even after depletion of the top 12 abundant plasma proteins. Of all the proteins detected in plasma, 4.5% originated from *O. volvulus*. All the *O. volvulus* proteins detected here by LC-MS/MS had less than three peptides used for protein identification, and many were identified by a single peptide. *O. volvulus* proteins in plasma are likely present below the detection limit for MS/MS, and the more abundant peptides of the complex biological mixtures will tend to 'drown out' or suppress ion signals from the less abundant peptides.

All but one of the *O. volvulus* proteins were still present in one or more individuals 21 months after treatment with doxycycline. This indicates adult worms were still present in the host and, actively or not, excreting or shedding proteins. This may mean treatment was not completely efficacious, or that the 21 month follow-up time period was too short to observe a significant change in the onchocerciasis plasma proteome following macrofilaricidal treatment. Filarial worm proteins, such as the CFA marker for *W. bancrofti*, have been shown to markedly decline but not completely clear from plasma by two years following macrofilaricidal treatment (263, 264). Doxycycline is an effective macrofilaricide that permanently sterilises female worms and causes a slow and sustained killing of the adult parasites, causing the worms to die or degenerate after 18–27 months (158). However, it has frequently been observed that not all worms are dead by 21 months follow up. In the Turner *et al* study from which our patient samples originated (157), a 6-week doxycycline (200 mg/day) treatment course resulted in the death of 65% of adult female worms from the seven patients examined at 21 months (157). In another study providing a 6-week course of 200 mg/day doxycycline and ivermectin at six months, no macrofilaricidal effect was observed by six months, while at months 20 and 27 a macrofilaricidal activity in female worms of more than 60% was observed (152). A shorter 5-week course of doxycycline at 100 mg/day resulted in 51% of the female worms still alive after two years, indicating a reduced level of macrofilaricidal activity of doxycycline with this treatment regimen (156). The incidence of new infections in areas with ongoing transmission after treatment with doxycycline could also potentially confound the identification of a biomarker that shows a dynamic change as an outcome of treatment. New drug-naïve adult worm infections can become established over the 21 month period, thus diluting the perceived antifilarial effects and therapeutic efficacy of treatment in different patients evaluated at

different times thereafter (158). Individuals may have deep onchocercomas with live adult worms, or new prepatent infections that are not yet producing mf. Although it is unknown whether these *O. volvulus* proteins are immunogenic and form immune-complexes in plasma, the parasite proteins may have an extended presence in plasma due to an association with immune complexes (385). Different parasite proteins may also have a different half-life in plasma due to the highly size and charge selective glomerular barrier, where filtration of larger proteins is almost totally restricted (386). The molecular weight cutoff for glomerular filtration is believed to be 70 kDa (387), and half of the 16 *O. volvulus* proteins were >70 kDa in mass.

The majority (13 of 16) of the identified *O. volvulus* proteins shared high protein sequence ID with two geographically relevant filarial worms, *W. bancrofti* and *L. loa*. However, 10 of the 16 proteins were shown to have lower (< 70%) sequence similarity along the total length of the protein. The potential marker for female worm infection prevalence, A0A044VCM8, had only 26.3% total sequence similarity with the top matching orthologous *L. loa* protein, while the *O. volvulus* protein detected less frequently at month 21 relative to baseline, A0A044SN57, had a high level of sequence identity with a *L. loa* protein, but a low level of sequence similarity over the total length of the protein (88.2% ID, with 35.0% similarity over the protein length). Although it cannot be directly inferred from our LC-MS/MS analyses whether these proteins are immunoreactive, or the potential for antibody cross-reactivity from total protein sequence similarity, higher levels of sequence homology with co-infective parasite species would render proteins less robust as potential diagnostic candidates. Peptides could be of use as diagnostic markers if one were to raise antibodies to recombinant peptides representing only the nonconserved region(s) of the candidate protein. However, this area of the protein sequence may not contain the epitope(s) that interacts with the antibody, and there still may be a risk of cross-reactivity (271). Achieving the necessary specificity and sensitivity has been a major bottleneck for the development of antigen detection diagnostic test for onchocerciasis (388). For example, a recent multi-omics study that attempted to identify candidate antigens for serodiagnosis of onchocerciasis using immunoprecipitation techniques found 181 of the 241 *O. volvulus* immunoreactive proteins identified in their study shared over 70% amino acid sequence identity over more than 70% of the entire protein length with proteins from geographically

relevant species (271). The issue of specificity has not been limited to onchocerciasis. The ICT, a point-of-care test for detecting lymphatic filariasis CFA has been widely used since the mid 2000's to detect active infection with adult *W. bancrofti*. However, in recent years it has been shown to produce false positives when there is a high infection prevalence of *L. loa* (389, 390). The *O. volvulus* short peptides experimentally detected here using LC-MS/MS were found to be *O. volvulus* specific for 75% of the proteins identified, verifying the definite parasite origin of these peptides.

Notable heterogeneity was observed between the plasma proteomes of individuals from the trial using LC-MS/MS. With the exception of three outlier samples, expression profiles of proteins clearly clustered by the individual rather than time point. Although the inter-individual variability between samples may have hampered the identification of a potential biomarker in the human proteome, these findings confirm that our experimental analyses were robust enough to capture the natural variation between individual patients, and even distinguish between men and women (by differential expression levels of PZP). The plasma proteome is known to have much greater inter- than intra-individual variability (367, 391, 392), and the nature of the disease and treatment under investigation, which included large gaps in time between sampling time points with potential re-infections, make it very challenging to capture and discern potentially relevant changes in protein levels related to treatment. There is also the variability of response to treatment among individuals, for example individuals with lower levels of infection may show a different circulating biomarker profile over time compared to individuals with higher parasite burdens (some may clear the worm protein by 12 months, some >27 months). The host response to onchocerciasis infection will also consist of individual-specific dynamic immune and cellular interactions with the parasite (393, 394). From the host proteome perspective, an additional caveat is that countless diseases provoke the same response, such as inflammation, which are not specific.

In conclusion, of the sixteen *O. volvulus* proteins identified in onchocerciasis plasma proteome, half could be potential markers of infection prevalence as they consistently persisted in individuals over the duration of the trial. One of these uncharacterised proteins, A0A044VCM8, which shares a low level of overall sequence similarity to a *L. loa* protein, could be a marker of the adult female worm.

However, no individual showed a complete absence of parasite proteins at the final follow up, and all but one *O. volvulus* protein was still detected in plasma at 21 months. No proteins met our prespecified biomarker criteria, and a convincing biomarker of infection clearance in the onchocerciasis plasma proteome by 21 months post-treatment was not identified. At least for this sample set, 21 months was too short a follow-up time to observe a macrofilaricidal effect on parasite protein profile in the host plasma. Our findings may be confounded by persisting living worms, persistence of plasma proteins and new worms acquired during the two-year follow-up.

Chapter 5. Nucleic acid markers of *Onchocerca volvulus* in plasma

Abstract

Diagnosis of onchocerciasis has typically been achieved through use of the 'gold standard' skin snip and morphological evaluation of emergent microfilariae (mf) by microscopy. However, this test has reduced sensitivity when mf densities in the skin are low, as is often the case for several months following annual mass drug administration (MDA) with ivermectin. Parasite-derived miRNAs and DNA as potential circulating biomarkers of *Onchocerca volvulus* in blood provide clear benefits over invasive skin snips that do not detect adult worm infections. The aim of this study was to assess whether *O. volvulus* miRNA markers miR-71 and lin-4 (previously identified by sequencing serum from individuals with onchocerciasis in Cameroon) and the specific DNA marker O-150 could be used for diagnosis of onchocerciasis from host plasma. We utilised a longitudinal plasma sample set from Cameroon to assess the potential of the molecular markers for detecting infection at baseline and in the follow up period after receiving microfilaricidal, macrofilaricidal, or a combination of the two treatments. The parasite-derived miRNAs, cel-miR-71-5p and bma-lin-4, were detected in 2.8% of the longitudinal plasma sample set at very low abundance, even after extensive optimisation of the RT-qPCR protocol. The two miRNAs were also detected in RNA extracted from both *Onchocerca ochengi* and *Loa loa* at distinct life cycle stages by RT-qPCR. Cel-miR-71-5p and bma-lin-4 therefore do not have the necessary specificity or sensitivity to be circulating diagnostic markers for onchocerciasis. By comparison, the *O. volvulus*-specific TaqMan qPCR assay for the O-150 repeat DNA sequence identified a higher proportion of individuals at baseline (44.4%) by qPCR in the longitudinal plasma sample set, with a decline in the frequency of positive individuals detected after receiving any treatment. This may indicate mf as a source of circulating DNA. A small number of mf negative participants were also positive by qPCR. However, 62.1% of qPCR negative samples had microfilaridermia. The detection of either parasite-derived miRNAs or DNA in host plasma does not have the necessary sensitivity to be used for diagnostic purposes in elimination 'end game' strategies.

Introduction

Diagnosis of onchocerciasis is typically achieved through use of the 'gold standard' skin snip and morphological evaluation of emergent mf by microscopy. While skin snips are specific and more sensitive than clinical examinations, this test has reduced sensitivity when mf densities in the skin are low (182), as is often the case for several months following annual MDA with ivermectin (231) and in populations with long-term exposure to CDTi. To increase sensitivity, skin snips/skin scratches can be analysed for *Onchocerca* genus-specific 150 bp tandem repeat sequence using PCR (194, 195). Over 4000 copies of this sequence were thought to be present per haploid genome of *O. volvulus* (195), however a recent estimate of the true genome-wide copy number of the O-150 repeats is 5,920 (199). To achieve species-specificity, hybridisation with an *O. volvulus* specific probe can also be used (198). In addition to conventional PCR analysis, real time qPCR assays and loop mediated isothermal amplification (LAMP) methods have been developed for highly sensitive and specific amplification of *O. volvulus* DNA targets (200-204).

Detection of the O-150 repeat sequence in skin snips by molecular testing offers improved sensitivity and specificity over parasitological and immunological methods, however there are also inherent limitations. In order to detect *O. volvulus* DNA from skin snips by PCR, mf must have initially been present in the skin. This test is therefore not appropriate for use for a number of months following ivermectin treatment, and results may also be confounded by DNA detected from dead or dying mf. Furthermore, skin snips are unpopular and invasive, and the procedure has been refused by entire communities (181). An attractive alternative would be the diagnosis of onchocerciasis from a circulating *O. volvulus* molecular marker, where blood sample collection is less invasive and detection is not reliant on the presence of mf in the skin. PCR has been used to detect O-150 DNA repeats from *Onchocerca gibsoni* in cattle serum (395); however, to the best of our knowledge, PCR of the O-150 sequence has solely focussed on skin snips for *O. volvulus* diagnosis in humans. The onchocercomas where adult worms reside are highly vascularised (249, 250), and therefore parasite DNA may be detectable in the blood using a sensitive qPCR platform. The detection of an *O. volvulus*-specific DNA sequence in the host circulation has the potential to identify active infection by adult worms irrespective

of mf status, and the levels of parasite DNA detected may provide an indication of infection intensity.

Another avenue that has been proposed for onchocerciasis diagnostics is the detection of parasite small RNAs in the host circulation. RNA-based methods may be of particular use in diagnosing filarial infections, as this could distinguish active infection, as well as facilitate the identification of species- and stage-specific expression (289, 290). MicroRNAs (miRNAs) are small (~22 nt in length) non-coding RNAs that function as post-transcriptional gene regulators, typically by inducing gene silencing of their target (281). In nematodes, miRNAs have been implicated in several important physiological processes such as development, differentiation and homeostasis, and possibly drug resistance (284). The small RNAs are also present in mammalian extracellular body fluids such as plasma, where they are believed to be particularly stable due to their association with specific proteins or by encapsulation in small lipoprotein vesicles (298, 299). In recent years, it has been established that miRNAs secreted/excreted by parasitic nematodes, including filarial worms such as *O. volvulus, O. ochengi, L. loa, D. immitis, B. pahangi* and *L. sigmodontis*, and trematodes, *S. japonicum* and *S. mansoni*, can be detected in the serum of their respective animal hosts (251, 287, 291, 294-297). In addition, preliminary studies have shown that miRNAs originating from *S. mansoni* enabled the differentiation between uninfected and infected serum in humans (295).

Six *O. volvulus* miRNAs were identified in the serum and plasma of individuals with onchocerciasis from Ghana and Cameroon using Illumina high-throughput sequencing (291). Of these, lin-4 and miR-71 were the only parasite-derived miRNAs identified in the Cameroon serum. These two miRNAs were also detected in bovine nodule fluid from *O. ochengi*, and in the plasma of baboons infected by *L. loa* through deep-sequencing (296), but have not yet been experimentally confirmed in the parasites using RT-qPCR. Although several studies have demonstrated the conserved nature of miRNA secretion by nematodes (251, 287, 291, 296, 307), the identification of novel miRNAs from *O. ochengi* in nodule fluid holds promise that *O. volvulus*-specific miRNAs may also be present in the host circulation (291). Verifying conserved circulating *O. volvulus*-associated miRNAs would therefore provide information on the diagnostic potential of parasite-derived miRNAs for onchocerciasis.

Aim of the study

The aim of this study was to assess the potential of *O. volvulus* nucleic acid markers in host plasma for diagnosis of active infection and antifilarial treatment efficacy. A longitudinal plasma sample set from Cameroon was screened to assess the potential of molecular markers for detecting adult worm infection pre-treatment, and in the two year follow-up period after receiving microfilaricidal (ivermectin), macrofilaricidal (doxycycline), or a combination of the two treatments. Lin-4 and miR-71 were selected as the *O. volvulus* miRNA targets for investigation, as they have previously been detected by sequencing plasma from individuals with onchocerciasis in Cameroon (291). A TaqMan qPCR assay (201) for the *O. volvulus* specific O-150 tandem repeat sequence was selected to detect circulating *O. volvulus* DNA in the host.

Methods

Plasma samples

Plasma from onchocerciasis infected-individuals was collected over 2003 - 2005 as part of a randomised Phase II community based trial conducted in the market town of Widikum, in the North West Province of Cameroon. Full details of the trial and original sample acquisition can be found in the study report (157), and relevant details have been outlined in Chapter 2. In brief, enrolled individuals were aged between 15 - 60 with *O. volvulus* microfilaridermia (>10 mf/mg skin snip), and they were assigned to one of three drug regimens:

(i) DOXY: Doxycycline (2 × 100 mg capsules daily) for six weeks plus non-matching ivermectin-dummy pill at month four (lactose tablet).

(ii) DOXY+IVM: Doxycycline (2 × 100 mg capsules daily) for six weeks plus ivermectin (150 µg/kg oral dose) at month four.

(iii) IVM: Matching doxycycline-placebo for six weeks plus ivermectin (150 µg/kg oral dose) at month four.

Plasma from the trial participants was collected at baseline and then at four, 12 and 21 months after the start of DOXY or DOXY-placebo treatment. At each time

point, *O. volvulus* microfilaridermia was assessed by microscopy. Some patients had or developed co-infections with *L. loa* and *M. perstans* over the duration of the trial. As the parasite miRNAs miR-71 and lin-4 are believed to also be present in *L. loa* and their expression is unknown in *M. perstans*, individuals infected only by *O. volvulus* across the entire trial follow-up were selected for the longitudinal study. After de-risking co-occurrence of *L. loa/M. perstans* infections by deselecting those samples derived from patients who were positive for *L. loa/M. perstans* mf at any time point, and those with insufficient sample volumes, the final sample set included: DOXY group (n = 9), DOXY+IVM (n = 5) and IVM (n = 4). Their median age was 39 years, with a range from 15 to 55 years. The ratio of female to male participants was 1:1, and they were evenly distributed between the three treatment groups. Parasitological details of patients selected for this study can be found in Table 5.1. European control plasma was obtained from the national health service (NHS), UK. All plasma samples were stored at -80 ^{o}C prior to use.

miRNA extraction

Small RNA was extracted from 200 µl human plasma samples using the miRCURY™ RNA Isolation Kit – Biofluid (Exiqon), following the manufacturer's instructions. Further details can be found in Chapter 2. A synthetic RNA spike-in mixture (Exiqon) was added to the lysis buffer to monitor technical variation between samples. Exiqon RNA spike-in mixture is used to monitor RNA isolation, and consists of three pre-mixed synthetic miRNAs Sp2, Sp4 and Sp5, corresponding to high, medium and low abundance miRNAs, respectively. On-column DNase treatment was applied, and the eluted small RNA was stored at -80 ^{o}C pending use. RNA used in downstream applications was based on sample volume input.

Adult male *O. ochengi* and L4 *L. loa* were sourced from a biobank at the LSTM, UK stored at -80 ^{o}C in RPMI. Due to scarcity of *O. volvulus* material and as the miRNAs of interest have also been reported in the closely related *O. ochengi* (291), total RNA was extracted from *O. ochengi* to validate the two parasite miRNA qPCR assays and use as a positive control. Total RNA was obtained from two adult male *O. ochengi* using the miRCURY™ RNA Isolation Kit – Cell and Plant (Exiqon), following the manufacturer's instructions. On-column DNase treatment was performed and eluted RNA was stored at -80 ^{o}C pending use. This extraction

procedure was also used to extract total RNA from two L4 *L. loa* worms. Total RNA and absence of contaminating DNA was quantified using the Qubit RNA BR Assay Kit and Qubit dsDNA HS Assay Kit, respectively, for Qubit 3.0 Fluorometer.

Patient ID	Treatment	Baseline mf (mf/mg)	T4 mf (mf/mg)	T12 mf (mf/mg)	T21 mf (mf/mg)
1 (a.1)	DOXY	40	1	2	0
2	DOXY	73.5	0	23.5	1
3	DOXY	9.5	14	37.5	0
4	DOXY	124.5	0	5.5	0
a.1	DOXY	40	1	2	0
a.2	DOXY	15.5	34	6.5	0
a.3	DOXY	14	2	0	0
a.4	DOXY	20.5	10	0	0
a.5	DOXY	16.5	2	0	3.5
a.6	DOXY	23.5	1	0	8.5
a.7	DOXY	13	0	1	0
a.8	DOXY	19	93	11.5	0
a.9	DOXY	45	6	0	0
b.1	DOXY+IVM	18	9	1.5	0
b.2	DOXY+IVM	24	1	0	0
b.3	DOXY+IVM	34.5	13	0.5	0
b.4	DOXY+IVM	88	0	0	1
b.5	DOXY+IVM	61.5	28	0	0
c.1	IVM	90.5	99	0.5	0
c.2	IVM	12	0	0	0.5
c.3	IVM	15.5	1	0	2
c.4	IVM	23.5	2	30	8.5

Table 5. 1. Parasitology of participants selected for the current study.
Parasitology of the 18 onchocerciasis-infected individuals eligible for longitudinal analysis (*a.1 - c.4*) and the four included for pilot studies (1 - 4). For each participant, the allocated treatment group and the mean number of mf/mg skin snip at baseline, and four, 12, and 21 months after starting the trial, is detailed. Patient 1 was also included in the longitudinal analysis, designated *a.1* here, as they had sufficient sample volumes and met the inclusion criteria of being *O. volvulus* positive and *M. perstans/L. loa* mf negative at every time point. DOXY, doxycycline; DOXY+IVM, doxycycline + ivermectin; IVM, ivermectin.

miRNA primers

All miRNAs in plasma and parasite RNA samples were reverse transcribed into cDNA using a universal reverse transcription (RT) reaction. Prior to cDNA synthesis, the synthetic miRNA spike-in Sp6 (Exiqon) was added to plasma RNA samples to monitor technical variation in the RT step.

LNA-enriched miRNA-specific qPCR primers from Exiqon were used to enhance specificity for target templates. Lin-4 and miR-71 are here referred to as bma-lin-4 and cel-miR-71-5p, respectively, following the naming convention assigned by their homology to miRNAs listed in miRBase (release 21, http://www.mirbase.org). The linearity of cel-miR-71-5p and bma-lin-4 qPCR assays (Exiqon) was determined by preparing five $\log_{10}$ serial dilutions of *O. ochengi* cDNA for each assay, with each dilution performed in triplicate. Assay reproducibility was assessed by repeating experiments three times on consecutive days to enable calculation of the inter- and intra-assay coefficient of variation (CV) for cel-miR-71-5p and bma-lin-4. The limit of detection (LOD) for the parasite qPCR assays was determined by preparing a 1:10 dilution series spanning over 10^5 to 10^0 copies from amplicon stocks of cel-miR-71-5p and bma-lin-4. Nine reactions were conducted per dilution. The 95% LOD for each assay was determined using a probit regression analysis. Specificity of the parasite miRNA assays was evaluated using European control plasma and by melt curve analysis.

Six human miRNA qPCR assays were tested with European control plasma to identify an endogenous control for plasma samples: hsa-miR-16-5p, hsa-miR-103a-3p, hsa-miR-425-5p, hsa-miR-93-5p, hsa-miR-191-5p, and hsa-miR-484. The linearity of the hsa-miR-16-5p qPCR assay was determined by preparing standard curves with five $\log_{10}$ serial dilutions of European control plasma cDNA, in three replicates. The experiment was repeated three times on consecutive days. Assays provided by Exiqon for synthetic miRNA spike-ins, Sp2, Sp4, Sp5 and Sp6, were also used to monitor technical reproducibility and extraction efficiency.

miRNA RT-qPCR

For both plasma and parasite samples, the two-step miRCURY LNA™ Universal RT microRNA PCR (Exiqon) methodology was utilised. For clinical human

samples, RNA and cDNA input volumes into the RT and qPCR systems, respectively, were empirically determined in European control plasma and a subset of four trial plasma samples. RNA volumes tested were 2 µl, 4 µl and 7 µl (maximum volume for RT reaction), and cDNA was prepared in dilutions of 1:5, 1:10, 1:20 and 1:40.

All experiments included a positive control, a no reverse transcriptase (–RT) control for each sample, and a 'no template' control (NTC) obtained from a mock RNA extraction. Each sample was initially tested in duplicate. A qPCR assay was considered positive if the amplification signal crossed the threshold in fewer than 40 cycles and was amplified in both replicates. A single peak at the correct melting temperature (T_m) was also required for each product, as determined by the melt curve analysis. The anticipated T_m for bma-lin-4 and cel-miR-71-5p in clinical samples was determined from repeated standard curves prepared from *O. ochengi* cDNA. Samples with amplification in one reaction were re-tested in triplicate, and were only considered positive if amplification occurred in two or more reactions, with a Cq < 40 and the correct T_m in the melt curve.

DNA extraction

DNA was extracted from 200 µl plasma using the QIAamp DNA Blood Mini Kit (Qiagen), following the manufacturer's instructions. To control for technical variation between samples, phocine herpes virus 1 (PhHV-1) was also spiked into the lysis buffer prior to DNA extraction. The eluted DNA was stored at -80 ^{o}C pending use. Plasma DNA input used in downstream applications was based on initial sample volume input.

O. volvulus DNA was sourced from a biobank at LSTM, UK. The DNA had been extracted from a human onchocercoma and stored at -80 ^{o}C.

Primers for *Onchocerca volvulus* O-150 DNA experiments

For detection of *O. volvulus* DNA, a pre-validated TaqMan qPCR assay specific to *O. volvulus* tandem repeat O-150 DNA sequence (accession no. J04659) (201) was used. The details of the primers/probe and their design have been reported elsewhere (201). O-150 qPCR assay specificity was verified by testing in European control plasma and NTC reactions. The linearity of the TaqMan assay was assessed

from standard curves prepared from five 1:1 serial dilutions of *O. volvulus* DNA, in three replicates. Three standard curves were prepared over consecutive days. The LOD for the assay has been reported elsewhere (201).

A qPCR assay (Sigma) for the plasma endogenous control glyceraldehyde 3-phosphate dehydrogenase (GAPDH) was assessed by preparing a series of five 1:1 dilutions of European control plasma DNA, in three replicates. Standard curves were repeated three times on alternate days. Primers for viral spike-in PhHV-1 were also obtained (IDT).

qPCR for *Onchocerca volvulus* O-150 DNA experiments

Experiments included a positive control and a NTC obtained from a mock DNA extraction. Each sample was initially tested in duplicate. A qPCR assay was considered positive if the amplification signal had a Cq < 40 and was amplified in both replicates. Samples with amplification in one reaction were re-tested in triplicate, and were only considered positive if amplification occurred in two or more reactions.

Statistical analysis

All analyses were performed using GraphPad Prism 5 with the exception of the probit regression analysis, which was performed using SPSS (Version 23, IBM Corp). Relative levels of the plasma reference miRNA and DNA between the different treatment groups at each time point were both compared using non-parametric Kruskal-Wallis test. To assess whether the endogenous molecular marker levels were consistent in individuals over time for each treatment group, non-parametric Friedman's test, followed by Dunn's post hoc test (with 95% confidence intervals) was used.

Results

Parasite miRNA qPCR assays

Both bma-lin-4 and cel-miR-71-5p miRNAs were detected in RNA extracted from adult male *O. ochengi* and in L4 *L. loa*. The efficiency of the cel-miR-71-5p qPCR assay was 99.9%, with an R^2 value of 0.979 (Fig. 5.1A). The overall inter and intra assay coefficient of variation (CV) from three qPCR experiments was 1.87% and 0.15%, respectively. The average (± SD) efficiency of the qPCR across the three experiments was 102.7% (3.41). The linear dynamic range of the assay was over 10^5 to 10^2 copies, and the mean Cq value across nine reactions at the last linear point of the curve was 34.13 ± 1.50 (± SD). Probit regression analysis determined the 95% LOD as 140 copies (95% confidence interval, CI: 95 - 325 copies) of cel-miR-71-5p. Melt analysis detected a single peak at a T_m of 69.5 ^oC.

The efficiency of the bma-lin-4 qPCR assay was 97.3%, and the R^2 was 0.993 (Fig. 5.1B). The overall inter and intra assay CV was 1.76% and 0.09%, respectively. The average (± SD) efficiency of the qPCR across the three experiments was 95.0% (3.08). The linear dynamic range of the bma-lin-4 assay was 10^5 to 10^2 copies, with a mean Cq value of 35.30 ± 0.76 (± SD) at the final linear point of the curve. The 95% LOD was 73 copies (95% CI: upper and lower bound could not be determined). Both parasite miRNA qPCR assays tested negative in control plasma, and in NTC and –RT reactions. Melt analysis detected a single peak at a T_m 71.5 ^oC.

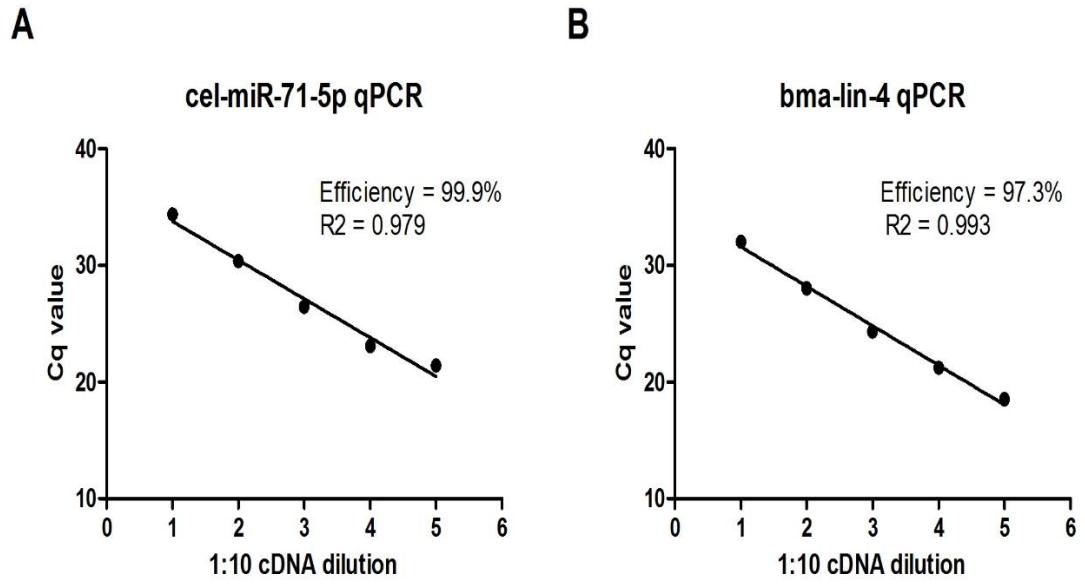

Fig. 5. 1. Standard curves of two parasite miRNA qPCR assays.

A. Efficiency and precision of the cel-miR-71-5p qPCR assay tested over five cDNA 1:10 dilutions. The average of three reactions and ± SD per dilution is shown.

B. Efficiency and precision of the bma-lin-4 qPCR assay over five 1:10 cDNA dilutions. The mean of three replicates and ± SD per dilution are displayed.

Plasma miRNA qPCR assays

Six qPCR assays were tested to identify a plasma endogenous control miRNA: hsa-miR-16-5p, hsa-miR-103a-3p, hsa-miR-425-5p, hsa-miR-93-5p, hsa-miR-191-5p and hsa-miR-484. Hsa-miR-16-5p was the most abundant miRNA in the European control plasma and was selected as the reference control (Fig. 5.2A). The efficiency of the hsa-miR-16-5p qPCR assay was 106.7%, with an R^2 of 0.990 (Fig. 5.2B). The overall inter and intra assay CV over three qPCR experiments was 1.34% and 0.04%, respectively. The average (± SD) efficiency of the qPCR assay across the triplicate qPCR experiments was 109.9% (3.20).

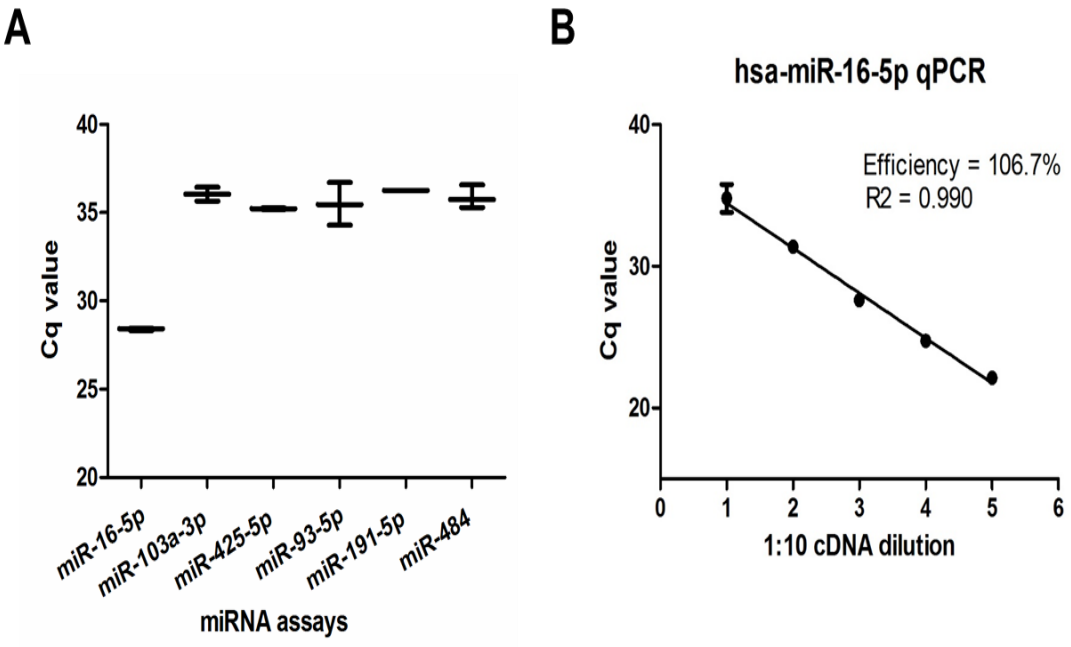

Fig. 5. 2. Assessment of plasma reference miRNAs.

A. Six miRNA qPCR assays were evaluated to determine a suitable endogenous control for plasma samples. Hsa-miR-16-5p was the most abundant miRNA in European control plasma. For each assay, the mean of three replicates with minimum and maximum values are displayed.

B. Efficiency and precision of the hsa-miR-16-5p qPCR assay tested over five 1:10 cDNA dilutions. Graph shows average of three replicate reactions and ± SD.

miRNA RT-qPCR

To verify that the RNA extraction and RT-qPCR methods were comparable in different plasma samples for miRNAs, a pilot study was conducted with European control plasma and plasma taken at baseline from four participants in the DOXY group. The plasma endogenous miRNA hsa-miR-16-5p and synthetic miRNAs, Sp2, Sp4, Sp5 and Sp6, were used as quality controls (Fig. 5.3).

The expression of hsa-miR-16-5p was comparable in samples from different individuals, with an average Cq of 24.16 ± 0.3 (SEM). The synthetic miRNAs Sp2, Sp4 and Sp5, corresponding to miRNAs at high, medium and low abundance, respectively, added to plasma prior to RNA extraction were comparably detected in all samples by RT-qPCR. The synthetic spike-in Sp6, added to the RNA eluate prior to RT, was also similarly detected in the plasma samples. The spike-ins

demonstrated that the RNA extraction and RT steps were both reproducible, and the expression levels of hsa-miR-16-5p showed that extracellular miRNA concentrations between plasma samples were comparable. The extraction spike-ins, Sp2, Sp4 and Sp5, and hsa-miR-16-5p were less abundant in the European control plasma relative to the four trial plasma samples, indicating there may be some PCR inhibition in this sample.

The four trial samples were negative for parasite miRNAs cel-miR-71-5p and bma-lin-4, as were the NTC and –RT reactions. However, the Sp5 spike-in corresponding to low abundance miRNAs was not always detected in all sample replicate reactions. Therefore, other low abundance miRNAs in the plasma samples, such as parasite miRNAs, may also be undetected using the current method.

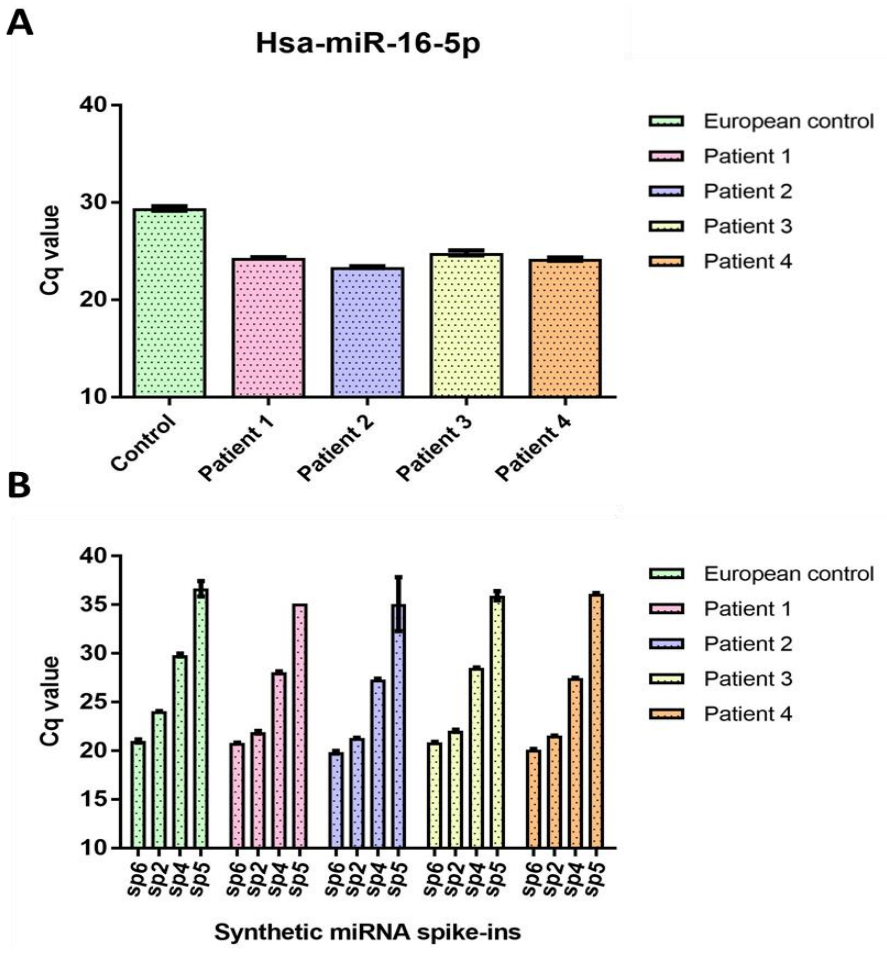

Fig. 5. 3. Plasma reference and spike-in miRNA controls.

A. Expression of plasma endogenous control miRNA hsa-miR-16-5p was comparable in plasma samples collected at baseline from four trial participants, confirming the presence of extracellular miRNAs and a similar RNA input across trial samples. European control

plasma had notably lower abundance of hsa-miR-16-5p detected relative to trial individuals. Graph shows mean of three replicates and ± SD for each sample.
B. To monitor RNA extraction**,** synthetic miRNAs, Sp2, Sp4, Sp5, were spiked into plasma prior to RNA extraction at a pre-mixed volume corresponding to high, medium and low abundance miRNAs, respectively. The synthetic miRNA Sp6 was spiked into RNA eluate to monitor RT. Spike-ins were comparably detected across the plasma samples collected at baseline from four trial participants, indicating that the extraction and RT of samples was performed with similar efficiency. The mean of three replicates and ± SD are displayed for each sample.

Optimisation of the miRNA RT-qPCR workflow

RNA from European control plasma and the four trial plasma samples was added in incremental volumes to the RT reaction mix, and the resultant cDNA for each sample was progressively concentrated. The qPCR assay for plasma reference miRNA hsa-miR-16-5p was used to monitor PCR inhibition, which can occur when RT or qPCR inhibitors present in a sample become more concentrated. The expression levels of hsa-miR-16-5p showed that inhibition did not occur in the trial plasma samples with increasing volumes of RNA and cDNA input (Fig. 5.4B-E). However, the hsa-miR-16-5p assay showed signs of inhibition at higher RNA volumes in the European control plasma sample (Fig. 5.4A).

Increasing the volumes of RNA and cDNA into RT-qPCR workflow identified one of the four trial participants as positive for worm miRNA cel-miR-71-5p (Fig. 5.5). Patient 4 was very weakly positive for cel-miR-71-5p, with average Cq values > 37. However, the parasite miRNA was consistently detected at several of the increased RNA and cDNA inputs. The three other trial samples were negative after repeat testing in triplicate reactions.

The absence of observable PCR inhibition and the detection of a worm miRNA (albeit at very low abundance) justified increasing the RNA input from the initial volume of 2 μl to the maximum 7 μl, and concentrating the cDNA from a 1:40 dilution to a 1:5 dilution for subsequent RT-qPCR analyses.

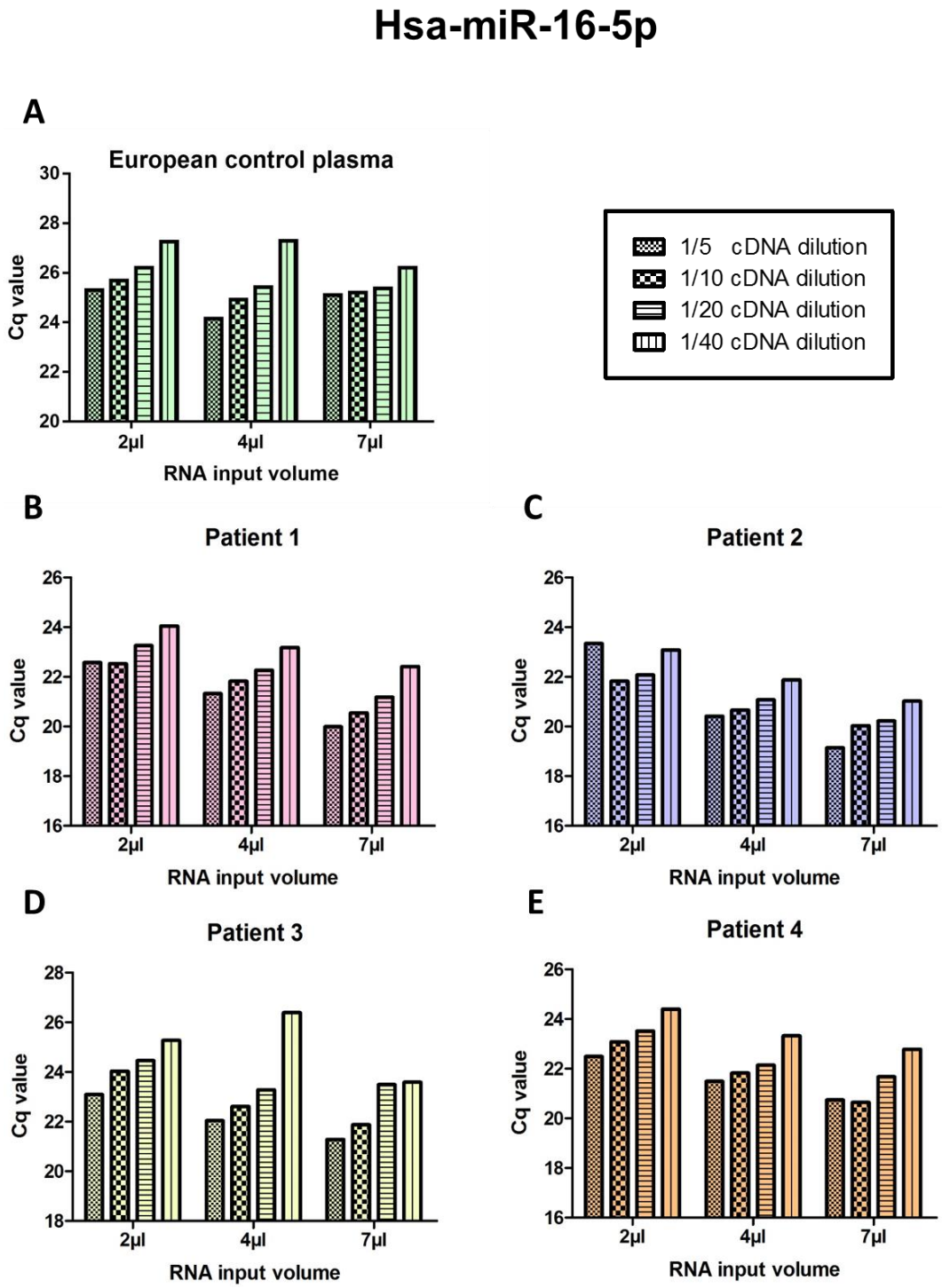

Fig. 5. 4. Monitoring PCR inhibition using a plasma endogenous control miRNA. A-E. The relative change in Cq value of plasma reference miRNA hsa-miR-16-5p in European control plasma **(A)** and plasma taken at baseline from four individuals from the trial (**B**-**E**). No inhibition appeared to occur in the trial samples after increasing RNA and cDNA inputs into the RT and qPCR reactions, respectively. Inhibition occurred in the European control plasma with 7 µl RNA. Graph shows the result of single wells due to limitions on RNA sample volumes.

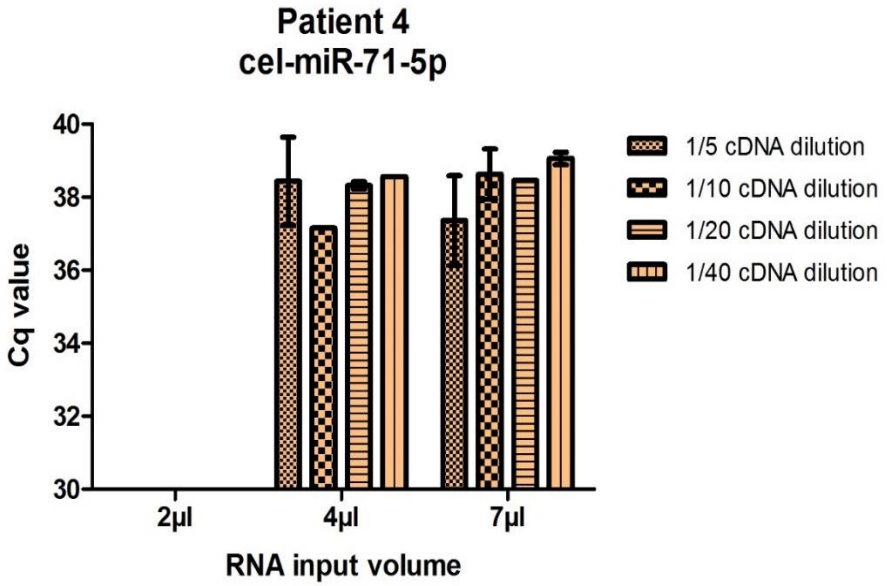

Fig. 5. 5. Detection of a parasite miRNA in plasma after optimising the RT-qPCR. Parasite miRNA cel-miR-71-5p was detected in one onchocerciasis positive individual at baseline after increasing the RNA volume and concentrating the resultant cDNA. The average of two replicates and the ± SD are displayed.

Detection of parasite miRNAs in clinical plasma samples

To further evaluate whether cel-miR-71-5p was positive in plasma as a result of onchocerciasis infection at baseline, plasma RNA from patient 4 (testing positive at baseline) collected pre-treatment and at months four, 12 and 21 post-doxycycline treatment was compared to plasma RNA from patient 2 (testing negative at baseline). Patient 4 was positive for cel-miR-71-5p at baseline and month four, and negative at months 12 and 21 (Fig. 5.6A). In patient 4, the relative level of cel-miR-71 was higher at month four compared to baseline; however, we noted a co-infection with *M. perstans* had developed by this time (n = 60 mf/ml blood). Therefore, we can not be certain the cel-miR-71-5p positive in the plasma of patient 4 originated from *O. volvulus* at month four. Patient 2 was negative at all time points.

The endogenous control hsa-miR-16-5p showed that the patient samples had comparable initial levels of extracellular miRNAs. The spike-in miRNA Sp5, corresponding to low abundance miRNAs, showed that miRNAs present at low levels were consistently detected and the samples were processed with equivalent efficiency (Fig. 5.6B).

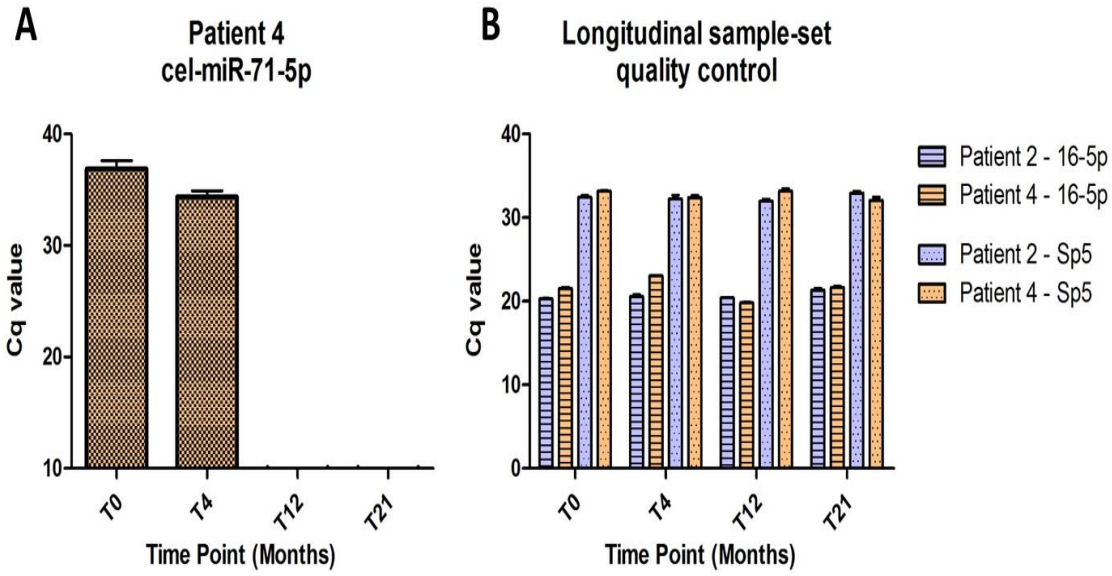

Fig. 5. 6. Longitudinal evaluation of cel-miR-71-5p in two individuals with onchocerciasis before and after doxycycline-treatment.

A. Patient 4 was positive for cel-miR-71-5p at baseline and at four months of the trial, and negative at months 12 and 21. Graph shows mean of two replicates and ± SD.

B. Relative levels of the endogenous control miRNA hsa-miR-16-5p and synthetic spike-in Sp5 were comparable between patient 2 and patient 4 at baseline, and at months four, 12 and 21 of the trial post-doxycycline treatment. The mean of two replicates and ± SD per sample are displayed.

Longitudinal analysis of parasite-derived miRNAs in plasma following antifilarial treatment

A larger longitudinal analysis was conducted to test individuals *O. volvulus* positive and *M. perstans/L. loa* mf negative before and after receiving one of three antifilarial treatment regimens. To reduce the risk of detecting cel-miR-71-5p as a result of a co-infecting parasite, we selected individuals from the DOXY group (n=9), the DOXY+IVM group (n=5), and the IVM group (n=4) infected with *O. volvulus* mf and with no detectable *M. perstans/L. loa* mf. From the 18 individuals tested at the four time points, 32 samples were re-tested in triplicate after one of two qPCR reactions was positive for a parasite miRNA. Two of the 72 samples in total (2.8%) were accepted as positive after re-testing. Cel-miR-71-5p was very weakly positive in one DOXY group patient at month four, and bma-lin-4 was also weakly

positive in one patient in the DOXY group at month 12 (Table. 5.2). All qPCR controls tested negative for worm miRNAs.

Patient ID	Treatment	Time point	miRNA	Cq (± SD)
a.5	DOXY	T4	cel-miR-71-5p	38.02 ± 0.33
a.7	DOXY	T12	bma-lin-4	36.75 ± 0.21

Table 5. 2. Clinical plasma samples positive for worm miRNAs.
Average Cq from three replicates and SD for the two trial individuals positive for worm miRNAs, cel-miR-71-5p and bma-lin-4, by qPCR.

The plasma endogenous control miRNA hsa-miR-16-5p was consistently detected in all samples and no significant difference (Kruskall Wallis test, P = >0.05) in expression levels was found between the three treatment groups at any time point of sampling (Fig. 5.7A). The IVM group and DOXY+IVM group also showed no significant change in hsa-miR-16-5p expression in individuals across sampling time-points (Friedman's test, P = >0.05). However, a statistically significant difference in expression levels of hsa-miR-16-5p was detected in participant samples from the DOXY group over time (Friedman test, P = 0.0191). Dunn's post hoc test revealed that a significant difference was observable between months four and 12 (Dunn's multiple comparisons, P = <0.05).

Hsa-miR-16-5p had higher average Cq values in plasma samples at month four relative to samples taken at month 12 from the same individuals in the DOXY group. This was also observed to a lesser extent with the spike-in Sp5. The difference in time points is therefore likely a result of a small degree of inhibition in some samples at month four relative to those from month 12. Overall, Sp5 was consistently and comparably detected in all treatment groups and time points of sampling (Fig. 5.7B). Therefore, we have verified that number of parasite miRNA-negative individuals was not as a result of the quality of the samples or methodology used.

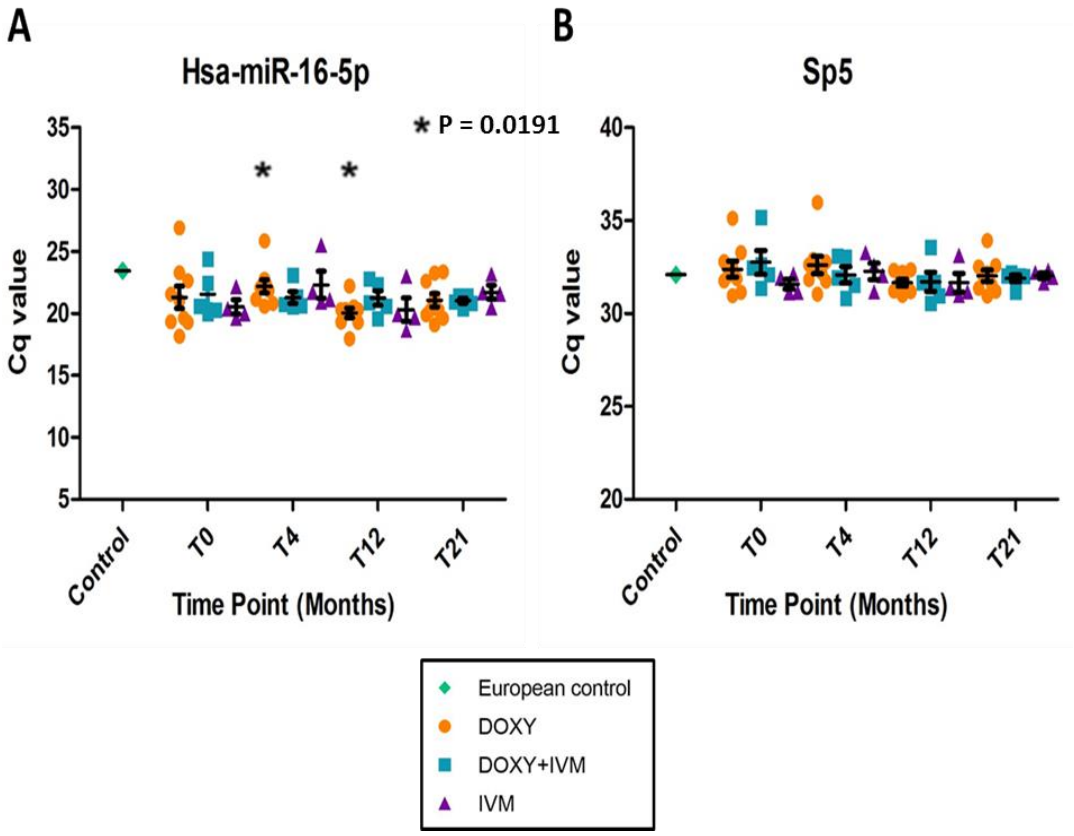

Fig. 5. 7. Longitudinal detection of plasma endogenous control and spike-in miRNAs in trial individuals before and after following one of three antifilarial treatment regimens.
A. The plasma endogenous control miRNA hsa-miR-16-5p was detected in the European control plasma and all trial participant plasma samples. Graph shows the mean of duplicate reactions for individual samples, and the ± SEM for each treatment group at each time point. There were no significant differences in hsa-miR-16-5p between groups at any time point. Differences in the miRNA marker over time in the IVM and IVM+DOXY group were also non-significant. A significant difference (P = 0.0191) in hsa-miR-16-5p in individuals over time in the doxycycline group was detected. Dunn's post hoc test identified a significant difference in these individuals between month four and month 12.
B. The spike-in miRNA Sp5 was positive in the European control and all trial participant plasma samples. The average of two replicates for each individual, and the ± SEM for the treatment groups at each time point are displayed.

qPCR assay for *Onchocerca volvulus* O-150 DNA

We next sought to establish whether *O. volvulus* DNA could be detected in the host plasma. An *O. volvulus*-specific TaqMan qPCR assay for the O-150 DNA sequence was assessed. The efficiency of the O-150 qPCR assay when tested with

1:2 serial dilutions of *O. volvulus* DNA was 97.7%, with an R^2 value of 0.964 (Fig. 5.8A). The overall inter and intra assay CV over the three qPCR experiments was 0.69% and 0.04%, respectively. The average (± SD) efficiency of the qPCR across the three experiments was 97.4% (7.05). The O-150 qPCR assay tested negative in European control plasma and in NTC reactions.

The efficiency of the qPCR assay for the endogenous plasma control GAPDH when tested with European control plasma DNA was 100.1%, with an R^2 value of 0.942 (Fig. 5.8B). The overall inter and intra assay CV over three experiments was 1.46% and 0.19%, respectively. The average (± SD) efficiency of the qPCR across the three experiments was 110.7% (11.54).

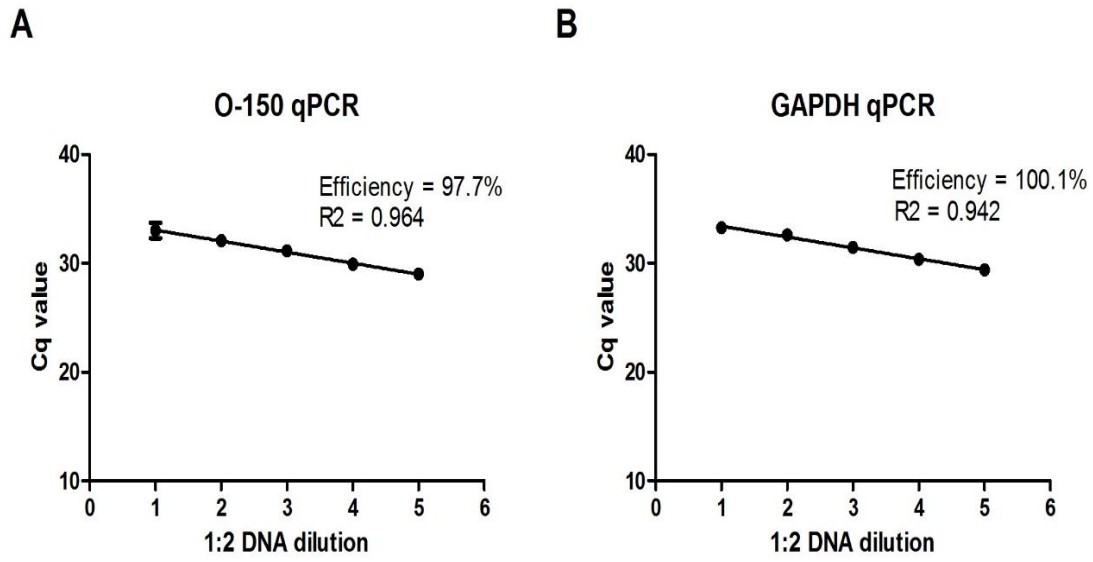

Fig. 5. 8. Standard curve of the *O. volvulus* O-150 qPCR assay and endogenous plasma control GAPDH qPCR assay.

A. Efficiency and precision of the O-150 DNA qPCR assay tested over five 1:2 *O. volvulus* DNA dilutions. The average of three reactions and ± SD per dilution are displayed.

B. Efficiency and precision of the GAPDH qPCR assay over five 1:2 plasma DNA dilutions. The mean of three replicates and ± SD per dilution is shown.

Detection of O-150 DNA in clinical plasma samples

The O-150 qPCR assay was initially assessed in plasma collected at baseline from four individuals in the DOXY group. Two of the four individuals, patients 3 and 4, tested positive for O-150 (Fig. 5.9A). Of note, patient 4 was also positive for parasite miRNA cel-miR-71-5p in the miRNA pilot study. The European control

plasma and NTC reactions were negative for O-150. The endogenous control GAPDH assay was detected at comparable levels across the control and trial participant samples, with the exception of patient 4. Patient 4 had higher levels of GAPDH DNA relative to the other individuals tested, and the highest level of *O. volvulus* DNA detected (Figure 5.9B). However, patient 3 was also positive for O-150 and had comparable levels of GAPDH relative to the other individuals tested.

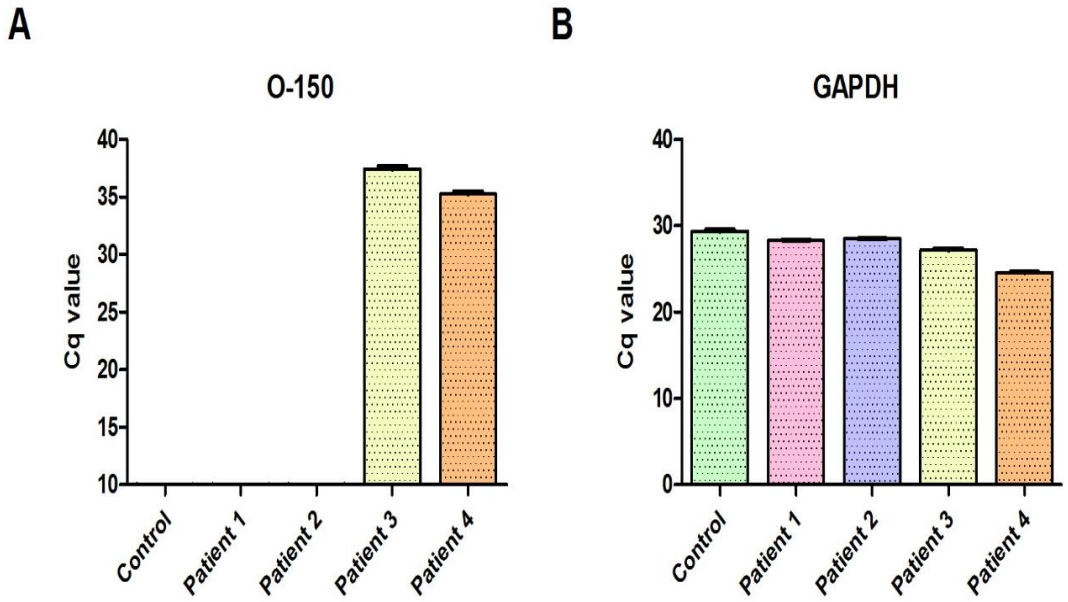

Fig. 5. 9. *O. volvulus* DNA positive and endogenous control DNA positive individuals.
A. The qPCR assay for the *O. volvulus* O-150 DNA sequence was positive in two of the four baseline plasma samples tested from trial individuals, and negative in the European control plasma. Graph shows mean of two replicates and ± SD for each sample.
B. The plasma endogenous control DNA GAPDH was detected in the control plasma and in samples collected at baseline from the four trial individuals. GAPDH DNA was comparably detected in all samples except patient 4, where levels were higher in this sample relative to the others. The mean of two replicates and ± SD for each sample are shown.

Longitudinal analysis of O-150 DNA in plasma following antifilarial treatment

To verify the detection of O-150 in the plasma of individuals with onchocerciasis and determine whether treatment affects detection over time, the O-150 qPCR assay was used to assess the 18 participants screened in the miRNA study. The O-150 assay was positive in eight of 18 (44.4%) baseline samples with skin snip-confirmed onchocerciasis. At month four, four of 18 (22.2%) plasma samples were positive for

O-150 by qPCR, and this declined to one (5.6%) positive sample detected at both months 12 and 21. The positive and negative samples among the 72 samples tested are provided in Table 5.3.

		O-150 qPCR			
Patient	**Treatment**	**Baseline**	**Month 4**	**Month 12**	**Month 21**
a.1	DOXY	Neg	Neg	Neg	Neg
a.2	DOXY	39.26 ± 1.24	Neg	Neg	Neg
a.3	DOXY	37.28 ± 1.05	Neg	Neg	Neg
a.4	DOXY	38.22 ± 1.24	Neg	Neg	Neg
a.5	DOXY	Neg	Neg	Neg	Neg
a.6	DOXY	Neg	Neg	Neg	Neg
a.7	DOXY	34.31 ± 0.54	36.88 ± 0.44	38.43 ± 1.02	37.47 ± 0.65
a.8	DOXY	Neg	Neg	Neg	Neg
a.9	DOXY	Neg	Neg	Neg	Neg
b.1	DOXY+IVM	Neg	Neg	Neg	Neg
b.2	DOXY+IVM	Neg	Neg	Neg	Neg
b.3	DOXY+IVM	38.79 ± 0.52	Neg	Neg	Neg
b.4	DOXY+IVM	38.37 ± 1.66	38.61 ± 0.84	Neg	Neg
b.5	DOXY+IVM	38.61 ± 0.46	Neg	Neg	Neg
c.1	IVM	38.26 ± 0.26	36.03 ± 0.38	Neg	Neg
c.2	IVM	Neg	Neg	Neg	Neg
c.3	IVM	Neg	Neg	Neg	Neg
c.4	IVM	Neg	38.42 ± 0.99	Neg	Neg

Table 5. 3. Individuals positive and negative for O-150 in plasma by qPCR.
Trial participants that were positive and negative for *O. volvulus* O-150 DNA sequence in plasma by qPCR over the duration of the trial. The time point of positive or negative qPCR detection for each individual is listed. Mean Cq value and ± SD for positive results are displayed. Neg, Negative.

The proportion of O-150 positive patients in each treatment group is shown in Fig. 5.10A. For all treatment groups, the greatest number of O-150 positive results were at baseline and month four. By month four, the number of O-150 positive patients had declined from four to one (75% decrease) in the DOXY group, and three to one (66.7% decrease) in the DOXY+IVM group. The number of O-150 positive individuals increased in the IVM group from one to two (50% increase) by month

four, however IVM was not provided until month four of the trial. Two individuals, one from DOXY+IVM group and one from IVM group, were positive both at baseline and at month four, but negative at months 12 and 21. One individual treated with DOXY was positive at every time point over the two years of the trial (Fig. 5.10B). This patient had 13 mf/mg at baseline, and <1 mf/mf at all subsequent time points of sampling. Of note, this patient was also positive for bma-lin-4 at month 12.

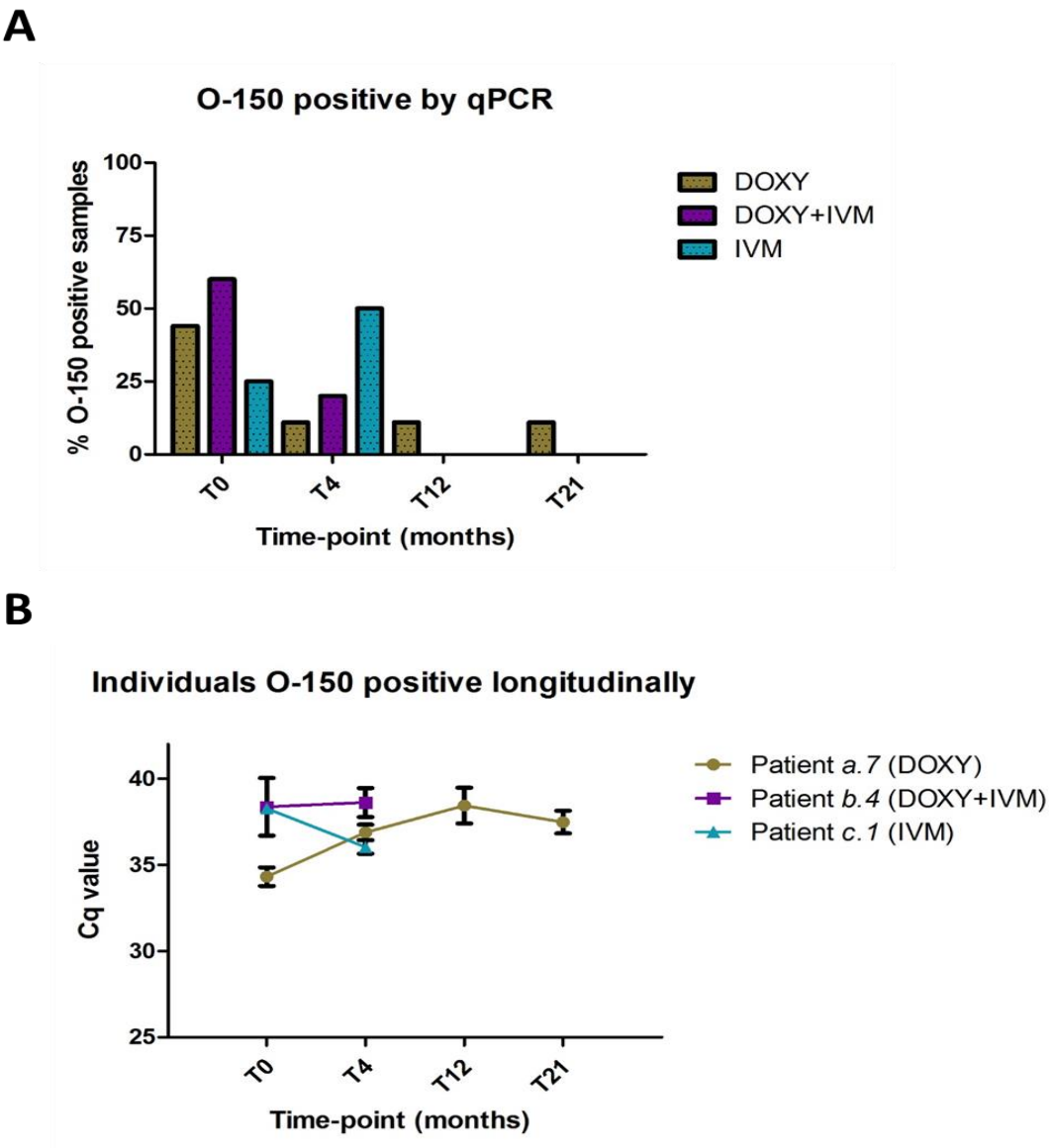

Fig. 5. 10. O-150 positive plasma samples by treatment group and time point.

A. Percentage of O-150 positive individuals in each treatment group at each time point.

B. The three individuals that were positive for O-150 by qPCR at more than one time point. Patient *a.7* was positive at all time points, while patients *b.4* and *c.1* were only positive at baseline and month four. Average Cq from three reactions and ± SD are shown for each sample.

Around 1/3 of all samples tested were negative for *O. volvulus* by both qPCR and skin snip. Of the total 14 O-150 qPCR positive plasma samples, 11 (78.6%) had microfilaridermia, and two of these mf positive individuals (18.2%) had <10 mf/mg. The vast majority of the O-150 positive samples were therefore positive by skin snip; however, some individuals with very low or negative mf burdens in skin were also positive by qPCR of plasma. Of the 58 samples in total that were negative for O-150 by qPCR, 36 (62.1%) had microfilaridermia. Of these mf positive individuals, 20 (55.6%) had <10 mf/mg. Therefore, over half of the mf positive individuals negative by qPCR had very low mf burdens. The number and proportion of individuals that were qPCR or mf positive, or both, at each time point is shown in Table 5.4.

	Baseline		**Month 4**		**Month 12**		**Month 21**	
Test	**Positive**	**Negative**	**Positive**	**Negative**	**Positive**	**Negative**	**Positive**	**Negative**
qPCR	8 (44.4%)	10 (55.6%)	4 (22.2%)	14 (77.8%)	1 (5.6%)	17 (94.4%)	1 (5.6%)	17 (94.4%)
Skin snip	18 (100%)	0 (0%)	15 (83.3%)	3 (16.7%)	8 (44.4%)	10 (55.6%)	6 (33.3%)	12 (66.6%)
Both	8 (44.4%)	0 (0%)	2 (11.1%)	2 (11.1%)	1 (5.6%)	10 (55.6%)	0 (0%)	11 (61.1%)

Table 5. 4. Test results obtained by qPCR of plasma and by mf detection in skin snips. Results obtained by qPCR of *O. volvulus* DNA in plasma and by microscopy of mf in skin snips in the 18 individuals with onchocerciasis at baseline, and at subsequent time points after receiving one of three antifilarial treatments.

The endogenous control GAPDH was detected in all samples (Fig. 5.11A), and relative levels did not significantly differ between different treatment groups at any time point (Kruskall-Wallis test, P = >0.05), or in individuals over time (Friedman's test, P = >0.05). This demonstrated that the O-150 positivity or negativity of samples was not a result of different initial DNA levels in individual plasma samples. A viral control PhHV-1, additionally spiked into plasma samples prior to DNA extraction, also showed that DNA was extracted uniformly across all samples (Fig. 5.11B).

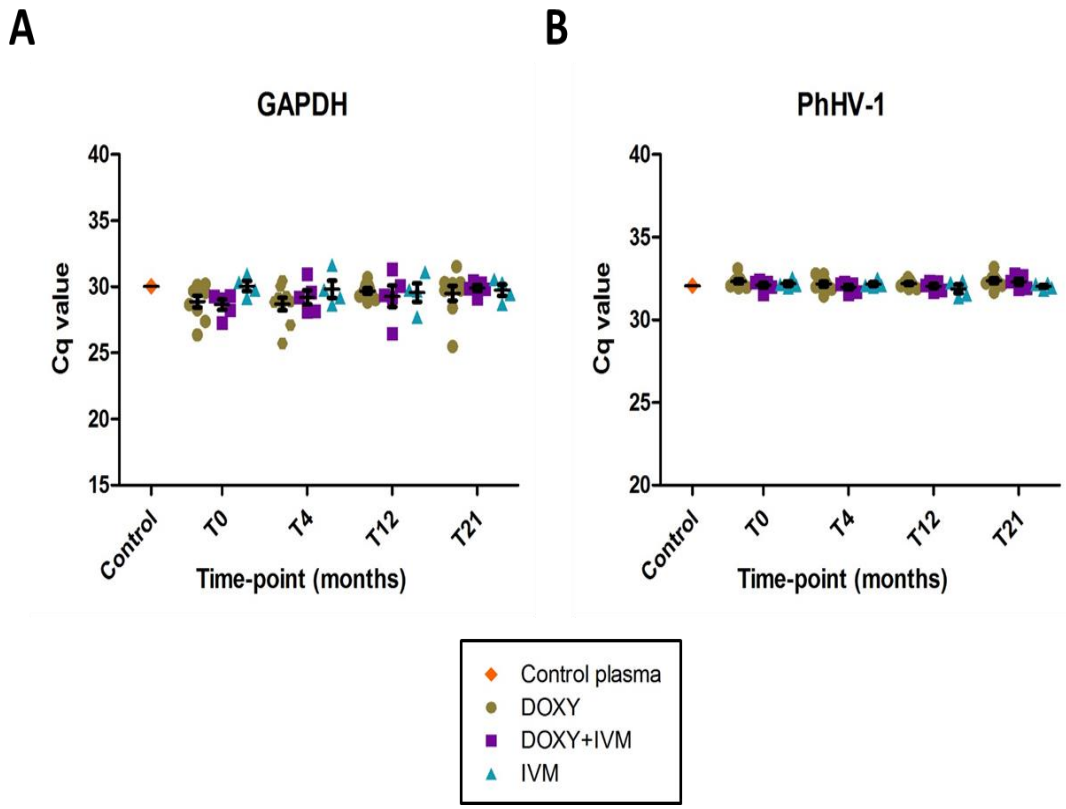

Fig. 5. 11. Plasma reference and spike-in DNA controls.

A. The plasma reference DNA marker GAPDH was detected in the European control plasma and all trial plasma samples. Graph shows the mean of two replicates for individual samples, and the ± SEM for each treatment group at successive time points.

B. The viral spike-in PhHV-1 was detected uniformly in the uninfected control and all trial plasma samples. The mean of two replicates for individual samples, and the ± SEM for each treatment group at each time point are displayed.

Discussion

This study reports the first use of RT-qPCR and qPCR for the detection of *O. volvulus* miRNAs and DNA, respectively, in plasma from individuals in an onchocerciasis-endemic community before and after macrofilaricidal or microfilaricidal treatment. The parasite-derived miRNAs, cel-miR-71-5p and bma-lin-4, were both detected in a very small subset of plasma samples by RT-qPCR. However, almost all samples tested negative, even after extensive optimisation of the RT-qPCR protocol. We also confirmed by RT-qPCR that the two miRNAs are expressed in *L. loa*, and therefore conclude that cel-miR-71-5p and bma-lin-4 therefore do not have the necessary specificity or sensitivity to be circulating diagnostic markers for onchocerciasis. Future work could investigate miRNAs in individuals with *O. volvulus* and *L. loa* or *M. perstans* co-infections, where the mf reside in the blood, to better understand the dynamics of parasite-derived circulating miRNAs for onchocerciasis. By comparison, the *O. volvulus*-specific O-150 DNA marker was detected in plasma in almost half the individuals at baseline, with a decline in positive patients detected after treatment with microfilaricidal, macrofilaricidal, or a combination of the two treatments. However, a high proportion of samples that were positive by parasitological evaluation of *O. volvulus* in skin snips were negative by qPCR in plasma. Therefore, qPCR of *O. volvulus* DNA in the host plasma did not have sufficient sensitivity to be a diagnostic test for onchocerciasis.

The results presented here demonstrate that even though *O. volvulus* does not reside in the circulatory system of the host, parasite miRNAs and DNA are detectable in plasma, albeit sporadically and in very low copy numbers. This has provided important information with regard to the diagnostic utility of these markers compared to the gold standard skin snip for detecting onchocerciasis positive individuals. Additionally, the use of a unique longitudinal sample set comprising patients enrolled in one of three filaricidal treatment regimens allowed us to assess the influence of treatment on detection of the parasite-derived nucleic acids over time. In a miRNA pilot study of four individuals with onchocerciasis sampled at baseline, one individual was positive for cel-miR-71-5p and all were negative for bma-lin-4. The same individual, patient 4, was also positive for O-150 DNA at baseline. The mf density in the skin of patient 4 was notably higher than in the other

three individuals (n = 124.5 mf/mg skin snip, compared to 73.5, 40 and 9.5 mf/mg), suggesting that cel-miR-71-5p may be correlated with higher infection intensity. The same individual was positive for cel-miR-71-5p four months after starting a six week course of daily doxycycline treatment, but was negative at 12 and 21 months. At four months this patient was *O. volvulus* mf negative, but a co-infection with *M. perstans* had developed (n = 60 mf/ml blood). It is not currently known whether cel-miR-71-5p is expressed in *M. perstans*, however its conservation across several nematode species renders it difficult to ascertain the origin of the miRNA at month four.

Testing an additional 18 participants infected solely with *O. volvulus* before and after their assignment to one of the three antifilarial treatment regimens identified only two of 72 samples as positive for a parasite miRNA. One participant was very weakly positive for cel-miR-71-5p, and one was weakly positive for bma-lin-4. While both worm miRNA positive individuals were from the doxycycline treated group, their positivity was not related to mf counts (mf density was < 2 in both patients), or sampling time. This study was unique in comparison to other *O. volvulus* miRNA studies conducted thus far (251, 291, 297) in that the use of plasma samples from *O. volvulus*-infected patients and excluding those with detectable co-infection at baseline suggested the miRNAs detected originated from *O. volvulus*.

A recent study also investigated cel-miR-71-5p and bma-lin-4 (there referred to as ‘ov-miR-71 23nt’ and ‘ov-lin-4’, respectively), as well as 15 other putative *O. volvulus* miRNAs, in plasma of individuals with onchocerciasis using LNA-enriched RT-qPCR (297). In their work, plasma samples from 23 nodule positive individuals and 20 microfilaridermic individuals were tested using a similar methodology, and the authors reported that seven parasite-derived miRNAs (including the ‘ov-miR-71 23nt’) showed a detectable signal. To validate their assays, 5′-phosphorylated miRNA oligoribonucleotides were synthesised for three variants of miR-71 plus plasma reference miRNAs. However, as a result of a significant difference in the melt curve analysis T_m for the synthetic worm miRNAs and worm miRNAs in clinical samples, they concluded that the amplification detected was non-specific and did not reflect true positive signals. Their work is in agreement with the current study in a number of ways. Namely, levels of these extracellular parasite-derived miRNAs are very low, if they are present at all in the plasma of individuals with onchocerciasis. Lagatie and colleagues (297) detected few worm miRNAs in

samples, and the miRNAs were not universally present in all or most infected individuals. Inadequate specificity was also highlighted as a concern due to the detection of worm-derived miRNAs in supposedly healthy samples, as well discrepancy in miRNA qPCR melt curve analyses.

Our work differed from the Lagatie study in several ways. While they reported considerably more parasite-miRNA positive individuals relative to our study, they did not rule out the potential for co-infected samples. As miRNAs from blood-localised parasites appear to more abundant in host circulation relative to parasites in other tissues (251, 287), there is a possibility that the miRNAs detected in their study originated from another parasite. Variants of miR-71 and their corresponding synthetic templates were also not assessed here as the assays were validated in relevant biological reference species. The T_m for cel-miR-71-5p and bma-lin-4 were the same when tested with RNA from both *O. ochengi* and *L. loa*, and only clinical samples with the correct T_m and meeting all other criteria outlined were accepted as positive. Additionally, the European control sample and NTC were negative. Specificity can be an issue for miRNA studies, as the very short length and sequence similarity of miRNAs pose unique challenges to assay design. A caveat of SYBR Green is unspecific amplification through primer-dimer formation, and this may confound defining weak positives and unspecific products, particularly as primer dimers will be of similar length to miRNAs. While these caveats raise caution over the source of miRNA in the few very weakly positive samples detected in our work, the consistent detection of cel-miR-71-5p in patient 4 over various RNA and cDNA concentrations supports the likelihood of a true positive.

Although our findings did not support the use of extracellular parasite-derived miRNAs as diagnostic markers for onchocerciasis, their potential for detection of blood-borne filarial infections and other parasitic worms have been investigated (251, 287, 291, 294-297). From a diagnostic standpoint, the utility of parasite-derived miRNAs as a marker for infection will depend on how consistently they are secreted/excreted into extracellular fluids and their stability once in plasma. Individuals infected by worms with life cycle stages in the blood will also likely have higher concentrations of parasite-derived miRNAs in their circulation relative to individuals with parasites infecting other tissues. For example, Tritten *et al.* consistently detected the parasite miRNAs miR-71 and miR-34 in the circulation of

dogs infected by *D. immitis* and *B. pahangi*, where the mf are present in peripheral blood, and adult worms of *D. immitis* also reside in the pulmonary arteries (251). Of note, in this study the infected dogs had significantly higher infection intensities (> 8000 mf/ml in positive samples), whereas all but one participant tested in the current study had <100 mf/mg per skin snip. Other studies have identified parasite-derived miRNAs in the serum of mice infected by *L. sigmodontis* (localised in the pleural cavity) (287), however they were not identified in the serum of mice infected with *H. polygyrus* (localised in the gut lumen) (287).

Of the extracellular parasite-derived miRNAs that have been identified thus far, miR-71 has been detected in the host fluids and linked to several filarial worms, including *O. volvulus, O. ochengi, L. loa, L. sigmodontis, D. immitis* and *B. pahangi*, as well as in extracellular exosomes and vesicles from other helminths (285, 287, 297, 307). MiR-71 promotes longevity in *Caenorhabditis elegans* (396, 397) and miR-71 knockout worms had shortened lifespans from around 20 to 10 days. Levels of miR-71 are also up-regulated in L1 diapause and dauer larvae (398). With regard to parasitic worms, Poole *et al* discovered that miR-71 was one of the most abundantly expressed miRNAs in *B. malayi* mf, comprising ~27% of all miRNAs identified (289). The authors postulated that it may be involved in the regulation of mf longevity as the larval stage can persist in the host for up to a year (although the adult worms live considerably longer) (32). Lin-4 has also been identified from several parasitic worms in the host fluid and in secreted exosomes. Lin-4 was the first nematode miRNA to be discovered over 20 years ago in *C. elegans* (399), and its function has since been extensively characterised. In *C. elegans*, mature lin-4 amasses towards the end of first larval stage (L1), and is involved in regulating the transition from the L1 to later larval stages by repressing the heterochronic proteins LIN-14 and LIN-28 (400, 401). The literature therefore suggests that miR-71 and lin-4 may be more sensitive, albeit still non-specific, markers for the parasite larval stages.

The use of an *O. volvulus*-specific DNA marker for screening plasma of individuals with onchocerciasis identified a higher proportion of infected individuals than the worm-derived miRNAs. Of all the baseline samples assessed (including the pilot study), the O-150 qPCR assay identified 45.5% of positive trial participants that were all positive by skin snip. The number of positive individuals identified had

declined in the doxycycline and doxycycline + ivermectin groups by four months, although one patient from each group was still positive for O-150 at this time. One additional individual was identified as positive in the ivermectin group at month four relative to at baseline. By months 12 and 21, only one individual (patient code *a.7*) from the doxycycline group remained positive. This participant was positive consistently over the two years of the trial. While the adult worm status of this patient is unknown, other longitudinal studies tracking macrofilaricidal treatment efficacy on adult *O. volvulus* worms have shown that a period of 20 and 27 months is required to observe the macrofilaricidal effects (152). As most O-150 positive individuals were at baseline and four months and then negative at 12 and 21 months for all treatment groups, our results showed no discernible difference in treatment type on the dynamics of O-150 detection over time.

An important feature of this study is that it mimicked the typical situation of low mf densities encountered in communities undergoing ivermectin treatment, and in hypoendemic communities that will be targeted in elimination programs. Therefore, the utility of O-150 qPCR of plasma as a diagnostic tool for real-world elimination 'end game' scenarios could be assessed. The assay detected *O. volvulus* infection in almost half of the individuals at baseline that were also positive by skin snip. Additionally, the qPCR assay was positive in three mf negative individuals and two individuals with < 10 mf/mg. However, the skin snip was found to be far superior over qPCR of *O. volvulus* DNA in plasma. Around 2/3's of qPCR negative samples were mf positive. Over half of these samples with microfilaridermia had low numbers of mf (< 10 mf/mg), and they were not detected using qPCR. Therefore, qPCR of the *O. volvulus* O-150 DNA marker in plasma was not as sensitive as skin snip for detecting light infection with *O. volvulus*. The number and viability of the adult worm population, which can infect deeper tissues, over the duration of the trial is not known. The trial of Turner *et al* (157) demonstrated superior killing of adult worms in doxycycline + ivermectin and doxycycline groups, but some adult worms persisted at 21 months and low levels of mf were still detected in skin snips at 12 and 21 months for some participants. It is difficult to gauge the level of infection required to detect circulating DNA of adult worms in plasma of the host, but plasma qPCR will likely be more sensitive in meso- and hyperendemic areas with higher infection densities.

A recent study using the same O-150 qPCR assay for the detection of *O. volvulus* DNA in skin snips reported greater sensitivity in identifying positive samples compared to microscopy of skin snips and nodule palpation, and their results provided a semi-quantitative estimate of mf intensity (201). However, they also observed that 56.3% of individuals who did not have palpable nodules had positive qPCR or skin snip results. Likewise, they noted that 63.4% of individuals that had negative skin snip microscopy results had palpable nodules or positive qPCR results. A further 52 individuals had palpable nodules but were mf negative by both microscopy and qPCR. Thus, combining positive results from all three tests significantly increased the accuracy of diagnosis and assessment of the infection prevalence in the sampled population. The O-150 assay could therefore be useful for mapping endemic areas for adult worm infection using pooled representative plasma samples of populations or sentinel groups alongside taking skin snips. Pool screen PCR has been widely implemented for estimating filarial prevalence in insect vectors (206), as well as in human blood samples for estimating the filarial infection prevalence in Indonesia (402).

On a technical note, robust controls for DNA and RNA experiments were used to ensure plasma nucleic acids were not degraded or affected by plasma-derived inhibitors, and that RT-qPCR and qPCR analyses among different samples was consistent. The relative stability of the human extracellular miRNA hsa-miR-16-5p and GAPDH DNA in trial plasma samples showed that initial miRNA and DNA levels were comparable when using the same plasma starting volume. The synthetic miRNA spike-in Sp5 and viral spike-in PhHV-1 verified that the samples in miRNA and DNA experiments were extracted with similar efficiency, and the combined use of plasma reference nucleic acids and spike-ins controlled for inhibition. The negative samples for *O. volvulus* nucleic acids in plasma were therefore not as a result of sample or methodological quality. Plasma is naturally very low in host RNA and DNA, making detection and accurate quantification of host, let alone parasite nucleic acids, from this sample type particularly challenging (403-406). An advantage of molecular markers is that they can be amplified by qPCR preceding their detection. As this study aimed to detect multiple miRNAs in individual samples, universal primers for cDNA synthesis of all miRNAs were utilised, followed by amplification of target templates using LNA™-enhanced microRNA-

specific forward and reverse primers, with SYBR Green for detection. However, other miRNA detection platforms, such as stem-loop RT with TaqMan PCR, may produce a different outcome with regard to sensitivity and specificity for targets (407, 408). Greater sensitivity may have been achieved in these experiments by increasing the RNA/cDNA or DNA input into their respective reactions. However, the limitations imposed by commercial reaction mix components and potential presence of inhibitors in plasma, as well as the limited availability of clinical samples, places restrictions on the amount of sample that can be tested in practice. Enriching for parasite nucleic acids preceding their detection, such as through selective concentration of miRNA-harbouring exosomes (287), may improve the sensitivity in samples where the parasite material will be greatly exceeded by the host material.

The conclusions that can be drawn from the current work are therefore in-line with the findings of others investigating extracellular parasite-derived miRNAs; that they are present at very low concentrations in the host circulation, and for *O. volvulus*-derived miRNAs this is likely due to the parasite's locality in the host. The diagnostic utility of cel-miR-71 and bma-lin-4 for detecting onchocerciasis in plasma is therefore very limited due to insufficient technical sensitivity. The O-150 qPCR assay showed some potential as an indicator of infection and treatment efficacy, and could be used to screen pooled plasma samples from endemic areas alongside the use of other diagnostic tools. However, it could not be used to identify onchocerciasis infection in hypoendemic areas. In conclusion, detection of parasite derived miRNA and DNA in plasma by qPCR was not as sensitive as the skin snip for detecting infection with onchocerciasis.

Chapter 6. Discussion

Plasma proteomics for *Onchocerca volvulus* biomarker discovery

This thesis aimed to develop a discovery proteomic workflow for plasma, and then use this workflow to identify circulating protein markers of onchocerciasis that show a dynamic change in protein abundance or prevalence over 21 months following macrofilaricidal treatment. Following the development of an untargeted plasma proteomic method, this study has identified *O. volvulus* proteins in the circulation of individuals infected with onchocerciasis, and found that almost all the parasite proteins were still detectable in the host circulation 21 months post-doxycycline treatment (Chapters 3 and 4). No proteins from the *Wolbachia* obligate endosymbiont of the parasite were identified in the host circulation. Of the 16 *O. volvulus* proteins identified, half were detected in almost every individual at all four time points over 21 months, while three parasite proteins had increased or decreased in detection frequency among individuals by the final follow-up. The parasite proteins identified are not predicted to be secretory (269), and therefore are likely detected in the host circulation due to excretion or death of the adult worm. However, the onchocerciasis plasma proteome was found to be largely unchanging over 21 months after treatment, as no parasite or human proteins statistically significantly changed in abundance over time, and no proteins were present in all individuals at baseline and absent at a later time point. The *O. volvulus* proteins identified in this data set are therefore primarily candidates for adult worm infection prevalence, and three proteins may be markers of ongoing infection clearance. The persistence of circulating parasite proteins over years following macrofilaricidal treatment is in line with trials measuring CFA of *W. bancrofti*, where the antigen has been shown to markedly decline but not completely clear from plasma up to 24 months post-doxycycline treatment (263, 264). Although doxycycline causes a slow and sustained killing of the adult parasites after 18–27 months (157), it has regularly been observed that not all worms are dead by 21 months. A 6-week doxycycline (200 mg/day) regimen can result in >60% of adult female worm death 21 to 27 months post-treatment (152, 157). Importantly, an uncharacterised *O. volvulus* protein, A0A044VCM8, that was identified at every time point almost consistently in every individual has been shown to be enriched in female worms (269). This 11

kDa membrane protein could therefore be a circulating marker for the female worms in the host. Although this is a small protein, the closest orthologous protein from *L. loa* showed minimal (26.3%) sequence similarity over the total protein length, with a large continuous portion (73 aa) of the sequence showing no conservation with the orthologous *L. loa* protein. Similarly, although the short peptide (11 aa) identified by MS/MS and used for protein inference of A0A044VCM8 is also present in *L. loa* and *W. bancrofti*, the individuals tested were mf negative for co-infections by parasitological assessment. Therefore, A0A044VCM8 may provide a diagnostic marker of onchocerciasis to which antibodies could be raised. The major conclusion that can be drawn from this study is that 21 months was too short a follow-up to detect dynamic changes in the onchocerciasis plasma proteome as a result of treatment; however, further research in a larger cohort is needed to investigate whether these proteins form circulating immune-complexes in plasma, and determine whether A0A044VCM8 is a circulating marker of female worm infection, if this protein declines/disappears following infection clearance, and if so, how long is needed to clear it from the host circulation following treatment.

To increase the likelihood of detecting onchocerciasis-related proteins or protein changes in the plasma proteome, we first had to improve the protein coverage of discovery LC-MS/MS analyses (341, 343). Use of immunoaffinity depletion columns to selectively remove abundant plasma proteins enabled identification of considerably more novel proteins relative to in whole plasma. The number of proteins identified in both plasma and depleted plasma was also in line with what we could expect using similar methodologies (359-362). Furthermore, it was shown that many non-targeted plasma proteins remained bound to the spin-column, several of which were unique to the eluted abundant protein fraction (360, 361, 366, 368, 369). Analysing the depleted plasma fraction and eluted abundant protein fraction using LC-MS/MS and then concatenating the protein identifications *in silico* improved the proteome coverage relative to LC-MS/MS analysis of whole plasma or depleted plasma, as well as providing a better basis for quantitative analyses. The use of this proteomic method for onchocerciasis clinical plasma samples, with a longer RP-LC separation gradient (2 hours compared to 1 hour) prior to MS further increased the number of proteins identified per individual relative to the control plasma tested in Chapter 3. This result may have been due to differences in initial protein

concentrations, or due to use of different bioinformatic software to analyse the control and trial plasma samples (409); however, increasing RP-LC gradient time enables better peptide separation and therefore more proteins can be identified (359, 410). Our proteomic workflow for a comparative semi-quantitative analysis of the onchocerciasis plasma proteome was shown to be robust, with similar numbers of proteins identified and very little experimental variability in the LFQ protein intensities between individual samples.

Despite the detection of several *O. volvulus* proteins in all five individuals screened, the proteomic analysis of a longitudinal onchocerciasis sample set following treatment detected no parasite or human proteins that significantly changed in abundance, or were absent among all individuals post-treatment. We therefore did not detect a protein marker of infection clearance and treatment efficacy in our data set. As several potential markers of infection prevalence from *O. volvulus* were consistently detected over the 21 months, we may have failed to identify a protein significantly changing as the adult worm infection had not yet cleared (157), or proteins from dying/degraded worms were continuously detected. Furthermore, three proteins showed either a decrease (A0A044SN57 and A0A044U885), or increase (A0A044TBP5), in detection frequency among individuals at month 21 relative to baseline, which may have resulted in a more conclusive outcome if individuals had been observed over a longer period of time. Contrary to our proteomic findings, a metabolomic study identified a significant reduction in the concentration of an *O. volvulus* neurotransmitter-derived secretion metabolite, NATOG, in urine from individuals tested 20 months post-doxycycline treatment compared with untreated *O. volvulus*-positive patients and placebo-treated patients (275). However, NATOG was also not completely cleared from the host urine by 20 months, and this metabolite may be cleared faster than a protein marker due to its intimate relationship with the human host metabolic pathway (275).

While longitudinal analyses such as the current study are inherently useful and findings more applicable to real-world scenarios relative to diseased vs healthy cohorts (273, 274), a number of factors may have confounded such analyses. The nature of the disease and treatment under investigation, which included large gaps in time between sampling time points, make it very challenging to capture and discern potentially relevant changes in protein levels related to treatment. New adult worm

infections may have become established over the 21 month period, thus diluting the perceived antifilarial effects and therapeutic efficacy of treatment in different patients evaluated at different times thereafter (158). With respect to the human proteins, the plasma proteome is known to have much greater inter- than intra-individual variability (367, 391, 392), and plasma proteomes of individuals tested here were found to cluster together rather than by specific time points of the trial. The host response to onchocerciasis infection will consist of individual-specific dynamic immune and cellular interactions with the parasite (393, 394), which may have been over-looked by grouping individuals by time point. Proteins relating to onchocerciasis treatment that change in abundance over time may have also had differences in signals too subtle for our semi-quantitative untargeted MS analyses in a small sample set (309). Furthermore, proteins are inferred by identification of short peptide sequences in discovery LC-MS/MS, and therefore proteins that vary as cleavage products or according to post-translational modifications are also likely to be missed with this method (309).

For future efforts investigating biomarkers of active infection with onchocerciasis and infection clearance following macrofilaricidal treatment, it will be important to try and improve the sample sets analysed and reduce potential for confounding variables. Ideally, human sample sets would be collected from areas of low endemicity or in a confirmed elimination setting so that reinfections are less likely to occur over follow up (or from migrant populations that will not remain in the endemic area). Clinical samples would also be collected from areas where there are not coinfective parasites, such as *L. loa, M. perstans* or *W. bancrofti,* to ensure that biomarker(s) are from infection with *O. volvulus* only. Additionally, patients would respond well to treatment and show a total macrofilaricidal response. A macrofilaricide drug that elicits a total macrofilaricidal effect on the adult worms and acts rapidly would be preferable for identifying biomarkers compared to samples from people treated with doxycycline, where follow up time must be at least 21 months due to the slow (and potentially incomplete) killing of the adult worm population. In the absence of a perfect human sample set, animal models, such as new immunodeficient mouse models for onchocerciasis, would also be useful for conducting preclinical studies where samples can be readily obtained and conditions optimally controlled.

Parasite-derived nucleic acid markers in plasma for diagnosis of onchocerciasis

The final aim of this project was to verify whether parasite-derived miRNAs and DNA are detectable in the plasma of individuals with onchocerciasis, and if so, to determine whether the type of antifilarial intervention alters their detection over time post-treatment (Chapter 5). This study has identified both parasite-derived miRNAs and *O. volvulus*-specific DNA in the circulation of the host, and reports the first use of RT-qPCR and qPCR for the detection of *O. volvulus* nucleic acids in plasma from individuals in an onchocerciasis-endemic community before and after macrofilaricidal or microfilaricidal treatment. However, the longitudinal analysis of 18 participants infected solely with *O. volvulus*, before and after treatment with either doxycycline, doxycycline + ivermectin or ivermectin, identified only two of 72 samples as very weakly positive for parasite miRNAs cel-miR-71-5p and bma-lin-4. Therefore, almost all samples tested negative, even after extensive optimisation of the RT-qPCR protocol. We also verified by RT-qPCR that the two miRNAs are expressed in *L. loa*, and therefore have experimentally confirmed that cel-miR-71-5p and bma-lin-4 do not have the necessary specificity or sensitivity to be circulating diagnostic markers for onchocerciasis. Future work could investigate miRNAs in individuals with *O. volvulus* and *L. loa* or *M. perstans* co-infections, where the mf reside in the blood, to better understand the dynamics of parasite-derived circulating miRNAs in the host circulation. By comparison, the *O. volvulus*-specific O-150 DNA marker was detected in plasma in almost half of the same 18 individuals tested at baseline, with a decline in positive patients detected in all treatment groups over time. However, a high proportion of samples that were positive by parasitological evaluation of *O. volvulus* in skin snips were negative by qPCR in plasma. Therefore, qPCR of *O. volvulus* DNA in the host plasma had the necessary specificity but not the sensitivity to be a diagnostic test for onchocerciasis.

The results presented here demonstrate that even although *O. volvulus* does not reside in the circulatory system of the host, parasite miRNAs and DNA are detectable in plasma. This has provided important information with regard to the proposed diagnostic utility of these markers compared to the ‘gold standard’ skin snip for detecting onchocerciasis positive individuals. Additionally, the use of a unique longitudinal sample set comprising patients enrolled in one of three filaricidal treatment regimens allowed us to assess the influence of treatment on detection of

the parasite-derived nucleic acids over time. An important feature of this study is that it was representative of the typical situation of low mf densities encountered in communities undergoing ivermectin treatment, and in hypoendemic communities that will be targeted in elimination programs. Therefore, the utility of parasite nucleic acids in plasma as a diagnostic tool for real-world elimination 'end game' scenarios could be assessed. This study was also unique in comparison to other *O. volvulus* miRNA studies conducted thus far (251, 291, 297) in that plasma samples from *O. volvulus* positive and *M. perstans/L. loa* mf negative individuals were tested, as samples with co-infections assessed by parasitological evaluation were excluded. This enabled us to report the *O. volvulus* origin of the parasite-derived miRNAs with greater confidence. Our work is in agreement with a recent study investigating circulating miRNAs in individuals with onchocerciasis (297), in that levels of these extracellular parasite-derived miRNAs are very low, if they are present at all in the host plasma. Lagatie and colleagues (297) detected few worm miRNAs in diverse samples, and the miRNAs were not universally present in all or most infected individuals. However, this study did not rule out the potential for co-infected samples. As miRNAs from blood-localised parasites appear to more abundant in host circulation relative to parasites in other tissues (251, 287), there is a possibility that the miRNAs detected in their study originated from another parasite. From a diagnostic standpoint, the utility of parasite-derived miRNAs as a marker for infection will depend on how consistently they are secreted/excreted into extracellular fluids and their stability once in plasma. Although our findings did not support the use of extracellular parasite-derived miRNAs as diagnostic markers for onchocerciasis, their potential for detection of blood-borne filarial infections and other parasitic worms have been investigated (251, 287, 291, 294-297). Worms with life cycle stages in the blood have shown higher levels of parasite-derived miRNAs in the host circulation (251, 287), relative to individuals with parasites infecting other tissues (287, 297). Therefore, the conclusions that can be drawn from the current work are in-line with the findings of others, that parasite-derived miRNAs are present at very low concentrations in the host circulation, and for *O. volvulus*-derived miRNAs this is likely due to the parasite's locality in the host. There is no diagnostic utility of cel-miR-71 and bma-lin-4 for detecting onchocerciasis in plasma as they are likely below the limit of detection for RT-qPCR, and there is extensive homology with secreted/excreted miRNAs of other parasitic worms.

The use of an *O. volvulus*-specific DNA marker to screen plasma from individuals with onchocerciasis by qPCR identified a higher proportion of infected individuals in baseline samples, and the number of positive individuals detected declined over time following all treatment regimens. The qPCR assay was also positive in three mf negative individuals and two individuals with < 10 mf/mg. In addition, one doxycycline treated individual remained positive for O-150 by qPCR over the duration of the trial. However, parasitological evaluation of skin snips was found to be far superior over qPCR of *O. volvulus* DNA in plasma, as around 2/3's of qPCR negative samples were positive for mf by skin snip. The O-150 qPCR assay also did not detect many samples from individuals with low numbers of mf (< 10 mf/mg). Therefore, plasma qPCR may be a more sensitive in meso- and hyperendemic areas with higher infection densities. A recent study using this O-150 qPCR assay in skin snips reported greater sensitivity compared to skin snip microscopy and nodule palpation, and their results provided a semi-quantitative estimate of mf intensity (201). However, they also observed that 56.3% of individuals who did not have palpable nodules had positive qPCR or skin snip results. Likewise, they noted that 63.4% of individuals that had negative skin snip microscopy results had palpable nodules or positive qPCR results. A further 52 individuals had palpable nodules but were mf negative by both microscopy and qPCR. Therefore, combining positive results from all three tests significantly increased the accuracy of diagnosis and assessment of the infection prevalence in the sampled population. The O-150 qPCR assay showed some potential as an indicator of infection, and could be used for mapping endemic areas for adult worm infection using pooled representative plasma samples of populations or sentinel groups, alongside the use of other diagnostic tools. PCR with pooled blood samples has been used to gauge the filarial infection prevalence in Indonesia (402). However, it could not be used to identify onchocerciasis infection in hypoendemic areas or to reliably monitor efficacy of any antifilarial treatment.

Conclusion

A circulating biomarker for *O. volvulus* to detect active infection, determine infection intensity and/or monitor treatment efficacy would be highly advantageous over the currently available diagnostic tools for onchocerciasis. Despite several decades of active and ongoing research to identify markers with the necessary

specificity and sensitivity to diagnose current infection with *O. volvulus*, no potential biomarkers have been progressed to diagnostic development for field use. Particularly now, as we progress from an onchocerciasis control to an elimination programme in Africa, a robust biomarker for *O. volvulus* is urgently needed in order to accurately map hypoendemic areas with low levels of ongoing transmission, identify areas with recrudescence, and make informed decisions regarding treatment provision and intervention cessation. *O. volvulus* has a complex life cycle within the host and an overlapping geographic distribution with other co-infective parasite species. The challenge for diagnostic development of a circulating marker for *O. volvulus* for use in elimination programmes therefore lies in addressing and overcoming the issues of sensitivity and specificity (411, 412). The increasing availability of filarial worm genomes and advances in transcriptomics and proteomics will go a long way in helping to better understand the unique biology of the parasite and interaction with the human host (199, 269), and aid in identifying novel targets for diagnostic tools (269, 271), as well as novel drug targets (199) and vaccine candidates (269). Using discovery proteomics, this thesis has identified *O. volvulus* proteins in the plasma of individuals during patent infection with onchocerciasis and in the many months following macrofilaricidal treatment. Several of these proteins could be markers of infection in the host from excretion or death of adult worms, and one may be a marker of the female worm. Additionally, most of the proteins had low sequence similarity along the total protein length with orthologous proteins from *W. bancrofti* and *L. loa*. Detection of circulating DNA specific to *O. volvulus* showed variable sensitivity for identifying infected individuals, while diagnosis of *O. volvulus* by circulating parasite-derived miRNAs completely lacked specificity and sensitivity. Although three *O. volvulus* proteins showed some potential, no protein, DNA or miRNA markers of infection clearance and treatment efficacy were identified by 21 months post-doxycycline treatment among the individuals tested. Future work should determine whether the *O. volvulus* proteins detected are indeed markers of active infection, in order to progress specific and sensitive targets for future diagnostic development.

Bibliography

1. APOC. Final Communiqué of the 11th session of the Joint Action Forum (JAF) of APOC, Paris, France, 6–9 December 2005.2005. [Internet]. Available from: http://www.who.int/apoc/about/structure/jaf/jaf11_final_communique.pdf.
2. Murdoch ME, Murdoch IE. Onchocerciasis. In: Mabey D, editor. Principles of medicine in africa. 4th ed. Cambridge: Cambridge University Press. 2013. p. 456-65.
3. Tamarozzi F, Halliday A, Gentil K, Hoerauf A, Pearlman E, Taylor MJ. Onchocerciasis: the role of *Wolbachia* bacterial endosymbionts in parasite biology, disease pathogenesis, and treatment. Clinical Microbiology Reviews. 2011;24(3):459-68.
4. Oladepo O, Brieger WR, Otusanya S, Kale OO, Offiong S, Titiloye M. Farm land size and onchocerciasis status of peasant farmers in south-western Nigeria. Tropical Medicine and International Health. 1997;2(4):334-40.
5. Brieger WR, Oshiname FO, Ososanya OO. Stigma associated with onchocercal skin disease among those affected near the Ofiki and Oyan Rivers in western Nigeria. Social Science and Medicine. 1998;47(7):841-52.
6. Vlassoff C, Weiss M, Ovuga E, Eneanya C, Nwel PT, Babalola S, et al. Gender and the stigma of onchocercal skin disease in Africa. Social Science and Medicine. 2000;50(10):1353-68.
7. Tchounkeu YFL, Onyeneho NG, Wanji S, Kabali AT, Manianga C, Amazigo UV, et al. Changes in stigma and discrimination of onchocerciasis in Africa. Transactions of the Royal Society of Tropical Medicine and Hygiene. 2012;106(6):340-7.
8. WHO. Onchocerciasis and its control: Report of a WHO Expert Committee on Onchocerciasis Control.1995; WHO Technical Report Series 852 [Internet]. Available from: http://apps.who.int/iris/bitstream/10665/37346/1/WHO_TRS_852.pdf.
9. Coffeng LE, Stolk WA, Zoure HG, Veerman JL, Agblewonu KB, Murdoch ME, et al. African Programme for Onchocerciasis Control 1995–2015: model-estimated health impact and cost. PLoS Neglected Tropical Diseases. 2013;7(1):e2032.
10. WHO. Accelerating work to overcome the global impact of neglected tropical diseases: a roadmap for implementation: executive summary.2012. [Internet]. Available from: http://apps.who.int/iris/bitstream/10665/70809/1/WHO_HTM_NTD_2012.1_eng.pdf.
11. Taylor MJ, Hoerauf A, Bockarie M. Lymphatic filariasis and onchocerciasis. The Lancet. 2010;376(9747):1175-85.
12. Dietz K. The population dynamics of onchocerciasis. In: Anderson RM, editor. The population dynamics of infectious siseases: theory and applications. Boston: Springer; 1982. p. 209-41.
13. Okulicz JF, Stibich AS, Elston DM, Schwartz RA. Cutaneous onchocercoma. International Journal of Dermatology. 2004;43(3):170-2.
14. Plaisier A, Van Oortmarssen G, Remme J, Habbema J. The reproductive lifespan of *Onchocerca volvulus* in West African savanna. Acta Tropica. 1991;48(4):271-84.

15. Haffner A, Guilavogui AZ, Tischendorf FW, Brattig NW. *Onchocerca volvulus*: microfilariae secrete elastinolytic and males nonelastinolytic matrix-degrading serine and metalloproteases. Experimental Parasitology. 1998;90(1):26-33.
16. Kozek WJ, Marroquin HF. Intracytoplasmic bacteria in *Onchocerca volvulus.* American Journal of Tropical Medicine and Hygiene. 1977;26(4):663-78.
17. Taylor MJ, Bandi C, Hoerauf A. *Wolbachia* bacterial endosymbionts of filarial nematodes. Advances in Parasitology. 2005;60:245-84.
18. Basáñez M-G, Sébastien D, Churcher TS, Breitling LP, Little MP, Boussinesq M. River blindness: a success story under threat? PLoS Medicine. 2006;3(9):e371.
19. Murdoch M, Asuzu M, Hagan M, Makunde W, Ngoumou P, Ogbuagu K, et al. Onchocerciasis: the clinical and epidemiological burden of skin disease in Africa. Annals of Tropical Medicine and Parasitology. 2002;96(3):283-96.
20. Boatin BA, Richards Jr FO. Control of onchocerciasis. Advances in Parasitology. 2006;61:349-94.
21. Timmann C, van der Kamp E, Kleensang A, König IR, Thye T, Büttner DW, et al. Human genetic resistance to *Onchocerca volvulus*: evidence for linkage to chromosome 2p from an autosome-wide scan. Journal of Infectious Diseases. 2008;198(3):427-33.
22. Arndts K, Specht S, Debrah AY, Tamarozzi F, Schulz UK, Mand S, et al. Immunoepidemiological profiling of onchocerciasis patients reveals associations with microfilaria loads and ivermectin intake on both individual and community levels. PLoS Neglected Tropical Diseases. 2014;8(2):e2679.
23. Hoerauf A, Satoguina J, Saeftel M, Specht S. Immunomodulation by filarial nematodes. Parasite Immunology. 2005;27(10-11):417-29.
24. Brattig NW. Pathogenesis and host responses in human onchocerciasis: impact of *Onchocerca* filariae and *Wolbachia* endobacteria. Microbes and Infection. 2004;6(1):113-28.
25. Remme J. The global burden of onchocerciasis in 1990. World Health Organization, Geneva.2004 [Internet]. Available from: http://www.who.int/healthinfo/global_burden_disease/Onchocerciasis%201990.pdf.
26. Enk CD. Onchocerciasis—river blindness. Clinics in Dermatology. 2006;24(3):176-80.
27. Amazigo UV, Nnoruka E, Maduka C, Bump J, Benton B, Seketeli A. Ivermectin improves the skin condition and self-esteem of females with onchocerciasis: a report of two cases. Annals of Tropical Medicine and Parasitology. 2004;98(5):533-7.
28. Murdoch M, Hay R, Mackenzie C, Williams J, Ghalib H, Cousens S, et al. A clinical classification and grading system of the cutaneous changes in onchocerciasis. British Journal of Dermatology. 1993;129(3):260-9.
29. Thylefors B, Negrel A, Pararajasegaram R, Dadzie K. Global data on blindness. Bulletin of the World Health Organization. 1995;73(1):115.
30. Lewallen S, Courtright P. Blindness in Africa: present situation and future needs. British Journal of Ophthalmology. 2001;85(8):897-903.
31. Amazigo U, Noma M, Bump J, Benton B, Liese B, Yameogo L, et al. Onchocerciasis. In: Jamison DT, Feachem RG, Makgoba MW, Bos ER, Baingana FK, Hofman KJ, et al., editors. Disease and mortality in Sub-Saharan Africa. 2nd ed. Washington (DC): The International Bank for Reconstruction and Development/The World Bank; 2006. Chapter 15.

32. Simonsen PE. Filariases. In: Cook GC, Manson P, Zumla A, editors. Manson's tropical diseases. 22nd ed. London: W. B. Saunders; 2009. p. 1477–513.
33. Baker R, Abdelnur O. Onchocerciasis in Sudan: the distribution of the disease and its vectors. Tropical medicine and parasitology: official organ of Deutsche Tropenmedizinische Gesellschaft and of Deutsche Gesellschaft fur Technische Zusammenarbeit (GTZ). 1986;37(4):341-55.
34. Little MP, Basáñez M-G, Breitling LP, Boatin BA, Alley ES. Incidence of blindness during the onchocerciasis control programme in western Africa, 1971-2002. Journal of Infectious Diseases. 2004;189(10):1932-41.
35. Zimmerman P, Dadzie K, De Sole G, Remme J, Alley ES, Unnasch T. *Onchocerca volvulus* DNA probe classification correlates with epidemiologic patterns of blindness. Journal of Infectious Diseases. 1992;165(5):964-8.
36. Higazi TB, Filiano A, Katholi CR, Dadzie Y, Remme JH, Unnasch TR. Wolbachia endosymbiont levels in severe and mild strains of *Onchocerca volvulus.* Molecular and Biochemical Parasitology. 2005;141(1):109-12.
37. Thylefors B. Ocular onchocerciasis. Bulletin of the World Health Organization. 1978;56(1):63.
38. Bird A, Anderson J, Fuglsang H. Morphology of posterior segment lesions of the eye in patients with onchocerciasis. British Journal of Ophthalmology. 1976;60(1):2-20.
39. Hopkins A, Boatin BA. Onchocerciasis. In: Selendy JMH, editor. Water and sanitation-related diseases and the environment: Challenges, interventions, and preventive measures. New Jersey: John Wiley and Sons; 2011. Chapter 11.
40. Egbert P, Jacobson D, Fiadoyor S, Dadzie P, Ellingson K. Onchocerciasis: a potential risk factor for glaucoma. British Journal of Ophthalmology. 2005;89(7):796-8.
41. Etya'ale D. Vision 2020: update on onchocerciasis. Community Eye Health. 2001;14(38):19.
42. Murphy RP, Taylor H, Greene BM. Chorioretinal damage in onchocerciasis. American Journal of Ophthalmology. 1984;98(4):519-21.
43. Gillette-Ferguson I, Hise AG, Sun Y, Diaconu E, McGarry HF, Taylor MJ, et al. *Wolbachia*- and *Onchocerca volvulus*-induced keratitis (river blindness) is dependent on myeloid differentiation factor 88. Infection and Immunity. 2006;74(4):2442-5.
44. Saint Andre A, Blackwell NM, Hall LR, Hoerauf A, Brattig NW, Volkmann L, et al. The role of endosymbiotic *Wolbachia* bacteria in the pathogenesis of river blindness. Science. 2002;295(5561):1892-5.
45. Gillette-Ferguson I, Hise AG, McGarry HF, Turner J, Esposito A, Sun Y, et al. *Wolbachia*-induced neutrophil activation in a mouse model of ocular onchocerciasis (river blindness). Infection and Immunity. 2004;72(10):5687-92.
46. Cooper PJ, Guderian RH, Proano R, Taylor DW. Absence of cellular responses to a putative autoantigen in onchocercal chorioretinopathy: cellular autoimmunity in onchocercal chorioretinopathy. Investigative Ophthalmology and Visual Science. 1996;37(2):405-12.
47. McKechnie NM, Braun G, Klager S, Connor V, Kasp E, Wallace G, et al. Cross-reactive antigens in the pathogenesis of onchocerciasis. Annals of Tropical Medicine and Parasitology. 1993;87(6):649-52.
48. Pion SD, Kaiser C, Boutros-Toni F, Cournil A, Taylor MM, Meredith SE, et al. Epilepsy in onchocerciasis endemic areas: systematic review and meta-analysis of population-based surveys. PLoS Neglected Tropical Diseases. 2009;3(6):e461.

49. Boussinesq M, Pion SD, Demanga N, Kamgno J. Relationship between onchocerciasis and epilepsy: a matched case-control study in the Mbam Valley, Republic of Cameroon. Transactions of the Royal Society of Tropical Medicine and Hygiene. 2002;96(5):537-41.
50. Newell ED, Vyungimana F, Bradley JE. Epilepsy, retarded growth and onchocerciasis, in two areas of different endemicity of onchocerciasis in Burundi. Transactions of the Royal Society of Tropical Medicine and Hygiene. 1997;91(5):525-7.
51. Föger K, Gora-Stahlberg G, Sejvar J, Ovuga E, Jilek-Aall L, Schmutzhard E, et al. Nakalanga syndrome: clinical characteristics, potential causes, and its relationship with recently described nodding syndrome. PLoS Neglected Tropical Diseases. 2017;11(2):e0005201.
52. Colebunders R, Njamnshi AK, Oijen M, Mukendi D, Kashama JM, Mandro M, et al. Onchocerciasis-associated epilepsy: From recent epidemiological and clinical findings to policy implications. Epilepsia Open. 2017;2(2):145-52.
53. Colebunders R, Hendy A, Nanyunja M, Wamala JF, van Oijen M. Nodding syndrome-a new hypothesis and new direction for research. International Journal of Infectious Diseases. 2014;27:74-7.
54. Colebunders R, Hendy A, Nanyunja M, Wamala JF, van Oijen M. Nodding syndrome-a new hypothesis and new direction for research. International of Journal Infecticious Diseases. 2014;27:74-7.
55. Colebunders R, Hendy A, Mokili JL, Wamala JF, Kaducu J, Kur L, et al. Nodding syndrome and epilepsy in onchocerciasis endemic regions: comparing preliminary observations from South Sudan and the Democratic Republic of the Congo with data from Uganda. BMC Research Notes. 2016;9:182.
56. Colebunders R, Post R, O'Neill S, Haesaert G, Opar B, Lakwo T, et al. Nodding syndrome since 2012: recent progress, challenges and recommendations for future research. Tropical Medicine and International Health. 2015;20(2):194-200.
57. Johnson TP, Tyagi R, Lee PR, Lee MH, Johnson KR, Kowalak J, et al. Nodding syndrome may be an autoimmune reaction to the parasitic worm *Onchocerca volvulus*. Science Translational Medicine. 2017;9(377).
58. Johnson T, Tyagi R, Lee PR, Lee M-h, Johnson KR, Kowalak J, et al. Detection of auto-antibodies to leiomodin-1 in patients with nodding syndrome. Journal of Neuroimmunology. 2014;275(1):103.
59. Idro R, Opar B, Wamala J, Abbo C, Onzivua S, Mwaka DA, et al. Is nodding syndrome an *Onchocerca volvulus*-induced neuroinflammatory disorder? Uganda's story of research in understanding the disease. International Journal of Infectious Diseases. 2016;45(Supplement C):112-7.
60. WHO. Onchocerciasis Fact Sheet.2017 [Internet]. Available from: http://www.who.int/mediacentre/factsheets/fs374/en/.
61. Noma M, Zoure H, Tekle AH, Enyong P, Nwoke BE, Remme JH. The geographic distribution of onchocerciasis in the 20 participating countries of the African Programme for Onchocerciasis Control:(1) priority areas for ivermectin treatment. Parasite and Vectors. 2014;7:325.
62. Duke BOL, Lewis DJ, Moore PJ. *Onchocerca-Simulium* complexes. Annals of Tropical Medicine and Parasitology. 1966;60(3):318-36.
63. Adler PH, Cheke RA, Post RJ. Evolution, epidemiology, and population genetics of black flies (Diptera: *Simuliidae*). Infection, Genetics and Evolution. 2010;10(7):846-65.

64. Adler PH, Crosskey RW. World blackflies (Diptera: *Simuliidae*): a comprehensive revision of the taxonomic and geographical inventory [2017]. 2017. [Internet]. Available from: http://www.clemson.edu/cafls/biomia/pdfs/blackflyinventory.pdf
65. Post R, Mustapha M, Krueger A. Taxonomy and inventory of the cytospecies and cytotypes of the *Simulium damnosum* complex (Diptera: *Simuliidae*) in relation to onchocerciasis. Tropical Medicine and International Health. 2007;12(11):1342-53.
66. Boakye DA, Back C, Fiasorgbor GK, Sib AP, Coulibaly Y. Sibling species distributions of the *Simulium damnosum* complex in the west African Onchocerciasis Control Programme area during the decade 1984-93, following intensive larviciding since 1974. Medical and Veterinary Entomology. 1998;12(4):345-58.
67. Kale O. Onchocerciasis: the burden of disease. Annals of Tropical Medicine and Parasitology. 1998;92(Supplement 1):101-15.
68. CDC. Progress toward elimination of onchocerciasis in the Americas-1993-2012. MMWR Morbidity and Mortality Weekly Report. 2013;62(20):405.
69. Zimmerman PA, Katholi CR, Wooten MC, Lang-Unnasch N, Unnasch TR. Recent evolutionary history of American *Onchocerca volvulus*, based on analysis of a tandemly repeated DNA sequence family. Molecular Biology and Evolution. 1994;11(3):384-92.
70. Shelley AJ. *Simuliidae* and the transmission and control of human Onchocerciasis in Latin America. Cadernos de saude publica. 1991;7(3):310-27.
71. Gustavsen K, Hopkins A, Sauerbrey M. Onchocerciasis in the Americas: from arrival to (near) elimination. Parasite and Vectors. 2011;4:205.
72. Adler PH, Borkent A, Hamada N, McCreadie JW. Biodiversity of *Simulium metallicum* sensu lato (Diptera: *Simuliidae*), a complex of Neotropical vectors associated with human onchocerciasis. Acta Tropica. 2017;173:171-9.
73. Remme J, Zongo J. Demographic aspects of the epidemiology and control of onchocerciasis in West Africa. Demography and Vector-Borne Diseases. 1989:367-86.
74. Remme JH. Research for control: the onchocerciasis experience. Tropical Medicine and International Health. 2004;9(2):243-54.
75. Thylefors B. Eliminating onchocerciasis as a public health problem. Tropical Medicine and International Health. 2004;9(4):A1-A3.
76. Mectizan Expert Committee. The Mectizan Donation Program: Community—based mass treatment of onchocerciasis. Parts I & II. One Copenhill, Atlanta, GA 30307. 1990.
77. Boatin B. The Onchocerciasis Control Programme in West Africa (OCP). Annals of Tropical Medicine and Parasitology. 2008;102(Supplement-1):13-7.
78. Remme J. The African Programme for Onchocerciasis Control: preparing to launch. Parasitology Today. 1995;11(11):403-6.
79. WHO. Community directed treatment with ivermectin: report of a multi-country study.1996. [Internet]. Available from: http://apps.who.int/iris/bitstream/10665/63902/1/TDR_AFR_RP_96.1.pdf.
80. APOC. Community-directed treatment with ivermectin (CDTi): a practical guide for trainers of community-directed distributors.1998. [Internet]. Available from: http://www.who.int/apoc/publications/cdti_practical_guide_for_trainers_of_cdds.pdf?ua=1.
81. Ngoumou P, Walsh JF. A manual for rapid epidemiological mapping of onchocerciasis. Geneva: World Health Organization; 1993.

82. Prost A, Hervouet J, Thylefors B. The degree of endemicity of onchocerciasis. Bulletin of the World Health Organization. 1979;57(4):655-62.
83. Coffeng LE, Pion SD, O'Hanlon S, Cousens S, Abiose AO, Fischer PU, et al. Onchocerciasis: the pre-control association between prevalence of palpable nodules and skin microfilariae. PLoS Neglected Tropical Diseases. 2013;7(4):e2168.
84. WHO. Strategies for ivermectin distribution through primary health care systems. Geneva: World Health Organization. 1991.
85. Noma M, Nwoke BE, Nutall I, Tambala PA, Enyong P, Namsenmo A, et al. Rapid epidemiological mapping of onchocerciasis (REMO): its application by the African Programme for Onchocerciasis Control (APOC). Annals of Tropical Medicine and Parasitology 2002;96 Suppl 1:S29-39.
86. WHO. Certification of elimination of human onchocerciasis: criteria and procedures. Geneva: World Health Organization; 2001.
87. WHO. Guidelines for stopping mass drug administration and verifying elimination of human onchocerciasis: criteria and procedures. Geneva: World Health Organization; 2016.
88. WHO. World: Distribution and status of preventive chemotherapy for onchocerciasis, 2015. 2016. [Internet]. Available from: http://gamapserver.who.int/mapLibrary/Files/Maps/Onchocerciasis_2015.png.
89. Allotey P, Amazigo U, Adjei S, Seddoh A, Lusamba-Dikassa PS. 15 years of APOC-a lifetime of public health evidence. The Lancet. 2012;380(9851):1361-3.
90. Diawara L, Traore MO, Badji A, Bissan Y, Doumbia K, Goita SF, et al. Feasibility of onchocerciasis elimination with ivermectin treatment in endemic foci in Africa: first evidence from studies in Mali and Senegal. PLoS Neglected Tropical Diseases. 2009;3(7):e497.
91. Traore MO, Sarr MD, Badji A, Bissan Y, Diawara L, Doumbia K, et al. Proof-of-principle of onchocerciasis elimination with ivermectin treatment in endemic foci in Africa: final results of a study in Mali and Senegal. PLoS Neglected Tropical Diseases. 2012;6(9):e1825.
92. Tekle AH, Elhassan E, Isiyaku S, Amazigo UV, Bush S, Noma M, et al. Impact of long-term treatment of onchocerciasis with ivermectin in Kaduna State, Nigeria: first evidence of the potential for elimination in the operational area of the African Programme for Onchocerciasis Control. Parasites and Vectors. 2012;5:28.
93. APOC. Informal consultation on elimination of onchocerciasis transmission with current tools in Africa–"Shrinking the Map", Ouagadougou, Burkina Faso, 25 – 27 February 2009. 2009. [Internet]. Available from: http://www.mectizan.org/sites/www.mectizan.org/files/attachments/resources/Report%20of%20Informal%20consultation%20on%20elimination%20of%20oncho%20transmission%20with%20current%20tools%20in%20Africa.pdf.
94. WHO. World Health Organization's 2020 roadmap on NTDs 2012 [Available from: http://www.who.int/neglected_diseases/NTD_RoadMap_2012_Fullversion.pdf.
95. World Bank. Pushing back neglected tropical diseases in Africa. 2012. [Internet]. Available from: http://www.worldbank.org/en/news/feature/2012/11/17/pushing-back-neglected-tropical-diseases-in-africa.
96. WHO. WHO revises onchocerciasis guidelines as countries approach elimination target. 2016. [Internet]. Available from: http://www.who.int/neglected_diseases/news/WHO_revises_guidelines_for_river_blindness/en/.

97. WHO. Regional Strategy on Neglected Tropical Diseases in the WHO African Region 2014–2020. Brazzaville: WHO Regional Office for Africa; 2014.
98. WHO. Preventive chemotherapy in human helminthiasis: coordinated use of anthelminthic drugs in control interventions: a manual for health professionals and programme managers. Geneva: World Health Organization; 2006.
99. Hopkins AD. Neglected tropical diseases in Africa: a new paradigm. International Health. 2016;8 Suppl 1:i28-33.
100. Hopkins AD. From 'control to elimination': a strategic change to win the end game. International Health. 2015;7(5):304-5.
101. Bockarie MJ, Kelly-Hope LA, Rebollo M, Molyneux DH. Preventive chemotherapy as a strategy for elimination of neglected tropical parasitic diseases: endgame challenges. Philosophical Transactions of the Royal Society of London Series B, Biological sciences 2013;368(1623):20120144.
102. Duerr HP, Raddatz G, Eichner M. Diagnostic value of nodule palpation in onchocerciasis. Transactions of the Royal Society of Tropical Medicine and Hygiene. 2008;102(2):148-54.
103. Kamga GR, Dissak-Delon FN, Nana-Djeunga HC, Biholong BD, Mbigha-Ghogomu S, Souopgui J, et al. Still mesoendemic onchocerciasis in two Cameroonian community-directed treatment with ivermectin projects despite more than 15 years of mass treatment. Parasites and Vectors. 2016;9(1):581.
104. Lamberton PH, Cheke RA, Winskill P, Tirados I, Walker M, Osei-Atweneboana MY, et al. Onchocerciasis transmission in Ghana: persistence under different control strategies and the role of the simuliid vectors. PLoS Neglected Tropical Diseases. 2015;9(4):e0003688.
105. Molyneux DH, Hopkins A, Bradley MH, Kelly-Hope LA. Multidimensional complexities of filariasis control in an era of large-scale mass drug administration programmes: a can of worms. Parasites and Vectors. 2014;7:363.
106. Dadzie Y, Neira M, Hopkins D. Final report of the Conference on the eradicability of onchocerciasis. Filaria Journal. 2003;2(2):297-308.
107. Blanks J, Richards F, Beltran F, Collins R, Alvarez E, Zea Flores G, et al. The Onchocerciasis Elimination Program for the Americas: a history of partnership. Revista panamericana de salud publica = Pan American journal of public health. 1998;3(6):367-74.
108. Sauerbrey M. The Onchocerciasis Elimination Program for the Americas (OEPA). Annals of Tropical Medicine and Parasitology 2008;102 Suppl 1:25-9.
109. WHO. Elimination of onchocerciasis in the WHO Region of the Americas: Ecuador's progress towards verification of elimination. Weekly Epidemiological Record. 2014;89(37):401-8.
110. Abdul-Ghani R, Mahdy MA, Beier JC. Onchocerciasis in Yemen: time to take action against a neglected tropical parasitic disease. Acta Tropica. 2016;162:133-41.
111. Taylor HR. Recent developments in the treatment of onchocerciasis. Bulletin of the World Health Organization. 1984;62(4):509-15.
112. Albiez EJ. Assessment of onchocerciasis two years after nodulectomy in a region with interrupted transmission. Zentralblattfur Bakteriologie, L Abt Ref. 1980;167:313.
113. Albiez EJ. Microfilarial densities of *Onchocerca volvulus* in the skin after a single nodulectomy in Liberia. Zentralblattfir Bakteriologie, L Abt Ref. 1980;167:313.

114. Albiez EJ. Studies on nodules and adult *Onchocerca volvulus* during a nodulectomy trial in hyperendemic villages in Liberia and Upper Volta. I. Palpable and impalpable onchocercomata. Tropenmedizin und Parasitologie. 1983;34(1):54-60.
115. Guderian RH. Effects of nodulectomy in onchocerciasis in Ecuador. Trop Med Parasitol. 1988;39 Suppl 4:356-7.
116. Babalola OE. Ocular onchocerciasis: current management and future prospects. Clinical Ophthalmology 2011;5:1479.
117. Hawking F. Suramin: with special reference to onchocerciasis. Advances in Pharmacology and Chemotherapy. 1978;15:289-322.
118. Anderson J, Fuglsang H, de CMTF. Effects of suramin on ocular onchocerciasis. Tropenmedizin und Parasitologie. 1976;27(3):279-96.
119. Rolland A, Prost A, Thylefors B. Review, after 3 years of the treatment with suramine, of a village suffering from onchocerciasis under entomological protection. Revue internationale du trachome et de pathologie oculaire tropicale et subtropicale : organe de la Ligue contre le trachome avec la collaboration de l'International. 1980;57(2-3):99-106.
120. Mazzotti L. Possibility of using the allergic reactions due to the administration of Hetrazan as an auxiliary diagnostic test for onchocerciasis in Mexico. Revista del Instituto de Salubridad y Enfermedades Tropicales. 1948;9:235-7.
121. Duke BO. The effects of drugs on *Onchocerca volvulus*. 1. Methods of assessment, population dynamics of the parasite and the effects of diethylcarbamazine. Bulletin of the World Health Organization. 1968;39(2):137-46.
122. Awadzi K, Gilles HM. Diethylcarbamazine in the treatment of patients with onchocerciasis. British Journal of Clinical Pharmacology. 1992;34(4):281-8.
123. Anderson J, Fuglsang H, de C MT. Effects of diethylcarbamazine on ocular onchocerciasis. Tropenmedizin und Parasitologie. 1976;27(3):263-78.
124. Bird A, el-Sheikh H, Anderson J, Fuglsang H. Changes in visual function and in the posterior segment of the eye during treatment of onchocerciasis with diethylcarbamazine citrate. British Journal of Ophthalmology. 1980;64(3):191-200.
125. Greene BM, Taylor HR, Brown EJ, Humphrey RL, Lawley TJ. Ocular and systemic complications of diethylcarbamazine therapy for onchocerciasis: association with circulating immune complexes. Journal of Infectious Diseases. 1983;147(5):890-7.
126. Francis H, Awadzi K, Ottesen E. The Mazzotti reaction following treatment of onchocerciasis with diethylcarbamazine: clinical severity as a function of infection intensity. The American Journal of Tropical Medicine and Hygiene. 1985;34(3):529-36.
127. Rougemont A, Thylefors B, Ducam M, Prost A, Ranque P, Delmont J. Traitement de l'onchocercose par la suramine à faibles doses progressives dans les collectivités hyperendémiques d'Afrique occidentale. 1. Résultats parasitologiques et surveillance ophtalmologique en zone de transmission non interrompue. Bulletin of the World Health Organization. 1980;58(6):917-22.
128. Jones BR. Selected pharmaceutical developments required for prevention of massive blindness in developing countries. Institute of Medicine Conference Proceedings, Washington, DC; Washington: National Academy of Sciences 1979. p. 103-13.

129. Awadzi K, Orme ML, Breckenridge AM, Gilles HM. The chemotherapy of onchocerciasis VI. The effect of indomethacin and cyproheptadine on the Mazzotti reaction. Annals of Tropical Medicine and Parasitology. 1982;76(3):323-30.
130. Taylor HR, Greene BM. Ocular changes with oral and transepidermal diethylcarbamazine therapy of onchocerciasis. British Journal of Ophthalmology 1981;65(7):494-502.
131. Ottesen EA. The global programme to eliminate lymphatic filariasis. Tropical Medicine and International Health. 2000;5(9):591-4.
132. Basanez MG, Pion SD, Boakes E, Filipe JA, Churcher TS, Boussinesq M. Effect of single-dose ivermectin on *Onchocerca volvulus*: a systematic review and meta-analysis. Lancet Infectious Diseases. 2008;8(5):310-22.
133. Fox LM. Ivermectin: uses and impact 20 years on. Current Opinion in Infectious Diseases. 2006;19(6):588-93.
134. Wolstenholme AJ, Rogers AT. Glutamate-gated chloride channels and the mode of action of the avermectin/milbemycin anthelmintics. Parasitology. 2005;131 Suppl:S85-95.
135. Diallo S, Aziz M, Lariviere M, Diallo J, Diop-Mar I, N'dir O, et al. A double-blind comparison of the efficacy and safety of ivermectin and diethylcarbamazine in a placebo controlled study of Senegalese patients with onchocerciasis. Transactions of the Royal Society of Tropical Medicine and Hygiene. 1986;80(6):927-34.
136. Taylor HR, Greene BM. The status of ivermectin in the treatment of human onchocerciasis. The American Journal of Tropical Medicine and Hygiene. 1989;41(4):460-6.
137. Duke BO. Evidence for macrofilaricidal activity of ivermectin against female *Onchocerca volvulus*: further analysis of a clinical trial in the Republic of Cameroon indicating two distinct killing mechanisms. Parasitology. 2005;130(Pt 4):447-53.
138. Chijioke CP, Okonkwo PO. Adverse events following mass ivermectin therapy for onchocerciasis. Transactions of the Royal Society of Tropical Medicine and Hygiene. 1992;86(3):284-6.
139. Keiser PB, Reynolds SM, Awadzi K, Ottesen EA, Taylor MJ, Nutman TB. Bacterial endosymbionts of *Onchocerca volvulus* in the pathogenesis of posttreatment reactions. Journal of Infectious Diseases. 2002;185(6):805-11.
140. Zoure HG, Wanji S, Noma M, Amazigo UV, Diggle PJ, Tekle AH, et al. The geographic distribution of *Loa loa* in Africa: results of large-scale implementation of the Rapid Assessment Procedure for Loiasis (RAPLOA). PLoS Neglected Tropical Diseases. 2011;5(6):e1210.
141. Padgett JJ, Jacobsen KH. Loiasis: African eye worm. Transactions of the Royal Society of Tropical Medicine and Hygiene. 2008;102(10):983-9.
142. Metzger WG, Mordmuller B. *Loa loa*-does it deserve to be neglected? Lancet Infectious Diseases. 2014;14(4):353-7.
143. Gardon J, Gardon-Wendel N, Demanga N, Kamgno J, Chippaux JP, Boussinesq M. Serious reactions after mass treatment of onchocerciasis with ivermectin in an area endemic for *Loa loa* infection. Lancet. 1997;350(9070):18-22.
144. Boussinesq M, Gardon J, Gardon-Wendel N, Kamgno J, Ngoumou P, Chippaux JP. Three probable cases of *Loa loa* encephalopathy following ivermectin treatment for onchocerciasis. American Journal of Tropical Medicine and Hygiene. 1998;58(4):461-9.
145. Ducorps M, Gardon-Wendel N, Ranque S, Ndong W, Boussinesq M, Gardon J, et al. Secondary effects of the treatment of hypermicrofilaremic loiasis using ivermectin. Bulletin de la Société de Pathologie Exotique 1995;88(3):105-12.

146. Boussinesq M. Loiasis. Annals of Tropical Medicine and Parasitology. 2006;100(8):715-31.
147. Mectizan Expert Committee/Technical Consultative Committee. Recommendations for the treatment of onchocerciasis with Mectizan in areas co-endemic for onchocerciasis and loiasis. 2004. Available from: http://www.who.int/apoc/publications/englishmectccloarecs-june04.pdf.
148. Takougang I, Meremikwu M, Wandji S, Yenshu EV, Aripko B, Lamlenn SB, et al. Rapid assessment method for prevalence and intensity of *Loa loa* infection. Bulletin of the World Health Organization. 2002;80(11):852-8.
149. APOC. Final communiqué of the tenth session of the Joint Action Forum of the African Programme for Onchocerciasis Control. Geneva: World Health Organization; 2004.
150. Kelly-Hope LA, Cano J, Stanton MC, Bockarie MJ, Molyneux DH. Innovative tools for assessing risks for severe adverse events in areas of overlapping *Loa loa* and other filarial distributions: the application of micro-stratification mapping. Parasites and Vectors. 2014;7:307.
151. Kelly-Hope LA, Unnasch TR, Stanton MC, Molyneux DH. Hypo-endemic onchocerciasis hotspots: defining areas of high risk through micro-mapping and environmental delineation. Infectious Diseases of Poverty. 2015;4:36.
152. Hoerauf A, Specht S, Büttner M, Pfarr K, Mand S, Fimmers R, et al. *Wolbachia* endobacteria depletion by doxycycline as antifilarial therapy has macrofilaricidal activity in onchocerciasis: a randomized placebo-controlled study. Medical Microbiology and Immunology. 2008;197(3):295-311.
153. Hoerauf A, Mand S, Volkmann L, Buttner M, Marfo-Debrekyei Y, Taylor M, et al. Doxycycline in the treatment of human onchocerciasis: Kinetics of *Wolbachia* endobacteria reduction and of inhibition of embryogenesis in female *Onchocerca* worms. Microbes and Infection. 2003;5(4):261-73.
154. Hoerauf A, Volkmann L, Hamelmann C, Adjei O, Autenrieth IB, Fleischer B, et al. Endosymbiotic bacteria in worms as targets for a novel chemotherapy in filariasis. Lancet. 2000;355(9211):1242-3.
155. Hoerauf A, Mand S, Adjei O, Fleischer B, Buttner DW. Depletion of wolbachia endobacteria in *Onchocerca volvulus* by doxycycline and microfilaridermia after ivermectin treatment. Lancet. 2001;357(9266):1415-6.
156. Hoerauf A, Specht S, Marfo-Debrekyei Y, Buttner M, Debrah AY, Mand S, et al. Efficacy of 5-week doxycycline treatment on adult *Onchocerca volvulus*. Parasitology Research. 2009;104(2):437-47.
157. Turner JD, Tendongfor N, Esum M, Johnston KL, Langley RS, Ford L, et al. Macrofilaricidal activity after doxycycline only treatment of *Onchocerca volvulus* in an area of *Loa loa* co-endemicity: a randomized controlled trial. PLoS Neglected Tropical Diseases. 2010;4(4):e660.
158. Specht S, Hoerauf A, Adjei O, Debrah A, Buttner DW. Newly acquired *Onchocerca volvulus* filariae after doxycycline treatment. Parasitology Research. 2009;106(1):23-31.
159. Walker M, Specht S, Churcher TS, Hoerauf A, Taylor MJ, Basáñez M-G. Therapeutic efficacy and macrofilaricidal activity of doxycycline for the treatment of river blindness. Clinical Infectious Diseases. 2015;60(8):1199-207.
160. Albers A, Esum ME, Tendongfor N, Enyong P, Klarmann U, Wanji S, et al. Retarded *Onchocerca volvulus* L1 to L3 larval development in the *Simulium damnosum* vector after anti-wolbachial treatment of the human host. Parasites and Vectors. 2012;5:12.

161. Wanji S, Tendongfor N, Nji T, Esum M, Che JN, Nkwescheu A, et al. Community-directed delivery of doxycycline for the treatment of onchocerciasis in areas of co-endemicity with loiasis in Cameroon. Parasites and Vectors. 2009;2(1):39.
162. McGarry HF, Pfarr K, Egerton G, Hoerauf A, Akue JP, Enyong P, et al. Evidence against *Wolbachia* symbiosis in *Loa loa*. Filaria Journal. 2003;2(1):9.
163. Buttner DW, Wanji S, Bazzocchi C, Bain O, Fischer P. Obligatory symbiotic Wolbachia endobacteria are absent from *Loa loa*. Filaria Journal. 2003;2(1):10.
164. Hoerauf A. Filariasis: new drugs and new opportunities for lymphatic filariasis and onchocerciasis. Current Opinion in Infectious Diseases 2008;21(6):673-81.
165. Tamarozzi F, Tendongfor N, Enyong PA, Esum M, Faragher B, Wanji S, et al. Long term impact of large scale community-directed delivery of doxycycline for the treatment of onchocerciasis. Parasites and Vectors. 2012;5:53.
166. Churcher TS, Pion SD, Osei-Atweneboana MY, Prichard RK, Awadzi K, Boussinesq M, et al. Identifying sub-optimal responses to ivermectin in the treatment of River Blindness. Proceedings of the National Academy of Sciences. 2009;106(39):16716-21.
167. Osei-Atweneboana MY, Eng JK, Boakye DA, Gyapong JO, Prichard RK. Prevalence and intensity of *Onchocerca volvulus* infection and efficacy of ivermectin in endemic communities in Ghana: a two-phase epidemiological study. The Lancet. 2007;369(9578):2021-9.
168. Osei-Atweneboana MY, Awadzi K, Attah SK, Boakye DA, Gyapong JO, Prichard RK. Phenotypic evidence of emerging ivermectin resistance in *Onchocerca volvulus*. PLoS Neglected Tropical Diseases. 2011;5(3):e998.
169. Debrah AY, Specht S, Klarmann-Schulz U, Batsa L, Mand S, Marfo-Debrekyei Y, et al. Doxycycline leads to sterility and enhanced killing of female *Onchocerca volvulus* worms in an area with persistent microfilaridermia after repeated ivermectin treatment: a randomized, placebo-controlled, double-blind trial. Clinical Infectious Diseases. 2015;61(4):517-26.
170. Hoerauf A, Marfo-Debrekyei Y, Buttner M, Debrah AY, Konadu P, Mand S, et al. Effects of 6-week azithromycin treatment on the *Wolbachia* endobacteria of *Onchocerca volvulus*. Parasitology Research. 2008;103(2):279-86.
171. Richards FO, Jr., Amann J, Arana B, Punkosdy G, Klein R, Blanco C, et al. No depletion of *Wolbachia* from *Onchocerca volvulus* after a short course of rifampin and/or azithromycin. American Journal of Tropical Medicine and Hygiene. 2007;77(5):878-82.
172. Specht S, Mand S, Marfo-Debrekyei Y, Debrah AY, Konadu P, Adjei O, et al. Efficacy of 2- and 4-week rifampicin treatment on the *Wolbachia* of *Onchocerca volvulus*. Parasitology Research. 2008;103(6):1303-9.
173. Taylor MJ, Hoerauf A, Townson S, Slatko BE, Ward SA. Anti-*Wolbachia* drug discovery and development: safe macrofilaricides for onchocerciasis and lymphatic filariasis. Parasitology. 2014;141(1):119-27.
174. Klarmann-Schulz U, Specht S, Debrah AY, Batsa L, Ayisi-Boateng NK, Osei-Mensah J, et al. Comparison of doxycycline, minocycline, doxycycline plus albendazole and albendazole alone in their efficacy against onchocerciasis in a randomized, open-label, pilot trial. PLoS Neglected Tropical Diseases. 2017;11(1):e0005156.

175. Halliday A, Guimaraes AF, Tyrer HE, Metuge HM, Patrick CN, Arnaud KO, et al. A murine macrofilaricide pre-clinical screening model for onchocerciasis and lymphatic filariasis. Parasites and Vectors. 2014;7:472.
176. Aljayyoussi G, Tyrer HE, Ford L, Sjoberg H, Pionnier N, Waterhouse D, et al. Short-course, high-dose rifampicin achieves *Wolbachia* depletion predictive of curative outcomes in preclinical models of lymphatic filariasis and onchocerciasis. Scientific Reports. 2017;7:210.
177. Boeree MJ, Heinrich N, Aarnoutse R, Diacon AH, Dawson R, Rehal S, et al. High-dose rifampicin, moxifloxacin, and SQ109 for treating tuberculosis: a multi-arm, multi-stage randomised controlled trial. Lancet Infectious Diseases. 2017;17(1):39-49.
178. Abanobi OC, Edungbola LD, Nwoke BE, Mencias BS, Nkwogu FU, Njoku AJ. Validity of leopard skin manifestation in community diagnosis of human onchocerciasis infection. Applied Parasitology. 1994;35(1):8-11.
179. Bari AU. Clinical spectrum of onchodermatitis. Journal of College of Physicians and Surgeons Pakistan 2007;17(8):453-6.
180. Albiez EJ, Buttner DW, Duke BO. Diagnosis and extirpation of nodules in human onchocerciasis. Tropical Medicine and Parasitology. 1988;39 Suppl 4:331-46.
181. Wilson NO, Ly AB, Cama VA, Cantey PT, Cohn D, Diawara L, et al. Evaluation of lymphatic filariasis and onchocerciasis in three Senegalese districts treated for onchocerciasis with ivermectin. PLOS Neglected Tropical Diseases. 2016;10(12):e0005198.
182. Taylor HR, Munoz B, Keyvan-Larijani E, Greene BM. Reliability of detection of microfilariae in skin snips in the diagnosis of onchocerciasis. American Journal of Tropical Medicine and Hygiene. 1989;41(4):467-71.
183. Remme J, Ba O, Dadzie K, Karam M. A force-of-infection model for onchocerciasis and its applications in the epidemiological evaluation of the Onchocerciasis Control Programme in the Volta River basin area. Bulletin of the World Health Organization. 1986;64(5):667.
184. Thylefors B, Brinkmann UK. The microfilarial load in the anterior segment of the eye. A parameter of intensity of onchocerciasis. Bulletin of the World Health Organization. 1977;55(6):731-7.
185. Stingl P, Ross M, Gibson DW, Ribas J, Connor DH. A diagnostic "patch test" for onchocerciasis using topical diethylcarbamazine. Transactions of the Royal Society of Tropical Medicine and Hygiene. 1984;78(2):254-8.
186. Newland HS, Kaiser A, Taylor HR. The use of diethylcarbamazine cream in the diagnosis of onchocerciasis. Tropical Medicine and Parasitology. 1987;38(2):143-4.
187. Awadzi K, Opoku NO, Attah SK, Lazdins-Helds JK, Kuesel AC. Diagnosis of *Onchocerca volvulus* infection via skin exposure to diethylcarbamazine: clinical evaluation of a transdermal delivery technology-based patch. Parasites and Vectors. 2015;8:515.
188. Boatin B, Toe L, Alley E, Nagelkerke N, Borsboom G, Habbema J. Detection of *Onchocerca volvulus* infection in low prevalence areas: a comparison of three diagnostic methods. Parasitology. 2002;125(6):545.
189. Toe L, Adjami AG, Boatin BA, Back C, Alley ES, Dembele N, et al. Topical application of diethylcarbamazine to detect onchocerciasis recrudescence in west Africa. Transactions of the Royal Society of Tropical Medicine and Hygiene. 2000;94(5):519-25.

190. Boussinesq M, Kamgno J, Eloundou Onomo P, Befidi R, Gardon J. Evaluation du patch à la DEC chez les sujets infectés par Loa loa. Document du Laboratoire mixte CPC/ORSTOM d'Epidémiologie et de Santé publique no 98-16. 1998.
191. Ozoh G, Boussinesq M, Bissek AC, Kobangue L, Kombila M, Mbina JR, et al. Evaluation of the diethylcarbamazine patch to evaluate onchocerciasis endemicity in Central Africa. Tropical Medicine and International Health. 2007;12(1):123-9.
192. Mand S, Marfo-Debrekyei Y, Debrah A, Buettner M, Batsa L, Pfarr K, et al. Frequent detection of worm movements in onchocercal nodules by ultrasonography. Filaria Journal. 2005;4(1):1.
193. Darge K, Troeger J, Engelke C, Leichsenring M, Nelle M, Awadzi K, et al. Evaluation of ultrasonography for the detection of drug-induced changes in onchocercal nodules. The American journal of tropical medicine and hygiene. 1994;51(6):800-8.
194. Toé L, Boatin BA, Adjami A, Back C, Merriweather A, Unnasch TR. Detection of *Onchocerca volvulus* infection by O-150 polymerase chain reaction analysis of skin scratches. Journal of Infectious Diseases. 1998;178(1):282-5.
195. Meredith SE, Unnasch TR, Karam M, Piessens WF, Wirth DF. Cloning and characterization of an *Onchocerca volvulus* specific DNA sequence. Molecular and Biochemical Parasitology. 1989;36(1):1-10.
196. Zimmerman PA, Guderian RH, Aruajo E, Elson L, Phadke P, Kubofcik J, et al. Polymerase chain reaction-based diagnosis of *Onchocerca volvulus* infection: improved detection of patients with onchocerciasis. Journal of Infectious Diseases. 1994;169(3):686-9.
197. Nutman TB, Parredes W, Kubofcik J, Guderian RH. Polymerase chain reaction-based assessment after macrofilaricidal therapy in *Onchocerca volvulus* infection. Journal of Infectious Diseases. 1996;173(3):773-6.
198. Merriweather A, Unnasch TR. *Onchocerca volvulus*: development of a species specific polymerase chain reaction-based assay. Experimental Parasitology. 1996;83(1):164-6.
199. Cotton JA, Bennuru S, Grote A, Harsha B, Tracey A, Beech R, et al. The genome of *Onchocerca volvulus*, agent of river blindness. Nature Microbiology. 2016;2:16216.
200. Fink DL, Fahle GA, Fischer S, Fedorko DF, Nutman TB. Toward molecular parasitologic diagnosis: enhanced diagnostic sensitivity for filarial infections in mobile populations. Journal of Clinical Microbiology. 2011;49(1):42-7.
201. Lloyd MM, Gilbert R, Taha NT, Weil GJ, Meite A, Kouakou IM, et al. Conventional parasitology and DNA-based diagnostic methods for onchocerciasis elimination programmes. Acta Tropica. 2015;146:114-8.
202. Lagatie O, Merino M, Debrah LB, Debrah AY, Stuyver LJ. An isothermal DNA amplification method for detection of *Onchocerca volvulus* infection in skin biopsies. Parasites and Vectors. 2016;9(1):624.
203. Alhassan A, Osei-Atweneboana MY, Kyeremeh KF, Poole CB, Li Z, Tettevi E, et al. Comparison of a new visual isothermal nucleic acid amplification test with PCR and skin snip analysis for diagnosis of onchocerciasis in humans. Molecular and Biochemical Parasitology. 2016;210(1):10-2.
204. Thiele EA, Cama VA, Lakwo T, Mekasha S, Abanyie F, Sleshi M, et al. Detection of *Onchocerca volvulus* in skin snips by microscopy and real-time polymerase chain reaction. American Journal of Tropical Medicine and Hygiene. 2016;94(4):906-11.

205. Yameogo L, Toe L, Hougard JM, Boatin BA, Unnasch TR. Pool screen polymerase chain reaction for estimating the prevalence of *Onchocerca volvulus* infection in *Simulium damnosum* sensu lato: results of a field trial in an area subject to successful vector control. American Journal of Tropical Medicine and Hygiene. 1999;60(1):124-8.
206. Katholi CR, Toe L, Merriweather A, Unnasch TR. Determining the prevalence of *Onchocerca volvulus* infection in vector populations by polymerase chain reaction screening of pools of black flies. Journal of Infectious Diseases. 1995;172(5):1414-7.
207. Unnasch TR, Meredith SE. The use of degenerate primers in conjunction with strain and species oligonucleotides to classify *Onchocerca volvulus*. Methods in Molecular Biology. 1996;50:293-303.
208. Rodriguez-Perez MA, Katholi CR, Hassan HK, Unnasch TR. Large-scale entomologic assessment of *Onchocerca volvulus* transmission by poolscreen PCR in Mexico. American Journal of Tropical Medicine and Hygiene. 2006;74(6):1026-33.
209. Guevara AG, Vieira JC, Lilley BG, Lopez A, Vieira N, Rumbea J, et al. Entomological evaluation by pool screen polymerase chain reaction of *Onchocerca volvulus* transmission in Ecuador following mass mectizan distribution. American Journal of Tropical Medicine and Hygiene. 2003;68(2):222-7.
210. Marchon-Silva V, Caer JC, Post RJ, Maia-Herzog M, Fernandes O. Detection of *Onchocerca volvulus* (Nematoda: *Onchocercidae*) infection in vectors from Amazonian Brazil following mass mectizan distribution. Memorias do Instituto Oswaldo Cruz. 2007;102(2):197-202.
211. Alhassan A, Makepeace BL, LaCourse EJ, Osei-Atweneboana MY, Carlow CK. A simple isothermal DNA amplification method to screen black flies for *Onchocerca volvulus* infection. PLoS One. 2014;9(10):e108927.
212. Poole CB, Li Z, Alhassan A, Guelig D, Diesburg S, Tanner NA, et al. Colorimetric tests for diagnosis of filarial infection and vector surveillance using non-instrumented nucleic acid loop-mediated isothermal amplification (NINA-LAMP). PLoS One. 2017;12(2):e0169011.
213. Doyle SR, Armoo S, Renz A, Taylor MJ, Osei-Atweneboana MY, Grant WN. Discrimination between *Onchocerca volvulus* and *O. ochengi* filarial larvae in *Simulium damnosum* (s.l.) and their distribution throughout central Ghana using a versatile high-resolution speciation assay. Parasites and Vectors. 2016;9(1):536.
214. Harnett W, Bradley J, Garate T. Molecular and immunodiagnosis of human filarial nematode infections. Parasitology. 1999;117(7):59-71.
215. Marcoullis G, Grasbeck R. Preliminary identification and characterization of antigen extracts from *Onchocerca volvulus*. Tropenmedizin und Parasitologie. 1976;27(3):314-22.
216. Marcoullis G, Salonen EM, Grasbeck R. Sequential affinity chromatography for the purification of antigens extracted from *Onchocerca volvulus* adult worms. Tropenmedizin und Parasitologie. 1978;29(1):39-48.
217. Collins WE, Campbell CC, Collins RC, Skinner JC. Serologic studies on onchocerciasis in Guatemala using fixed-tissue sections of adult *Onchocerca volvulus*. American Journal of Tropical Medicine and Hygiene. 1980;29(6):1220-2.
218. Cabrera Z, Parkhouse RM. Identification of antigens of *Onchocerca volvulus* and *Onchocerca gibsoni* for diagnostic use. Molecular and Biochemical Parasitology. 1986;20(3):225-31.

219. Klenk A, Geyer E, Zahner H. Serodiagnosis of human onchocerciasis: evaluation of sensitivity and specificity of a purified *Litomosoides carinii* adult worm antigen. Tropenmedizin und Parasitologie. 1984;35(2):81-4.
220. Lujan R, Collins WE, Stanfill PS, Campbell CC, Collins RC, Huong AY. Comparison of heterologous adult *Brugia malayi* and homologous *Onchocerca volvulus* antigen in the enzyme-linked immunosorbent assay (ELISA) for Guatemalan onchocerciasis. Journal of Parasitology 1984;70(3):385-90.
221. Lucius R, Erondu N, Kern A, Donelson JE. Molecular cloning of an immunodominant antigen of *Onchocerca volvulus*. Journal of Experimental Medicine. 1988;168(3):1199-204.
222. Lobos E, Altmann M, Mengod G, Weiss N, Rudin W, Karam M. Identification of an *Onchocerca volvulus* cDNA encoding a low-molecular-weight antigen uniquely recognized by onchocerciasis patient sera. Molecular and Biochemical Parasitology. 1990;39(1):135-45.
223. Bradley J, Trenholme K, Gillespie A, Guderian R, Titanji V, Hong Y, et al. A sensitive serodiagnostic test for onchocerciasis using a cocktail of recombinant antigens. The American Journal of Tropical Medicine and Hygiene. 1993;48(2):198-204.
224. Nde PN, Pogonka T, Bradley JE, Titanji VP, Lucius R. Sensitive and specific serodiagnosis of onchocerciasis with recombinant hybrid proteins. The American Journal of Tropical Medicine and Hygiene. 2002;66(5):566-71.
225. Rodríguez-Pérez MA, Domínguez-Vázque A, Méndez-Galván J, Sifuentes-Rincón AM, Larralde-Coronal P, Barrera-Saldaña HA, et al. Antibody detection tests for *Onchocerca volvulus*: comparison of the sensitivity of a cocktail of recombinant antigens used in the indirect enzyme-linked immunosorbent assay with a rapid-format antibody card test. Transactions of the Royal Society of Tropical Medicine and Hygiene. 2003;97(5):539-41.
226. Burbelo PD, Leahy HP, Iadarola MJ, Nutman TB. A four-antigen mixture for rapid assessment of *Onchocerca volvulus* infection. PLoS Neglected Tropical Diseases. 2009;3(5):e438.
227. Ramachandran CP. Improved immunodiagnostic tests to monitor onchocerciasis control programmes — A multicenter effort. Parasitology Today. 1993;9(3):77-9.
228. Lobos E, Weiss N, Karam M, Taylor HR, Ottesen EA, Nutman TB. An immunogenic *Onchocerca volvulus* antigen: a specific and early marker of infection. Science. 1991;251(5001):1603-5.
229. Lustigman S, Brotman B, Huima T, Prince AM. Characterization of an *Onchocerca volvulus* cDNA clone encoding a genus specific antigen present in infective larvae and adult worms. Molecular and Biochemical Parasitology. 1991;45(1):65-75.
230. Bradley J, Helm R, Lahaise M, Maizels R. cDNA clones of *Onchocerca volvulus* low molecular weight antigens provide immunologically specific diagnostic probes. Molecular and Biochemical Parasitology. 1991;46(2):219-27.
231. Boatin B, Toe L, Alley E, Dembele N, Weiss N, Dadzie K. Diagnostics in onchocerciasis: future challenges. Annals of Tropical Medicine and Parasitology. 1998;92(sup1):S41-5.
232. Weil G, Ogunrinade A, Chandrashekar R, Kale O. IgG4 subclass antibody serology for onchocerciasis. Journal of Infectious Diseases. 1990;161(3):549-54.
233. Gbakima AA, Nutman TB, Bradley JE, McReynolds LA, Winget MD, Hong Y, et al. Immunoglobulin G subclass responses of children during infection with

Onchocerca volvulus. Clinical and Diagnostic Laboratory Immunology. 1996;3(1):98-104.
234. Neglected Tropical Diseases Support Centre. *Ov*-16 meeting notes, neglected tropical diseases support center, taskforce for global health, Decatur, GA, USA, May 2–3, 2016. 2016. [Internet]. Available from: http://www.ntdsupport.org/sites/default/files/uploads/docs/resources/Ov16%20Technical%20Meeting%20Report_May_2016.pdf.
235. Weil GJ, Steel C, Liftis F, Li B-W, Mearns G, Lobos E, et al. A rapid-format antibody card test for diagnosis of onchocerciasis. Journal of Infectious Diseases. 2000;182(6):1796-9.
236. Lipner EM, Dembele N, Souleymane S, Alley WS, Prevots DR, Toe L, et al. Field applicability of a rapid-format anti–*Ov*-16 antibody test for the assessment of onchocerciasis control measures in regions of endemicity. Journal of Infectious Diseases. 2006;194(2):216-21.
237. Program Coordinating Committee. Guide to detecting a potential recrudescence of onchocerciasis during the posttreatment surveillance period: the American paradigm. Research and Reports in Tropical Medicine. 2012;2012(3):21-33.
238. Lindblade KA, Arana B, Zea-Flores G, Rizzo N, Porter CH, Dominguez A, et al. Elimination of *Onchocercia volvulus* transmission in the Santa Rosa focus of Guatemala. American Journal of Tropical Medicine and Hygiene. 2007;77(2):334-41.
239. Rodríguez-Pérez MA, Unnasch TR, Domínguez-Vázquez A, Morales-Castro AL, Richards Jr F, Peña-Flores GP, et al. Lack of active *Onchocerca volvulus* transmission in the northern Chiapas focus of Mexico. American Journal of Tropical Medicine and Hygiene. 2010;83(1):15-20.
240. Oguttu D, Byamukama E, Katholi CR, Habomugisha P, Nahabwe C, Ngabirano M, et al. Serosurveillance to monitor onchocerciasis elimination: the Ugandan experience. American Journal of Tropical Medicine and Hygiene. 2014;90(2):339-45.
241. Katabarwa MN, Walsh F, Habomugisha P, Lakwo TL, Agunyo S, Oguttu DW, et al. Transmission of onchocerciasis in Wadelai focus of northwestern Uganda has been interrupted and the disease eliminated. Journal of Parasitology Research. 2012;2012:1-7.
242. Higazi TB, Zarroug IM, Mohamed HA, Elmubark WA, Deran TC, Aziz N, et al. Interruption of *Onchocerca volvulus* transmission in the Abu Hamed focus, Sudan. American Journal of Tropical Medicine and Hygiene. 2013;89(1):51-7.
243. Golden A, Steel C, Yokobe L, Jackson E, Barney R, Kubofcik J, et al. Extended result reading window in lateral flow tests detecting exposure to *Onchocerca volvulus*: a new technology to improve epidemiological surveillance tools. PloS One. 2013;8(7):e69231.
244. Golden A, Faulx D, Kalnoky M, Stevens E, Yokobe L, Peck R, et al. Analysis of age-dependent trends in *Ov*16 IgG4 seroprevalence to onchocerciasis. Parasites and Vectors. 2016;9(1):338.
245. Golden A, Stevens EJ, Yokobe L, Faulx D, Kalnoky M, Peck R, et al. A recombinant positive control for serology diagnostic tests supporting elimination of *Onchocerca volvulus*. PLoS Neglected Tropical Diseases. 2016;10(1):e0004292.
246. Paulin HN, Nshala A, Kalinga A, Mwingira U, Wiegand R, Cama V, et al. Evaluation of onchocerciasis transmission in Tanzania: preliminary rapid field

results in the Tukuyu Focus, 2015. American Journal of Tropical Medicine and Hygiene. 2017.
247. Bradley JE, Gillespie AJ, Trenholme KR, Karam M. The effects of vector control on the antibody response to antigens of *Onchocerca volvulus.* Parasitology. 1993;106(4):363-70.
248. Lont YL, Coffeng LE, de Vlas SJ, Golden A, de Los Santos T, Domingo GJ, et al. Modelling anti-*Ov*16 IgG4 antibody prevalence as an indicator for evaluation and decision making in onchocerciasis elimination programmes. PLoS Neglected Tropical Diseases. 2017;11(1):e0005314.
249. Smith R, Cotter T, Williams J, Guderian R. Vascular perfusion of *Onchocerca volvulus* nodules. Tropical Medicine and Parasitology. 1988;39:418-21.
250. George GH, Palmieri JR, Connor DH. The onchocercal nodule: interrelationship of adult worms and blood vessels. The American Journal of Tropical Medicine and Hygiene. 1985;34(6):1144-8.
251. Tritten L, Burkman E, Moorhead A, Satti M, Geary J, Mackenzie C, et al. Detection of circulating parasite-derived microRNAs in filarial infections. PLoS Neglected Tropical Diseases. 2014;8(7):e2971.
252. Ouaissi A, Kouemeni LE, Haque A, Ridel PR, Andre PS, Capron A. Detection of circulating antigens in onchocerciasis. American Journal of Tropical Medicine and Hygiene. 1981;30(6):1211-8.
253. Des Moutis I, Ouaissi A, Grzych JM, Yarzabal L, Haque A, Capron A. *Onchocerca volvulus:* detection of circulating antigen by monoclonal antibodies in human onchocerciasis. American Journal of Tropical Medicine and Hygiene. 1983;32(3):533-42.
254. Schlie-Guzman M, Rivas-Alcalá A. Antigen detection in onchocerciasis: correlation with worm burden. Tropical Medicine and Parasitology. 1989;40(1):47-50.
255. Mbacham WF, Titanji VP, Thunberg L, Holmdahl R, Rubin K. A monoclonal antibody-based immunodiagnostic assay for onchocerciasis. Tropical Medicine and Parasitology. 1992;43(2):83-90.
256. Thambiah G, Whitworth J, Hommel M, Devaney E. Identification and characterization of a parasite antigen in the circulating immune complexes of *Onchocerca volvulus* infected patients. Tropical Medicine and Parasitology. 1992;43(4):271-6.
257. Chandrashekar R, Ogunrinade AF, Henry RW, Lustigman S, Weil GJ. *Onchocerca volvulus:* monoclonal antibodies to immune complex-associated parasite antigens. Experimental Parasitology. 1993;77(2):224-34.
258. More SJ, Copeman DB. A highly specific and sensitive monoclonal antibody-based ELISA for the detection of circulating antigen in bancroftian filariasis. Tropical Medicine and Parasitology. 1990;41(4):403-6.
259. Weil GJ, Liftis F. Identification and partial characterization of a parasite antigen in sera from humans infected with Wuchereria bancrofti. Journal of Immunology. 1987;138(9):3035-41.
260. Chesnais CB, Missamou F, Pion SD, Bopda J, Louya F, Majewski AC, et al. Semi-quantitative scoring of an immunochromatographic test for circulating filarial antigen. The American Journal of Tropical Medicine and Hygiene. 2013;89(5):916-8.
261. Goodwin J-K. The serologic diagnosis of heartworm infection in dogs and cats. Clinical Techniques in Small Animal Practice. 1998;13(2):83-7.

262. Taylor MJ, Makunde WH, McGarry HF, Turner JD, Mand S, Hoerauf A. Macrofilaricidal activity after doxycycline treatment of *Wuchereria bancrofti:* a double-blind, randomised placebo-controlled trial. The Lancet. 2005;365(9477):2116-21.
263. Debrah AY, Mand S, Marfo-Debrekyei Y, Batsa L, Pfarr K, Buttner M, et al. Macrofilaricidal effect of 4 weeks of treatment with doxycycline on *Wuchereria bancrofti.* Tropical Medicine and International Health. 2007;12(12):1433-41.
264. Debrah AY, Mand S, Marfo-Debrekyei Y, Batsa L, Pfarr K, Lawson B, et al. Reduction in levels of plasma vascular endothelial growth factor-A and improvement in hydrocele patients by targeting endosymbiotic *Wolbachia* sp. in *Wuchereria bancrofti* with doxycycline. The American Journal of Tropical Medicine and Hygiene. 2009;80(6):956-63.
265. Mand S, Pfarr K, Sahoo PK, Satapathy AK, Specht S, Klarmann U, et al. Macrofilaricidal activity and amelioration of lymphatic pathology in bancroftian filariasis after 3 weeks of doxycycline followed by single-dose diethylcarbamazine. The American Journal of Tropical Medicine and Hygiene. 2009;81(4):702-11.
266. Harnett W, Worms M, Grainger M, Pyke S, Parkhouse R. Association between circulating antigen and parasite load in a model filarial system, *Acanthocheilonema viteae* in jirds. Parasitology. 1990;101(3):435-44.
267. Weil GJ, Chandrashekar R, Liftis F, McVay CS, Bosshardt SC, Klei TR. Circulating parasite antigen in *Brugia pahangi*-infected jirds. The Journal of Parasitology. 1990;76(1):78-84.
268. Weil GJ, Malane MS, Powers KG. Detection of circulating parasite antigens in canine dirofilariasis by counterimmunoelectrophoresis. The American Journal of Tropical Medicine and Hygiene. 1984;33(3):425-30.
269. Bennuru S, Cotton JA, Ribeiro JM, Grote A, Harsha B, Holroyd N, et al. Stage-specific transcriptome and proteome analyses of the filarial parasite *Onchocerca volvulus* and its *Wolbachia* endosymbiont. American Society for Microbiology. 2016;7(6):e02028-16
270. Gaze S, Driguez P, Pearson MS, Mendes T, Doolan DL, Trieu A, et al. An immunomics approach to schistosome antigen discovery: antibody signatures of naturally resistant and chronically infected individuals from endemic areas. PLoS Pathogens. 2014;10(3):e1004033.
271. McNulty SN, Rosa BA, Fischer PU, Rumsey JM, Erdmann-Gilmore P, Curtis KC, et al. An integrated multiomics approach to identify candidate antigens for serodiagnosis of human onchocerciasis. Molecular and Cellular Proteomics. 2015;14(12):3224-33.
272. Preidis GA, Hotez PJ. The newest "omics"—metagenomics and metabolomics—enter the battle against the neglected tropical diseases. PLoS Neglected Tropical Diseases. 2015;9(2):e0003382.
273. Denery JR, Nunes AA, Hixon MS, Dickerson TJ, Janda KD. Metabolomics-based discovery of diagnostic biomarkers for onchocerciasis. PLoS Neglected Tropical Diseases. 2010;4(10):e834.
274. Bennuru S, Lustigman S, Abraham D, Nutman TB. Metabolite profiling of infection-associated metabolic markers of onchocerciasis. Molecular and Biochemical Parasitology. 2017;215:58-69.
275. Globisch D, Moreno AY, Hixon MS, Nunes AA, Denery JR, Specht S, et al. *Onchocerca volvulus*-neurotransmitter tyramine is a biomarker for river blindness. Proceedings of the National Academy of Sciences. 2013;110(11):4218-23.

276. Globisch D, Specht S, Pfarr KM, Eubanks LM, Hoerauf A, Janda KD. *Litomosoides sigmodontis*: a jird urine metabolome study. Bioorganic and Medicinal Chemistry Letters. 2015;25(24):5804-7.
277. Globisch D, Eubanks LM, Shirey RJ, Pfarr KM, Wanji S, Debrah AY, et al. Validation of onchocerciasis biomarker N-acetyltyramine-O-glucuronide (NATOG). Bioorganic and Medicinal Chemistry Letters. 2017;27(15):3436-40.
278. Lagatie O, Ediage EN, Debrah LB, Diels L, Nolten C, Vinken P, et al. Evaluation of the diagnostic potential of urinary N-Acetyltyramine-O, β-glucuronide (NATOG) as diagnostic biomarker for *Onchocerca volvulus* infection. Parasites and Vectors. 2016;9(1):302.
279. Wewer V, Makepeace BL, Tanya VN, Peisker H, Pfarr K, Hoerauf A, et al. Lipid profiling of the filarial nematodes *Onchocerca volvulus*, *Onchocerca ochengi* and *Litomosoides sigmodontis* reveals the accumulation of nematode-specific ether phospholipids in the host. International Journal for Parasitology. 2017;S0020-7519(17):30205-9.
280. Chapman EJ, Carrington JC. Specialization and evolution of endogenous small RNA pathways. Nature Reviews Genetics. 2007;8(11):884-96.
281. Kim VN, Nam J-W. Genomics of microRNA. Trends in Genetics. 2006;22(3):165-73.
282. Gorski SA, Vogel J, Doudna JA. RNA-based recognition and targeting: sowing the seeds of specificity. Nature Reviews Molecular Cell Biology. 2017;18(4):215-28.
283. Cai P, Gobert GN, McManus DP. MicroRNAs in parasitic helminthiases: current status and future perspectives. Trends in Parasitology. 2016;32(1):71-86.
284. Devaney E, Winter AD, Britton C. microRNAs: a role in drug resistance in parasitic nematodes? Trends in Parasitology. 2010;26(9):428-33.
285. Fromm B, Trelis M, Hackenberg M, Cantalapiedra F, Bernal D, Marcilla A. The revised microRNA complement of *Fasciola hepatica* reveals a plethora of overlooked microRNAs and evidence for enrichment of immuno-regulatory microRNAs in extracellular vesicles. International Journal for Parasitology. 2015;45(11):697-702.
286. Fromm B, Ovchinnikov V, Hoye E, Bernal D, Hackenberg M, Marcilla A. On the presence and immunoregulatory functions of extracellular microRNAs in the trematode *Fasciola hepatica*. Parasite Immunology. 2017;39(2):e12399.
287. Buck AH, Coakley G, Simbari F, McSorley HJ, Quintana JF, Le Bihan T, et al. Exosomes secreted by nematode parasites transfer small RNAs to mammalian cells and modulate innate immunity. Nature Communications. 2014;5:5488.
288. Manzano-Roman R, Siles-Lucas M. MicroRNAs in parasitic diseases: potential for diagnosis and targeting. Molecular and Biochemical Parasitology. 2012;186(2):81-6.
289. Poole CB, Gu W, Kumar S, Jin J, Davis PJ, Bauche D, et al. Diversity and expression of microRNAs in the filarial parasite, Brugia malayi. PLoS One. 2014;9(5):e96498.
290. Winter AD, Weir W, Hunt M, Berriman M, Gilleard JS, Devaney E, et al. Diversity in parasitic nematode genomes: the microRNAs of *Brugia pahangi* and *Haemonchus contortus* are largely novel. BMC Genomics. 2012;13(1):4.
291. Quintana JF, Makepeace BL, Babayan SA, Ivens A, Pfarr KM, Blaxter M, et al. Extracellular *Onchocerca*-derived small RNAs in host nodules and blood. Parasites and Vectors. 2015;8(1):58.

292. Kato M, de Lencastre A, Pincus Z, Slack FJ. Dynamic expression of small non-coding RNAs, including novel microRNAs and piRNAs/21U-RNAs, during *Caenorhabditis elegans* development. Genome Biology. 2009;10(5):R54.
293. Winter AD, Gillan V, Maitland K, Emes RD, Roberts B, McCormack G, et al. A novel member of the let-7 microRNA family is associated with developmental transitions in filarial nematode parasites. BMC Genomics. 2015;16:331.
294. Cheng G, Luo R, Hu C, Cao J, Jin Y. Deep sequencing-based identification of pathogen-specific microRNAs in the plasma of rabbits infected with *Schistosoma japonicum*. Parasitology. 2013;140(14):1751-61.
295. Hoy AM, Lundie RJ, Ivens A, Quintana JF, Nausch N, Forster T, et al. Parasite-derived microRNAs in host serum as novel biomarkers of helminth infection. PLoS Neglected Tropical Diseases. 2014;8(2):e2701.
296. Tritten L, O'Neill M, Nutting C, Wanji S, Njouendoui A, Fombad F, et al. *Loa loa* and *Onchocerca ochengi* miRNAs detected in host circulation. Molecular and Biochemical Parasitology. 2014;198(1):14-7.
297. Lagatie O, Debrah LB, Debrah A, Stuyver LJ. Plasma-derived parasitic microRNAs have insufficient concentrations to be used as diagnostic biomarker for detection of *Onchocerca volvulus* infection or treatment monitoring using LNA-based RT-qPCR. Parasitology Research. 2017;116(3):1013-22.
298. Hoy AM, Buck AH. Extracellular small RNAs: what, where, why? Biochemical Society Transactions. 2012;40(4):886-90.
299. Valadi H, Ekström K, Bossios A, Sjöstrand M, Lee JJ, Lötvall JO. Exosome-mediated transfer of mRNAs and microRNAs is a novel mechanism of genetic exchange between cells. Nature Cell Biology. 2007;9(6):654-9.
300. Schwarzenbach H, Nishida N, Calin GA, Pantel K. Clinical relevance of circulating cell-free microRNAs in cancer. Nature Reviews Clinical Oncology. 2014;11(3):145-56.
301. Kim Y-K. Extracellular microRNAs as biomarkers in human disease. Chonnam Medical Journal. 2015;51(2):51-7.
302. He X, Sai X, Chen C, Zhang Y, Xu X, Zhang D, et al. Host serum miR-223 is a potential new biomarker for *Schistosoma japonicum* infection and the response to chemotherapy. Parasites and Vectors. 2013;6:272.
303. Cai P, Gobert GN, You H, Duke M, McManus DP. Circulating miRNAs: potential novel biomarkers for hepatopathology progression and diagnosis of *Schistosomiasis japonica* in two murine models. PLoS Neglected Tropical Diseases. 2015;9(7):e0003965.
304. Silakit R, Loilome W, Yongvanit P, Chusorn P, Techasen A, Boonmars T, et al. Circulating miR-192 in liver fluke-associated cholangiocarcinoma patients: a prospective prognostic indicator. Journal of Hepato-Biliary-Pancreatic Sciences. 2014;21(12):864-72.
305. Plieskatt J, Rinaldi G, Feng Y, Peng J, Easley S, Jia X, et al. A microRNA profile associated with *Opisthorchis viverrini*-induced cholangiocarcinoma in tissue and plasma. BMC Cancer. 2015;15:309.
306. Li BS, Zhao YL, Guo G, Li W, Zhu ED, Luo X, et al. Plasma microRNAs, miR-223, miR-21 and miR-218, as novel potential biomarkers for gastric cancer detection. PLoS One. 2012;7(7):e41629.
307. Zamanian M, Fraser LM, Agbedanu PN, Harischandra H, Moorhead AR, Day TA, et al. Release of small RNA-containing exosome-like vesicles from the human filarial parasite *Brugia malayi*. PLoS Neglected Tropical Diseases. 2015;9(9):e0004069.

308. Horgan RP, Kenny LC. 'Omic'technologies: genomics, transcriptomics, proteomics and metabolomics. The Obstetrician and Gynaecologist. 2011;13(3):189-95.
309. Rifai N, Gillette MA, Carr SA. Protein biomarker discovery and validation: the long and uncertain path to clinical utility. Nature Biotechnology. 2006;24(8):971-83.
310. Anderson NL, Anderson NG. The human plasma proteome history, character, and diagnostic prospects. Molecular and Cellular Proteomics. 2002;1(11):845-67.
311. Parker CE, Borchers CH. Mass spectrometry based biomarker discovery, verification, and validation--quality assurance and control of protein biomarker assays. Molecular Oncology. 2014;8(4):840-58.
312. Wanji S, Tendongfor N, Esum M, Yundze SS, Taylor MJ, Enyong P. Combined utilisation of rapid assessment procedures for loiasis (RAPLOA) and onchocerciasis (REA) in rain forest villages of Cameroon. Filaria Journal. 2005;4(1):2.
313. Perkins DN, Pappin DJC, Creasy DM, Cottrell JS. Probability-based protein identification by searching sequence databases using mass spectrometry data. Electrophoresis. 1999;20(18):3551-67.
314. UniProt Consortium. UniProt: the universal protein knowledgebase. Nucleic Acids Research. 2017;45(D1):D158-d69.
315. Nesvizhskii AI. A survey of computational methods and error rate estimation procedures for peptide and protein identification in shotgun proteomics. Journal of Proteomics. 2010;73(11):2092-123.
316. Elias JE, Haas W, Faherty BK, Gygi SP. Comparative evaluation of mass spectrometry platforms used in large-scale proteomics investigations. Nature Methods. 2005;2(9):667.
317. Matrix Science. Mascot database search - Decoy databases. [Internet]. Available from: http://www.matrixscience.com/help/decoy_help.html; (Accessed July 2017).
318. Matrix Science. MS/MS Results Interpretation. [Internet]. Available from: http://www.matrixscience.com/help/interpretation_help.html#GROUPING; (Accessed July 2017).
319. Cox J, Mann M. MaxQuant enables high peptide identification rates, individualized ppb-range mass accuracies and proteome-wide protein quantification. Nature Biotechnology. 2008;26(12):1367-72.
320. Cox J, Neuhauser N, Michalski A, Scheltema RA, Olsen JV, Mann M. Andromeda: a peptide search engine integrated into the MaxQuant environment. Journal of Proteome Research. 2011;10(4):1794-805.
321. Tyanova S, Temu T, Cox J. The MaxQuant computational platform for mass spectrometry-based shotgun proteomics. Nature Protocols. 2016;11(12):2301-19.
322. Cox J, Hein MY, Luber CA, Paron I, Nagaraj N, Mann M. Accurate proteome-wide label-free quantification by delayed normalization and maximal peptide ratio extraction, termed MaxLFQ. Molecular and Cellular Proteomics. 2014;13(9):2513-26.
323. Geiger T, Wehner A, Schaab C, Cox J, Mann M. Comparative proteomic analysis of eleven common cell lines reveals ubiquitous but varying expression of most proteins. Molecular and Cellular Proteomics 2012;11(3):M111.014050.
324. Tyanova S, Temu T, Sinitcyn P, Carlson A, Hein MY, Geiger T, et al. The Perseus computational platform for comprehensive analysis of (prote) omics data. Nature Methods. 2016;13(9):731-40.

325. Altschul SF, Gish W, Miller W, Myers EW, Lipman DJ. Basic local alignment search tool. Journal of Molecular Biology. 1990;215(3):403-10.
326. Sievers F, Wilm A, Dineen D, Gibson TJ, Karplus K, Li W, et al. Fast, scalable generation of high-quality protein multiple sequence alignments using Clustal Omega. Molecular Systems Biology. 2011;7:539.
327. Binns D, Dimmer E, Huntley R, Barrell D, O'Donovan C, Apweiler R. QuickGO: a web-based tool for Gene Ontology searching. Bioinformatics. 2009;25(22):3045-6.
328. Nielsen H. Predicting Secretory Proteins with SignalP. Methods in Molecular Biology. 2017;1611:59-73.
329. Ye J, Coulouris G, Zaretskaya I, Cutcutache I, Rozen S, Madden TL. Primer-BLAST: a tool to design target-specific primers for polymerase chain reaction. BMC Bioinformatics. 2012;13(1):134.
330. Hulsen T, de Vlieg J, Alkema W. BioVenn–a web application for the comparison and visualization of biological lists using area-proportional Venn diagrams. BMC Genomics. 2008;9(1):488.
331. Anderson L. Candidate-based proteomics in the search for biomarkers of cardiovascular disease. The Journal of Physiology. 2005;563(1):23-60.
332. Omenn GS. Exploring the human plasma proteome. Proteomics. 2005;5(13):3223-5.
333. Baker ES, Liu T, Petyuk VA, Burnum-Johnson KE, Ibrahim YM, Anderson GA, et al. Mass spectrometry for translational proteomics: progress and clinical implications. Genome Medicine. 2012;4(8):63.
334. Domon B, Aebersold R. Options and considerations when selecting a quantitative proteomics strategy. Nature Biotechnology. 2010;28(7):710-21.
335. Zhang Y, Fonslow BR, Shan B, Baek M-C, Yates III JR. Protein analysis by shotgun/bottom-up proteomics. Chemical Reviews. 2013;113(4):2343-94.
336. Zubarev RA. The challenge of the proteome dynamic range and its implications for in-depth proteomics. Proteomics. 2013;13(5):723-6.
337. Todd J, Simpson P, Estis J, Torres V, Wub AH. Reference range and short- and long-term biological variation of interleukin (IL)-6, IL-17A and tissue necrosis factor-alpha using high sensitivity assays. Cytokine. 2013;64(3):660-5.
338. Slebos RJ, Brock JW, Winters NF, Stuart SR, Martinez MA, Li M, et al. Evaluation of strong cation exchange versus isoelectric focusing of peptides for multidimensional liquid chromatography-tandem mass spectrometry. Journal of Proteome Research. 2008;7(12):5286-94.
339. Sprung RW, Brock JW, Tanksley JP, Li M, Washington MK, Slebos RJ, et al. Equivalence of protein inventories obtained from formalin-fixed paraffin-embedded and frozen tissue in multidimensional liquid chromatography-tandem mass spectrometry shotgun proteomic analysis. Molecular and Cellular Proteomics. 2009;8(8):1988-98.
340. Beck HC, Overgaard M, Rasmussen LM. Plasma proteomics to identify biomarkers–application to cardiovascular diseases. Translational Proteomics. 2015;7:40-8.
341. States DJ, Omenn GS, Blackwell TW, Fermin D, Eng J, Speicher DW, et al. Challenges in deriving high-confidence protein identifications from data gathered by a HUPO plasma proteome collaborative study. Nature Biotechnology. 2006;24(3):333-8.
342. Malmström J, Lee H, Aebersold R. Advances in proteomic workflows for systems biology. Current Opinion in Biotechnology. 2007;18(4):378-84.

343. Michalski A, Cox J, Mann M. More than 100,000 detectable peptide species elute in single shotgun proteomics runs but the majority is inaccessible to data-dependent LC− MS/MS. Journal of Proteome Research. 2011;10(4):1785-93.
344. Laemmli UK. Cleavage of structural proteins during the assembly of the head of bacteriophage T4. Nature. 1970;227(5259):680-5.
345. Qian WJ, Jacobs JM, Camp DG, Monroe ME, Moore RJ, Gritsenko MA, et al. Comparative proteome analyses of human plasma following in vivo lipopolysaccharide administration using multidimensional separations coupled with tandem mass spectrometry. Proteomics. 2005;5(2):572-84.
346. Schenk S, Schoenhals GJ, de Souza G, Mann M. A high confidence, manually validated human blood plasma protein reference set. BMC Medical Genomics. 2008;1(1):41.
347. Liu H, Sadygov RG, Yates JR. A model for random sampling and estimation of relative protein abundance in shotgun proteomics. Analytical Chemistry. 2004;76(14):4193-201.
348. Fasano M, Curry S, Terreno E, Galliano M, Fanali G, Narciso P, et al. The extraordinary ligand binding properties of human serum albumin. The International Union of Biochemistry and Molecular Biology Life. 2005;57(12):787-96.
349. Hodge K, Ten Have S, Hutton L, Lamond AI. Cleaning up the masses: exclusion lists to reduce contamination with HPLC-MS/MS. Journal of Proteomics. 2013;88:92-103.
350. Ye H, Sun L, Huang X, Zhang P, Zhao X. A proteomic approach for plasma biomarker discovery with 8-plex iTRAQ labeling and SCX-LC-MS/MS. Molecular and Cellular Biochemistry. 2010;343(1-2):91-9.
351. Ernoult E, Bourreau A, Gamelin E, Guette C. A proteomic approach for plasma biomarker discovery with iTRAQ labelling and OFFGEL fractionation. Journal of BioMed Research. 2009;2010:1-8.
352. Bandow JE. Comparison of protein enrichment strategies for proteome analysis of plasma. Proteomics. 2010;10(7):1416-25.
353. Hakimi A, Auluck J, Jones GD, Ng LL, Jones DJ. Assessment of reproducibility in depletion and enrichment workflows for plasma proteomics using label-free quantitative data-independent LC-MS. Proteomics. 2014;14(1):4-13.
354. Millioni R, Tolin S, Puricelli L, Sbrignadello S, Fadini GP, Tessari P, et al. High abundance proteins depletion vs low abundance proteins enrichment: comparison of methods to reduce the plasma proteome complexity. PloS One. 2011;6(5):e19603.
355. Gong Y, Li X, Yang B, Ying W, Li D, Zhang Y, et al. Different immunoaffinity fractionation strategies to characterize the human plasma proteome. Journal of Proteome Research. 2006;5(6):1379-87.
356. Yocum AK, Yu K, Oe T, Blair IA. Effect of immunoaffinity depletion of human serum during proteomic investigations. Journal of Proteome Research. 2005;4(5):1722-31.
357. Echan LA, Tang HY, Ali-Khan N, Lee K, Speicher DW. Depletion of multiple high-abundance proteins improves protein profiling capacities of human serum and plasma. Proteomics. 2005;5(13):3292-303.
358. Kim YJ, Domon B. Sample preparation and profiling: mass-spectrometry-based profiling strategies. In: Horvatovich P, Bischoff R, editors. Comprehensive biomarker discovery and validation for clinical application. Cambridge: Royal Society of Chemistry; 2013. p. 136-61.

359. Dayon L, Kussmann M. Proteomics of human plasma: A critical comparison of analytical workflows in terms of effort, throughput and outcome. EuPA Open Proteomics. 2013;1:8-16.
360. Tu C, Rudnick PA, Martinez MY, Cheek KL, Stein SE, Slebos RJ, et al. Depletion of abundant plasma proteins and limitations of plasma proteomics. Journal of Proteome Research. 2010;9(10):4982-91.
361. Liu T, Qian W-J, Mottaz HM, Gritsenko MA, Norbeck AD, Moore RJ, et al. Evaluation of multiprotein immunoaffinity subtraction for plasma proteomics and candidate biomarker discovery using mass spectrometry. Molecular and Cellular Proteomics. 2006;5(11):2167-74.
362. Omenn GS, States DJ, Adamski M, Blackwell TW, Menon R, Hermjakob H, et al. Overview of the HUPO Plasma Proteome Project: Results from the pilot phase with 35 collaborating laboratories and multiple analytical groups, generating a core dataset of 3020 proteins and a publicly-available database. Proteomics. 2005;5(13):3226-45.
363. Gupta N, Pevzner PA. False discovery rates of protein identifications: a strike against the two-peptide rule. Journal of Proteome Research. 2009;8(9):4173-81.
364. Veenstra TD, Conrads TP, Issaq HJ. Commentary: What to do with" one-hit wonders"? Electrophoresis. 2004;25(9):1278-9.
365. Elias JE, Gygi SP. Target-decoy search strategy for mass spectrometry-based proteomics. Proteome Bioinformatics. 2010:55-71.
366. He P, He HZ, Dai J, Wang Y, Sheng QH, Zhou LP, et al. The human plasma proteome: analysis of Chinese serum using shotgun strategy. Proteomics. 2005;5(13):3442-53.
367. Geyer PE, Kulak NA, Pichler G, Holdt LM, Teupser D, Mann M. Plasma proteome profiling to assess human health and disease. Cell Systems. 2016;2(3):185-95.
368. Yadav AK, Bhardwaj G, Basak T, Kumar D, Ahmad S, Priyadarshini R, et al. A systematic analysis of eluted fraction of plasma post immunoaffinity depletion: implications in biomarker discovery. PLoS One. 2011;6(9):e24442.
369. Bellei E, Bergamini S, Monari E, Fantoni LI, Cuoghi A, Ozben T, et al. High-abundance proteins depletion for serum proteomic analysis: concomitant removal of non-targeted proteins. Amino Acids. 2011;40(1):145-56.
370. Engvall E, Ruoslahti E. Affinity of fibronectin to collagens of different genetic types and to fibrinogen. Journal of Experimental Medicine 1978;147(6):1584-95.
371. Nielsen MJ, Moestrup SK. Receptor targeting of hemoglobin mediated by the haptoglobins: roles beyond heme scavenging. Blood. 2009;114(4):764-71.
372. Ball CH, Roulhac PL. Multidimensional techniques in protein separations for neuroproteomics. In: Alzate O, editor. Neuroproteomics. Boca Raton: CRC Press; 2009. p. 25-49.
373. Qian W-J, Kaleta DT, Petritis BO, Jiang H, Liu T, Zhang X, et al. Enhanced detection of low abundance human plasma proteins using a tandem IgY12-SuperMix immunoaffinity separation strategy. Molecular and Cellular Proteomics. 2008;7(10):1963-73.
374. Addona TA, Shi X, Keshishian H, Mani D, Burgess M, Gillette MA, et al. A pipeline that integrates the discovery and verification of plasma protein biomarkers reveals candidate markers for cardiovascular disease. Nature Biotechnology. 2011;29(7):635-43.

375. Cao Z, Tang H-Y, Wang H, Liu Q, Speicher DW. Systematic comparison of fractionation methods for in-depth analysis of plasma proteomes. Journal of Proteome Research. 2012;11(6):3090-100.
376. Keshishian H, Burgess MW, Gillette MA, Mertins P, Clauser KR, Mani D, et al. Multiplexed, quantitative workflow for sensitive biomarker discovery in plasma yields novel candidates for early myocardial injury. Molecular and Cellular Proteomics. 2015:M114. 046813.
377. Yin P, Lehmann R, Xu G. Effects of pre-analytical processes on blood samples used in metabolomics studies. Analytical and bioanalytical chemistry. 2015;407(17):4879-92.
378. Davies MJ. The oxidative environment and protein damage. Biochimica et Biophysica Acta (BBA)-Proteins and Proteomics. 2005;1703(2):93-109.
379. Anderson NL, Anderson NG, Pearson TW, Borchers CH, Paulovich AG, Patterson SD, et al. A human proteome detection and quantitation project. Molecular and Cellular Proteomics. 2009;8(5):883-6.
380. Surinova S, Schiess R, Hüttenhain R, Cerciello F, Wollscheid B, Aebersold R. On the development of plasma protein biomarkers. Journal of Proteome Research. 2010;10(1):5-16.
381. Farrah T, Deutsch EW, Aebersold R. Using the Human Plasma PeptideAtlas to study human plasma proteins. In: Simpson RJ, Greening DW, editors. Serum/Plasma Proteomics. New York: Humana Press; 2011. p. 349-74.
382. Folkersen J, Teisner B, Grunnet N, Grudzinskas J, Westergaard J, Hindersson P. Circulating levels of pregnancy zone protein: normal range and the influence of age and gender. Clinica Chimica Acta. 1981;110(2-3):139-45.
383. Harnett W. Secretory products of helminth parasites as immunomodulators. Molecular and Biochemical Parasitology. 2014;195(2):130-6.
384. McKerrow JH, Caffrey C, Kelly B, Loke Pn, Sajid M. Proteases in parasitic diseases. Annual Review of Pathology: Mechanisms of Disease. 2006;1:497-536.
385. Slifka MK. Mechanisms of humoral immunity explored through studies of LCMV infection. In: Oldstone MB, editor. Arenaviruses II: The molecular pathogenesis of arenavirus infections. 263. Berlin: Springer Science & Business Media; 2012. p. 66-79.
386. Haraldsson B, Nystrom J, Deen WM. Properties of the glomerular barrier and mechanisms of proteinuria. Physiological Reviews. 2008;88(2):451-87.
387. Lote CJ. Glomerular filtration. In: Lote CJ, editor. Principles of renal physiology. 5th ed. New York: Springer; 1994. p. 33-44.
388. Chandrashekar R, Curtis K, Weil G. Molecular characterization of a parasite antigen in sera from onchocerciasis patients that is immunologically cross-reactive with human keratin. Journal of Infectious Diseases. 1995;171(6):1586-92.
389. Pion SD, Montavon C, Chesnais CB, Kamgno J, Wanji S, Klion AD, et al. Positivity of antigen tests used for diagnosis of lymphatic filariasis in individuals without *Wuchereria bancrofti* infection but with high Loa loa microfilaremia. The American Journal of Tropical Medicine and Hygiene. 2016;95(6):1417-23.
390. Wanji S, Amvongo-Adjia N, Koudou B, Njouendou AJ, Ndongmo PWC, Kengne-Ouafo JA, et al. Cross-reactivity of filariais ICT cards in areas of contrasting endemicity of *Loa loa* and *Mansonella perstans* in Cameroon: Implications for shrinking of the lymphatic filariasis map in the Central African Region. PLoS Neglected Tropical Diseases. 2015;9(11):e0004184.

391. Liu Y, Buil A, Collins BC, Gillet LC, Blum LC, Cheng LY, et al. Quantitative variability of 342 plasma proteins in a human twin population. Molecular Systems Biology. 2015;11(2):786.
392. Abdullah L, Paris D, Luis C, Quadros A, Parrish J, Valdes L, et al. The influence of diagnosis, intra-and inter-person variability on serum and plasma Aβ levels. Neuroscience Letters. 2007;428(2):53-8.
393. Soboslay PT, Geiger SM, Weiss N, Banla M, Luder CG, Dreweck CM, et al. The diverse expression of immunity in humans at distinct states of *Onchocerca volvulus* infection. Immunology. 1997;90(4):592-9.
394. Mackenzie CD, Williams JF, Sisley BM, Steward MW, O'Day J. Variations in host responses and the pathogenesis of human onchocerciasis. Reviews of Infectious Diseases. 1985;7(6):802-8.
395. Fahrial Y, Catmul J, Copeman B. Duration of persistence of *Onchocerca gibsoni* DNA in cattle blood. Jurnal Sain Veteriner. 2013;21(1):33-7.
396. De Lencastre A, Pincus Z, Zhou K, Kato M, Lee SS, Slack FJ. MicroRNAs both promote and antagonize longevity in *C. elegans*. Current Biology. 2010;20(24):2159-68.
397. Isik M, Korswagen HC, Berezikov E. Expression patterns of intronic microRNAs in *Caenorhabditis elegans*. Silence. 2010;1(1):5.
398. Karp X, Hammell M, Ow MC, Ambros V. Effect of life history on microRNA expression during *C. elegans* development. RNA. 2011;17(4):639-51.
399. Lee RC, Feinbaum RL, Ambros V. The *C. elegans* heterochronic gene lin-4 encodes small RNAs with antisense complementarity to lin-14. Cell. 1993;75(5):843-54.
400. Ambros V. A hierarchy of regulatory genes controls a larva-to-adult developmental switch in *C. elegans*. Cell. 1989;57(1):49-57.
401. Ambros V, Horvitz H. Heterochronic mutants of the nematode *Caenorhabditis elegans.* Science. 1984;226:409-16.
402. Supali T, Ismid IS, Wibowo H, Djuardi Y, Majawati E, Ginanjar P, et al. Estimation of the prevalence of lymphatic filariasis by a pool screen PCR assay using blood spots collected on filter paper. Transactions of the Royal Society of Tropical Medicine and Hygiene. 2006;100(8):753-9.
403. Elshimali YI, Khaddour H, Sarkissyan M, Wu Y, Vadgama JV. The clinical utilization of circulating cell free DNA (CCFDNA) in blood of cancer patients. International Journal of Molecular Sciences. 2013;14(9):18925-58.
404. Moldovan L, Batte KE, Trgovcich J, Wisler J, Marsh CB, Piper M. Methodological challenges in utilizing miRNAs as circulating biomarkers. Journal of Cellular and Molecular Medicine. 2014;18(3):371-90.
405. Witwer KW. Circulating microRNA biomarker studies: pitfalls and potential solutions. Clinical Chemistry. 2015;61(1):56-63.
406. Zampetaki A, Mayr M. Analytical challenges and technical limitations in assessing circulating miRNAs. Thrombosis and Haemostasis. 2012;108(4):592.
407. Mestdagh P, Hartmann N, Baeriswyl L, Andreasen D, Bernard N, Chen C, et al. Evaluation of quantitative miRNA expression platforms in the microRNA quality control (miRQC) study. Nature Methods. 2014;11(8):809-15.
408. Chen C, Ridzon DA, Broomer AJ, Zhou Z, Lee DH, Nguyen JT, et al. Real-time quantification of microRNAs by stem–loop RT–PCR. Nucleic Acids Research. 2005;33(20):e179-e.
409. Paulo JA. Practical and efficient searching in proteomics: a cross engine comparison. WebmedCentral. 2013;4(10):1-15.

410. Tang H-Y, Nadeem A-K, Echan LA, Levenkova N, John J. Rux, Speicher DW. A novel fourdimensional strategy combining protein and peptide separation methods enables detection of low abundance proteins in human plasma. In: Omenn GS, editor. Exploring the human plasma proteome. New Jersey: John Wiley & Sons; 2006. p. 135-58.
411. Alhassan A, Li Z, Poole CB, Carlow CK. Expanding the MDx toolbox for filarial diagnosis and surveillance. Trends in Parasitology. 2015;31(8):391-400.
412. Vlaminck J, Fischer PU, Weil GJ. Diagnostic tools for onchocerciasis elimination programs. Trends in Parasitology. 2015;31(11):571-82.